Surface Chemical Functionalization based on Plasma Techniques

Politecnico di Torino
Dipartimento di Scienza Applicata e Tecnologia

Doctorate Course in Electronic Devices – cycle XXIV

"Surface Chemical Functionalization based on Plasma Techniques"

Candidate: Serena Ricciardi

Tutors: Prof. Fabrizio Pirri

Dr.ssa Paola Rivolo

Acknowledgments

The PhD period has been an important experience for me not only from the professional point of view, as I have extended my knowledge to new scientific fields and I have learned new important techniques for my education, but also it has been fundamental for my personal growth, as it has given to me the possibility to know people who have offered their precious experience and have supported me throughout all the important steps of this period.

First of all, I am very grateful to Professor Pirri, who has given to me the opportunity to participate to the Doctorate selection and to join to this workgroup and to my supervisor, Dr.ssa Paola Rivolo, who has been a constant presence through all these years, not only as a "reference point" for the research activity but also from the human point of view. Thanks to her support and her practical suggestions I have learned new techniques concerning the chemical field and I have started to be confident with a "new" world as she has offered to me her precious knowledge and has guided me during the most important steps of this project.

Certainly, I would like to thank all my colleagues who have participated to develop the subject of this thesis, in particular Dr.ssa Francesca Frascella, who has shared with me all the important moments of this period and has become more than a workmate, giving to me an essential support and precious suggestions whenever I needed; Dr.ssa Gabriella Digregorio and Dr.ssa Rossana Gazia, my colleagues and my friends, who have supported me with their kindness and their scientific suggestions.

A kind thank to Dr. Ivan Ferrante and Dr. Riccardo Castagna, for their essential contribution in some important results but also for their friendship and their help showed in every moment of my working life.

I am very grateful to Dr. Pietro Mandracci for the help in many practical situations and for the important instructions which has enabled me to face some difficult situations with success, and to Dr. Emiliano Descrovi and Dr. Mirko Ballarini for their scientific support and for the collaboration in different activities.

I am very thankful to my officemates, Dr.ssa Monica Capone, Dr.ssa Ninfa Radicella and Dr. Emiliano Capolongo, for all the affection and all the nice moments enjoyed together during these three years.

I would also like to thank the research group of the Leibniz Institute in Dresden, in particular Dr. Mirko Nitschke and all the scientific staff, as they have kindly received me offering the possibility to work in an excellent institute and to approach to several facilities and characterization techniques important for my study, supporting me with their knowledge and their experience.

Finally my family, always present in my life and always supporting me during this academic iter; without them the realization of this important goal could never have been possible and all the important persons of my life for the unconditional love and the huge appreciation which have sustained me every day.

Index

8. “Plasma polymerization from styrene vapours: thin film deposition of styrene-polymers and styrene-co-polymers with acrylic acid”

Introduction

Biomaterials research has undergone a variety of evolutionary developments in recent years. In this perspective, bulk materials properties and biomechanics took relevance in view of the stringent mechanical and tribological demands of the bio-implants. However, such issues cannot be the sole determinants of clinical outcome. Interest in bulk properties has inevitably shifted to the important consideration of the **surface** with the interfacial phenomena, conditioning their performance. These events are extremely important for **biosensor devices**. The application focus of biosensors has also broadened with time and whilst clinical diagnostics probably remains the single biggest area, roles are also being found in environmental (including food) monitoring, personal security (including warfare), drug discovery, and basic biological research.

The development of suitable materials for biosensor applications requires a thorough understanding of the **structure** and **chemistry** of the solid-liquid interface when such a material has to work in the actual context. The research domain is complex due to the diversity of materials and applications of interest and the variety of biological species the biosensor device has to interface.

In order to begin to follow the interactions that may occur when a material is placed in a particular environment, it is of fundamental importance to have information on the composition and structure of the top few atomic layers. In general, the statement that surface properties of a material differ from that of the bulk can be also applied to biomaterials.

Thus, since the interaction between the material and the biological species occur at their interface, that is at molecular level in a narrow interface zone (< 1 nm), the surface properties of the material can greatly influence the biomaterial tissue/cell/protein interaction.

Surface modification techniques have become a key method for designing materials to produce specific biological and chemical interactions.

Modification of surface properties by altering the surface functionalities or by thin film deposition allow us to create and optimize surfaces with desired chemical and physical properties suitable for subsequent biological evaluation and indeed, for such applications as the promotion of specific cell/protein responses to a surface.

Nowadays, the wet chemical conventional methods, used for surface functionalization, involve in some cases the use of toxic liquid reagents thus environment detrimental; for this

reason they are progressively being replaced by other techniques, in particular by **plasma surface modification processes.**

Low-temperature plasmas are produced by electrical discharge sustained by gases at low-pressure condition. They consist of a mixture of highly reactive species, i.e., ions, radicals, electrons, photons and excited molecules.

The nature of plasmas, the modalities of transferring electric or electromagnetic field intensities to the reaction systems, the geometry of reactor (shape and volumes of the reaction vessel, geometrical location of electrodes and substrates, etc.) and the selected experimental conditions (pressure, power, flow rates of gases, temperature of the substrates, etc.) crucially influence the gas-phase and surface-related plasma chemistry.

Recently, surface treatments and modification based on vapor phase plasma-assisted techniques have been widely applied to several biomedical fields. These processes are able to provide specific mono-type chemical functionalities, exposed at materials surfaces. Respect to traditional liquid phase procedures, advantages such as the high process control and the use of small quantities of reagents, are crucial for the enhancement of efficiency of the interactions that materials must perform according to the application.

In particular, procedures for in situ plasma polymerization, starting from vapor released by liquid monomers, are presently used to synthesize innovative polymeric thin films applicable as substrates for cell culture, as adhesion promoter in prosthetic implants and for molecular recognition in sensors and biosensors.

This method achieves the chemical and morphological modification of surfaces leaving the bulk properties practically intact, thus enabling its applicability to a great variety of materials independently from their chemical properties.

By plasma treatment completely different chemistry, hydrophilicity or surface roughness can be obtained in final resulting materials. Advantages of plasma polymerization include the possibility to obtain conformal thin films, pinhole free, deposited on most substrates, by means of a relatively simple one-step coating. Additionally, a wide range of compounds can be chosen as a monomer for plasma polymerization, even saturated hydrocarbons, providing a great diversity of possible surface modifications.

Among these compounds, **Acrylic Acid** is an important monomer, finding applications as a coating in a great number of biological experiments, for example, as a novel cell-delivery vehicle. Using acrylic acid as a monomer for plasma polymerization, layers, containing **carboxylic acid groups** (**-COOH**), can be produced to make surfaces reactive towards different biomolecules containing **amino groups** (**NH_2**).

In this kind of applications the density of the carboxylic functionalities exposed at the surface of the plasma polymer is a crucial point.

The modulation of the applied power, typically through variation of the pulse frequency and duty cycle, enables greater control over the processing plasma properties, for instance, the retention of the degree of monomer functional groups in the resulting polymer structure.. It worth of note that, by selectively acting the monomer fragmentation, through the plasma discharge pulsing, it is possible to promote the chain propagation of the polymer without affecting the chemical structure of the functional groups and so obtaining a high density of reactive surface species.

These advantages have resulted in the rapid development of plasma technology, during the past decades, for applications ranging from adhesion to composite materials, protective coatings, printing, membranes, biomedical applications and so on.

1) Concerning the first part of the experimental work of this thesis, a twofold aim can be singled out:
   - by means of the study and the optimization of **plasma polymerization processes**, the achievement of thin films exposing the desired properties of **stability**, **biocompatibility** and bioreactivity
   - the experimental validation of such films performance in **biosensor devices**

   For these purposes, thin functional films deposited by plasma-polymerization process, were applied to different devices, in particular a plasma poly-acrylic acid thin film was used for the surface functionalization of a Microarray platform for **biodiagnostic detection analysis**. Then, a patterned functional polymer obtained by the combination of a non-bio-adhesive layer of plasma **poly-styrene** and the functional coating of the plasma poly acrylic acid, was used for the functionalization of a photonic mono-dimensional crystal able to couple **Bloch Surface Waves** on its surface to **Fluorescence emission** specifically **localized** to poly-acrylic acid guides for **photonic biosensing** .

2) A last chapter of this thesis is dedicated to the study and optimization of **maleic anhydride functionalization** according to different technical approaches, compared in terms of technical feasibility and achievable surface properties, in order to obtain a stable surface functionalization with a sufficient anhydride density for subsequent protein binding.

Chapter I

Biosensor Technology

1.1. What is a biosensor?

The name "sensor" is referred to a device able to convert a physical quantity into a different signal (usually electrical) that can be detected and measured.

A simple example is represented from a mercury thermometer using a physical effect to measure external temperature. Even in nature some examples of sensor occur: all living organisms have natural sensors with biological functions similar to those of artificial sensors suitable for detection of physical (light, temperature, movement), metabolic (oxygen and glucose levels) and biochemical (interactions with hormones, cytokines) phenomena [1].

In particular a biosensor is an electronic device that employs biological elements (such as antibodies, enzymes, receptor proteins, lectins, nucleic acids, cells, or tissue sections) as the analyte sensor and couples the element to a transducer. Specific interactions between the target analyte and the biorecognition element produce a physico-chemical change, which is detected and measured by the transducer. Indeed, the transducer converts the biochemical signal into an electronic signal that is processed into an analog or digital format. The amount of generated signal generated is directly proportional to the concentration of the analyte, allowing for both quantitative and qualitative real-time measurements [2].

Figure 1.1 Fiber-optic, fully automated biosensor performs four immunoassays simultaneously in 5 to 10 minutes and shows the results on an LCD screen in words

Unlike many standard immunoassays which use biological elements without the transducing component, “Biosensors combine the exquisite selectivity of the biological molecule with the processing power of modern microelectronics and optoelectronics to offer powerful new analytical tools with applications in medical diagnostics, environmental monitoring, and food processing [3].

The detection of a specific molecule could be achieved due to the molecular recognition occurring between the surface of the sensor, opportunely modified, and the target molecule. Thanks to suitable surface modifications, the sensor can be made selectively reactive towards the specific target and so able to detect it even in complex biological matrices.

The difficulty associated to such device is related to the activity in vivo due to the use of the liquid phase bio-reagents that can alter the attendant optimized solution parameters of pH, pI and concentration thus compromising biosensor efficiency in the detection mechanism.

1.2. Commercial biosensors

The first biosensor appeared in 1956 and is related to an enzymatic electrode used for measuring oxygen amount.

In 1975 the Yellow Springs Instrument Co. (Ohio, USA) brought out the glucose biosensor, based on the reaction performed by the enzyme glucose oxidase which, by consuming oxygen, transforms glucose into gluconic acid. Hydrogen peroxide is a by-product of oxidation and oxygen consumption is revealed by amperometric detection.

Blood-glucose monitoring kits for diabetics are by far the most successful commercial biosensors to date, thanks to the handheld devices offered by MediSense, LifeScan, Bayer, and Boehringer Mannheim. Scientists are exploring the development of optical devices for glucose monitoring, based on subcutaneous membrane implants and on in vivo glucose needle enzyme electrodes, in which the sensor is implanted beneath the skin.

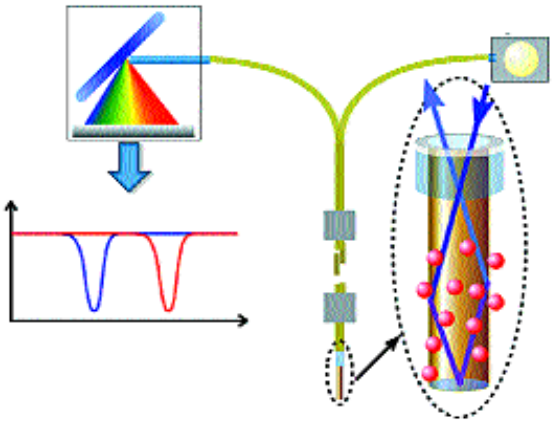

Figure 1.2 White light passes through the optical fiber into the gold-tipped sensor probe, where biomolecular binding events cause changes in the refractive index thus affecting the spectrum of the reflected light

Another important field of application is related to the food industry. Prompted by the rise in food-borne illnesses, the U.S. Department of Agriculture plans to institute new regulations that will require more thorough testing for pathogens, thus reflecting a demand for automated

biosensors capable of rapidly detecting contaminants in meat, poultry, seafood, fruits, and vegetables. Compared to conventional detection methods, which are quite long if used with perishable food, biosensor technology can produce measurements more quickly, sometimes within hours, and detect smaller amounts of pathogens, with fewer false positives.

A laser-based biosensor developed by researchers at the Georgia Institute of Technology integrates optics, immunoassay, and surface chemistry to detect *Salmonella* in meat; and scientists at Lawrence Berkeley National Laboratory have produced a biosensor that detects the particularly virulent 0157:H7 strain of *E. coli*. The University of Florence in Italy has developed a piezoelectric biosensor to detect the potentially deadly *Listeria* bacteria in milk products, while Sensor Solutions is using electrochemical biosensors to determine the sugar/alcohol ratio in wine [2].

In figure 1 is represented another example of optical biosensor based on the integration of different activities on the same device. The optically based BIAcore sensor from Biacore AB (Uppsala, Sweden) is primarily sold to bioscience R&D laboratories for real-time analysis of biological interactions, and it is also used for high-throughput screening in pharmaceutical development. Biacore plans to target the food-processing industry as well, particularly for vitamin analysis in fortified food products and drug residue analysis in meat and milk products.

Concerning different areas, in environmental monitoring, Ligler's group at NRL has

developed a fully automated fiber optic biosensor that performs four immunoassays simultaneously in 10 minutes and displays the results on an LCD screen in simple words (Figure 1.2).

Other emerging applications for biosensors include an array of medical diagnostics. By means the sensors, clinical analyses can be performed at the bedside, in critical-care units, and in doctors'offices, and the test results can be acted upon immediately, thus avoiding the delays associated with having to send samples to centralized laboratories. BioStar's (Boulder, CO) optical immunoassay technology offers point-of-care diagnostic testing for strep A and B infections. "Affinity Sensors" optical biosensors can rapidly detect, measure, and characterize antibodies in human blood serum [2].

1.3. Biosensor components

Three main units compose biosensors:

- a biomolecule, the probe, the biological element of the sensor able to recognize the target
- the analyte, the target molecule, binding the biological element
- the transducer, able to convert the signal related to the biological interaction between the biological element and the analyte into a measurable signal

1.3.1. The biological elements: the interaction between the probe and the analyte

In the most common biosensor implementation, a probe molecule is affixed to a sensing platform and used to recognize or detect a target molecule which is complementary to the probe. As an example, a protein antibody may serve as the probe, used to detect a specific protein antigen, or a single stranded oligonucleotide may be used as a biorecognition probe for the complementary segment of single-stranded DNA.

The main features related to biomolecules that can be used in biosensor are the affinity and the specificity for the analyte.

Typical biomolecules which can be integrated in biosensors are:

- DNA or RNA molecules able to bind proteins and suitable for the screening

- Proteins, usually receptor molecules able to bind a specific ligand or antibodies, mostly used for their great specificity and for the type of binding with their antigen (versatility and high binding energy).

DNA

Life is specified by **genomes**. Every organism, including humans, has a genome that contains all of the biological information needed to build and maintain a living example of that organism. The biological information contained in a genome is encoded in its **deoxyribonucleic acid (DNA)** and is divided into discrete units called **genes**.

A single gene consists of a unique sequence of DNA that provides the complete instructions to make a functional product, called a protein. Genes instruct each cell type (such as skin, brain, and liver) to make discrete sets of proteins at just the right times, and it is through this specificity that unique organisms arise [4].

DNA, or deoxyribonucleic acid, is the hereditary material in humans and almost all other organisms. Nearly every cell in a person's body has the same DNA. Most DNA is located in the cell nucleus (where it is called nuclear DNA), but a small amount of DNA can also be found in the mitochondria (where it is called mitochondrial DNA or mtDNA).

The information in DNA is stored as a code made up of four chemical bases: adenine (A), guanine (G), cytosine (C), and thymine (T). Human DNA consists of about 3 billion bases, and more than 99 percent of those bases are the same in all people. The order, or sequence, of these bases determines the information available for building and maintaining an organism, similar to the way in which letters of the alphabet appear in a certain order to form words and sentences.

DNA bases pair up with each other, A with T and C with G, to form units called base pairs. Each base is also attached to a sugar molecule and a phosphate molecule. Together, a base, sugar, and phosphate are called a nucleotide [5].

Individual nucleotides are linked through the phosphate group forming two long strands that create a spiral called a double helix. The structure of the double helix is somewhat like a ladder, with the base pairs forming the ladder's rungs and the sugar and phosphate molecules forming the vertical sidepieces of the ladder. Each strand, has a sense of direction, in which one end is chemically different than the other. The so-called 5' end terminates in a 5' phosphate group ($-PO_4$); the 3' end terminates in a 3' hydroxyl group (-OH). This is important because DNA strands are always synthesized in the 5' to 3' direction. The precise order, or sequence of nucleotides determines the product made from that gene.

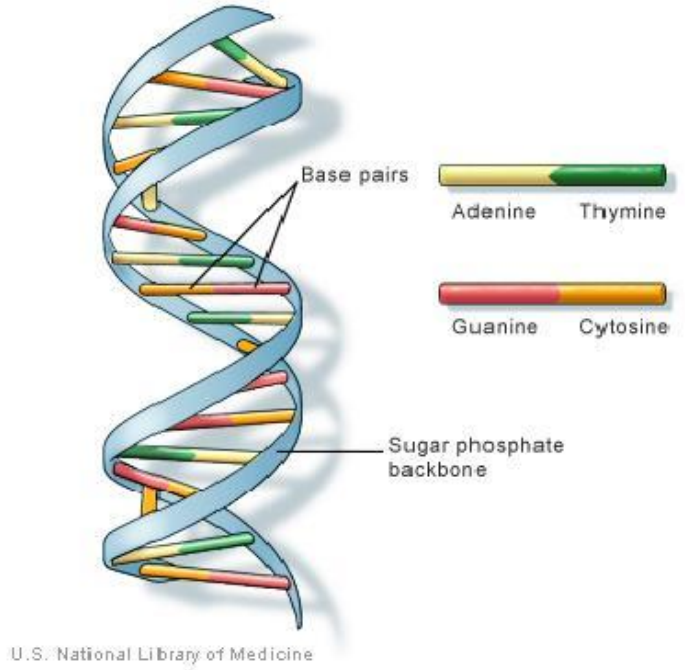

Figure 1.3 DNA is a double helix formed by base pairs attached to a sugar-phosphate backbone

A gene is the basic physical and functional unit of heredity. Genes, which are made up of DNA, act as instructions to make molecules called proteins. In humans, genes vary in size from a few hundred DNA bases to more than 2 million bases. The Human Genome Project has estimated that humans have between 20,000 and 25,000 genes.

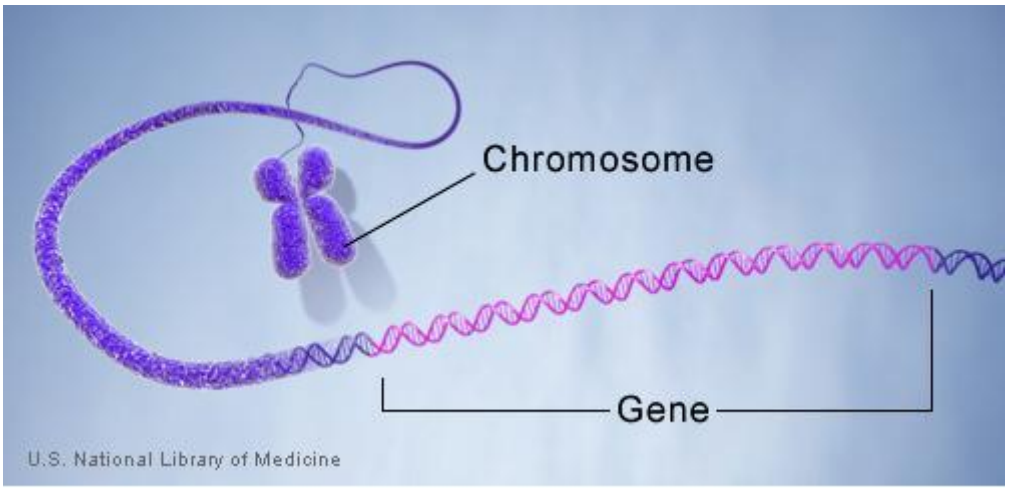

Figure 1. 4 Gene are made up of DNA. Each chromosome contains many genes

Proteins

Although DNA is the carrier of genetic information in a cell, proteins do the bulk of the work. Proteins are long chains containing as many as twenty different kinds of amino acids. Each cell contains thousands of different proteins: **enzymes** that make new molecules and catalyze nearly all chemical processes in cells; **structural components** that give cells their shape and help them move; **hormones** that transmit signals throughout the body; **antibodies** that recognize foreign molecules; and **transport molecules** that carry oxygen. The genetic code carried by DNA is what specifies the order and number of amino acids and, therefore, the shape and function of the protein.

The "**Central Dogma**", a fundamental principle of molecular biology, states that genetic information flows from DNA to RNA to protein. Ultimately, however, the genetic code resides in DNA because only DNA is passed from generation to generation. Yet, in the process of making a protein, the encoded information must be faithfully transmitted first to RNA then to protein. Transferring the code from DNA to RNA is a fairly straightforward process called **transcription**. Deciphering the code in the resulting mRNA is a little more complex. It first requires that the mRNA leave the nucleus and associate with a large complex of specialized RNAs and proteins that, collectively, are called the **ribosome**. Here the mRNA is translated into protein by decoding the mRNA sequence in blocks of three RNA bases, called **codons**, where each codon specifies a particular amino acid. In this way, the **ribosomal complex** builds a protein one amino acid at a time, with the order of amino acids determined precisely by the order of the codons in the mRNA [5].

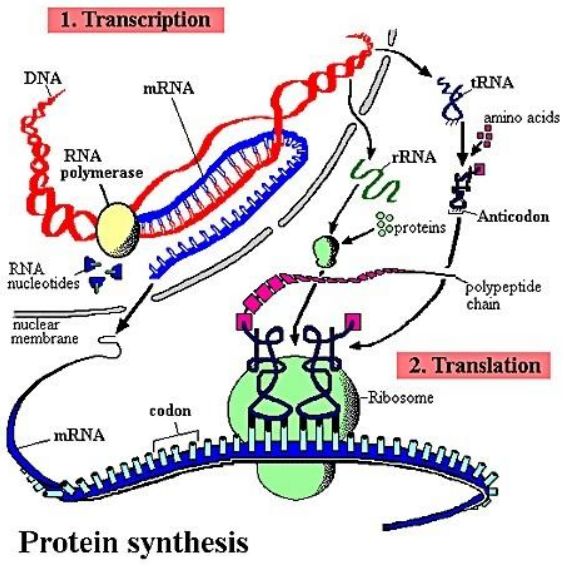

Figure 1.5 The Central Dogma: from DNA to proteins

1.3.2. The substrate: the choice of the material to be functionalized

In any biosensing technology a crucial point is the stability of the recognizing biomolecules immobiliezed on the substrate. The development of various stabilization techniques has helped to address that problem. The sophisticated manufacturing processes, including miniaturization and full automation, have moved in this direction.

Vacuum technology has had a significant impact on the design and construction of biosensors, from the clean-room environments needed to manufacture the devices to control of the fluidics of biosensing systems. Researchers are also using vacuum technology to create modified surface substrates that better preserve the biological activity required for sensing purposes. Because most of the biological reactions take place at a solid-liquid interface, the better scientists understand the behaviour of biomolecules at interfaces, the better the molecules and their reactions can be controlled in biosensing systems. Surface Plasmon resonance and optical spectroscopic techniques are also finding use as tools for understanding the biosensor interface and the biological interactions at surfaces.

A crucial role in projecting a biosensor is also played by the choice of the substrate. Substrates usually available for biofunctionalization procedures are: silicon, corning or gold but also many polymeric substrates are suitable for this purpose such as poly(met)acrylates, polystyrene, polypirrol, silicon, teflon and have been quite used for the fabrication of biosensors, MEMS or microarray systems.

Material system	Advantages	Disadvantages
Silicon	Low cost Mature processing techniques	Limits in operating frequency range
Compound semiconductors	High carrier mobility, high frequency operation Suitability for optoelectronics Capability for bandgap engineering and epitaxially-grown layers	Cost
Organic semiconductors	Ease of application (inkjet, spin casting) Suitability for flexible substrates Suitability for optoelectronics	Low carrier mobility Not amenable to standard process flows
Nanomaterials	Novel physicochemical and electronic properties	Not amenable to standard process flows Unproven safety profile

Table 1.1 Advantages and disadvantages associated with various relevant material systems

In Table 1.1 a list of specific materials and material systems which have received significant attention for their potential for biological application, in particular, for sensing applications in molecular diagnostics.

Silicon, thanks to its unique properties, has resulted in profound technological advances over the last half-century. Silicon exhibits a crystal structure in which each silicon atom bonds covalently with four neighboring atoms in a tetrahedral arrangement, forming a so-called diamond lattice [6].

It's classified as "semiconductor" because at temperature of absolute zero, all outer shell electrons are confined to covalent bonds, leaving no free electrons for conduction; as temperature rise above absolute zero, thermal energy can result in the liberation of electrons available for conduction.

Its electrical properties can be readily altered through the addition of a very small number of impurity atoms ("doping") and directed to specific regions of a silicon substrate it allows for the spatial definition of electronically-active devices which can then be interconnected to perform complex circuit functions [7].

Other semiconductor materials can be formed by the combination of elements from column III and column V of the periodic table in 1:1 stoichiometric ratio and used to form crystalline materials. These substrates exhibit semiconducting properties similar to that of silicon and germanium even if they are more expensive than their silicon counterparts. The advantage is related to the higher electron mobility and suitability for use at high frequencies. These materials also exhibit higher resistivity than silicon, allowing for their use in applications which demand very low leakage currents and high sensitivities and also have unique properties which render them useful for photonic and (bio-photonic) applications, such as fluorescence detection.

Another class of semiconductor materials is that of organic semiconductors, typically based on carbon-containing compounds and polymers. The electron distribution in organic molecules composed of π-conjugated systems (i.e. carbon-containing molecules composed of repeating double-bond/single bond units) is delocalized, allowing for relative ease of electron (current) flow in these materials. In addition, proper selection of the conjugation length allows for interesting optoelectronic activity, hence these materials have found great use as organic light-emitting diodes (OLEDs) and as photovoltaic materials. Organic semiconducting materials may be deposited onto rigid or flexible substrates using low-cost inject printing or spin-casting techniques but these materials are relatively less amenable to traditional photolithographic techniques for patterning and device definition. Although this may be

advantageous for simple devices, it can complicate the processing for more complex devices or integrated circuits.

Different from to the other class of substrates is the class of the nanomaterials; this term has been applied to materials that incorporate structures having dimensions in the range 1-100 nm and whose electrical and/or chemical properties are also influenced by their small dimensional scale. These materials have a wide variety of morphologies, including nanotubes, nanowires, nanoparticles also termed quantum dots), and sheet-like two dimensional structures. The unique optical, electrical, mechanical and chemical properties of nanomaterials have attracted considerable interest (these properties are influenced by quantum mechanical effects, and may vary from those of the individual constituent atoms or molecules, as well as those of the corresponding bulk materials. As the prototypal example carbon nanotubes have been the subject of great research focus, given their great strength, high thermal and electrical conductivity, and chemical stability.

The type of material used in biosensors can affect the subsequent functionalization step, for this reason this choice is a crucial point in fabricating a biosensor device.

Usually the materials used as substrates are: metals, glass and ceramics and polymers.

Metals

Metals are solids that have metallic chemical bonding where the atoms are bonded by the "sea" of electrons. Typically, metals are ductile, have some degree of fracture toughness, and have appreciable electrical conductivity. Gold is the only metal that does not form a natural oxide; metals are usually covered with an oxide layer that is the natural or real surface of the material. In some cases the oxide layer is removed from the metal before film deposition takes place but in many cases the film is deposited on the oxide surface. Metal oxides have a high surface energy so a clean metal oxide will adsorb low energy adsorbates, such as hydrocarbons, in order to lower its surface energy. These adsorbates are the contaminants that must be removed before film deposition.

Metals can react with each other to form compounds (intermetallic compounds) that have a high degree of ionic chemical bonding. Aluminum is an amphoteric metal that can form intermetallic compounds with other metals either by giving up or accepting an electron. Intermetallic compounds can play an important role in the galvanic corrosion of surfaces, interfaces, and films when they are present [8].

Ceramics and glasses

Ceramics and glasses are generally multicomponent solids that are chemically bonded by ionic or covalent bonding such that there are no free electrons. Therefore, the electrical conductivity and the thermal conductivity are low and the material is brittle. If there is crystallinity the material is called a ceramic and if there is no crystallinity (i.e. the material is amorphous) the material is called a glass.

Ceramics and glasses are characterized by low ductility and low fracture toughness. Some elemental materials, such as boron, carbon, and silicon, can be formed as amorphous materials, so the definitions must be taken with some exceptions [8].

Polymers

A polymer is a large molecule formed by bonding numerous small molecular units, called monomers, together. The most common polymers are the organic polymers, which are based on carbon–hydrogen units that may or may not contain other elements such as nitrogen, oxygen, metals, etc. Polymers can also be formed from other monomer units such as silicon–hydrogen, boron–hydrogen, etc. In building a polymer, many bonds are formed which have various strengths, bond orientations, and separations (bond lengths) between atoms and functional groups. These bonds and the associated chemical environment determine the IR absorption and photoelectron emission characteristics of the material. Table 1.2 gives the repeating monomer units for some common polymers.

The chemical properties of the polymer surface will depend on the functional groups present on the surface and may depend on the vapor in contact with the surface. For example, the surface may be different if it has been put into contact with an inert atmosphere (argon, nitrogen) or with a water vapor-containing atmosphere.

The mechanical properties of the surface region will depend on the amount and type of cross-linking of the polymer material. Often the near-surface region of a polymer material has quite different mechanical properties from the bulk of the material [8].

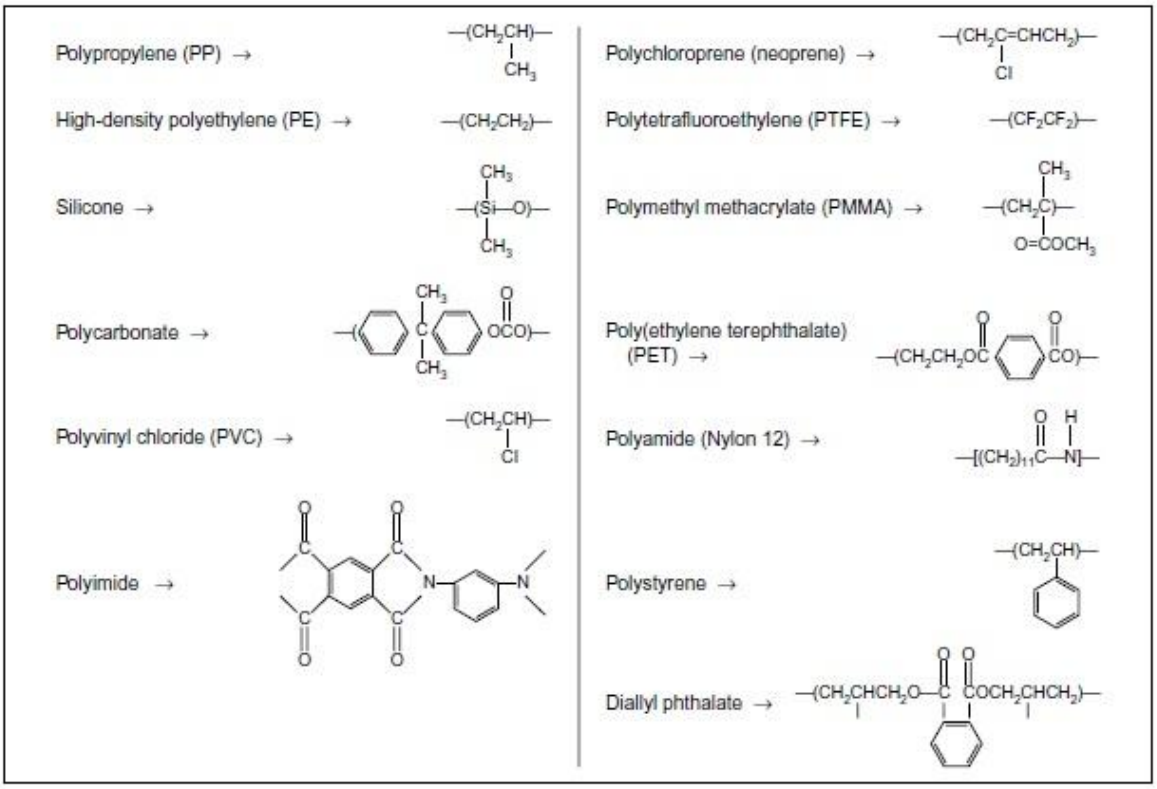

Table 1.2 Repeating Units for Some Common Polymers

Once selected the specific support and the opportune biomolecule for the biosensor fabrication, another crucial step is the attachment of the biological element to the surface as it cannot be removed during the binding to the target molecule to be recognized.

Techniques for immobilizing biomolecules can broadly be divided into two categories: chemical and physical methods.

Chemical methods of immobilization involve the formation of at least one covalent bond between one or more enzyme molecules and the polymer matrix. These processes are usually irreversible.

Physical methods include adsorption (e.g. electrostatic interaction) and entrapment within micro-compartments (e.g. entrapment of molecule within gel matrices or semi-permeable microcapsules, etc.) and are usually based on reversible bond formations.

In case of enzymes, covalent attachment to a solid-phase matrix must involve only functional groups of the enzyme that are not essential for catalytic action. This immobilization approach is much more complex and less mild than those based on physical adsorption and ionic binding procedures. These procedures will be discussed in details in Chapter II.

In order to optimize the functionalization step many important surface properties have to be considered such as surface wettability, biocompatibility and the presence of functional

groups in the molecule.

1.3.3. The transducer: how to convert a biological event into a measurable signal

The transducer is the element able to convert the biochemical reaction between the biomolecule and the probe into a measurable electrochemical signal. Usually in biosensors they are electrochemical, electro-optical, acoustic and mechanical components.

Various physicochemical properties of sensing structures have been used to detect the presence of a target molecule in analyte solution. Binding of a target with an immobilized probe molecule may result in changes which can be detected using electromagnetic energy across the spectrum (from low frequencies used in impedimetric sensors to very high frequencies involved in the detection of radiolabeled target molecules). As another example, changes in optical properties at the sensor surface may be used in various detection schemes (for example, a fluorescence emission or a change in optical reflectance at a sensor surface may be used to reveal the presence of a target molecule.

Other parameters, such as the acoustic waves produced by surface-acoustic wave devices or the mass of a resonant structure may be altered by probe-target binding. The same parameters may also serve to transduce a binding event into a detectable signal. This signal can then be further processed to provide a qualitative or quantitative metric of the presence of the target biomolecule.

Concerning the type of detection, transducers can be distinguished in direct or indirect: the former are based on a real-time direct detection of the biological reaction commonly using non catalytic components such as cellular receptors and antibodies, the latter mediate an indirect detection using a secondary element, usually an enzyme, characterized by catalytic activity. The first class includes detectors based on plasmon resonance, piezolelectric sensors which measure the variation in the acoustic resonance due to the analyte adhesion on the substrate, optomechanical sensors (microcantilever) which measure the deflection of the beam caused by the interaction between the analyte and the antibody immobilized on the surface of the beam.

On the other hand, electrochemical transducers (measuring the oxidation or the reduction of an element associated to the secondary element) and the potentiometric sensors (where the signal is produced by the electrochemical and physical changes induced in a conducting polymer) are considered.

The application areas of biosensors is extremely wide: from clinical chemistry, medicine, pharmaceutical industry (drugs quality) to agriculture, food industry (quality control, process monitoring), fermentation processes, environmental monitoring and control.

The great use in medicine diagnostic is mostly related to clinical biosensors based on antigen-antibody recognition or to biosensors based on the use of an enzyme as the selector [1,9].

1.4. Microarray: an example of multiple biosensor

The great success related to sensing platforms able to recognize one single molecule has encouraged the development of devices containing thousands of sensors, able to the detect at the same time the presence of several analytes. With this type of devices is possible to reduce drastically the time of the measure, the amount of the sample needed for the detection and the costs. Several companies and research laboratories have already developed prototype multichannel systems. Multisensor chips are expected to revolutionize analytical chemistry, much as integrated circuits transformed the computer industry. These devices are particularly promising for drug development and in monitoring genetic expression to determine whether a specific gene is functioning.

Microarray analysis is based on standard molecular biology, with a principal advantage being higher throughput and greater precision than traditional filter and blotting techniques [10]. Generally, microarrays use high-density microscopic array elements, planar substrates, low reaction volumes, multicolor fluorescent labelling, high binding specificity, high-speed instrumentation for manufacture and detection, and sophisticated software for data analysis and modelling.

The array elements react specifically with labelled mixtures, producing signals that reveal the identity and concentration of each labelled species in solution. These attributes provide miniature biological assays that allow the exploration of any organism on a genomic scale.

Using expression (transcript) profiling, researchers are able to generate quantitative gene expression information for many genes in many samples, using one- and two-color fluorescent schemes: in one-color analysis expression profiles for each sample are generated on a different chip using a single fluorescent label (for example, phycoerythrin) and then the different images are compared, in two-color formats two RNA samples are labeled separately with different fluorescent tags (for example, cyanine 3 and cyanine 5 (Cy3, Cy5)), hybridized to a single microarray and scanned to generate fluorescent images from the two channels

Both the two strategies allow comparisons of tissue types such as heart versus brain, normal versus diseased tissue samples, or time-course samplings of cell cultures subjected to different treatments or conditions, and both schemes yield high-quality gene expression data [11].

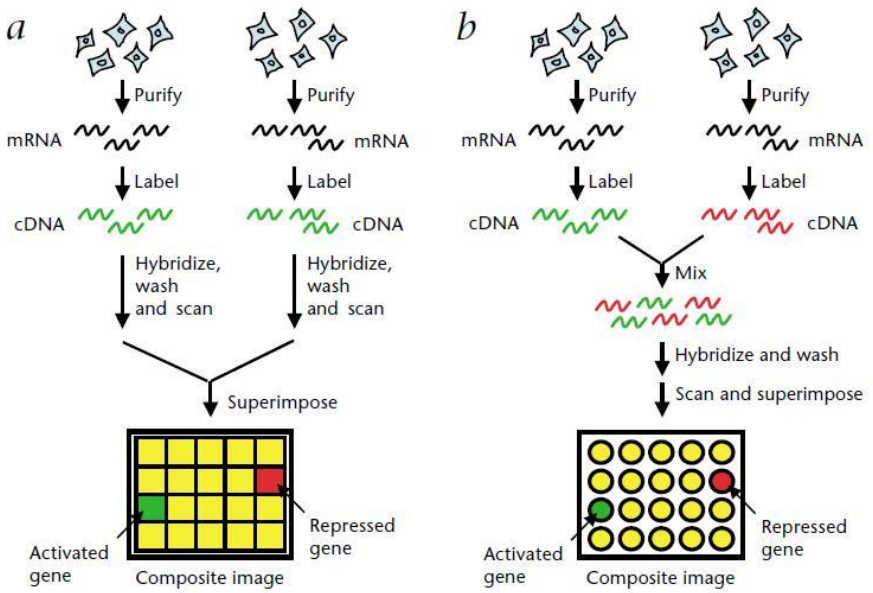

Figure 1.6 Expression analysis by microarray: one-color expression analysis (a) using a single fluorescent label (green wavi lines) and two chips and two-color expression analysis (b) using two different fluorescent label (green and red wavy lines) and a singlr chip to generate expression profiles for two different cell samples

Nucleic acid microarrays primarily use short oligonucleotides (15–25 nt), long oligonucleotides (50–120 nt) and PCR-amplified cDNAs (100–3,000 base pairs) as array elements.

Concerning the manufactory technology microarray can be divided into two main categories: synthesis and delivery [12]. In the synthesis approaches, microarrays are prepared in a stepwise fashion by the in situ synthesis of nucleic acids and other biopolymers from biochemical building blocks. With each round of synthesis, nucleotides are added to growing chains until the desired length is achieved. The delivery technologies, by contrast, use the exogenous deposition of pre-prepared biochemical substances for chip fabrication. Molecules such as cDNAs are amplified by PCR and purified, and small quantities are deposited onto known locations using a variety of delivery technologies

Fluorescent probes for expression profiling are typically prepared from total RNA or messenger RNA (mRNA) by reverse transcription, although many different labeling strategies are available. Control and experimental samples can be labeled separately with fluors that have non-overlapping emission spectra, including cyanine, Alexa, and other fluorescent

derivatives. Two samples labeled with different fluors can be hybridized to a single chip to derive absolute and comparative expression information in the two samples.

The detection, resulting in graphical images, can be accomplished using a variety of fluorescence detection technologies including instruments that contain confocal optics, photomultiplier tubes (PMTs), and charge-coupled devices (CCD).

Over the years, Microarray density, defined as the number of array elements per square centimeter of substrate, has also increased steadily permitting the manufacture of microarrays with tens of thousands of array elements and the analysis of entire genomes on single chips [13-15].

References

[1] Battisti A., Solaro R., "Biosensori, Biochip e Microarray. Principi ed applicazioni nel settore biomedico", *AIM Magazine*, **2011**, 1, p. 14-23.

[2] Ouellette J., "Biosensors: Microelectronics marries biology" *The Industrial Physicist*, **1998**, p. 11-14.

[3] Alcock J., Turner A.P.F., *In vivo chemical sensors : recent developments*, Cranfield Press: Cranfield (UK), **1993.**

[4] National Center for Biotechnology Information http://www.ncbi.nlm.nih.gov

[5] Genetic Home Reference http://ghr.nlm.nih.gov/handbook/basics/dna

[6] Sze S.M., Ng, K.K., *Physics of Semiconductor Devices*, Wiley: Hoboken, NJ, **2006.**

[7] Klemer D.P., *Microelectronic Biosensors: Materials and Devices*, University of Winconsin- Milwaukee: Milwaukee, Winconsin, **2009.**

[8] Mattox D.M., Andrew W., *Handbook of Physical Vapor Deposition (PVD) Processing, II edition*, Elsevier: London, **2010.**

[9] Serra P.A., *Biosensors - Emerging Materials and Applications*, InTech , **2011.**

[10] Grunstein M., Hogness D.S., "Colony hybridization: a method for the isolation of cloned DNAs that contain a specific gene" *Proc. Natl. Acad. Sci. USA*, **1975,** 72, p. 3961–3965.

[11] Yuen T., Wurmbach E., Pfeffer R.L., Ebersole B.J., Sealfon S.C. "Accuracy and calibration of commercial oligonucleotide and custom cDNA microarrays", *Nucleic Acids Res*., **2002**, 30, p. 48.

[12] Schena M. et al., "Microarrays: biotechnology's discovery platform for functional genomics", *Trends Biotechnol*. **1998**, 16, p. 301–306.

[13] DeRisi J.L., Iyer V.R., Brown P.O., "Exploring the metabolic and genetic control of gene expression on a genomic scale", *Science*, **1997**, 278, p. 680–686.

[14] Hughes T.R. et al., "Widespread aneuploidy revealed by DNA microarray expression profiling", *Nature Genet*. **2000**, 25, p. 333–337.

[15] Sudarsanam P., Iyer V.R., Brown P.O., Winston F., "Whole-genome expression analysis of snf/swi mutants of Saccharomyces cerevisiae", *Proc. Natl. Acad. Sci. USA*, **2000**, 97, p. 3364–3369.

Chapter II

Surface modification techniques

The huge quantity of studies concerning "surfaces" is related to the great importance they have in the material's properties because they dominate the behaviour of materials.

They are very difficult to study due to the fact that surfaces usually lack the high symmetry and purity of the bulk of a solid and are often strongly influenced by adsorbed impurities from the environment.

Phenomena experienced in everyday life such as corrosion, adhesion, adsorption, friction and lubrication all occur at surfaces. More intimately, the crucial role played by surfaces in biocompatibility gives them an importance in the design of materials used in dentistry, contact lenses and medical implants such as hip joints and knee replacements. Industrial processes that occur at surfaces have a great impact on our lives and include crystal growth, semiconductor device manufacture and heterogeneous catalysis. Surface properties will also have a dominant influence on the emerging field of nanotechnology. The control of surface properties is thus essential to the function of a wide variety of materials. Clearly, then, a primary aim of surface scientists is to get a sufficient understanding of surfaces to make it possible the control of its properties.

2.1. Crystal surfaces and real surfaces

The majority of experimental surface studies have been performed on single crystals in order to simplify the atomic and electronic structure of the surface. Crystal surfaces can be prepared in order to obtain relatively large flat terraces made up of atoms of similar atomic coordination, with relatively few atoms associated with defect sites such as steps. The majority of single crystals grow in one of the four unit cells: simple cubic (SC), face centred cubic (FCC), body centred cubic (BCC) or hexagonal close packed (HCP). When a single crystal is terminated by a surface, then, depending on the angle of the termination, different atomic arrangements are exposed. These different surfaces are described by the Miller indices [1].

Different crystal planes have different atomic densities and hence differences in free energy at the surface. The free energy of a surface is an important determinant of its behavior.

Real surfaces usually lack the high symmetry and purity of the interior of a solid and are often strongly influenced by adsorbed impurities from their environment. They dominate the behavior of the material, playing a crucial role in biocompatibility and so influencing the design of the material in the emerging field of nanotechnology. The control of surface properties is thus essential to the function of a wide variety of materials. Clearly, then, a primary aim of surface scientists is to obtain a sufficient understanding of surfaces to make it possible to control surface properties. the experimental investigation of the fundamental properties of surfaces have mostly taken place in UHV where the pressure is typically 10-10 mbar ± thirteen orders of magnitude lower than atmospheric pressure. A UHV environment is required to prepare a well-defined clean surface and maintain it for a sufficient time for experimental studies. In addition to surface preparation, a good vacuum is also a prerequisite for many of the experimental probes used to study surfaces since these probes are often based upon controlling the trajectories of electrons and ions. Vacuum technology has developed pumping systems capable of maintaining a UHV environment within stainless steel chambers for indefinite periods of time.

Experiments are not exclusively performed on clean surfaces in UHV and the recent development of experimental probes that are capable of operating in a non-UHV environment is giving rise to an increasing trend of experimental studies of surfaces in ambient and liquid environments.

2.2. What is a biomaterial surface?

In the past, biomaterial biocompatibility was considered to be passive behavior towards the biological system. This requires the biomaterial to be non-thrombogenic, non-allergenic, non-carcinogenic, and non-toxic. Williams defined biocompatibility, however, as `the ability of a material to perform with an appropriate host response in a specific application. With this term we refer the whole range of interactions that exist between a biomaterial implant and its biological surroundings, as well as the orchestrated sequence of responses the body invokes to essentially reject that implant as non-self. In the case of invasive in vivo monitoring, an electrochemical biosensor requires intimate, direct contact with the sample matrix in order to function properly, notwithstanding the intensity of the body's reactive response to its constituent materials. As a consequence, the observed performance of the biosensor is highly

vulnerable to the local accumulation of surface-active agents from the body such as cells, proteins and other less well identified constituents such as colloidal and lipid aggregates. This accumulation of biological compounds on the surface of the sensing device is known as "biofouling", and will with time alter and degrade the biosensor response and performance.

Furthermore, biosensors are not bio-inert, not only because of the active redox components they may incorporate but also because of the polymeric materials, as well as the coated or uncoated metal and carbon electrode interfaces they present towards the living tissues.

A variety of properties determine biocompatibility. Among these are the mechanical and chemical/physical properties of a material, both bulk and surface; the surface exerts the heavier influence because it is the component where the biomaterial and the biological system meet each other and interact. The properties of the surface that have utmost importance are:

- the chemical structure
  - hydrophilicity
  - presence of chemical groups that could initiate reactions in the biological system
- the morphology
  - the distribution and abundance of hydrophilic/hydrophobic and crystalline/amorphous phases
  - surface topography, i.e. surface roughness and the presence of physical structures

When the implant comes into contact with the biological system the following reactions are observed:

1. within the first few seconds molecules (especially proteins and lipids) from the surrounding body liquids and tissue are deposited. In blood the properties of this adsorbed protein layer determines hemocompatibility, while in tissues it controls further reactions of the cell system. The nature of the adsorbed proteins is dependent on the surface characteristics of the implanted material.
2. upon implantation, the tissue neighboring the implant undergoes mechanical, chemical or physical damage or a combination of these. This damage could be acute (short-term and intense) or chronic (long-term) depending on the degree of stability of the material surface. In any case a period of inflammation is observed.
3. a biocompatible implant, if inert, is surrounded by a thin layer, mainly consisting of collagen.
4. a biocompatible implant, if not stable will undergo some sort of degradation and/or erosion in the harsh biological medium. This will continue until the implant is completely removed from the medium.

5. a non biocompatible implant, if not stable and inert, will undergo degradation and erosion but its products will initiate a variety of undesirable reactions.

Since the surface is the outermost region of the implant interfacing tissue, it should fulfill the requirements of biocompatibility.

2.3. Surface modification and functionalization techniques

In general, some materials which have excellent bulk physical and chemical properties often do not possess suitable surface properties required for specific applications.

For this reason, surface-modification techniques, that can transform these materials into valuable finished products, become an important part of surface science and technology.

The techniques, developed in the last decade, are able to simply modify surface morphology of materials or give rise to nanostructured coatings aimed to simply affect the adhesion or anti-adhesion properties, mainly hydrophilicity and hydrophobicity, or to promote specific bonding with other species. These features can be a crucial advantage in several applications in the fields of protective, antiadhesion, adhesion coatings, friction and wear, composites, microelectronics and thin-film technology, molding and lithography, technical fabrics, biomaterials, sensing and in particular biosensing.

2.3.1. Surface modification depending on materials chemistry

The simplest method to attach antibodies or antigens to metallic surfaces is to exploit the natural tendency of proteins to adsorb by means of nonspecific interactions to most surfaces. This method is simple, rapid and effective but suffers from several limitations. Uncontrolled, nonspecific interactions between proteins and surfaces may lead to nonspecific protein adsorption (giving rise to false positives) and partial denaturation or loss of biological activity of the protein. The mere fact that nonspecific protein adsorption is a stochastic process will cause a fraction of the proteins to interact with the surface in an unfavorable orientation for binding to soluble analytes (e.g., when the antigen binding site in an antibody faces the surface, they will be unavailable for interaction with antigens even if the protein has not been denatured). Additionally, proteins adsorbed by means of nonspecific interactions are prone to be displaced by other proteins with larger surface affinity. The latter may result in a decreased response of the biosensor with time, increased nonspecific interactions, or both. Because of

this, it is desirable to count with facile methods of protein immobilization that minimize the aforementioned problems. An ideal method would have to allow robust immobilization of the biomolecules. Such method must minimize nonspecific adsorption of proteins, be conducive to maintaining the biological activity of the proteins, allow uniform and optimal orientation of immobilized receptors, and should provide for robust attachment of the desired biomolecules such that displacement and/or degradation does not proceed to a significant extent. These requirements point to the need for well-defined surface chemistries that can be produced in a reproducible manner.

Generally, these surface-modification methods can be divided into two classes: physical modifications and chemical modifications [2]. The key advantage of these techniques is that the surface of the materials can be modified or tailored to acquire very distinctive properties through the choice of different grafting precursors, while maintaining the substrate properties.

The crucial point is to single out the suitable molecule to be grafted according to the chemistry of the material substrate, that is, the kind of atoms/groups with which the substrate is truncated with. Before the grafting step, commonly a surface activation is needed in order to create reactive sites on the substrate surface or enhance the amount of the ones naturally already present.

Practically, one can generate reactive groups through UV, high-energy electrons, γ irradiation, plasma treatment, ozone exposure [2] and chemical reactions performed in liquid and vapor phase. The kind of activation treatment heavily depends on materials.

For sake of simplicity, the different types of derivatizing treatments and the related materials activation procedures will be considered according to substrate chemistry.

2.3.1.1. Chemical derivatization: the formation of Self-Assembled Monolayer (SAM)

Generally, among the surface-modification techniques, the formation of a Self-Assembled Monolayer (SAM) has been intensively studied. SAM is a kind of “bottom-up” technique which provides advantages regarding the surface modification. It leads to a structure which is at, or close to, thermodynamic equilibrium, and thus tends to self-healing/defect rejection and leads to a closely packed, well-ordered, and stable configuration on the surface [2]. SAMs offer unique opportunities to increase fundamental understanding of self-organization, structure-property relationships, and interfacial phenomena. The ability to tailor both head and tail groups of the constituent molecules makes SAMs excellent systems for a more fundamental understanding of phenomena affected by competing intermolecular, molecular-

substrates and molecule-solvent interactions like ordering and growth, wetting, adhesion, lubrication, and corrosion.

SAMs provide the needed design flexibility, both at the individual molecular and at the material levels, and offer a vehicle for investigation of specific interactions at interfaces and of the effect of increasing molecular complexity on the structure and stability of two-dimensional assemblies.

The key factors characterizing the SAM precursor molecules consist in the i) "head", the ii) "tail" and the iii) body chain length of the molecule (Figure 2.1).

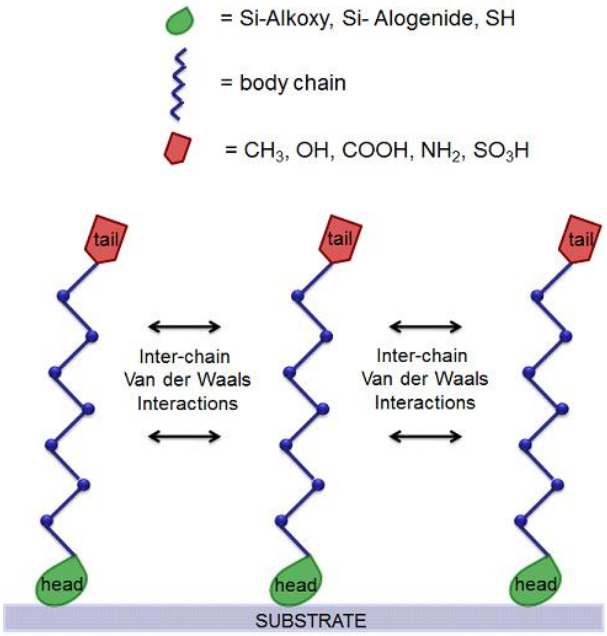

Figure 2.1 Scheme of a general SAM formed on the surface of a substrate

The "head" is one of the terminal group of these normally linear species and has the role to anchor the surface by a favored and fast reaction producing the formation of a usually stable (covalent) bond linking the surface. The choice of this termination is driven by the chemistry of the material substrate.

The "tail" of the molecule, that is the termination opposite to the "head", is deputed to perform the desired effect at the SAM surface. So as a rule of thumb, it can be a methyl termination (-CH_3), a perfluoroalkyl termination that generate at the most a hydrophobic or super-hydrophobic and repulsive behavior or a functional group such as –SH, -OH, -NH_2, -COOH able to carry out a subsequent reaction with other molecule (for example biomolecules, polymers, suitable linker molecules) or simply express hydrophilic and adhesion properties.

The molecule length (the hydrocarbons chains can range, for instance, from C_3 to C_{24}) will strongly depends on the application for which SAM structures are needed.

In particular, such monolayers have been generated mostly on metal surfaces, such as Au, Ag, and Cu, using the thiol chemistry [2]. Nuzzo and Allara, reported in 1983, [3] the procedure of bi-functional organic sulfides species self-assembly on the surface of Au (111) freshly evaporated substrates in the liquid phase by simply putting in contact the samples with a diluted (milliMolar range) solution of the reagent, for some hours. Successively many authors observed with other n-alkyl thiolates that in the first few seconds the species are able to bind the gold surface and in more than 1h, they self–assemble into a compact, well-ordered flat inter-crossed molecular monolayer. The –SH head is able to establish a strong Au-S bond and the chain-to-chain interaction performed by the adjacent grafted molecules is dominated by weak dispersion forces if non-functional interacting groups are present in the middle of the aliphatic chain. In this case, H-bond or other stronger Van der Waals forces can exerted. The inter-chain forces are able to produce, as calculated by Godin [4] an equilibrium separation between two alkyl chains of 0,44 nm. The alkanethiol SAM is formed as a densely packed structure showing $(\sqrt{3} \times \sqrt{3})R30°$ overlayer on gold surface where the molecule is tilted about 30° from the surface normal with the sulfur atom chemically bonded to gold atoms. This implies that a compressive surface-stress has to be generated during the self-assembly, and this stress will increase with increasing alkyl chain length.

Patel et al [5] studied the effect of chain length on the reactivity of SAMs towards protein immobilization generating SAMs from short- and long-chain carboxylic acid terminating alkyl thiols, 11-MercaptoUndecanoic Acid (11-MUA), 3-MercaptoPropanoic Acid (3-MPA) and from the mixture, 1:10, of the both. The accessibility of the carboxylic groups by the amino- group of a lysine termination exposed by the protein, *catalase*, to be anchored, decreases in the order Mixed > 11-MUA > 3-MPA. The experiment was performed by previously activating the carboxylic groups by a water soluble 1-ethyl-3-[3-(dimethylamino) propyl]carbodiimide hydrochloride (EDC) and N-hydroxysuccinimide (NHS). Successful formation of the NHS ester intermediate is reliant on the accessibility of the terminal carboxylate groups. It was assessed that a steric packing of these acid groups can limit the rate of intermediate formation with full conversion of accessible acid groups only occurring after several repeated reaction cycles. The co-adsorption of different alkyl-thiols provides the system a degree of disorder which is strategic for an efficient protein immobilization.

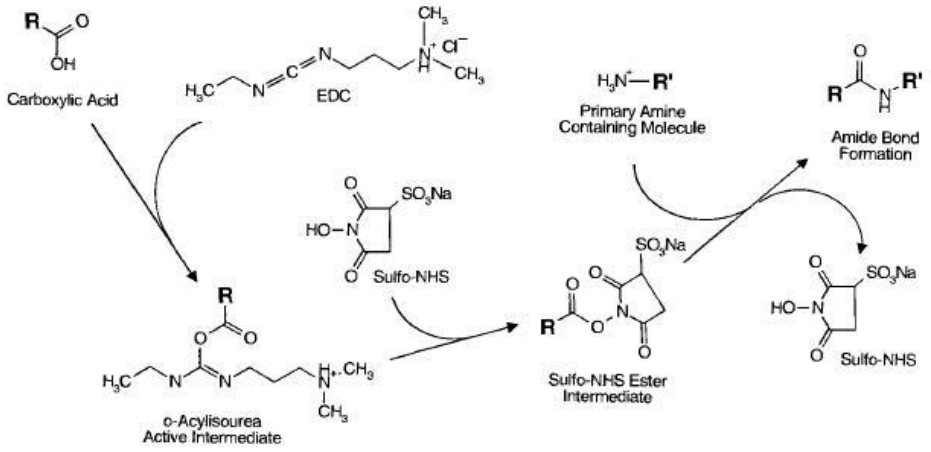

Figure 2.2 The efficiency of an EDC-mediated reaction may be increased through the formation of a sulfo-NHS ester intermediate. The sulfo-NHS ester survives in aqueous solution longer than the active ester formed from the reaction of EDC alone with a carboxylate. Thus, higher yields of amide bond formation may be realized using this two-stage process

For inorganic oxides, the typical molecules used to form SAMs monolayers are organosilanes. They are characterized by a variability of possible structures and by the easiness of reaction performed both in the liquid and in the vapor phase.

In particular, Silicon/Silica (Si/SiO_2), glass and quartz surfaces, Aluminum/Alumina (Al/Al_2O_3), fillosilicates such as mica, magnetic materials such as maghemite (γ-Fe_2O_3) nanoparticles, germanium oxide [2] and Zinc oxide (ZnO) [6] exposing naturally hydroxyl-terminated (-OH) surfaces or zinc selenide [2] and Gallium Nitride (GaN) Alluminum Nitride (AlN) and Silicon Nitride (SiN) [7-9], where the –OH species can be easily created by a pretreatment, react with alkylchlorosilanes and alkylalkoxysilanes. Stable siloxy linkages [10, 11] are formed between hydroxylated Silica and 3-aminopropyltriethoxysilane (3-APTES). The reaction proceeds through the hydrolysis of silane alkoxy-terminations and the condensation with surface hydroxyls and elimination of an alcohol molecule. Further condensation between adjacent molecules already grafted to the surfaces take part stabilizing the SAM through the formation of siloxane bridges (Si-O-Si).

Glass and Si/SiO_2 are the most common inorganic materials used in many technological applications as optical and electrical materials and as MEMS (MicroElectroMechanical Systems). One major factor that limits the widespread use and reliability of MEMS is adhesion. Adhesion is a result of the dominance of surface forces, such as capillary, hydrogen bonding, electrostatic, and Van der Waals forces, over body forces at the micro-scale. When internal restoring forces of microstructures cannot overcome surface adhesive forces, the devices are said to suffer from stiction. Many procedures based on organosilanes SAMs formation are reported to impart to MEMS antistiction properties. Comparing the SAM

formation from dimethyldichlorosilane ($(CH_3)_2SiCl_2$, DDMS) and tridecafluoro-1,1,2,2-tetra-hydrooctyltrichlorosilane ($CF_3(CF_2)_5(CH_2)_2SiCl_3$ - FOTS) [11], by a liquid (thermal annealing about 65°C in anhydrous toluene solution) and a vapor procedure (dosage of organosilane vapor pressure on an Oxygen plasma pre-activated surface in a low pressure CVD style reactor), it results that the vapor phase method avoids vertical polymerization of precursor molecule producing a flatter SAM with the same efficiency in antistiction properties. 3-APTES has been shown to be an efficient SAM precursor [10, 12] for biosensing of protein tumoral markers based on micro-cantilever devices.

Both the functionalization routes described above are efficient in reducing the mass effect of the functional coating which is detrimental for the device sensitivity and in providing a maximum coverage in the order of 10^{14} -NH_2 groups/cm^2 [10].

The no-oxides surfaces, such as nitrides, can be easily hydroxilated in order to exploit organosilanes chemistry in order to achieve surface functionalization. The well assessed procedure consist in the substrate immersion in H_2SO_4:H_2O_2 (3:1) solution, also called Piranha solution, for 20 min, rinsed with deionized water and dried under Nitrogen flux prior to silanization. The highly oxidizing reagents produce, for GaN (deposited by MetalOrganic Chemical Vapor Deposition - MOCVD), an oxide layer exposing hydroxyl species. For AlN (also obtained by MOCVD) which is already covered by a native oxide layer, the only effect is surface hydroxyliation [7].

The Piranha solution is used also on crystalline Silicon and on SiO_2 thermally grown from crystalline Silicon. On SiN (deposited by Plasma Enhanced Chemical Vapour Deposition, PECVD), a solution with 10% nitric acid (HNO_3) at 80 °C for 20 min [8] or a mixture of CH_3COOH and H_2O_2 for 3 h [9] is used to activate the silanols (Si-OH); for the both water is used for rinsing and N_2 for drying.

Also polymers can be activated in order to react with organosilane “head” (trialkoxy- or trichloro- terminations) as suggested by Kühn et al. in [13]. The double procedure consists in an Oxygen plasma step in order to produce mixed oxygen containing species OH, C=O, C-O-C, CHO, COOH, C-O-OH, CO_3, C=C, etc. on a polyolefinic polymer such as PolyEthylene (PE) or PolyPropylene (PP) and then a reduction step in diborane (gaseous procedure) or $LiAlH_4$ solution in order to obtain a monotype homofunctional surface exposing hydroxyls.

2.3.1.2. Chemical derivatization: graft polymerization

Silicon/Silica and Diamond surface can be also directly derivatized through polymers grafting. On their own, polymers expose functionalities which are able to give further reactions.

Surface graft polymerization is a chemical modification method. In surface graft polymerization, the modification is achieved by grafting suitable macromolecular chains on the surface of materials through covalent bonding. The key advantage of these techniques is that the surface of the materials can be modified or tailored to acquire very distinctive properties through the choice of different grafting monomers, while maintaining the substrate properties. It also ensures an easy and controllable introduction of graft chains with a high density and exact localization onto the surface. Compared with the physically coated polymer chains, the covalent attachment of the grafted chains onto a material surface avoids their desorption and maintains a long-term chemical stability of the introduced chains.

Chiari et al used a *ter*-polymer of N,N-dimethylacrylamide, N-acryloyloxysuccinimide and 3-(trimethoxysilyl)propyl methacrylate [14]. The co-polymer (DMA-NAS-MAPS) graft the SiO_2 surface of oxidized silicon or glass by a simple and robust procedure consisting in the dip coating in an aqueous solution, of substrates of different shapes in a short time span (less than 1 h) and in mild conditions without harmful treatments with harsh washing solutions. The film formed on the surface is thin, on the order of a few nanometers. For fluorescent microarray chips, this is a suitable coating as it does not affect the fluorescence intensification provided by the silicon/silicon oxide substrate. The trimethoxysilyl terminations react with surface silanols, as well as an organosilane, the acryloyloxysuccinimidyl ends give rise to covalent bonds with amino-groups of biomolecules and the DMA units form the structural backbone of the polymer.

Recently, Oxidized Ultranocrystalline diamond (UNCD) has been successfully coated with poly(styrene) (PS) using the self-initiated photografting and photopolymerization (SIPGP) approach with styrene as the monomer, within 16 h, under constant irradiation with UV light (λ_{max}=350 nm) [15]. The obtained coating stable grafted to surface is then easily derivatized by sulphonation, nitration and amido-alkylation carried out according to well-known liquid chemistry routes and so allowing the incorporation of additional functional molecules, such as fluorescent labels. This will open the way for designing more advanced biosensing schemes, incorporating multifunctional elements and with a higher loading capacity for biomolecules.

Ruckenstein et al reported the graft polymerization reaction on already SAMs coated surfaces of glass and silicon wafers in order to introduce additional reactive sites. The method

involves the aniline substitution at Br-terminated SAM, through the aniline amino termination and further the surface oxidative graft polymerization of aniline on the modified glass surface via the covalently immobilized aniline sites. A PolyAnyline (PANI) coating is so obtained by performing the reaction in the polymerization solution containing aniline, and due to its well-known conductivity (conductive polymer) this can be a suitable substrate to be used as biosensor and biomaterial.

Another route to further derivatize an organosilane surface for biosensing purposes consists in the grafting, from a 8.5 pH solution, of homofunctional linkers such as Glutaraldehyde (OHC-CH_2-CH_2-CH_2-CHO) which is able through an aldehyde end to react with NH_2 exposed at amino-SAM modified surface and, then, through the second aldehyde termination to immobilize biomolecules exposing amino-terminations.

This method has been successfully applied by Ricciardi et al. [12] for functionalization of cantilever based biosensors aimed to the detection of tumoral markers (Angiopoietin).

2.3.2. Surface modification no-depending on materials chemistry

Among the surface modification techniques, deposition of coating obtained by plasma polymerization presents, respect to surface derivatization discussed in the previous paragraph, the advantage to allow the tailoring of properties of any kind of surface without involving the substrate surface chemistry in the functionalization mechanism.

Macromolecular plasma chemistry [16] has developed in the last two decades in the following directions: plasma-enhanced synthesis (deposition and/or grafting) of thin layer macromolecular structures; surface functionalization of polymeric materials; and etching of inorganic or polymeric substrate surfaces. Plasma enhanced synthesis involves the dissociation of starting materials and reorganization of the resulting neutral and charged molecular fragments into macromolecular structures on the surfaces located inside or outside of the plasma zone. When the starting materials are common monomers the recombination processes are more complex due to the development of simultaneous conventional polymerization reactions along with the fragment-recombination mechanisms initiated by the plasma-created and surface-attached active species (e.g. ions, free radicals). In these cases, complex structures result and structural identification is difficult. However, an advantage of conventional monomer- based processes are that specific functionalities can be retained in the polymer structures and consequently some characteristics can be more easily predicted and designed into the final product.

Macromolecular thin layers can also be synthesized by the plasma-generation of active sites (e.g. ions, free radicals) or reactive functionalities (primary amine groups, etc.) on substrate surfaces, followed by the development of graft-polymerization reactions in the absence of the plasma in the presence of 'true monomers'.

As a result, molecular precursors can be physically or through covalent bonding incorporated through surface-located charged and neutral (e.g. free radicals) active species, into the nascent macromolecular layers. Plasma-assisted functionalization processes will be discussed in details in the following chapters.

References

General Book:

Vadgama P., *Surfaces and Interfaces for Biomaterials*, Woodhead Publishing Ltd, **2005.**

Rivolo P., *Encyclopedia of Nanotechnology* "Nanostructures for surface functionalization and surface properties" Springer Science+Business Media B.V., DOI 10.1007/978-90-481-9751-4, B. Bhushan (ed.), **2012**.

[1] Attard G., Barnes C., *in Surfaces*, Oxford University Press, **1998.**

[2] Ruckenstein E., Li Z.F., "Surface modification and functionalization through the self-assembled monolayer and graft polymerization", *Adv. Colloid Interface Sci.,* **2005,** 113, p. 43-63.

[3] Nuzzo R.G., Allara D.L., "Adsorption of bifunctional organic disulfides on gold surfaces", *J. Am. Chem. Soc*., **1983**, 105, p. 4481-4483.

[4] Godin M., "Surface stress, kinetics and structure of alkanethiol self-assembled monolayers", PhD Thesis, McGill University, Canada, **2004.**

[5] Patel N., Davies M.C., Heaton R.J., Roberts C.J., Tendler S.J.B., Williams P.M., "A scanning probemicroscopy study of the physisorption and chemisorption of protein molecules onto carboxylate terminated self-assembledmonolayers", *Appl. Phys. A,* **1998,** 66, p. S569–S574.

[6] SelegÅrd L., Khranovskyy V., Söderlind F., Vahlberg C., Ahrén M., Käll P.-O., Yakimova R., Uvdal K., "Biotinylation of ZnO Nanoparticles and Thin Films: A Two-Step Surface Functionalization Study", *ACS Appl. Mater. Interfaces,* **2010,** 2, p. 2128–2135.

[7] Baur B., Steinhoff G., Hernando J., Purrucker O., Tanaka M., Nickel B., Stutzmann M., Eickhoff M., "Chemical functionalization of GaN and AlN surfaces", *Appl. Phys. Lett.,* **2005**, 87, p. 263901.

[8] Tlili A., Jarboui M.A., Abdelghani A., Fathallah D.M., Maaref M.A., "A novel silicon nitride biosensor for specific antibody–antigen interaction", *Mater. Sci. Eng. C-Biomimetic Supramol. Syst.*, **2005,** 25, p. 490–495.

[9] Lee S.-H., Lee C.-S., Shin D.-S., Kim B.-G., Lee Y.-S., Kim Y.-K., "Micro protein patterning using a lift-off process with fluorocarbon thin film", *Sens. Actuator B-Chem.*, **2004**, 99, p. 623–632.

[10] Fiorilli S., Rivolo P., Descrovi E., Ricciardi C., Pasquardini L., Lunelli L., Vanzetti L., Pederzolli C., Onida B., Garrone E., "Vapor-phase self-assembled monolayers of aminosilane on plasma-activated silicon substrates", *J. Colloid Interface Sci.*, **2008**, 321, p. 235–241.

[11] Ashurst W.A., Carraro C., Maboudian R., Frey W., "Wafer level anti-stiction coatings for MEMS", Sens. Actuator A-Phys., **2003**, 104, p. 213–221.

[12] Ricciardi C., Fiorilli S., Bianco S., Canavese G., Castagna R., Ferrante I., Digregorio G., Marasso S.L., Napione L., Bussolino F., "Development of microcantilever-based biosensor array to detect Angiopoietin-1, a marker of tumor angiogenesis", *Biosens. Bioelectron,* **2010**, 25, p. 1193–1198.

[13] Kühn G., Weidner S., Decker R., Ghode A., Friedrich J., "Selective surface functionalization of polyolefins by plasma treatment followed by chemical reduction", *Surf. Coat. Technol.*, **1999**, 116–119, p. 796–801.

[14] Cretich M., Di Carlo G., Longhi R., Gotti C., Spinella N., Coffa S., Galati C., Renna L., Chiari M., "High Sensitivity Protein Assays on Microarray Silicon Slides", *Anal. Chem.*, **2009**, 81, p. 5197–5203.

[15] Steenackers M., Lud S.Q., Niedermeier M., Bruno P., Gruen D.M., Feulner P., Stutzmann M., Garrido J.A., Jordan R., "Structured Polymer Grafts on Diamond", *J. Am. Chem. Soc.*, **2007**, 129, p. 15655-15661.

[16] Denes F.S., Manolache S., "Macromolecular plasma-chemistry: an emerging field of polymer science", *Prog. Polym. Sci.,* **2004**, 29, p. 815–885.

Chapter III

Techniques for Under Vacuum Deposition

Processes for the so called “under vacuum” coatings are performed in al low pressure (sub-atmospheric) environment and in presence of an atomic or molecular condensable gas/vapor source. The low pressure conditions are used not only to reduce gas particle density but also to limit gaseous contamination, establish partial pressures of inert and reactive gases and control gas flow.

The vapor source may be from a solid or liquid surface (Physical vapor deposition –PVD), or from a chemical vapor precursors (chemical vapor deposition –CVD). The terms “physical vapor deposition” and “chemical vapor deposition” seem to have originated with C.F. Powell, J.H. Oxley, and J.M. Blocher, Jr., in their 1966 book *Vapor Deposition* to differentiate between the types of vapor sources [1].

In older literature this term is often used instead of PVD; in PVD processing the vaporization may be generated by thermal heating of a solid (sublimate) or liquid (evaporate) surface or by the non-thermal process of sputtering (physical sputtering). When different species in the gaseous phase react together in order to form a deposited compound on a substrate it is called reactive deposition. If the vapor source is from a solid molecular species (such as silicon oxide), some of the more volatile constituents may be lost upon vaporization. If these lost species are replaced by a reactive species from the deposition environment, the process may be called quasi-reactive deposition. The particle density in the vacuum may be such as to sustain a plasma discharge that provides ions and electrons. This plasma “activates” reactive gases for reactive deposition processes and aids in the decomposition of chemical vapor precursors (“plasma deposition” or plasma-enhanced chemical vapor deposition –PECVD).

In some cases PVD and CVD processes are combined in the same chamber at the same time to deposit the material in a “hybrid process”. For example, the deposition of titanium carbonitride (TiCxNy or Ti(CN)) may be performed using a hybrid process where the titanium may come from sputtering titanium; the nitrogen is from a gas and the carbon is from acetylene vapor. Alloys, mixtures, compounds and composite materials can be deposited using a single source of the desired material or multiple sources of the constituents.

In many instances the term “thin film” is used when discussing PVD vacuum deposits. This is because most early applications did not rely on the mechanical properties of the deposited material; they relied on the optical and electrical properties of thin deposits. In many recent applications the vacuum deposited materials have been used for mechanical, electrical and tribological applications, and the deposit thickness has become greater.

The term “thin film” is generally used for deposits less than about 0,5 microns (5000 Ångstroms or 500 nanometers) in thickness.

The history of vacuum coating processes is closely associated with the history and the development of vacuum technology, electricity, magnetism, gaseous chemistry, plasma technology, thermal evaporation, arcing and sputtering [3].

The first piston-type vacuum pump appeared in about 1640; Otto von Guericke fabricated this “air pump”, as he called it, patterned after the water pumps that had been used for many years to remove water from mines. Piston-type vacuum pumps came into widespread use, but vacuum experiments had to be continually pumped because of the poor vacuum seals available at that time.

In 19th century materials obtained from the sap of trees have been used for this type of machines; it was only in 1857 that H. Geisser invented the platinum-to-glass seal that allowed “sealed-off” vacuum tubes to be produced. This was a major advance in vacuum technology. Neoprene (“artificial”) rubber was invented by DuPont in 1933 and molded seals of this material began to be used by the vacuum community in the late 1930s and replaced wax sealing. As late as the 1960s, findings and fixing vacuum leaks was a major part of vacuum facility, many of the early experiments used hydrogen flushing to augment vacuum pumping to reduce oxygen in the chamber. During WWII, the Germans used phosphorus pentoxide, a dessicant, in the vacuum chamber to remove water vapor when depositing optical coatings [3].

In the following years, with the advent of reactive deposition and hybrid processing, the control of gas composition and mass flow has become an important aspect of vacuum engineering and technology. This includes partial pressure control and gas manifolding in processing chamber. Many vacuum measurement instruments cannot be used for measurement of total gas pressure in the presence of a plasma in the range of interest for several PVD processes (0,5 to 20 mTorr).

Differential pumped mass spectrometers can be used to monitor and control partial pressures of gases. In 1984 a mass spectrometric feedback method of controlling the partial pressure of reactive gases in reactive sputter deposition was patented. Optical emission

spectroscopy is also used to control the partial pressures of reactive gases in reactive sputter deposition. Optical emission has been used for many years to detect the “end-point” in plasma etching for semiconductor processing.

The use of vacuum equipment for deposition (and etching) processes also introduces problems associated with pumping and disposing of possibly toxic, flammable, and corrosive process gases, as well as reactive gases used for *in situ* cleaning of the vacuum systems. Specialized vacuum equipment and *in situ* chamber plasma-etch-cleaning techniques have been developed to address these concerns [3].

An important aspect of under vacuum coating processing often deals with the rapid creation of vacuum and the quick decrease of water vapor contamination. The problem of water vapor displacement from its point of origin towards the vacuum pump, particularly slow due to “adsorption-desorption” events on surfaces represents often the predominant factor in the removing water vapor from the chamber [2].

Deposition technology has a key role for the creation of devices such as computers, since microelectronic solid-state devices are all based on material structures created by thin-film deposition.

Electronic engineers have continuously demanded films of improved quality and complexity for solid-state devices, requiring a rapid evolution of deposition technology. Equipment manufacturers have made successful efforts to meet the requirements for improved and more economical deposition systems and for in situ process monitors and controls for measuring film parameters. Another important reason for the rapid growth of deposition technology is the improved understanding of the physics and chemistry of films, surfaces, interfaces, and microstructures. This was thanks to the remarkable advances in analytical instrumentation during the past twenty years. A better fundamental understanding of materials leads to extended applications and new designs of devices that incorporate these materials.

A good example of the crucial importance of deposition technology is the fabrication of semiconductor devices, an industry that is totally dependent on the formation of thin solid films of a variety of materials by deposition from the gas/vapor, liquid, or solid phase. The starting materials, epitaxial films of semiconductors, are usually grown from the gas phase.

Chemical vapor deposition of a single-crystal silicon film on a single-crystal silicon substrate of the same crystallographic orientation, a process known as homoepitaxy, is accomplished by hydrogen reduction of dichlorosilane vapors. If a single-crystal film of silicon is deposited on a non-silicon crystal substrate, the process is termed heteroepitaxy.

Layers of single-crystal compound semiconductors are produced with a thickness of a few atom layers by molecular beam epitaxy.

Subsequent steps in the fabrication process create electrical circuit that require the deposition of an insulating or dielectric layer, such as an oxide, glass, or nitride, by one of several types of chemical vapor deposition (CVD) processes, by plasma-enhanced chemical vapor deposition (PECVD), or by any one of the sputtering deposition methods. The deposition of conductor films for contact formation and interconnections can be accomplished by vacuum evaporation or sputtering.

CVD processes are especially suitable if polysilicon, polycides, or refractory metals are to be deposited.

3.1. The Good Vacuum (Low Pressure) Environment

The "good" vacuum environment provides a long mean free path for collision between the vaporization source and the substrate. It also allows control of the amount of gaseous and vapor contamination during processing. The "good" vacuum environment is generated by a vacuum equipment that includes the deposition chamber, load-lock chambers, if used, vacuum pumping system ("pumping stack"), exhaust system, gas inlet system, and associated plumbing.

In addition, the fixturing and tooling used to hold, position, and move the substrates (manipulator) are important to the system design. Substrate materials cleaned outside the deposition system may be recontaminated in the system during evacuation ("pumpdown") by "system-related contamination." During deposition, the film can be contaminated by system-related contamination and by "process-related contamination." The goal of good vacuum system design, construction, operation, and maintenance is to control these sources of contamination.

A "vacuum" is a condition where the gas pressure in a container is less than that of the ambient pressure. The pressure difference can be small, such as that used to control gas flow in a system, or large, such as that used in vacuum-based PVD systems to give a long mean free path for vaporized particles and to allow the control of gaseous and vapor contamination to any desired level. A "rough" vacuum ($>10^{-3}$ Torr) corresponds to a pressure of about 10^{-6} of that of the atmosphere or about 1013 molecules/cm^3. A "good" vacuum ($\approx 10^{-6}$ Torr) implies a pressure of about 10^{-9} that of the atmosphere or 1010 molecules/cm^3. In a very ultrahigh vacuum (VUHV) (10^{-12} Torr) there are about 10^4 molecules per cubic centimeter.

The advantages of performing a vacuum deposition process are different:

1. The vacuum is a clean and reproducible environment, coatings realized under these conditions will be with the desired properties and without any contaminations
2. These deposition processes are environment-friendly compared to the other deposition techniques
3. During the deposition of the coating, the majority of materials, in atmospheric conditions will get oxidized or contaminated
4. The major part of devices used for thin film deposition are able to work only in vacuum conditions
5. In atmospheric condition the mean free path of gaseous species is very short (< 1 mm) so they could be not able to reach the substrate for deposition

Under Vacuum Deposition techniques can be divided into two major categories: **Physical Vapor Deposition** (**PVD**) and **Chemical Vapor Deposition** (**CVD**).

3.2. Physical vapor deposition

Physical vapor deposition processes (often just called thin film processes) are atomistic deposition processes in which the material is vaporized from a solid or liquid source in the form of atoms or molecules and transported in the form of a vapor through a vacuum or low pressure gaseous (or plasma) environment to the substrate, where it condenses. Typically, PVD processes are used to deposit films with thicknesses in the range of a few nanometers to thousands of nanometers; however, they can also be used to form multilayer coatings, graded composition deposits, very thick deposits, and free-standing structures. The substrates can range in size from very small to very large, for example the 10’·12’ glass panels used for architectural glass [4].

The substrates can range in shape from flat to complex geometries such as watchbands and tool bits. Typical PVD deposition rates are 10–100Å (1–10 nanometers) per second.

Physical vapor deposition processes can be used to deposit films of elements and alloys as well as compounds using reactive deposition processes. In reactive deposition processes, compounds are formed by the reaction of the depositing material with the ambient gas environment such as nitrogen (e.g. titanium nitride, TiN) or with a co-depositing material (e.g. titanium carbide, TiC). Quasi-reactive deposition is the deposition of films of a compound

material from a compound source where loss of the more volatile species or less reactive species during the transport and condensation process is balanced by the partial pressure of reactive gas in the deposition environment: for example, the quasi-reactive sputter deposition of ITO (indium–tin oxide) from an ITO sputtering target using a partial pressure of oxygen in the plasma.

The main categories of PVD processing are vacuum deposition (evaporation), sputter deposition, arc vapor deposition and ion plating,

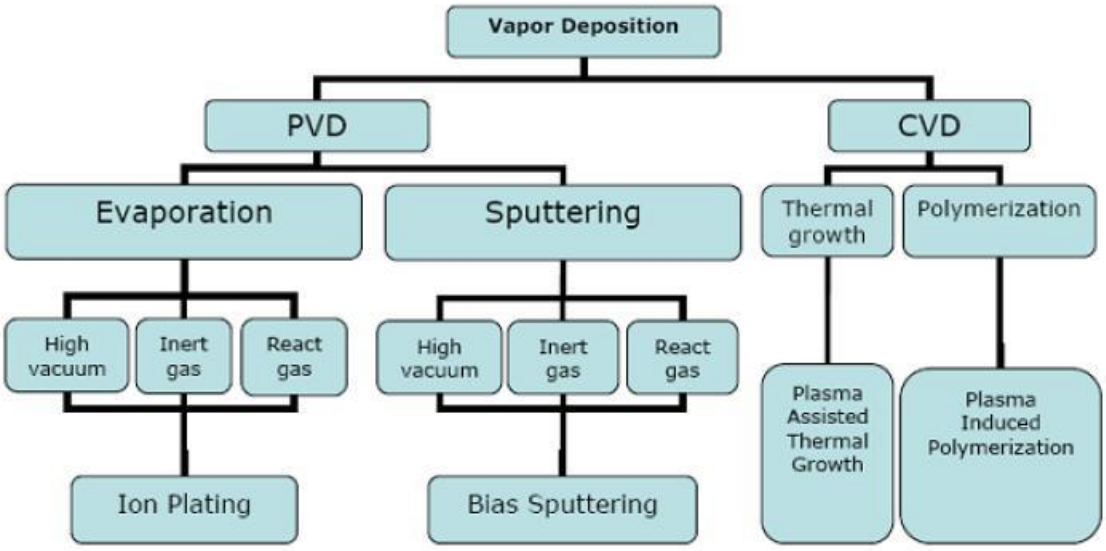

Figure 3.1 Scheme: Vapor Deposition Techniques

3.2.1. Vacuum Deposition

Vacuum deposition, which is sometimes called vacuum evaporation, is a PVD process in which material from a thermal vaporization source reaches the substrate with a few or without collision with gas molecules in the space between the source and substrate. The trajectory of the vaporized material is "line of sight." The vacuum environment also promotes the reduction of gaseous contamination in the deposition system. Typically, vacuum deposition takes place in the gas pressure range of 10^{-5} Torr to 10^{-9} Torr, depending on the level of gaseous contamination that can be tolerated in the deposition system [4]. The thermal vaporization rate can be very high if compared to other vaporization methods. The material vaporized from the source has a composition which is proportional to the relative vapor pressures of the material in the molten source material. Thermal evaporation is generally done using thermally heated sources such as tungsten wire coils or by high energy electron beam

(e-beam) heating of the source material itself. Generally, the substrates are mounted at an appreciable distance away from the evaporation source to reduce radiant heating of the vapor source on the substrate.

Vacuum deposition is used to form optical interference coatings, mirror coatings, decorative coatings, permeation barrier films on flexible packaging materials, electrically conducting films, wear resistant coatings, and corrosion protective coatings.

3.2.2. Sputter Deposition

Sputter deposition is defined as the deposition of particles vaporized from a surface ("target") by the physical sputtering process. Physical sputtering is a non-thermal vaporization process where surface atoms are physically ejected from a solid surface by momentum transfer from an atomic-sized energetic bombarding particle, which is usually a gaseous ion, accelerated from a plasma. This PVD process is sometimes just called sputtering, i.e. "sputtered films of -," which is an improper term given that the film is not being sputtered. Generally the source-to-substrate distance is short compared to vacuum deposition. Sputter deposition can be performed by energetic ion bombardment of a solid surface (sputtering target) in vacuum by using an ion gun or low pressure plasma (<5 mTorr) where the sputtered particles suffer (few or no one) gas phase collisions in the space between the target and the substrate.

Sputtering can also be done in a higher plasma pressure (5–30 mTorr) where energetic particles sputtered or reflected from the sputtering target are "thermalized" by gas phase collisions before they reach the substrate surface. The plasma used in sputtering can be confined near the sputtering surface or may fill the region between the source and the substrate. The sputtering source can be an element, alloy, mixture, or a compound and the material is vaporized retaining the composition of the bulky target. The sputtering target provides a long-lived vaporization source that can be mounted so that vapours can run in any direction.

Compound materials such as TiN and zirconium nitride (ZrN) are commonly "reactively sputter deposited" by using a reactive gas in the plasma. The presence of the plasma "activates" the reactive gas ("plasma activation"), making it more chemically reactive.

Sputter deposition is widely used to deposit thin film metallization on semiconductor material, coatings on architectural glass, and reflective coatings on compact discs (CDs), and

for magnetic films, dry film lubricants, hard coatings (tools, engine parts) and decorative coatings [4].

3.2.3. Arc Vapor Deposition

Arc vapor deposition uses a high current, low voltage arc to vaporize the material of a cathodic electrode (cathodic arc) or anodic electrode (anodic arc) and deposit the vaporized species on a substrate. The vaporized material is highly ionized and usually the substrate is biased in order to accelerate the ions ("film ions") to the substrate surface.

Arc vapor deposition is used to deposit hard and decorative coatings. The ions ("film ions") that are formed in arc vaporization are useful in the ion plating process [4].

3.2.4. Ion Plating

Ion plating, which is sometimes called ion-assisted deposition (IAD) or ion vapor deposition (IVD), utilizes concurrent or periodic bombardment of the depositing film by atomic-sized energetic particles to modify and control the properties of the depositing film.

In ion plating the energy, flux, and mass of the bombarding species along with the ratio of bombarding particles to depositing particles are important processing variables. The depositing material may be vaporized either by evaporation, sputtering, arc erosion, or by decomposition of a chemical vapor precursors.

The energetic particles used for bombardment are usually ions of an inert or reactive gas, or, in some cases, ions of the condensing film material ("film ions"). Ion plating may be done in a plasma environment where ions for bombardment are extracted from the plasma or it may be done in a vacuum environment where ions for bombardment are formed in a separate "ion gun." The latter ion plating configuration is often called ion beam-assisted deposition (IBAD).

By using a reactive gas in the plasma, films of composite materials can be deposited. Ion plating can provide dense coatings at relatively high gas pressures where gas scattering can enhance surface coverage [4].

3.3. Non PVD Thin Film Atomistic Deposition Processes

3.3.1. Chemical Vapor Deposition

Thermal CVD (or vapor plating) is the deposition of atoms or molecules by the high temperature reduction or decomposition of a chemical vapor precursor species, which contains the material to be deposited. Reduction is normally accomplished by hydrogen, at elevated temperature.

Decomposition is accomplished by thermal activation. The deposited material may react with other gaseous species in the system to give compounds (e.g. oxides, nitrides). Chemical vapor deposition processing is generally accompanied by volatile reaction byproducts and unused precursor species. Chemical vapor deposition has numerous other names and adjectives associated with it such as vapor phase epitaxy (VPE) when CVD is used to deposit single crystal films, metal-organic CVD (MOCVD) when the precursor gas is a metal-organic species, plasma-enhanced CVD (PECVD) when a plasma is used to induce or enhance decomposition and reaction.

Plasmas may be used in CVD reactors to “activate” and partially decompose the precursor species. This allows deposition at a temperature lower than thermal CVD and the process is called plasma-enhanced CVD (PECVD) or plasma-assisted CVD (PACVD). The plasmas are typically generated by radio frequency (rf) techniques. Figure 2 shows a parallel plate CVD reactor that uses rf power to generate the plasma. This type of PECVD reactor is commonly used in the semiconductor industry to deposit silicon nitride (Si_3N_4) and phosphosilicate glass (PSG), encapsulating layers a few microns thick with deposition rates of 5–100 nm/min. At low pressures, concurrent energetic particle bombardment during deposition can affect the properties of films deposited by PECVD.

Plasma-based CVD may also be used to deposit polymer films (plasma polymerization). In this case the precursor vapor is a monomer that plasma decomposes and recombines by cross-linking on the surface to form an organic or inorganic polymer film. These films have very low porosity and give excellent surface coverage [4].

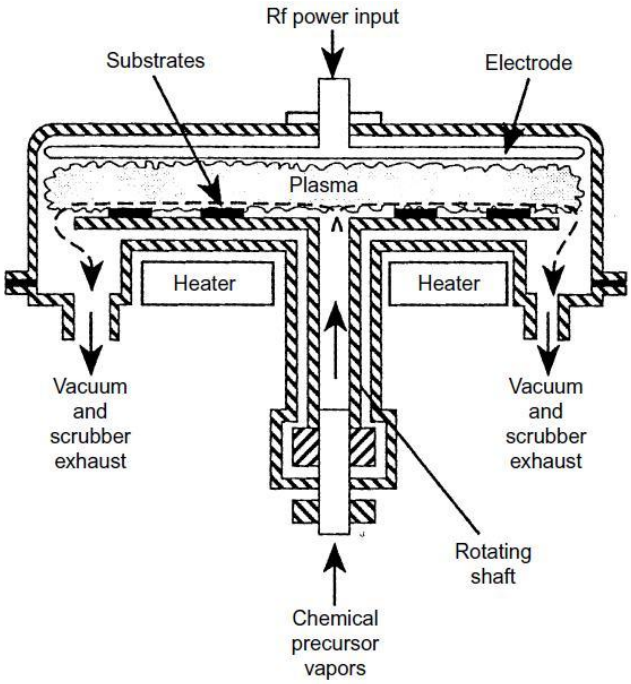

Figure 3.2 Parallel Plate Plasma-enhanced Chemical Vapor Deposition (PECVD) Reactor. Typical Parameters are: Radio Frequency (rf) – 50 kHz to 13.56 MHz; Temperature – 25 to 700°C; Pressure – 100 mTorr to 2 T orr; Gas Flowrate – 200 sccm

3.3.2. Electroplating, Electroless Plating and Displacement Plating

Electroplating is the deposition on a cathode (normally the substrate) of metals ions from the electrolyte ionic species in an electrolitc cell. Only about 10 elements (Cr, Ni, Zn, Sn, In, Ag, Cd, Au, Pb, and Rh) are commercially deposited from aqueous solutions. Some alloy compositions such as Cu–Zn, Cu–Sn, Pb–Sn, Au–Co, Sn–Ni, Ni–Fe, Ni–P and Co–P are commercially deposited.

Conductive oxides such as PbO_2 and Cr_2O_3 can also be deposited by electroplating. A thin film of material deposited by electroplating is often called a "flash" and is in the order of 40 millionths of an inch thick. Typically, the anode of the electrolytic cell is made of the material to be deposited and is consumed during the deposition process. In some cases, the anode material is not consumed and the material to be deposited comes only from the solution, which must be continually replenished. For example, lead oxide, PbO_2, can be electrodeposited from a lead nitrate plating bath using carbon anodes. Stainless steel and platinum are also often used as non-consumable anode materials.

In electroless or autocatalytic plating, no external voltage/current source is required. The voltage/current is supplied by the chemical reduction of an agent at the deposit surface. The

reduction reaction is catalyzed by a material, which is often boron or phosphorous. Materials that are commonly deposited by electroless deposition are: Ni, Cu, Au, Pd, Pt, Ag, Co, and Ni–Fe alloys. Displacement plating consists in the deposition of ions in solution on a surface and results from the difference in electronegativity between the surface element and the ionic species [4].

3.3.3. Chemical Reduction

Some thin films can be deposited from chemical solutions at low temperatures by immersion

in a two-part solution that gives a reduction reaction. “Chemical silvering” of mirrors and vacuum flasks are some common examples [5].

The glass surface to be silvered is cleaned very thoroughly then nucleated using a hot acidic stannous chloride solution or by vigorous swabbing by a saturated solution of $SnCl_2$. The surface is then immediately immersed in the silvering solution where a catalyzed chemical reduction causes silver to be deposited on the glass surface. Copper oxide (Cu_2O) films can be deposited from mixing solutions of $CuSO_4$ + $Na_2S_2O_3$ (sodium thiosulfate) and NaOH. Elemental materials such as platinum, gold, tin, and indium can be deposited by the thermal decomposition of a chemical solution. For example, platinum can be deposited by the thermal decomposition of platinum chloride solution on the surface.

References

[1] Powell C.F, Oxley J.H., Blocher J.M., *Vapor Deposition*, John Wiley, NY , **1996.**

[2] Mattox D.M., “Steady State and ‘Transit’ Conduction”, *Vac. Technol. Coat.*, **2001**, 2 (6),

[3] Mattox D.M., *The Foundations of Vacuum Coating Technology*, Noyes Publication, New York, **2003**.

[4] Mattox D.M., *Handbook of Physical Vapor Deposition (PVD) Processing*, *2nd Edition*, Elsevier: London, **2010.** p. 20.

[5] Lowenheim F.A., *Chemical methods of film deposition* Chap. III-1, in: J.L. Vossen, W. Kern (Eds.), Thin Film Processes, Academic Press, **1975.**

Chapter IV

The Theory of Plasma

Gases do not ordinarily conduct electricity and are electrical insulators. William Crookes (1879), in order to probe the structure of atoms and molecules, investigated the properties of gases at low pressures on exposure to electric fields. He concluded from his experiments that the electrified gases contained in an enclosure and characterized by uniform electrical and optical properties behave as a new state of matter.

Tonks and Langmuir (1929) coined the term plasma to denote the state of matter inside the glow discharge to differentiate it from ordinary gases. The energy provided by an external power source is sufficient to strip the electrons from atoms and molecules thereby creating an equal number of oppositely charged particles. The electrons are thus liberated from the atom and acquire freedom of motion. Since charges exist as separate entities and can transport current when subjected to electric and magnetic fields we infer that the plasma becomes a conducting state. It is possible to shape and mold the ions and electrons in the plasma by the shape of the containers, and move and energize them by electromagnetic forces.

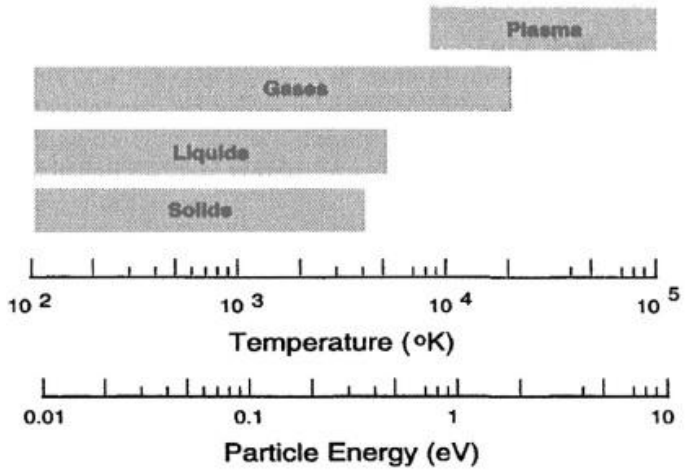

Figure 4.1 State of matter versus temperature

Hence, the name plasma is derived from the Greek root plassein, which means ‘‘to shape or mold’’. Plasma fills therefore every crevice in a vacuum vessel [1].

Plasma is a partially ionized gas consisting of equal numbers of positively and negatively charged particles, the remainder made up of unionized neutral particles and electromagnetic radiation.

4.1. The Plasma State

Unlike the potential energy of attraction between an electron and a proton in a neutral atom, the potential energy of a typical plasma particle due to its neighbors in the plasma is much smaller than its kinetic energy. Therefore, the existence of ions and electrons as separate entities in the plasma, exerting forces on each other, gives plasma some of its unique properties that make it different from gases. Each charged particle in the plasma interacts simultaneously with all other charged particles resulting in important collective effects. In the plasma, the charged particles can be ordered and forced to move in a regular fashion in cohesive groups by applied magnetic and electric fields.

In the undisturbed plasma, the charges move around in a constant electric field since the sums of all the interactions tend to cancel and the plasma shows a behavior of quasi-neutrality. Deviations from electrical neutrality give raise to electric fields and these fields can be very large. Even small deviations from electrical neutrality lead to large electric fields, whose creation demands an immense amount of energy. A one percent deviation in the ion and electron densities at a known separation distance creates a large electrostatic force, which far exceeds the pressure force per unit volume from the motion of particles at any given temperature and pressure.

Charge separation in the plasma is nevertheless a distinct feature of the plasma state. The separation of charges results in an electric field, the establishment of which requires energy. If there are no external sources of energy, this energy must come from thermal energy. At the same time, plasma interacts internally with itself and with externally applied fields and forces. The maintenance of a plasma state is possible when electron and ion densities are in a steady state. Very low degrees of ionization (say 1%) are sufficient for the gas to exhibit electromagnetic properties of plasma. The process of ionization that tries to keep the charges apart must be in balance with the process of recombination that tends to neutralize the charges, under the influence of external energy source.

The negative charges in the plasma are virtually all electrons, even though a fraction of negative ions may be present. The positive charges are essentially due to atoms, molecules and molecular fragments that have lost one or more electrons. The ions may be singly charged or multiply charged. Examples of positive and negative ions are reported in Figure 4.2.

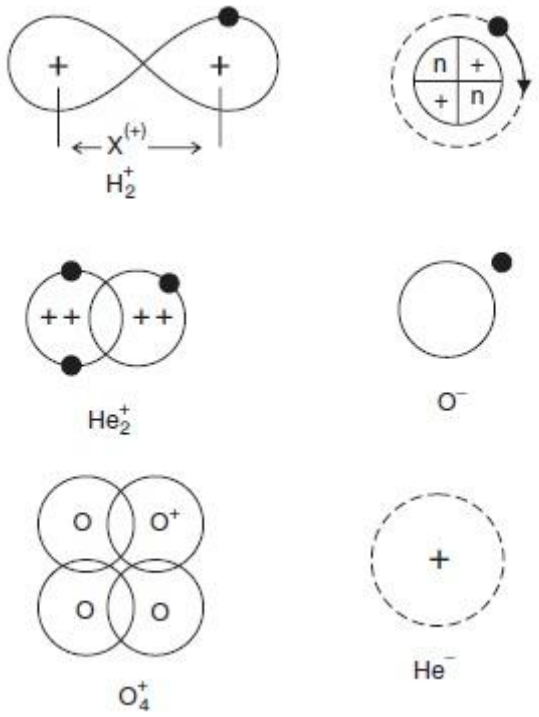

Figure 4.2 Positive and negative ions in a plasma

There are also radicals in the plasma. An example of radical reactions occurring in a plasma is reported below:

$O^2 + e^- = O^* + O^*$

$F^2 + e^- = F^* + F^*$

$e^- + CF_4 = CF_3 + F + e^-$

$H_2O + e^- = OH^+ + H + 2e^-$

$H_2O + e^- = OH + H^+ + 2e^-$

The continuous random motion of the various particles in the plasma due to thermal energy is normally insufficient to maintain a steady state condition but serves to randomize the energies of charge carriers and neutrals through various collision processes and interactions.

In order to maintain the plasma in a steady state, it is essential to replenish the charge lost by diffusion and recombination by some mechanism of generating charges, such as by the presence of external electric and magnetic fields. Ordinarily, gases contain a few ions and electrons due to the effect of cosmic rays or ambient ultraviolet radiation on the gas. These electrons are accelerated by an electric field and are able to generate additional ions and electrons. The nature of the interaction occurring in a plasma due to external forces influences the kinds of particles present in a plasma, their densities and the distribution of their energies.

The presence of charged particles in the plasma means the existence of electric fields that vary with distance r from the location of the charge according to an r^{-2} law. The electric field emanates spherically in all directions with the charge as the center but the volume of the spherical shell increases in proportion to r^2. The product of the electric field times the spherical shell volume determines the effectiveness of the electric field and is a constant, independent of distance. Thus, each charged particle in the plasma influences other charged particles in the plasma at large distances from one another.

A neutral atom or molecule on the other hand has a dipole moment that creates an electric field that has a distance dependence that varies according to a rule r^{-n} where $n \geq 3$. Neutral atoms and molecules exert forces on each other over a very small range of distances. The influence of charges in the plasma on one another acting over large distances is the principal reason for its behavior as distinct from gases of neutral atoms and molecules. Also the magnetic field associated with a moving charge produces a force on other moving charges. The path of particles in a gas follows a zigzag path as the particles travel between collisions along a straight line. However, the path of an ion or an electron in the plasma between collisions is quite different. The path between collisions of a charged particle in the plasma cannot be straight-line segments. Each of the charged particles in the plasma is always in the electric field of the remaining electrons and ions. This electric field is subject to continuous fluctuation in both magnitude and direction. The velocity of the charged particle thus varies continuously. Nevertheless, the trajectory of the charged particle shows a random walk nature, due to the very frequent small deflections that combine in accordance with statistical laws to give rise to a gradual variation in the direction of the moving particle.

The interactions of charged particles in the plasma over large distances imply that they seldom come close to one another and suffer a hard collision. However, the densities of charged particles in the plasma and the temperature of the plasma are important in determining the importance of hard collisions. If the density of charged particles in the plasma is high, the charged particles in the plasma may appear to present a dipole-like appearance to

other charges and consequently hard collisions are important. At low temperatures, electrons and ions rapidly combine to form neutral atoms and molecules. Therefore, heating of a gas to a high temperature is one way to maintain plasma and clearly the density of charged particles increases with increase in temperature.

There are several useful ways of generating the plasma in a gas. The most common method is based on the application of electric and magnetic field to a gas at low pressure in a closed space. Since the gas is normally non-conducting, the first few charges in the gas are due to the influence of cosmic or ultraviolet radiation on the gas. The electric field then takes over and produces all the remaining charged particles to activate and sustain the plasma. Radio frequency waves, shock waves, lasers and high-energy particle beams are other means able to generate plasma.

Moreover plasma exist also in nature, in fact it is estimated that more than 99% of the known universe is in the plasma state, with the exception of cold celestial bodies and planetary systems. The stars of the universe including our sun have extremely high temperatures and they consist entirely of plasmas. It is also suggested that the space between the stars and galaxies are star-origin, radiation-induced, rarefied plasmas. The degrees of ionization are not total even at star surfaces, due to energy losses from radiation processes.

Also meteoritic impacts on the atmosphere of the earth create plasma states. Molecular fragmentation and ionization processes are initiated as a consequence and the plasma state is generated.

4.2. Classification of plasmas

At atmospheric pressures and temperatures around 5000 K materials only exist in the gaseous phase. Above 10,000 K ions are the main constituent particles of matter. Under these conditions and at even higher temperatures, matter is considered to be in the plasma state.

Plasma states can be divided in two main categories: **Hot Plasmas** (near-equilibrium plasmas) and **Cold Plasmas** (non-equilibrium plasmas).

Hot plasmas are characterized by very high temperatures of electrons and heavy particles, both charged and neutral, and they are close to maximal degrees of ionization (100%). Cold plasmas are composed of low temperature particles (charged and neutral molecular and atomic species) and relatively high temperature electrons and they are associated with low degrees of ionization (1024–10%).

Hot plasmas include electrical arcs, plasma jets of rocket engines, thermonuclear reaction generated plasmas, etc. while cold plasmas include low-pressure direct current (DC) and radio frequency (RF) discharges (silent discharges), discharges from fluorescent (neon) illuminating tubes. Corona discharges are also identified as cold plasmas [2].

4.2.1. Low Pressure, non-equilibrium plasmas

Low-pressure non-equilibrium discharges (cold plasmas) [3-5] are initiated and sustained by DC, RF, or microwave (MW) power transferred to a low-pressure gas environment, with or without an additional electric or magnetic field. Ultimately, all these discharges are initiated and sustained through electron collision processes under the action of the specific electric or electromagnetic fields. Accelerated electrons (energetic electrons) induce ionization, excitation and molecular fragmentation processes leading to a complex mixture of active species, which will undergo, depending on the specific plasma mode (e.g. direct or remote plasma environments), recombination processes in the presence or absence of the plasma. The recombination reaction mechanisms are very different reaction mechanisms from those for conventional chemical processes. If electrons with specific energy distribution functions initiate and control all the processes in glow discharges it might appear obvious that similar electron energy distribution environments created using different power sources (DC, RF, MW, etc.) should initiate similar chemistries; and consequently, the type of the plasma would be of less importance for the generation of specific processes. However, due to the electrode, antenna and reactor geometries, their chemical nature, their relative positions in the reaction chambers, and owing also to the individual specificity of the processes (e.g. DC discharges require electrodes with electrically conductive surfaces) plasma non-uniformities can be highly variable. Therefore proper selection and control of plasma parameters are necessary for efficient approaches to specific applications.

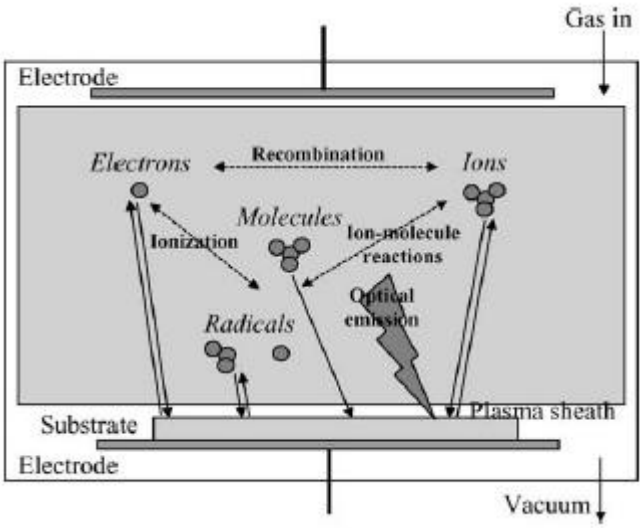

Figure 4.3 Interactions of plasma-generated species with the substrate

4.2.2. Hot plasmas (near-equilibrium plasmas)

Hot plasmas [6-10] have an extremely high energy content, which induce fragmentation of all organic molecules to atomic levels and as a consequence, these plasmas can only be used for generating extremely high caloric energy or to modify thermally stable inorganic materials (metals, metal oxides, etc.).

Hot plasma approaches considered for materials processing have been initiated with the use of plasma arc heaters, and later on, three distinct application areas emerged: synthesis, melting and deposition. Progress in thermal plasma processing has been limited by an unsatisfactory understanding of the extremely complex reaction kinetics, transport properties, heat transfer, and particle dynamics during gas–solid, gas–gas and solid–gas interactions. As a result, thermal plasma processing has only in a few instances progressed beyond laboratory and pilot scale stages.

In this dissertation the processes described will refer to low-pressure, non-equilibrium plasmas.

4.3. Physic of Plasma

Plasmas are characterized by the following main parameters: mean free path, Debye length, plasma temperature and mean electron energy. The free path $\bar{\lambda}$ is the distance a

particle traverses between two successive collisions and, because of the probabilistic nature of the collisions, it has a specific distribution. It can generally be described by the following equation

$$\bar{\lambda} = \frac{1}{\pi\,(r_1 + r_2)N}$$

where r_1 , r_2 are the radii of colliding particles; N is the number particle density (number of particles per unit volume).

The electrical neutrality of plasma is true only in the macroscopic sense. The electric field of each particle interacts with the electric charges of surrounding particles. Neutrality of the majority of the systems is achieved when the field of each particle is negligible outside the zone where shielding occurs. The characteristic parameter that describes the electrical shielding (when the potential of each particle is shielded by charges of the surrounding particles) is called the **Debye length** λ_D; and it defines the volume (Debye sphere) within which the neutrality rule can be violated.

This parameter can be approximated by the following equation

$$\lambda_D = \sqrt{\frac{\mathcal{E}_0 \mathcal{K} T_e}{n_e\, e^2}}$$

where ε_0 is the permittivity of free space; e is the charge of the electron; $\mathcal{K}$ is the Boltzmann's constant; T_e is the temperature of electrons, and n_e is the electron density (number of electrons per unit volume). An ionized gas is considered plasma only if the Debye length is much smaller than the physical dimensions of the plasma region and if the number of the particles within the Debye sphere is much larger than unity (the number of electrons in the Debye sphere of cold plasma is in the range of 10^{-4}–10^{-7}).

Charged and neutral particles collide in the gas phase and with surfaces, which confine the discharge, and undergo recombination and neutralization reaction mechanisms. Electrons that have much higher thermal velocities than ions and neutral molecular and atomic-species, reach surfaces much faster and create a negative potential (negative self-bias). This results in a positively charged plasma layer in the vicinity of the surface of a thickness of several Debye length. This positively charged plasma layer is recognized as the plasma sheath.

Across the sheath potential the flux of the electrons equals the flux of ions reaching the surface; the net current through the sheath is zero. The thickness of the plasma sheath, *ds*, confines a region where the electron density is negligible, and its value depends on the frequency of the electromagnetic field and the pressure in the system. Collision or collision-free sheath conditions will dominate depending on the magnitude of the collisional free path.

The electrical potential developed across the plasma sheath is called the sheath potential and is given for a planar and for a spherical surface by [11]

$$V_S = \frac{K\,T_e}{2E}\,\ln\left(\frac{m_e}{2{,}3\,m_i}\right) \quad \text{(planar surface)}$$

where V_S is the sheath potential and m_i the mass of ions.

$$V_S = \frac{K\,T_e}{2E}\,\ln\left(\frac{\pi\,m_e}{2\,m_i}\right) \quad \text{(spherical surface)}$$

where m_e stands for the mass of the electron. The transport of ions and electrons to the surface through the sheath is mediated by ambipolar diffusion and controlled by the Bohm sheath criterion, which states that only ions with velocities v_i higher than the critical velocity value given by

$$V_e = \left(\frac{K\,T_e}{m_i}\right)^{1/2}$$

will reach the surface.

The plasma temperature is defined as the mean translational energy of the particles in the discharge.

As a result of the substantial mass difference existent between the electrons and heavy species, these particle populations can often be considered as two systems in their own ‘thermal equilibrium’. A plasma would be in thermodynamic equilibrium if the temperatures of the electrons and neutral species, including the ionization, excitation, dissociation and radiation temperatures, were all equal. Because of the presence of a constant energy loss at the plasma boundaries (mainly by convection or radiation), complete thermodynamic equilibrium cannot be reached.

The electron energy distribution of non equilibrium (low-pressure) plasmas can be often described by a Druyvesteyn approximation where the temperature of the electrons is

considered much higher than that of the ions, and when it is assumed that the only 'energy losses' are by elastic collisions (the electric field strength in the plasma is sufficiently low to neglect inelastic collisions).

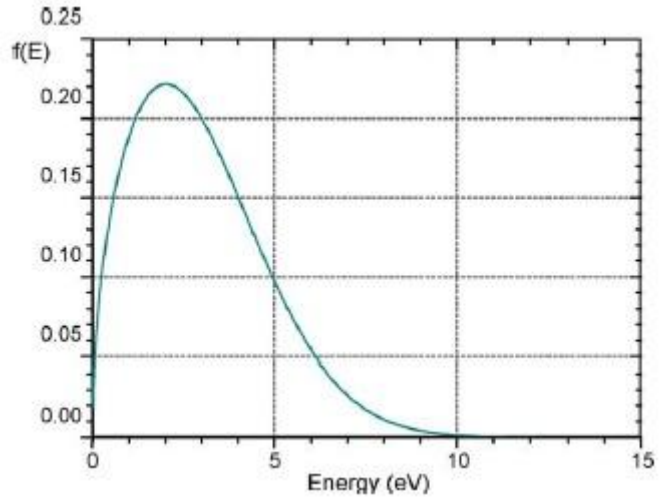

Figure 4.4 Druvesteyn electron energy distribution of a cold plasma (average electron energy: 3 eV)

However, at higher degrees of ionization the influence of the electron density on the energy distribution can be significant [5-6]. It can be observed that a small number of electrons have relatively high energies (5–15 eV) while the bulk of the electrons belong to the low-energy electron range (0.5–5 eV). Since the ionization potentials of the atoms of common organic structures (e.g. C^+= 1.26 eV; H^+ = 13.6 eV; O^+ = 13.6 eV; N^+= 14.53 eV, etc.) belong to the tail region of the electron energy distribution, the low degrees of ionization of cold plasmas appear obvious.

However, this argument is somewhat circular since the inelastic process of ionization is in large part what determines the electron temperature needed to sustain the discharge.

It is extremely important to note that the energy range of most of the electrons (2–5 eV) is intense enough to dissociate almost all chemical bonds involved in organic structures, and organic structures containing main group elements, and to create free radical species capable of reorganizing into macromolecular structures. As a consequence, the structures of all volatile compounds can be altered and/or converted into high molecular weight compounds, even if they do not have the functionalities which are present in common monomer structures. Higher energies are usually required for the dissociation of unsaturated linkages and the formation of multiple free radicals. Accordingly, initial or plasma-generated unsaturated bonds will have a better 'survival rate' under plasma conditions, in comparison to the σ

linkages. Thus, it can be understood why plasma generated macromolecular structures are usually characterized by unsaturated, branched and cross-linked architecture.

The plasma-synthesized macromolecular networks generated by *Plasma-State* processes, directly from the recombination of plasma species on surfaces, which confine the discharge, do not retain the structural characteristics of the starting materials They are not based on repeating units and consequently, the term 'plasma-polymers', which is often used, is inappropriate for describing these structures.

In contrast, Plasma-Induced reactions involve plasma-generated active sites (e.g. free radicals and charged functionalities) located on plasma-exposed substrate surfaces, which initiate conventional polymerization processes from conversion of monomers in the absence of a plasma (e.g. remote plasma zones and pulsed plasma environments).

Besides the recombination mechanisms developed on the surfaces, which confine the plasma, the active species of the discharge interact and continuously tailor the artificially exposed (reactor walls, various substrates, etc.) and self-generated (e.g. plasma-synthesized macromolecular structures) surface layers. The competition between the recombination-deposition processes and the 'destructive' interaction of plasma species with the nascent macromolecular structures will control the intensities and the predominance of ablation, surface functionalization and macromolecular-film-formation reactions.

4.3.1. Modulated plasmas (pulsed plasmas)

Modulated discharges (pulsed plasma) are created by using an RF carrier, switched on and off at a low frequency (longer period time). One of four general types of modulation is pulse-FM or 'chirp' modulation where a carrier is swept over a wideband during a given pulse interval. Pulse is a variation of a voltage or current normally having a constant value. This variation is characterized by a rise and a decay approaching infinitesimal duration. The main parameters that characterize modulated discharges are: the carrier frequency, the pulse period (the time it takes to complete a pulse cycle) and the duty cycle (measures ON period, as a percentage of total period—ON and OFF) are given by

$$\text{Period} = T_{on} + T_{off}$$

$$\text{Duty} = \frac{T_{on}}{T_{on} + T_{off}} \times 100$$

The regimes present in modulated-power discharges (Fig. 10) are Turn-ON (≈ 10–500 ms; rising electron density; larger electron average energy; low ion flux density; ion density rising; power not well matched because of the varying plasma impedance; plasma sheaths forming and changing with plasma ignition; often a larger plasma potential), Steady State (ON; large nearly constant electron density; medium electron energy; large positive ion flux density; power well matched to nearly constant plasma impedance; plasma sheaths oscillating in steady state fashion; medium plasma potential), Turn-OFF (falling electron density; rapidly decreasing electron average energy; rapidly falling ion flux density; plasma potential falling; power falling; plasma sheaths disintegrating with electron density decay; plasma potential falling with electron energy and density) and Late Afterglow (zero power; small electron density; near thermal electron average energy; small ion flux density; negative ions can reach surfaces; plasma sheaths disintegrated with electron density decay; plasma potential zero or even negative).

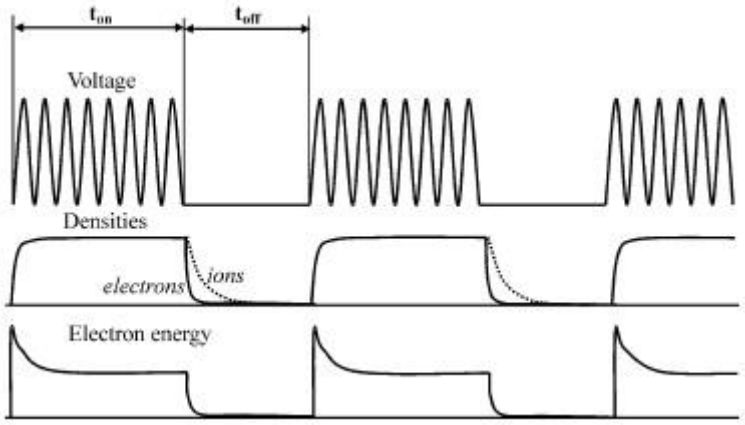

Figure 4.5 Evolution of main parameters of pulsed plasma

To get negative ions out, the sheath must be reversed for a long enough period of time. It ordinarily sets up to repel negative ions (and electrons). Negative ions do not have enough energy to overcome it and it is necessary to absorb the electron current to reverse this electric field (in steady state). This current can be initially large (≈ 5000 A/m2 at 1011 cm^{-3} or 162 A to an 8″ wafer) but it decreases as the electron density decreases.

Pulsed plasmas help in extracting negative ions since electron density decreases quickly during the turn-off and late afterglow and it becomes significantly easier to reverse the electric field direction and extract negative ions. The sheath does not disintegrate in constant wave (CW) plasmas so negative ions are trapped and can polymerize for long times. The rf

power is modulated in pulsed discharges and the sheaths disintegrate periodically. As a consequence, negative ions can be lost to the walls before they polymerize.

Using pulsed plasma, 'dust' particle formation can be diminished (negative ions are not trapped in the glow by the plasma sheaths to format particulates) and the discharge chemistry can be altered. The properties of deposited films can be altered with pulsed plasmas and the etch/deposition rate can be maintained despite lower power. The time variation in the source power changes the electron energy and density; consequently, both higher and lower energy electrons can be formed for reaction. When the power is off the electron energy drops and attachment of fragments can become large. This negative ion chemistry can be different than neutral or positive ion chemistry and loss rates for neutral radicals can vary significantly. When the power is turned on, the electron energy can spike, increasing dissociation and ionization.

Discharge chemistry can be altered by pulsed plasma. It was demonstrated that the ratio of CF and CF_2 radical densities to CF_3 radical density can be controlled through variation of the duty cycle for a 100 ms modulation period [12]. Modulating an ECR plasma enables the control of the CF_2 radical and the F atom density ratio in CHF_3 [13]. The density ratio CFx/F (x = 2,3) increases with decreasing RF ontime in CF_4/H_2 ICP [14].

Properties of deposited films can be altered with pulsed plasmas. Films deposited from modulated glows have significantly smaller optical bandgaps than those deposited from comparable CW discharges [15]. Modulation brought about an improvement in the deposition rate of a-Si:H films and in the film quality [16]. Modulation also caused a drastic suppression of powder concentration in the discharge space [16]. The negative ions are involved in powder formation under these plasma conditions where the particles appear slowly, many seconds after plasma ignition [17].

Etch/deposition rate can be maintained despite lower power in pulsed plasmas. For SF_6 Si etching with pulse durations less than 10 ms, the etch rate is increased to the level of continuous discharge when the duty cycle is kept constant at 20% [18].

For SiO_2 deposition, as the pulse frequency increases from 0.1 to 100 Hz, the deposition rate increases and equals that from a continuous plasma [19].

Trenching, notching and charging damage can be reduced with pulsed plasmas. Highly selective, highly anisotropic, notch-free and charge-build-updamage- free polycrystalline silicon etching is performed by using a electron cyclotron resonance Cl_2 plasma modulated at a pulse timing of a few tens of microseconds [20]. The notching in gate poly-Si etching, is suppressed in a pulsed-power chlorine inductively coupled plasma (ICP) [21]. The low

frequency biased UHF plasma drastically reduces the charge accumulation on the resist mask because negative and positive ions can both be inserted alternately through RF oscillation; thus, the surface is quickly neutralized [22]. The Si etching rate, at 400 kHz RF bias is maximum at the same pressure as that for the F-density, confirming that the negative ion etching was effective [23].

4.4. Plasma Process Parameters

There is large variety of parameters which have a direct effect on the chemical and physical characteristics of a plasma and which therefore also affect the surface chemistry obtained by the plasma modification. An overview of the most important parameters influencing glow discharge processes is shown in Table 4.1.

Parameter	Variations	Main effect	References
Apparatus parameters			
Reactor type	Tube or bell jar		
Frequency	0 (DC)-10^{10} Hz	Energy density of plasma	67
Electrodes			
-Placement	Internal or external	Internal electrodes affect chem. Compositon of plasma	77
-Coupling	Capacitively or inductively	Homogeneity of plasma	
-Shape			
-Surface area ratio		Only important for internal electrodes	
Pumping			
-Base pressure	10^{-2}-10^{-8} mbar	Cleanness of system	78
-Capacity	2-250 m³/h	Residence time	
Magnetic field		Confinement and homogeneity of plasma	
Discharge parameters			
Gas		Type of process	
		Etching or deposition	
Substrate			44
Flow	0-1000cm³/min	Residence time in plasma	
		Etching/deposition rate	
Pressure	10^{-2}-10 mbar	Energy density of plasma	79
Power	1-1000W	Energy density of plasma	
Biasing	self bias-500V	Etching rate	80
Substrate temperature	77-500 K	Surface composition	79,81-85
Procedure parameters			
Cleaning of reactor	Chemical, thermal or plasma	Removal of impurities	
Evacuation time	cleaning	Cleanness of system	
Treatment time	1 s- several hours	Intensity of modification	
Quenching gas	0.01 s- several hours	Surface chemistry	

Table 4.1 Process Parameters and their effect in plasma treatments

Furthermore the main effect of varying a particular parameter is given, although it should be noted that several other effects might simultaneously occur. The parameters are divided into three classes: apparatus parameters, which are set by the design of the equipment, discharge parameters and procedure parameters. Especially the importance of apparatus and discharge parameters have been acknowledged in the literature. The importance of procedure parameters is generally accepted but scarcely documented.

The effect of the most important apparatus and discharge parameters have been extensively reviewed. The energy density of a plasma can be increased by the increasing the frequency of the electric field, by using a magnetic field to confine the plasma, by decreasing the plasma volume (by varying the place, positions, shape and surface ratio of the electrodes) and by increasing the input power.

The final chemical composition of the surface is affected by the chosen gas, the energy density of the plasma, the selected substrate (of minor importance during plasma polymerization processes), the bias voltage, the substrate temperature and the quenching gas. According to the gas type, either etching or deposition occurs. By increasing the flow rate, the etching or deposition rate increases until after a certain point the rate of the process is limited by the power input.

Yasuda has correlated an overall parameter, power input per mass 'monomer' to the etching rate [25].

$$W/F \cdot M$$

in which W is the electrical power input, F is molar or volume flow rate, and M is the molecular weight of gas [26]. The units of this composite parameter are J/kg, i.e., energy per mass of gas.

The numerical value of $W/F \cdot M$ in J/kg can be calculated from W in Watt, F in sccm, and M in g/mol by

$$[W\ /\ (F \cdot M) \quad in\ J\ /\ kg] = W/(F \cdot M)\ \times\ (1{,}34\ \times\ 10^9)$$

Since F is proportional to the molar flow rate, $F \cdot M$ represents the mass flow rate. Because the deposition rate is generally given in unit of mass per unit area and unit time the power input parameter should be also expressed using the mass unit. Flow rate of gases are generally expressed by the volume or molar flow rate. Therefore, the molecular weight, M, must be included.

If only one monomer or gas is used, M is a constant and, consequently, the similar dependence of results can be obtained by W/F as an operational parameter; however, if more than one monomer or gas, e.g., methane, ethane, propane, and butane, are compared, multiple curves representing each gas rather than one universal curve are obtained. These multiple curves converge into a master curve representing for the homologous series of hydrocarbons [26].

In a simple set of experiments with only a single gas at a given flow rate, experiments could be carried out adequately by changing the value of W, which erroneously gives the impression that W is the process parameter of plasma treatment or plasma polymerization or both. Many papers published currently use W as the process parameter, which indicates the importance of the operational parameter is being neglected. The misinterpretation of the operational parameter hinders the true understanding of the processing aspect of plasma treatment and plasma polymerization as well as the proper scale-up of a laboratory experiment to a larger industrial-scale operation.

Although this parameter can be used for general comparisons, two other important parameter are neglected. These are pressure and residence time of the gas in the plasma. Furthermore different sets of conditions yield similar W/FM values, but totally different surface compositions.

Because all plasma processes are combinations of etching, sputtering and deposition processes, all materials in contact with a plasma influence the chemical composition of the surface. Therefore the cleanness of the reactor, the type of vacuum joints used, the chemical composition of materials surrounding the plasma (including reactor, electrodes and substrates) and evacuation times and pressures have influence on the chemical composition of the surface of the substrate. To circumvent most of these problems, long plasma treatment times are used. The plasma has etched or coated all its surroundings and a steady state surface composition is obtained.

The large number of parameters makes glow discharge processes sometimes difficult to reproduce. Although a minimal experimental set up is needed to create plasmas, for a good control (and good reproducibility) of the process well designed and rather expensive equipment is needed. The large number of parameters also means that on the other hand the reproduction of experiments of other authors is extremely difficult. Because glow discharge processes can be operated in many different ways, a large degree of freedom in engineering these processes exists. This makes glow discharges an extremely versatile technique to modify polymer surfaces with totally different shapes.

References

[1] Cecchi J. L., *in Handbook of Plasma Processing Technology*, eds. Stephen M. Rossnagel, Jerome J. Cuomo and William D. Westwood, Park Ridge, NJ: Noyes Publications, **1990**.

[2] Denes F.S., Manolache S., "Macromolecular plasma-chemistry: an emerging field of polymer science", *Prog. Polym. Sci*., **2004**, 29, p. 815–885.

[3] Venugopalan M, *Reaction under cold plasma conditions,* vol. 1., Wiley/Interscience: New York, **1971.**

[4] Nasser E., *Fundamentals of gaseous ionization and plasma electronics*, Wiley/Interscience: New York, **1971.**

[5] Hollahan J.R., Bell A.T., *Techniques and applications of plasma chemistry*, Wiley: New York, **1974.**

[6] Herman H., "Plasma-sprayed coatings", *Sci. Am*., **1988**, 259(3), p. 112–117.

[7] Mac Rae D.R., "Plasma arc process systems, reactors, and applications", *Plasma Chem. Plasma Process*, **1989**, 9(1, Suppl). p. 85S–118S.

[8] Smith R.W., Wei D., Apelian D., "Thermal plasma materials processing-applications and opportunities", *Plasma Chem. Plasma Process*, **1989**, 9(1, Suppl), p. 135S–65S.

[9] Leveroni E., Pfender E., "A unified approach to plasma-particle heat transfer under noncontinuum and nonequilibrium conditions", *Int J Heat Transfer,* **1990**, 33(7), p. 1497–509.

[10] Chang C.H., Pfender E., "Nonequilibrium modeling in lowpressure argon plasma jet. Part II: turbulent flow", *Plasma Chem Plasma Process*, **1990**, 10(3), p. 493–500.

[11] Grill A., *Cold plasma in materials fabrication-from fundamentals to applications*. IEEE Press: New York, **1994**.

[12] Takahashi K., Hori M., Goto T., Jpn J., "Control of fluorocarbon radicals by on-off modulated electron cyclotron resonance plasma", *Appl. Phys. Part 2 Lett.*, **1993**, 32(8A), p. L1088–1091.

[13] Samukawa S., Furuoya S., "Time-modulated electron cyclotron resonance plasma discharge for controlling generation of reactive species", *Appl. Phys. Lett.*, **1993**, 63(15), p. 2044–2046.

[14] Sugai H., Nakamura K., "Diagnostics and control of radicals in an inductively coupled etching reactor", *J. Vac. Sci. Technol. A,* **1995**, 13, p. 887–893.

[15] Overzet L.J., Verdeyen J.T., Roth R.M., Carasco F.F., "The effects of modulation on an RF discharge in silane and on the deposited amorphous hydrogenated silicon", *Mater. Res. Soc. Symp. Proc.,* **1987**, 98, p. 321–326.

[16] Watanabe Y., Shiratani M., Kubo Y., Ogawa I., Ogi S., "Effects of low-frequency modulation on rf discharge chemical vapour deposition", *Appl. Phys. Lett.*, **1988**, 53(14), p. 1263–1265.

[17] Courteille C., Dorier J.L., Hollenstein Ch., Sansonnens L., Howling A.A., "Partial-depth modulation study of anions and neutrals in low-pressure silane plasmas", *Plasma Sources Sci. Technol.*, **1996**, 5(2), p. 210–215.

[18] Boswell R.W., Henry D., "Pulsed high rate plasma etching with variable Si/SiO2 selectivity and variable Si etch profiles", *Appl. Phys. Lett.*, **1985**, 47(10), p. 1095–1097.

[19] Charles C., Boswell R.W., Kuwahara H., "SiO2 deposition from oxygen/silane pulsed helicon diffusion plasmas", *Appl. Phys. Lett.*, **1995**, 67(1), p. 40–42.

[20] Samukawa S., Mieno T., "Pulse-time modulated plasma discharge for highly selective, highly anisotropic and charge-free etching", *Plasma Sources Sci. Technol.*, **1996**, 5(2), p. 132–138.

[21] Ahn T.H., Nakamura K., Sugai H., "Negative ion measurements and etching in a pulsed-power inductively coupled plasma in chlorine", *Plasma Sources Sci. Technol.*, **1996**, 5(2), p. 139–144.

[22] Samukawa S., Tsukada T., "Effects of electron temperature in high-density Cl_2 plasma for precise etching processes", *Appl. Phys. Lett.*, **1996**, 69(8), p. 1056–1058.

[23] Shibayama T., Shindo H., Horiike Y., "Silicon etching by alternating irradiations of negative and positive ions", *Plasma Sources Sci. Technol.*, **1996**, 5(2), p. 254–259.

[24] Yasuda H.K., "Some Important Aspects of Plasma Polymerization", *Plasma Process. Polym.* **2005**, 2, p. 293–304.

[25] Yasuda H. K., *Luminous Chemical Vapor Deposition & Interface Engineering*, Marcel Dekker: New York, **2004**.

[26] Yasuda H. K., *Plasma Polymerization*, Academic Press: Orlando, **1985**.

Chapter V

Plasma Activation and Plasma Polymerization Processes for Biomedical Applications

In the biomaterial research low-pressure plasma process has been widely recognized as a technology of choice for surface modification of biomedical devices. Plasma process presents the advantages to modify the very first layers of the surface, keeping the bulk material properties.

In particular, modification of the surface energetics of the materials can improve the adhesion strength, surface and coating properties, and biocompatibility.

Succinctly speaking, plasma-based techniques offer the following advantages with regard to biomaterials engineering:

1. Plasma engineering is usually reliable, reproducible, non-line-of-sight, relatively inexpensive, and applicable to different sample geometries as well as different materials such as metals, polymers, ceramics, and composite. Plasma processes can be monitored quite accurately using in situ plasma diagnostic devices [1].

2. Plasma treatment can result in changes of a variety of surface characteristics, for example, chemical, tribological, electrical, optical, biological, and mechanical. Proper applications yield dense and pinhole free coatings with excellent interfacial bonds due to the graded nature of the interface [2].

3. Plasma processing can provide sterile surfaces and can be scaled up to industrial production relatively easily. On the contrary, the flexibility of non-plasma techniques for different substrate materials is smaller [3].

4. Plasma techniques are compatible with masking techniques to enable surface patterning [4] a process that is commonly used in the microelectronics industry.

As a result, plasma-surface modification (PSM) as an economical and effective materials processing technique is gaining popularity in the biomedical field. It is possible to change in

continuum the chemical composition and properties such as wettability, metal adhesion, dyeability, refractive index, hardness, chemical inertness, lubricity, and biocompatibility of materials surfaces.

In the biomedical context, ‘‘good biocompatibility’’ refers to that a prosthesis or biomaterial device is non-toxic, does not induce deleterious reactions from the bio-medium, performs properly all the functions they have been designed for, and has a reasonable lifetime. The application of plasma-based techniques is quite diverse, and examples of applications include cleaning/sterilization, coating or depositing, and implantation modification of surface chemistry of a substrate.

5.1. Plasma Surface Modification techniques

Biocompatibility (biological performance) can be broadly defined as a satisfactory performance of materials during their interaction with living systems and it is extensively investigated by scientists and engineers who dealing with medical and biological problems. It is a complex phenomenon and its mechanisms are not fully understood, mainly due to the lack of detailed knowledge of in vivo conditions.

The degree of biocompatibility sets the limits to engineering solutions required for biomedical problems. Conventional wet-chemistry approaches employed for changing the physical–chemical characteristics of material surfaces often have application limitations owing to the complexity of the techniques, the requirement of environmentally non-friendly processes, and labor-intensive and expensive methodologies.

Non-equilibrium low- and atmospheric-pressure cold plasma techniques have been recognized for a long time as efficient surface modification techniques, and accordingly the plasma approach was also considered for the generation of biocompatible surfaces. Surface functionalization processes involving non-depositing plasma-gases, and plasma-enhanced deposition reactions have been investigated for the modification of biomaterial surfaces.

5.1.1. Plasma Treatment: cleaning, activation and etching

Thanks to a plasma treatment, by choosing the right configuration and processing parameters, it is possible to produce specific effects upon the surface. In particular, by plasma, the substrate can be cleaned, activated and etched.

Plasma cleaning is a proven, effective, economical and environmentally safe method for critical surface preparation. As example, plasma cleaning with oxygen eliminates natural and technical oils and grease at the nano-scale and reduces contamination up to six fold when compared with traditional wet cleaning methods, including solvent cleaning residues themselves. Plasma cleaning produces a pristine surface, ready for bonding or further processing, without any harmful waste material. In this case the cleaning effect is due not only to the ultra-violet light generated in plasma but also to the oxygen species able to react with the organic contaminants to form mainly water and carbon dioxide which are continuously removed (pumped away) from the chamber during processing.

With plasma activation this effect is increased because reactive species from the plasma bind to active surface sites all over the material, creating a surface that is highly 'active' to bonding agents.

This effect could be applied to plastics, i.e. polypropylene or PTFE (polytetrafluoroethylene), but also glass and ceramics can be plasma activated similarly. Technically oxygen is usually used as the process gas, however, many plasma activations can also be carried out with just ambient air. Parts remain active for a few minutes up to several months, depending on the particular material that has been plasma treated. Polypropylene for example can still be reprocessed several weeks after treatment.

In case of a polymer, the interaction between a plasma and the surface leads to two competitive reactions, namely modification and degradation [5]. When the modification effect dominates, the properties of the polymer will change due to ion beam interaction, plasma-graft co-polymerization, and plasma polymerization. When degradation is prominent, etching will take place on the polymer surface.

Plasma etching in biomaterials research mainly focuses on argon plasma exposure of polymer materials. An etching reaction is a degradation reaction occurring at the surface of the polymers, and when polymers are exposed to plasma for a long enough time, the exposed layers of the polymers are etched off. The rate of weight loss is strongly dependent on the nature of the polymer as well as the energy of the plasma. Polymers containing oxygen functionalities such as ether, carboxylic and ester groups show high plasma susceptibility. On the other hand polyolefins with no substituents exhibit low plasma susceptibility. Such weight loss is restricted to the topmost layers of the polymer whereas in the inner layer, this weight loss process scarcely occurs. Therefore, polymers subjected to the plasma etching process possess similar chemical and physical properties similar to the original polymers. The elemental composition, chemical structure, degree of polymerization and crystallinity of the

treated polymers are hardly altered and are similar to those of the original polymers. The weight loss in the etching process is mainly due to bonds breaking and reactions of the radicals generated in the polymer chains upon plasma exposure. In addition to the chemical etching process, physical sputtering occurs frequently when polymers are exposed to plasma [6,7].

5.1.2. Plasma Deposition: plasma polymerization

Plasma polymerization is gaining importance for last several years as a tool to modify material surfaces. In plasma polymerization, the transformation of low-molecular-weight molecules (monomers) into high-molecular-weight molecules (polymers) occurs with the assistance of energetic plasma species such as electrons, ions, and radicals. Plasma polymerization is chemically different from conventional polymerization involving radicals and ions. In many cases, polymers formed by plasma polymerization have different chemical compositions as well as chemical and physical properties from those formed by conventional polymerization, even if the same monomers are used in plasma polymerization and conventional radical or ionic polymerization. This uniqueness results from the reaction mechanism of the polymer-forming process.

The nature of plasmas, the modalities of transferring electric or electromagnetic field intensities to the reaction systems, the geometry of reactor (shape and volumes of the reaction vessel, geometrical location of electrodes and substrates, etc.) and the selected experimental conditions (pressure, power, flow rates of gases, temperature of the substrates, etc.) crucially influence the gas-phase and surface-related plasma chemistry. Consequently, the comparison of experimental results obtained from a large variety of plasma systems, even for identical starting components, is extremely difficult.

Cold-plasma-mediated processes involve both gas phase and surface reaction mechanisms. The gas phase reaction mechanisms involve the interaction of ab initio existing and nascent neutral and charged plasma-created species, including atoms, molecules, free radicals, ions of either polarity, excited species, electrons and photons. Besides the recombination mechanisms developed on the surfaces which confine the plasma, the active species of the discharge interact and continuously tailor the artificially exposed (reactor walls, various substrates, etc.) and self-generated (e.g. plasma-synthesized macromolecular structures) surface layers. The competition between the recombination-deposition (deposition, grafting, functionalization) processes and ‘destructive-interaction’ of plasma species (etching) with the nascent

macromolecular structures will control the intensities and the predominance of ablation, surface functionalization and macromolecular-film-formation reactions.

The mechanisms of surface functionalization of polymeric substrates are different from the gas-phase processes. While electrons play the most important role in the plasma state, positive ions also play a significant role in the surface chemistry during the interactions of plasma species with polymers. The resulting valence-ionized polymer chains undergo neutralization reactions leading to sufficiently intense localized internal energy concentrations (electronically excited states), which can induce homolytic bond cleavages. Free-radical and unsaturated-bond development can result in cross-linking of polymeric layers. Free radicals can further induce chemical reactions involving plasma species in situ and affect reactions controlled by specific chemical environments (gas-phase or condensed-phase compounds, including, oxygen, monomer molecules, etc.) in the absence of plasma.

Qualitative and quantitative evaluation of charged and neutral species of the gas phase and identification of charged and neutral surface functionalities on substrate surfaces is essential for understanding the plasma-induced reaction mechanisms and physical processes. Adaptation of in situ diagnostic techniques (including real time measurements) for relatively high and low pressure (100–1000 mTorr) plasma environments is a research area where many questions still remain un-answered. Continued research will promote the development of novel and/or improved processes for tailoring materials surface characteristics and the development of advanced laboratory plasma installations, required for scaling up plasma processes to industrial levels.

Hydrocarbons such as methane, ethane, ethylene, acetylene, and benzene are widely used in the synthesis of plasma polymerized hydrogenated carbon films. The enhanced micro-hardness, optical refractive index, and impermeability result in good abrasion resistance.

Plasmas of fluorine containing inorganic gases, such as fluorine, hydrogen fluoride, nitrogen trifluoride, bromine trifluoride, sulfur tetrafluoride, and sulfur hexafluoride monomers are used to produce hydrophobic polymers.

Plasma polymers fabricated using organo-silicon monomers have excellent thermal and chemical resistance and outstanding electrical, optical, and biomedical properties. The common organo-silicon precursors include silane, disilane (SiSi), disiloxane (SiOSi), disilazane (SiNHSi), and disilthiane (SiSSi) [7-9].

Recently, surface treatments and modification based on vapor phase plasma-assisted techniques have been widely applied to several biomedical fields. These processes are able to provide specific mono-type chemical functionalities, exposed at materials surfaces. Respect to

traditional liquid phase procedures, advantages such as the high process control and the use of small quantities of reagents, are crucial for the enhancement of efficiency of the interactions that materials must perform according to the application.

In particular, procedures for in situ plasma polymerization, starting from vapor released by liquid monomers, are presently used to synthesize innovative polymeric thin films applicable as substrates for cell culture [10], as adhesion promoter in prosthetic implants and for molecular recognition in sensors and biosensors.

The low pressure plasma polymerization, starting from the same reagent and only varying the process parameters (modulation of the plasma discharge, monomer or mixture of monomers/process gas, reactant vapor partial pressure, etc.) leads to the deposition of polymeric materials with different features in terms of density of functional groups, wettability (hydrophilicity/hydrophobicity) and chemical stability [11].

The most studied polymers in biomedical and sensing fields, display as functional groups mainly carboxyls (-COOH) and amines ($-NH_2$), hydroxyls (-OH), and aldehydes (-CHO). Fewer reports exist on hydroxy and aldehyde surfaces prepared by plasma methods. Hydroxy surfaces can be prepared by water plasma treatment or the plasma polymerization of alkyl alcohol vapors. Water plasma treatment on many polymer substrates suffers from aging, with surface adaptation leading to the movement of surface modification effects into the polymer. Both hydroxy and aldehyde surfaces have been used for the covalent immobilization of biologically active molecules. Aging effects are less well documented than for amine surfaces [29].

Aminated surfaces have been fabricated using various plasma vapors or mixtures (allylamines, ethylenediamine, diaminopropane, n-eptilamine [11]) and have found wide use for biointerface applications. However, in many cases the amine surfaces have a rather limited shelf life, with post-plasma oxidation reactions and surface adaptation leading to the disappearance of amine groups from the surface. Aging is a widespread phenomenon that often has not been recognized, particularly in some of the earlier studies on the use of plasma-fabricated surfaces for bio-interfacial applications, and can markedly alter the surface chemistry [10].

Plasma-fabricated surfaces that contain carboxyl groups have also been well documented. For example are obtained, by acrylic acid [10] and vinyl acetic acid or applying CO_2 plasma on olefin polymers [11].

In order to better tune the distribution and density of functional groups, are also widely known processes of plasma co-polymerization, where the monomer containing functional

groups of interest is mixed with a precursor which does not contain specific functionalities (e.g.. styrene or octadiene [12]) and which has the function to dilute the reactive groups at the surface. For example, carboxylate co-polymer surfaces have shown excellent ability to support the colonization of some human cell lines of clinical interest. Immobilization of proteins onto plasma-carboxylated surfaces is also well established. Generally, these surface chemistries show good ability to support cell colonization, though the effectiveness seems to depend on the process vapor and the plasma conditions.

An example in which process parameters affect the final properties of the plasma-polymer film is reported by Detomaso et al. [10]. Starting from Acrylic Acid vapor, processes obtained by Continous Wave (CW) plasma discharge and by Modulated Wave (MW), that is pulsed, plasma discharge are compared respect to the efficiency of the final polymer coating towards cells growth. The –COOH terminated polymer obtained by MW, with a Duty Cycle (D.C.= (T_{on} / T_{on} + T_{off}) of 5, where T_{on}=5ms and T_{off}=95 ms, is less useful to murine fibroblast growth than the CW plasma film, because more soluble in water due to the higher density of –COOH groups and the higher retention of the monomer (Acrylic Acid) structure (low cross-linking and backbone chain propagation).

5.1.3. The advantages of pulsing the plasma discharge

Over the last decades, tremendous progress has been made in understanding and utilization of plasma to obtain coatings and surfaces with desired properties. Improvements are generally attributed to ‘activation’ of condensing particles and enhancement of surface mobility, which usually bleads to denser films, affecting a wide range of mechanical, optical, electrical and other properties. To further optimize properties of coatings and surface structures, plasma can be ‘engineered, with emphasis on pulsed plasmas.

The use of pulsed radio-frequency-excited plasmas has become important in the deposition of chemically functional polymeric surfaces [13]. Control over the plasma parameters through manipulation of the pulsing waveform (usually in the hertz to kilohertz range) allows the incorporation and maximisation of desired chemical groups at the surface. For instance, it has been found that the duty cycle is a key parameter in determining the degree to which there is retention of the chemical nature of the starting compound (monomer) in the deposited films [13,14].

As described in chapter 4 the *Duty Cycle (DC)* is the ratio between the time in which the plasma discharge is on (T_{on}) and the period corresponding to the length of the pulsation (T_{on} + T_{off}), where T_{off} corresponds to the break between plasma impulses.

$$DC = \frac{T_{on}}{T_{on}+T_{off}}$$

In pulsed plasma depositions the Average Power (P_{ave}) received from the substrate is expressed in this equation:

$$P_{AVE} = P_{RF}\, DC$$

For this reason, low DC can be applied with high value of inner power during the period of T_{on} thus resulting in a low Average Power for all the period of the pulsing and so in an high functional retention.

Compared to Continous Wave (CW) Processes, Modulated Wave (MW) Plasma-generated reactive species are consumed both in plasma-on and plasma-off periods but by different reaction mechanisms. It is believed that the charged species in the plasma-off intervals are converted extremely rapidly into neutral active species (e.g. free radicals, excited species) which can initiate recombination reactions with the dominant un-modified plasma-gas molecules. When conventional monomer gas or vapour environments are the plasma media, free radical initiated conventional polymerization reactions will develop simultaneously with the random recombination into macromolecular structures of plasma-generated species. Obviously, in the plasma-off periods, the characteristic plasma effects, including development of self-bias, generation of UV radiation, thermal effects on the substrates as a result of the bombardment of surfaces with plasma species, will be absent and consequently molecular fragmentation processes will be substantially diminished. During this period conventional recombination reactions including polymerization, entrapment of non-reacted molecules into the nascent macromolecular thin-layer networks and the formation of structurally non-homogeneous layers will be dominant. At the same time, free radical sites and conventional monomer molecules entrapped into the nascent networks might continue to generate specific recombination reactions during the entire plasma-on/plasma-off period with the generation of structures that retain more of the original plasma-gas structure.

Consequently, understanding of film-formation rates and reaction mechanisms and relating film characteristics, including chemical composition, adhesion, surface roughness, to plasma

parameters are very difficult. Thermal and time stability of structural and morphological characteristics of the pulsed-plasma films will also have a dynamic character due to the incorporated, more or less reactive molecular and molecular-fragment species.

Despite the difficulties in understanding the complex multi-mechanism nature of the formation of pulsed-plasma films, literature data indicate that this plasma approach provides additional ways for controlling plasma-deposited film chemistry and composition, and film-formation rates with potential application in the areas of thin layer biomaterials, adhesives, electrically conductive organic layers, low dielectric constant films and generation of super hydrophobic coatings [15,16].

5.2. Plasma-polymerized acrylic-acid thin film deposition

Native and plasma-modified polymers with oxygen containing surface groups generally support protein and cell adhesion.

Efforts were run to individuate the effect of each individual group (hydroxyl, carbonyl, carboxyl, etc.) on cell adhesion/growth, but the investigation is not over yet. Such groups favor the formation, through ion–ion, ion–dipole and similar interactions, of a protein layer on surfaces exposed to biological media, which drives the behaviour of cells that, soon after, come in contact with.

This work will however focus on plasma polymerization of acrylic acid, since COOH-dense surfaces can have important biomedical applications.

Negative charged groups, e.g. carboxylates, have been recognized as cell adhesion promoters [17-21].

It was shown that endothelium cells strongly prefer surfaces rich with carboxylic and/or hydroxyl groups [22]. MacNeil et al. [23] studied the attachment of keratinocytes to coatings deposited from acrylic acid (AA)/octadiene plasmas, containing carboxylic and hydroxyl groups, and found a strong preference of cells for the former groups. For the same coatings, Short et al. [24] reported an optimum concentration of surface carboxyl groups, above and below which the proliferation of osteoblast-like cells fails. Ertel et al. [25], instead, have shown that the growth of bovine aortic endothelial cells correlates with the density of carbonyl groups

Moreover, carboxylic acid groups are sensitive to pH changes of the solution in which they are immersed: this behaviour could be used in drug delivery systems to release a certain amount of a drug in an environment characterized by a specific pH.

Plasma polymerization of acrylic acid allows to obtain thin functional films, stably attached to the substrates surface and exposing specific properties according to the working conditions applied during deposition.

As an example, significant fragmentation of the feed generally occurs in glow discharges and this results into a wide range of functional groups appearing in the coating [26,27].

The fragmentation can be minimized by carefully tuning parameters such as power input and duty cycle, to obtain a high degree of monomer structure retention in the film.

It has been demonstrated in several studies that higher monomer structure retention and so higher percentage of carboxylic functionalities can be obtained in the final films when low power and/or low duty cycle are applied during plasma polymerization resulting in low molecular fragmentation of the precursor in the plasma (i.e. acrylic acid).

On the other hand, as the power increases, the fragmentation increases itself resulting in a higher reticulation degree and so a lower carboxylic groups density in the final films.

PPAA coatings with tunable carboxyl surface density are able to influence adhesion and spreading of keratinocytes within 24 h of culture [28]. Films with high carboxyl density can result unstable in water due to swelling, leaching of unreacted fragments or/and de-lamination. Coatings that support cell growth for a certain time while they degrade may be attractive as biodegradable materials; more often, though, stable functional surfaces are requested, e.g. for long-term cell adhesion or for biomolecule immobilization.

Concerning this application the stability at least in water should be tested.

A lower number of carboxylic groups increases film stability due to the higher cross-linking degree of the polymer which is more reticulated and so more suitable for biological applications where the sample has to be in contact with aqueous biological fluids.

For this reason the choice and the optimization of plasma process parameters are crucial steps in the functionalization procedure based on PPAA films.

References

[1] Sioshansi P., Tobin E.J., “Surface treatment of biomaterials by ion beam processes”, S*urf. Coatings Technol*., **1996**, 83, p. 175.

[2] Szycher M., Sioshansi P., Frisch E. E., *Biomaterials for the 1990s: Polyurethanes. Silicones and Ion Beam Modification Techniques* (Part 11), Spire Corporation, Patriots Park, Bedford, **1990.**

[3] Ohl A., Schroder K., "Plasma-induced chemical micropatterning for cell culturing applications: a brief review", *Surf. Coatings Technol.*, **1999**, 116–119, p. 820–830.

[4] Vargo T.G., Bekos E.J., Kim Y.S., Ranieri J.P., Bellamkonda R., Aebischer P., Margevich D.E., Thompson P.M., Gardella Jr. J.A., "Synthesis and characterization of fluoropolymeric substrata with immobilized minimal peptide sequances for cell adhesion studies", *J. Biomed. Mater. Res*., **1995**, 29, p. 767;

[5] Chappel P.J.C., Brown J.R., George G.A., Willis H.A., *Surf. Interf. Anal*., **1991**, 17, p 143.

[6] Chan C.M., Ko T.M., Hiraoka H., "Polymer surface modifications by plasmas and photons", *Surf. Sci. Rep*., **1996**, 24, p. 223-227.

[7] Inagaki N., *Plasma-surface Modification and Plasma Polymerization*, Technomic Publishing Company, Inc., Pennsylvania, **1996.**

[8] Lewis H.G.P., Edell D.J., Gleason K.K., "Pulsed-PECVD Films from Hexamethylcyclotrisiloxane for Use as Insulating Biomaterials", *Chem. Mater*., **2000**, 12, p. 3488.

[9] Dai L., St. John H.A.W., Bi J., Zientek P., Chatelier R.C., Griesser H.J., "Biomedical coatings by the covalent immobilization of polysaccharides onto gas-plasma-activated polymer surfaces", *Surf. Interf. Anal*., **2000**, 29, p. 46.

[10] Detomaso L., Gristina R., D'Agostino R., Senesi G.S., Favia P., "Plasma deposited acrylic acid coatings: Surface characterization and attachment of 3T3 murine fibroblast cell lines", *Surf. Coat. Technol.*, **2005**, 200, p. 1022–1025.

[11] Siow K.S., Britcher L., Kumar S., Griesser H.J., "Plasma Methods for the Generation of Chemically Reactive Surfaces for Biomolecule Immobilization and Cell Colonization" A Review. *Plasma Process. Polym*., **2006**, 3, p. 392-418.

[12] Swaraj S., Oran U., Friedrich J.F., Lippitz A., Unger W.E.S., "Surface chemical analysis of plasma-deposited copolymer films prepared from feed gas mixtures of ethylene or styrene with allyl alcohol", *Plasma Process. Polym*., **2007**, 4, p. 376-389.

[13] Yasuda H., Hsu T., "Some aspects of plasma copolymerization of acetylene with N_2 and/or water", *J. Polym. Chem. Ed*., **1977**, 15, p. 817.

[14] Rinsch C.L., Chen X., Panchalingam V., Eberhart C., Wang J.-H., Timmons R.B., "Pulsed Radio Frequency Plasma Polymerization of Allyl Alcohol: Controlled Deposition of Surface Hydroxyl Groups", *Langmuir*, **1996**, 12 , p. 2995.

[15] Denes F.S., Manolache S., "Macromolecular plasma-chemistry: an emerging field of polymer science", *Prog. Polym. Sci*., 2004, 29, p. 815–885.

[16] Calderon J.G., Timmons R.B., "Surface molecular tailoring via pulsed plasma-generated acryloyl chloride polymers: synthesis and reactivity", *Macromolecules,* **1998**, 31(10), p. 3216–3224.

[17] Maroudas N.G., "Adhesion and spreading of cells on charged surfaces", *J. Theor. Biol*. **1975**, 49, p. 417–42.

[18] Lombello C.B., Malmonge S.M., Wada M.L.F., "PolyHEMA and polyHEMA-poly(MMA-co-AA) as substrate for culturing Vero cells", *J. Mater-Sci Mater M*, **2000**, 11, p. 541–546.

[19] Sugimoto Y., "Effect on the adhesion and locomotion of mouse fibroblasts by their interacting with differently charged substrates: a quantitative study by ultrastructural method", *Exp. Cell. Res*. **1981**, 135, p. 39–45.

[20] Lee J.H, Lee J.W., Khang G., Lee H.B., "Interaction of cells on chargeable functional group gradient surfaces", *Biomaterials,* **1997**, 18, p. 351–8.

[21] Gupta B., Plummer C., Bisson I., Frey P., Hilborn J., "Plasma-induced graft polymerization of acrylic acid onto poly(ethylene terephthalate) films: characterization and human smooth muscle cell growth on grafted films", *Biomaterials,* **2002**, 23, p. 863–871.

[22] Tidwell C.D., Belu A.M., Ratner B.D., Tarasevich B., Atre S., Allara D.L., *Transactions of the Society of Biomaterials, 23rd Annual Meeting*, vol. 20; 1997. P.. 203

[23] France R.M., Short R.D., Dawson R.A., Macneil S., "Attachment of human keratinocytes to plasma co-polymers of acrylic acid/1,7 octadiene and allylamine/1,7 octadiene", *J. Mater. Chem.* **1998**, 8, p. 37–42.

[24] Daw R., Candan S., Beck A.J., Devlin A.J., Brook I.M., Macneil S., Dawson R.A., Short R.D., "Plasma copolymer surfaces of acrylic acid/1,7 octadiene: surface characterisation and the attachment of ROS 17/2.8 osteoblast-like cells", *Biomaterials*, **1998**, 19, p. 1717–25.

[25] Ertel S.I., Chilkoti A., Horbett T.A., Ratner B.D., "Endothelium cell growth on oxygen-containing films deposited from radiofrequency plasma: the role of surface carbonyl groups", *J. Biomat-Sci Polym. E,* **1991**, 3, p. 163–83.

[26] Kelly J.M., Short R.D., Alexander M.R., "Experimental evidence of a relationship between monomer plasma residence time and carboxyl group retention in acrylic acid plasma polymers", *Polymer*, **2003**, 44(11), p. 3173–3176.

[27] Sciarratta V., Vohrer U., Hegemann D., Muller M., Oehr C., "Plasma functionalization of polypropylene with acrylic acid", *Surf. Coat. Technol*., **2003**,174–175, p. 805–810.

[28] Favia P., Sardella E., Gristina R., Milella A., D'Agostino R., "Functionalization of biomedical polymers by means of plasma processes: plasma treated polymers with limited hydrophobic recovery and PE-CVD of –COOH functional coatings", *J. Photopolym. Sci. Technol.,* **2002**,15, p. 341–350.

[29] Rivolo P., *Encyclopedia of Nanotechnology* "Nanostructures for surface functionalization and surface properties" Springer Science Business Media B.V., DOI 10.1007/978-90-481-9751-4, B. Bhushan (ed.), **2012**.

Experimental Section

Chapter VI

Plasma-polymerized acrylic acid thin films deposition: working conditions

6.1. Materials selected as substrates

The deposition of the plasma-polymerized acrylic acid PPAA) coatings (has been carried out on different substrates for the investigation and the optimization of the chemical-physical properties resulting in the final films according to the applied process parameters.

In particular conventional flat substrates, such as silicon (CZ/1-0-0, Boron/P-Type), polyethylene (Low Density PE; thickness 2.3 mm; Good Fellow) and corning (Danville) glass were used for the deposition of PPAA.

The characterizations performed on the different materials have confirmed the homogeneity of the surface coatings achieved by plasma polymerization, where the chemistry of the materials used during deposition does not affect the resulting film, since the functionalization mechanism is limited to the outer surface layers.

Moreover to investigate chemical properties by Infrared Spectroscopy, substrates with absorption in different spectral range were used. Spectra of deposited PPAA films were collected on PE and Corning glass substrates (Silicon was not used owing to its Refractive Index higher than the Diamond one). For Corning and PE, substrate contributions hide PPAA features in different complementary part of the selected spectral range thus allowing the investigation of the plasma polymer vibrational modes absorption in the 400-4000 cm^{-1} range.

In order to improve the adhesion of the polymers at the surface, substrates were rinsed in ethanol and dried under N_2 flux before putting in the chamber.

6.2. The experimental apparatus: the PECVD reactor

Plasma treatments were carried out at room temperature in a PECVD reactor composed of a stainless-steel vacuum chamber with cylindrical geometry (diameter = 320 mm; height = 200 mm), provided with lateral window for optical inspection and connected to a rotary pump.

Two horizontal parallel plates of 15 cm in diameter, placed at 4 cm far away from each other, act as electrodes.

The system is equipped by 4 different gas/vapour lines, one connected directly to the chamber and the other ones intercepted by the corresponding *reservoirs* (stainless steel cylinder 40 mm diameter and 100mm height) used for the storage of the liquid monomers. The *gas carrier*, Ar, flows into the line, passes through the reservoir containing the liquid monomer and is bubbled in the liquid.

Mass Flow Controllers (MFC - MKS), connected to pneumatic shutoff valves, control the Ar flow in the different lines while the gas-vapor mixture out-flow from the reservoir is regulated by a manual metering valve.

Figure 6.1 The inner of the vacuum chamber of the PECVD reactor

It is possible to apply an external heating "jacket", equipped with a thermocouple for the temperature monitoring, to the reservoir to increase the vapor pressure of the liquid reagent and completely convert it into the vapor phase.

The gas-vapour mixture, passing through its line, is then uniformly distributed in the reactor by the upper showerhead electrode (with pinholes of 2 mm diameter). Substrates are placed on the circular sample-holder that is the grounded electrode, parallel to the shower.

A rotative pump evacuates the chamber maintaining the base pressure at about 23 mTorr; this pump is connected to a zeolites trap able to absorb organic vapor residuals and prevent the oil pump reflux. It is possible to modify the chamber pressure by a throttle valve.

An absolute capacitive sensor, (maxima pressure sustained=10 torr) connected to the reactor by a lateral flange of the vacuum chamber, is used to measure the pressure.

Plasma activation is mediated by a radiofrequency generator working at a fixed frequency of 13,56 MHz and connected to the shower electrode.

A semi-automated impedance matching network (Hüttinger Elektronik GmbH) between the generator and the electrode allows to minimize the reflected power.

A function generator is used to pulse the plasma properly varying the on/off time (on time = T_{on}; off time = T_{off}) of the plasma discharge, with times of ON and times of OFF indipendently tunable between 1 ms and 999 ms.

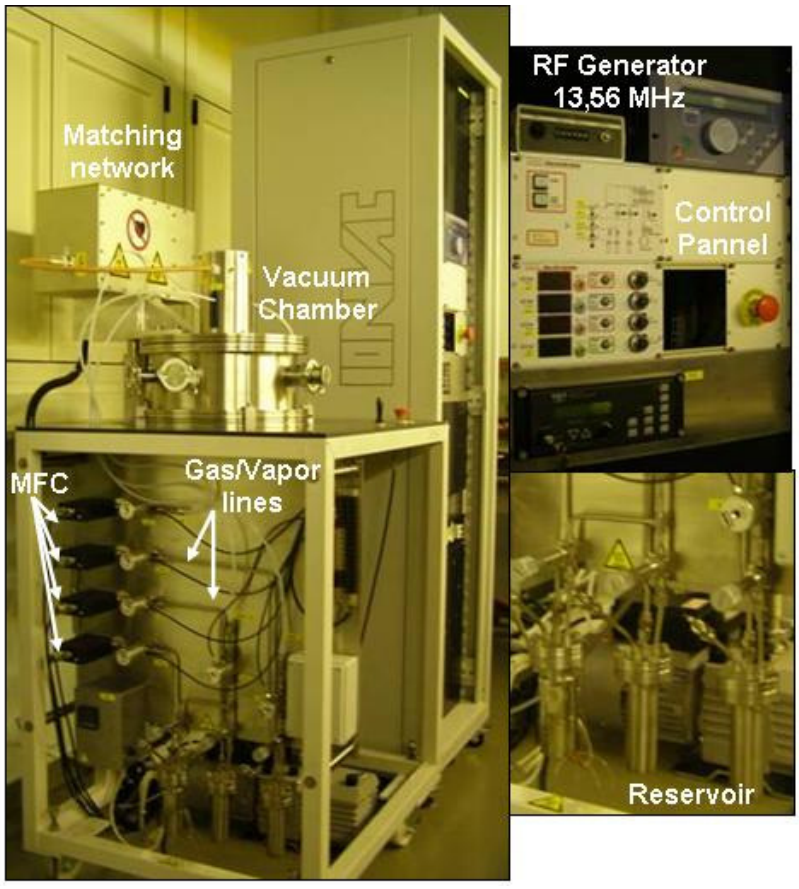

Figure 6.2 The PECVD reactor with its components

In the case of acrylic acid, the reagent containing reservoir is maintained at room temperature, without additional heating.

Argon (Ar) is used as gas carrier (flow =20sccm) and made bubbled in liquid AAc in order to enhance vapors formation (AA Vapor Pressure = 3.1 Torr @ 20C°) and transport them into the chamber.

The process pressure in presence of the Ar/AAc mix is set at 220 mTorr.

Modulated Waves processes are carried out; several duty cycle percentages (*D.C. %* = 100 * [$T_{on}/(T_{on}+T_{off})$]) and several pulsing periods ($T_{on}+T_{off}$) were tested for fixed *D.C. %* values. Finally different deposition times were explored for a certain process in order to correlate the dependence of film chemistry on PPAA coating thickness.

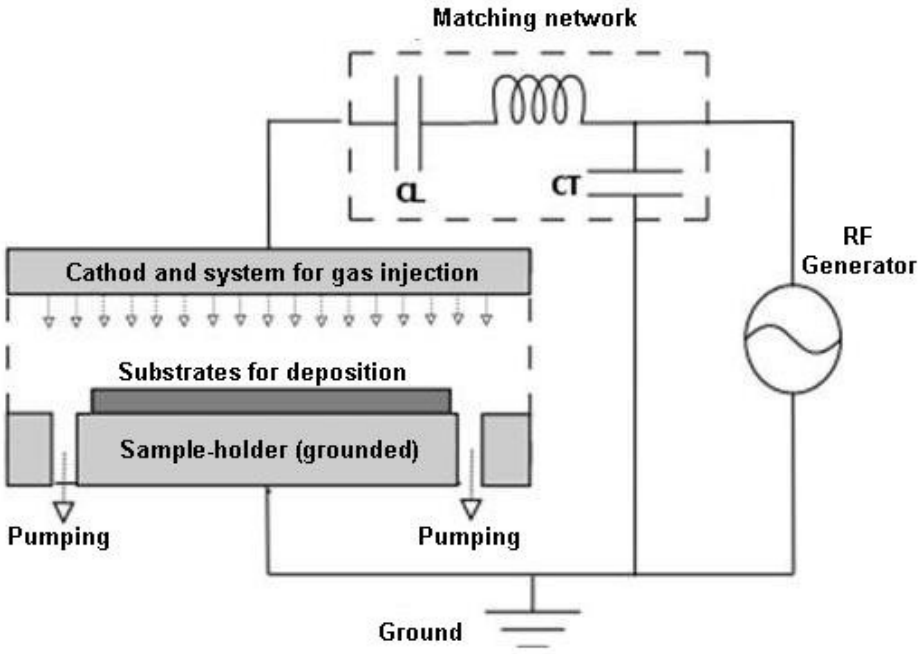

Figure 6.3 Scheme of the Plasma-Polymerization system

6.2.1. Measure of the vapor flow of the acrylic acid

The procedure for the surface functionalization by plasma processes usually needs the use of gas-vapor mixture, where the gas (usually Ar, N_2 or O_2) is applied to sustain the plasma discharge and eventually (in the case of molecular gases such as O_2 or N_2) to supply further radicals to the process reaction.

Organic vapors mixed to gas feed the system with active radicals deriving from the fragmentation of the starting molecules due to the anelastic collisions with the energetic electrons from the plasma.

The formation of the gas-vapor mixtures can be obtained in two different modes:

- The gas is injected separately by the line not passing through the *reservoir* and the liquid monomer is evaporated from the reservoir directly into the chamber without gas bubbling throughout the *reservoir*, in this case the mixture is formed in the expansion chamber of the shower electrode.

- The gas-vapor mixture is obtained by bubbling the gas throughout the liquid to evaporate contained in the *reservoir*, in this case the gas-vapor mixture is already formed when reaches the shower electrode.

In both cases the flow injected into the chamber can be regulated or measured with a good accuracy by the use of the Mass Flow Controllers connected to the lines; on the other hand the vapor flow mixed to the gas has to be measured by a different approach, using an indirect method based on the pressures relieved in the chamber.

Measuring the pressure (p) in the chamber is possible to calculate the overall flow $F_{gas+vapor}$ of gas and vapor, if note the efficient pumping rate S_{eff} by the following equation

$$F_{gas+vapor} = \frac{p\, S_{eff}}{RT}$$

It is relatively difficult to measure the efficient pumping rate S_{eff} so usually it is preferred to measure the flow $F_{gas+vapor}$ by indirect method, calculating the flow F_{equiv}able to produce the same pressure in the chamber at a fixed position of the throttle valve.

This procedure is correct with the approximation to consider the pumping rate the same for the gas-vapor mixture and for the gas only.

The low vapor/gas ratio in the mixture gives reason to this approximation.

Once known the overall flow of the mixture injected into the system, it is relatively easy to derivate by subtraction the flow related to vapor only, taking note of the flow value related to the bubbling gas by the mass Flow Controller reading

$$F_{vapor} = F_{gas+vapor} - F_{gas} \approx F_{equiv} - F_{gas}$$

Using these equations it has been possible to calculate the acrylic acid flow.

Practically, the total flow of the Ar+vapor mixture flowing out the *reservoir* was estimated by measuring the Ar gas flow which was needed to obtain the same pressure in the chamber, with the throttle valve set at the same position, thus having approximately the same pumping speed. The vapor flow without carrier was then estimated as the difference between the estimated total flow (Ar+vapor) and the measured Ar flow, and resulted to be approximately 3 sccm.

6.3. Plasma-Polymerization Processes from AA vapours

Pure Acrylic Acid, 99% (AA), liquid monomer was purchased by Sigma and used for the deposition of thin polymerized layers on different substrate using the PECVD reactor described in paragraph 6.2 . Depositions were carried out at room temperature, and the ground electrode is cooled.

Substrates to be functionalized were placed at the centre of the sample-holder.

Each plasma process described in the following paragraph is divided in two different steps. Before each deposition, in the same process, samples were treated for 3 or 5 minutes by plasma-etching with Ar or O_2 in order to clean the surface and improve its adhesion properties, activating it for the subsequent film deposition.

Several process parameters were investigated in order to single out the parameters combination suitable to obtain a stable thin coating characterized by a relatively-high density of surface functional groups, prone to give good reactivity.

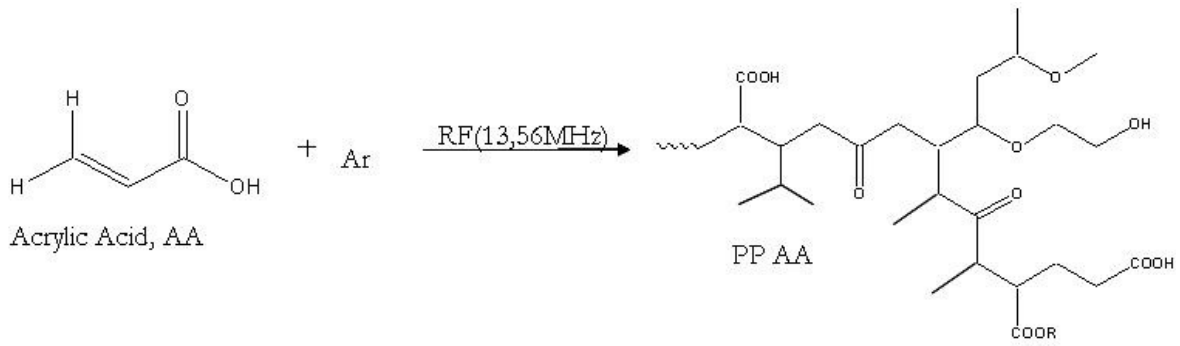

Figure 6.4 Plasma-poymerization of AA (RF plasma discharge sustained by Ar)

Plasma polymerization processes were performed in Continuous Wave (CW) and Modulated Wave (MW) mode respectively varying applied $Power_{RF}$, *D.C.%*, active discharge period and deposition time.

In Table 6.1 process parameters related to CW conditions are reported.

Processes Parameters	**Measured Value**
Ar flow	20 sccm
AAc flow	3 sccm
Working Pressure	206-248 mTorr
Deposition Time	20 min
Power (P_{RF})	5W, 25W, 50W, 60W, 70W, 100W

Table 6.1 Process parameters for plasma-polymerization of acrylic acid in Continous Wave

For CW processes, the discharge power was the only parameter varied, in order to investigate the effect of increasing the power on PPAA chemical composition.

In table 6.2 process parameters related to MW conditions are reported.

Processes Parameters	**Measured Value**
Ar flow	20 sccm
AAc flow	3 sccm
Working Pressure	206-248 mTorr
Deposition Time	5, 10, 20 min
Power (P_{RF})	100W, 200W
Duty Cycle (D.C.%)	5, 10, 20, 50
(T_{on}; T_{off})	(5;95) ms (20;80) ms (10;90) ms (50;50) ms (50;450) ms (20;180) ms

Table 6.2 Process parameters for plasma-polymerization of acrylic acid in Modulated Wave

In case of MW processes, not only Duty Cycle (related to the Average Power parameter) but also the associated T_{on} and T_{off} ratios for the same *D.C.* value were varied.

6.4. Characterization Analysis of PPAA films obtained in different conditions

After each deposition PPAA films were investigated using several characterization techniques in order to get both qualitative and quantitative information on the chemical-physical properties of the resulting polymers and to optimize, by tuning plasma process parameters, the final films characteristics in order to satisfy the particular application.

Samples, coated with PPAA films, were characterized just after the process and after rinsing in de-ionized water (de-H_2O). This step is of crucial importance due to the particular application: in any biological assay, samples are put in contact with aqueous fluids so they have to show water resistance. For this reason, after the process, plasma-polymerized films have been rinsed in de-H_2O for 20 minutes and then analyzed by the same methods performed before rinsing.

Moreover the use of complementary techniques give the possibility to have a detailed investigation on film properties for the subsequent study on the bio-reactivity of the film with biological species.

In the following paragraphs it is described how to apply the different surface characterization techniques (described in appendix A) for the analytical study on polymers structure and chemical composition.

6.4.1. Contact Angle Measurements

The surface properties, in particular wettability and hydrophilicity of deposited PPAA films have been investigated by OCA measurements on a OCAH 200 instrument (DataPhysic Instruments GmbH), equipped with a charge-coupled device camera and an automatic dosing system for the liquids. Deionized Water MilliQ grade (H_2O) and Diiodomethane (CH_2I_2 – Sigma Aldrich) were used as liquids (droplet volume = 1.5 µl), for the analysis using the sessile droplet method in static mode. Drop profiles were fitted through the Young–Laplace method, and contact angles between fitted function and base line were calculated by the SCA20 software.

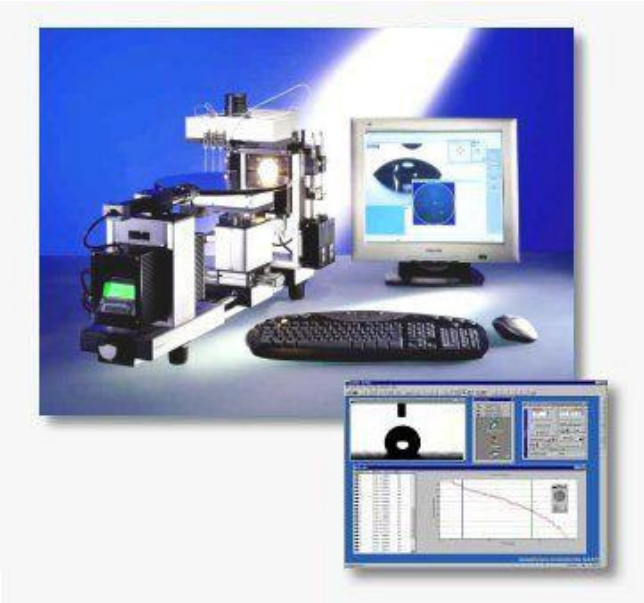

Figure 6.5 OCAH200 Contact Angle and relative software

Surface free energy of both the bare and the PPAA coated substrates (PE, corning glass, Silicon) was determined using Owens-Wendt-Kealble (OWK) method [1].

This method distinguishes between two components: one dispersive and one polar. The dispersive components is related to weak interactions such as London and Van der Waals forces, due to the presence of organic chains at the surface, while the polar components is related to Coulomb interactions (charge-charge interactions) mostly due to hydrogen bond formation. For this reason the measurements were carried out with two different liquids for the two different components, water (following the Ström model) and diiodomethane (following the Fowkes model) for the polar and the dispersive component respectively.

6.4.2. Attenuated Total Reflection-Fourier Transform Infra-Red Spectroscopy (ATR-FTIR) measurements

ATR FT-IR spectra were collected at 4 cm^{-1} resolution and 64 scans were accumulated for each spectrum on a Nicolet 5700 FTIR Spectrometer (ThermoFisher) equipped with a room temperature DTGS detector. Samples surface, put in intimate contact with a diamond crystal, were investigated by the Attenuated Total Reflection (ATR) mode.

Spectra of deposited PPAA films were collected on PE and Corning glass substrates (Silicon was not used as its Refractive Index is higher than the Diamond one) in order to observe the plasma polymer vibrational modes absorption in the 400-4000 cm^{-1} range.

Figure 6.6 Attenuated Total Reflection-Fourier Transform Infra Red spectroscopy

In fact, PE and Corning glass give rise to IR absorptions observable owing to the penetration depth of the produced evanescent wave that is greater than the nanometric thickness of the PPAA film. Therefore, substrate contributions hide PPAA features in different complementary part of the selected spectral range. In order to avoid instrumental fakes due to bare substrate spectrum subtraction, the spectra corresponding to the sum of PPAA and substrate contributions will be discussed without software elaboration. In table 6.3 several types of vibrational modes and their relative spectral ranges are reported.

Wave Number (cm^{-1})	**Type of Vibration**
2972-2880	C-H *stretching*
1470-1365	C-H *bending*
3650-3590	isolated -OH *stretching*
3550-3200	inter-molecule interacting –OH *stretching*
3200-2500	intra-molecule interacting –OH *stretching*
1725-1700	*stretching* C=O
1610-1550 1420-1300	*stretching* $-CO_2^-$
1320-1100	*stretching* C-O

Table 6.3 Correlation between the type of vibration of the chemical bonds (stretching or bending) and the corresponding wave number (cm^{-1}) values

6.4.3. X-Ray Photoelectron Spectroscopy (XPS)

The XPS measurements were carried out using a PHI 5000 *VersaProbe* Scanning ESCA microprobe. The photoelectrons emission from the surface of PPAAc films deposited on Silicon substrates were excited with a monochromatic Al$K\alpha$ radiation.

The survey spectra were acquired at 187.85 eV. A take off angle of 45° was used corresponding to a penetration depth of 7 nm.

The high resolution spectra of C1s and O1s were collected at 23.50 eV, with an overall energy resolution of 0.85 eV. All core-level peak energies were referenced to C1s peak at 285.0 eV assignable to the surface adventitious Carbon.

Figure 6.7 PHI Scanning X-Ray Microprobe

6.4.4. Ellipsometry

Ellipsometric measurements of the thin polymer films on reflecting surfaces were performed using a SE400adv ellipsometer (Sentech Instruments, Berlin, Germany). Δ and Ψ values for four angles of incidence, 50°, 60°, 65° and 75° were acquired at a wavelength of 633 nm. To calculate the thickness and the optical properties of the polymer films under investigation, fit procedures based on optical multi-layer models were applied to the ellipsometric data. The values for the refractive indices were taken from the literature. Nine measurements from different spots across each sample were averaged. The average values obtained by these measurements were compared to the ellipsometric data derived by the

measurements performed with a spectroscopic ellipsometer (J.A. Woollam Co., Inc. Ellipsometry Solutions), in order to validate these data.

Figure 6.8 Ellipsometer system

6.4.5. Electrokinetic (zeta potential characterization)

Streaming current (I_S) measurements were carried out at the Leibniz-Institut für Polymerforschung in Dresden using the in-house developed Microslit Electrokinetic Setup (MES). The instrument allows to perform streaming current measurements in dependence of the difference pressures (p) across a rectangular streaming channel formed by two sample surfaces (20 x 10 mm²) at variable channel height. As a key feature of the device the distance between the sample surfaces can be adjusted down to 1 µm keeping the surfaces parallel and without de-wetting of the samples.

For the characterization of a plasma-immobilized poly(acrylic acid) film a channel height of about 30 µm was used.

A cross-section of the sample carrier and positioning unit is shown in Fig. 6.8.

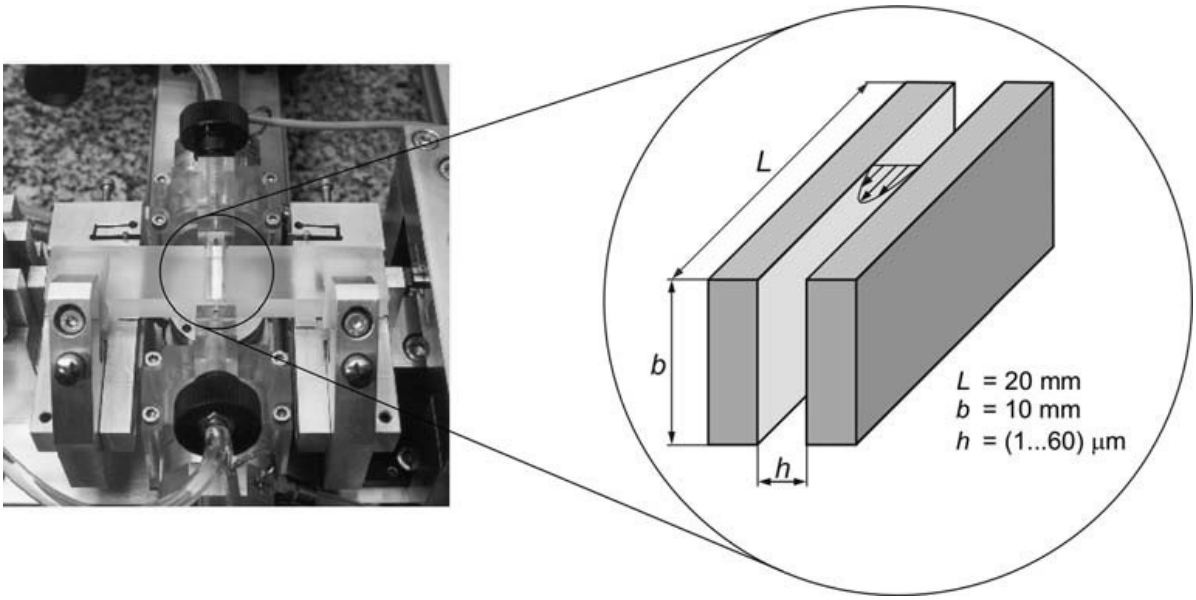

Figure 6.8 Microslit cell after alignment of the sample carriers (left) and schematic representation of the s streaming channel (right)

Polymer-coated sample carriers are fixed on a glass block and aligned in parallel under microscope. After the alignment, the slit formed by the sample carriers is sealed by silicon gaskets from all four directions simultaneously by a pneumatic system. Ag/AgCl electrodes for the measurement of the streaming potential and streaming current are positioned at the inlet and outlet of the channel. The precise distance adjustment is performed by means of a piezotranslator [2]

Streaming potential and streaming current measurements can be performed with the MES at varied pressure differences across the slit channel automatically including variation of electrolyte, its concentration and pH plus variation of the channel height, respectively.

The solutions for the measurements of plasma-polymerized films were prepared from vacuum-degassed DI water. The solution pH was adjusted by adding 0.1 M solutions of HCl or KOH. The titration was started in the alkaline pH range. At each pH the sample was equilibrated for about 40 min.

In order to make the results of the electrokinetic measurements better comparable with those obtained for other surfaces, apparent zeta potentials were calculated from the streaming current I_{str} applying the Smoluchowski equation.

$$I_{str}/\Delta P = \varepsilon_0 \varepsilon_r \mathrm{H} \ell \zeta / \eta L_0$$

where η is the dynamic viscosity of the fluid, ε_0, the permittivity of vacuum, ε_r, the dielectric constant of the fluid, p, the pressure difference across the slit channel, H, ℓ and L_0 are the channel dimensions , the height, the length and the width channel respectively

For electrokinetically ideal surfaces, i.e. surfaces without roughness, porosity, hairy layers or a patch-like distribution of chemical properties at the surface, the zeta potential is defined as the potential of an imaginary hydrodynamic shear plane separating an inner region where no fluid motion occurs and an outer region where fluid velocity takes non-zero values. However, in the case of soft interfaces, as for the thermo-responsive hydrogel films, such hydrodynamic shear plane does not exist. Therefore, the quantity calculated by the Smoluchowski equation is called apparent zeta potential.

6.4.6. Colorimetric Titration

The surface density of carboxylic groups available for a covalent binding with amino modified DNA probes was estimated by Toluidine Blue O (TBO, Sigma-Technical Grade) colorimetric titration. The amino group contained in TBO molecule (Fig. 6.9) reacts with a surface carboxylic group according to a 1:1 ratio [3].

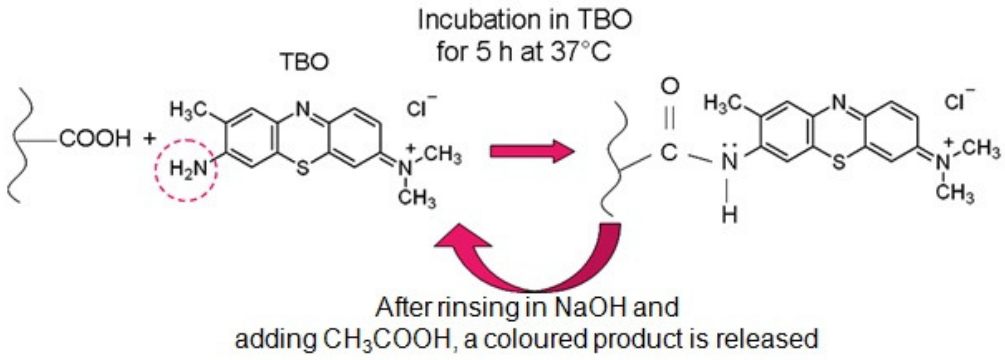

Figure 6.9 Toluidine Blueo O (TBO): colorimetric titration of the –COOH groups

Bare and PPAAc coated PE samples were contacted with 2 ml of 0.5 mM TBO aqueous solution (pH 10) at 30° C for 5 h. To remove unreacted dye, substrates were rinsed with copious amount of 0.1 mM NaOH solution (Fig. 6.9). The release of dye molecules reacted with –COOH terminations of the PPAAc film was promoted with 1ml of 50% (v/v) acetic acid solution. Dye maximum absorption in the recovered solutions (contained in quartz cuvette with an optical path of 0.5mm) was measured at 633 nm using an UV-Vis-NIR double

beam Varian Cary 500 spectrophotometer in transmission mode equipped with a specular reflectance unit with an angle of incidence 12°. This instrument contains a tungsten halogen visible source, a deuterium arc UV source, a R928 photomultiplier tube UV-Vis detector, and an electrothermally controlled lead sulfide photocell NIR detector. The result is an accessible wavelength range of 190-3200 nm. Wavelength dispersion is performed using dual double-sided gratings in a Littrow monochromator.

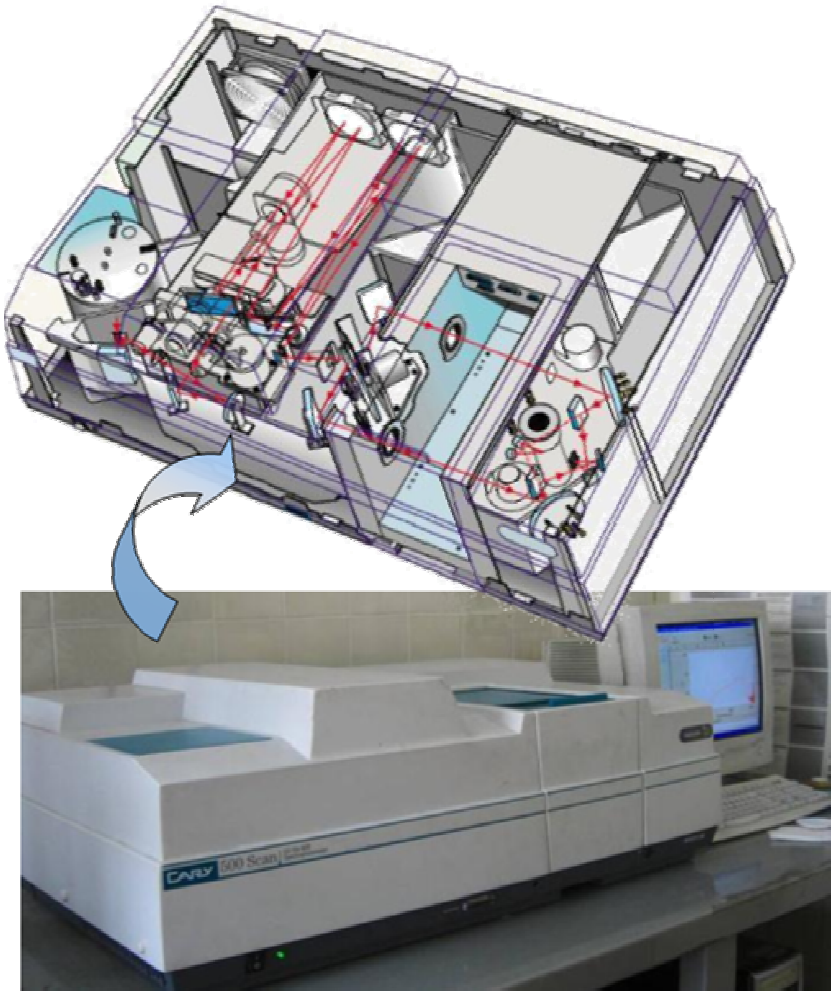

Figure 6.10 CARY 500 Scan UV-Vis-NIR Spectrophotometer and a schematical inner view of the system and the beam path

The advantage of a double beam instrument is the automatic compensation of instrumental phenomena such as source intensity and temperature fluctuations. Spectra were collected in 200-600 nm range at 2 nm resolution.

For a monochromatic radiation, the Absorbance, A_λ, of an absorbent specie in a solution with a certain concentration C is derived by Lambert-Beer law:

$$A_\lambda = \varepsilon_\lambda \, b \, C$$

where ε is the coefficient of molar absorbitivity and b is the path length of the sample.

For the measurements of TBO concentrations ε has to be necessarily constant. For this reason a calibration curve C/A_λ has been performed measuring the absorption of different solution having a known concentration of the absorbent specie (λ max = 633 nm), to calculate the slope of the curve corresponding to ε.

Once calculated ε,it is possible to proceed with the measures of TBO solutions resulting from the reaction with PPAA samples at the same wavelength (λ max = 633 nm).

According to Lambert-Beer Law, the estimation of number of reacted TBO molecules and subsequently, of PPAAc surface –COOH species was measured from the concentration C, taking into account effective area of measured samples.

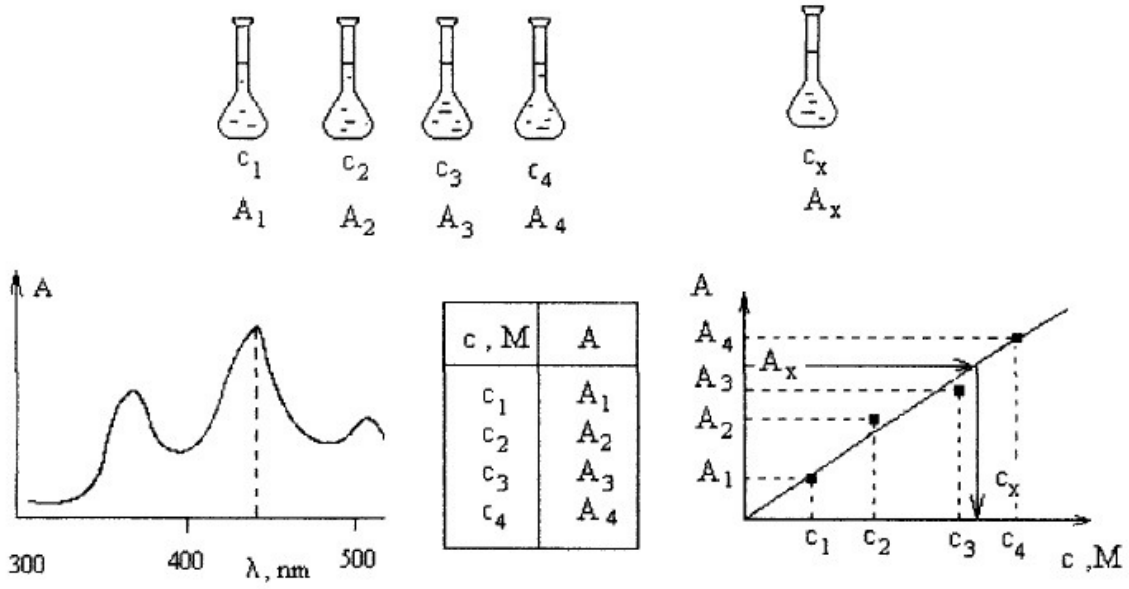

Figure 6.11 Calibration Curve of TBO solutions

6.5. Study of the reactivity of PPAA films towards biomolecules

Before the real application of the PPAA films to biosensors devices, the thin functional films were tested for their reactivity towards different biomolecules such as proteins A and bovine serum albumine (BSA).

Two different characterizations were applied in order to verify the formation of a stable binding between the carboxylic (-COOH) groups exposed at the surface and the amino groups ($-NH_2$) of the biomolecules. Before the incubation with the protein, the PPAA samples were rinsed in de-ionized water.

6.5.1. Fluorescence Microscopy

Fluorescence Microscopy was exploited in order to verify the presence of a labelled protein opportunely bound to the PPAA films. The protein A was conjugated with a fluorofor (Alexa-Fluor 546) thus enabling the detection by fluorescence emission.

A LEICA DM-LM microscope (objective 20X) equipped with a Hg vapour lamp (50W) and a digital camera DFC340 FX, was used. By an opportune combinations of the filters is possible to selectively detect the fluorescent markers for a large number of molecules. In this case L5 combination of filters was used for the detection of species conjugated with fluorescein label.

This technique is just a preventive step in order to verify the “bio- functionality” of the films deposited on Silicon and Corning substrates by plasma-polymerization.

6.5.2. Quartz Microbalance Technique

Microgravimetry is a generic name for sensitive analytical techniques based on measuring minor changes in the mass or density of an object. In the context of biomedical applications microgravimetry could allow the measuring of mass as small as that of single biomacromolecule. The most sensitive methods are based on piezoelectricity. Among them the most common technique is known as quartz crystal microgravimetry or microbalance technique usually abbreviated as QCM.

The QCM method, which detects mass change at nanogram scale, is the most widely used technique for exploration of complex interfacial phenomena. It is also sometimes called quartz microBalance (abbreviated QMB), quartz crystal resonance sensor (QCRS) or quartz crystal immittance (QCI, QCM-Δf-ΔR or QCM- ΔR).

In a quartz crystal microbalance, a mechanical oscillation is induced by an applied alternating current via the piezoelectric effect. Concerning the Quartz Microbalance with Dissipation (QCM-D setup), frequency shifts Δf and dissipation shifts ΔD that are due to additional surface layer and bulk solution effects (i.e., film adsorption or bulk viscosity change, respectively) can be measured at several overtones simultaneously. Here, for rigid films a linear dependency between Δf and the adsorbed surface density Γ is valid whereas for viscoelastic surface layers additional energy dissipation and a frequency (overtone)-dependent response have to be taken into account.

In describing the surface layer as a viscoelastic solid with a frequency-dependent complex shear modulus,

$$G = \mu_l + if\eta_l$$

in the Voigt–Voinova representation, [4] [5] Δf and ΔD can be assigned to a film with uniform thickness d_{visc}, density ϱ_l, elastic shear (storage) modulus μ_l, and shear viscosity (loss modulus) η_l.

Additionally the film deposited on the Au-coated electrode is assumed to be in contact with a Newtonian fluid under no-slip conditions.

An ellipsometry-compatible QCM-D module from Q-Sense was used (QELM 401, Q-Sense, Frölunda, Sweden) and installed on the ellipsometer base. The ellipsometry module is made of Teflon and titanium and is equipped with windows of quartz glass at an angle of incidence of 65°. The cell allows a small liquid volume (100 µl) above the crystal surface. Measurements were done in flow either with a constant flow rate of 0.4 ml/min or with stagnant solutions.

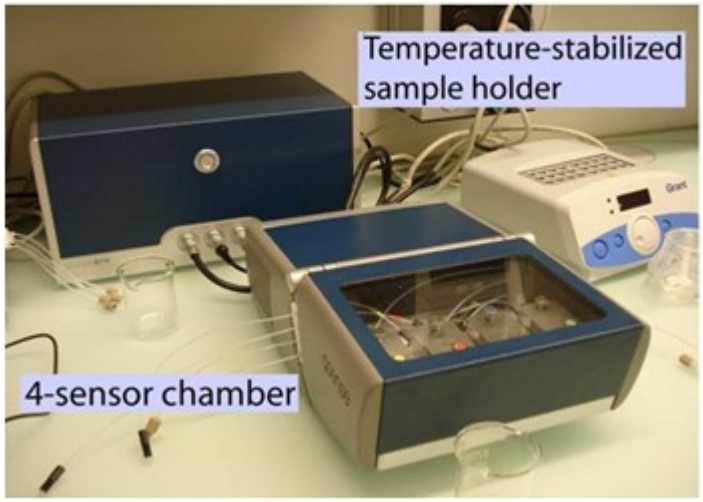

Figure 6.12 Quartz Microbalance (QCM) set-up

The temperature was monitored over the whole experiment and held constant at 23 °C. For the exchange of liquids a syringe pump (NE-500 OEM, New Era Pump Systems, Inc., Farmingdale, NY, USA) was applied to increase the flow gradually.

Experiments were carried out by starting with the PPAAc film in water and then exchanging the solution in constant flow at 0.4 ml/min to 0,1 mg/ml BSA in buffer solution (PBS) to perform the absorption on PPAAc films. Adsorption at constant flow conditions was monitored for 30 min at pH 5.2 (BSA IEP = 5,6). Desorptions were carried out in different conditions (with PBS pH 7,6 and with Sodium Dodecyl Sulfate, SDS)

References

[1] Owens D.K., Wendt R.C., "Estimation of the surface free energy of polymers", *J. Appl. Polym. Sci.,* **1969**, 13, p 1741-1747.

[2] Zimmermann R., Osaki T., Schweiß R., Werner C., "Electrokinetic microslit experiments to analyse the charge formation at solid/liquid interfaces", *Microfluid Nanofluid,* **2006**, 2, p 367–379.

[3] Chen J.P, Chiang Y.P, *J. Membr. Sci*., **2006**, 270, p 212-220.

[4] Voinova M. V., Jonson M., Kasemo B., "Dynamics of viscous amphiphilic films supported by elastic solid substrate", *J. Phys.: Condens. Matter,* **1997**, 9, p 7799.

[5] Voinova M. V., Jonson M., Kasemo B., "Missing mass effect in biosensor's QCM applications", *Biosens. Bioelectron.,* **2002**, 17, 835.

Chapter VII

Plasma-polymerized acrylic acid thin films deposition: experimental results

A preliminary study on the plasma-polymerization processes was carried out by acrylic acid monomer, experimenting different working conditions as described in Chapter VI.

In order to optimize the functionalization procedure by deposition of plasma-polymerized thin films, the physico-chemical properties of these coating were investigated after each deposition (Chapter VI) and results related to this characterization study are reported in this chapter.

In particular both Continous and Modulated Waves Processes were tested, to find the more suitable conditions of plasma discharge in order to obtain a stable coating deposited on the substrate with a relative high density of functional groups at the surface and resistant to contact with water and other liquid means.

7.1. Continous Wave (CW) plasma-polymerized acrylic-acid films

7.1.1. Contact Angle Results

PPAA coatings, as described in Chapter VI, were deposited on different substrates. The OCA angles were performed on Silicon (Si), Corning glass (Corning) and Polyethylene (PE) before plasma deposition in order to characterize substrate's properties before functionalization.

substrate	OCA_{H_2O} deg	$OCA_{CH_2I_2}$ deg	W_{sl} mN/m	W^d_{sl} Watt	W^h_{sl} min
Si	47±1	46±3	53,24	25,29	27,95
Corning	54±1,5	38±2	50,88	30,94	19,94
PE	90±3	49±3	34,94	33,02	1,92

Table 7.1 OCA measurements performed on Silicon, Corning and Polyethylene substrate before plasma polymerization

As reported in chapter VI (Table 6.1) several process parameters related to CW conditions were tested

Processes Parameters	Measured Value
Ar flow	20 sccm
AAc flow	3 sccm
Working Pressure	206-248 mTorr
Deposition Time	20 min
Power (P_{RF})	5W, 25W, 50W, 60W, 70W, 100W

Table 6.1 Process parameters for plasma-polymerization of acrylic acid in Continous Wave

The resulting plasma-polymerized acrylic-acid were analyzed by contact angle measurements using two different liquids (water, H_2O and diiodomethane, CH_2I_2), in order to investigate not only on hydrophilic/hydrophobic properties of the polymers but also to calculate the surface energy W_{sl} of these films expressed in the two components (see Chapter VI). On each sample four measurements of OCA_{H2O} and OCA_{CH2I2} were performed in order to determine the average value of the contact angle.

As described in Chapter VI measurements were performed on Silicon (Si), Corning and Polyethylene (PE) and results confirm the homogeneity conferred by plasma coatings, OCA angles in fact show very similar values for the three type of substrates, since the substrate chemistry is not involved in the functionalization mechanism if mediated by plasma

processes. Tables 7.2, 7.3 and 7.4 show OCA results with both the two liquids (H_2O and CH_2I_2) of PPAA films deposited in CW on Si, Corning and PE substrates respectively.

P_{RF} Watt	OCA_{H_2O} deg	$OCA_{CH_2I_2}$ deg	W_{sl} mN/m	W^d_{sl} mN/m	W^h_{sl} mN/m
5	17±1	37±2	70,16	26,05	44,11
25	12±1	39±2	71,38	25,26	46,12
50	13,3±0,8	36±2	71,29	26,58	44,71
75	47±2	35±2	55,39	31,03	24,36
100	62,3±0,9	28,3±0,9	49,33	37,22	12,11

Table 7.2 OCA measurements performed on Si substrates coated with PPAA films obtained in CW plasma processes

P_{RF} Watt	OCA_{H_2O} deg	$OCA_{CH_2I_2}$ deg	W_{sl} mN/m	W^d_{sl} Watt	W^h_{sl} min
5	17±1	34±2	70,17	27,36	42,81
25	9±3	40±3	72,05	24,34	47,71
50	12±2	33±3	71,73	27,79	43,94
75	55±2	33±1	51,64	33,59	18,05
100	62±1	26±2	50,07	37,94	12,13

Table 7.3 OCA measurements performed on Corning substrates coated with PPAA films obtained in CW plasma processes

P_{RF} Watt	OCA_{H_2O} deg	$OCA_{CH_2I_2}$ deg	W_{sl} mN/m	W^d_{sl} Watt	W^h_{sl} min
5	16±2	31±2	70,54	28,74	41,8
25	13±2	36±1	71,19	26,08	45,11
50	15±1	30,04±0,7	71,19	28,89	42,3
75	48±3	27±2	56,55	34,36	22,19
100	59	26	49,42	35,14	14,28

Table 7.4 OCA measurements performed on PE substrates coated with PPAA films obtained in CW plasma processes

Results from the tables confirm the uniformity of the surface coating achieved by plasma-polymerized thin films deposition. OCA_{H2O} measured on the corresponding PPAA coatings deposited on Silicon, Corning glass and Polyethylene show a similar trend confirming the absence of dependency of the film surface properties on the nature of the substrate, flatness being comparable.

This surface modification, in fact, does not depend on the bulk of the substrate but only the upper layers are involved in the reaction with the plasma polymers.

Figure 7.1 shows OCA water contact angles (OCA_{H2O}) on PPAA films obtained in Continuous Wave at increasing $Power_{RF}$ and deposited on PE substrates ($OCA_{H2O} \approx 82°$). According to Power increase, 5W → 100W, a progressive increasing in the OCA_{H2O} values as a consequence of the growing hydrophobicity of deposited PPAA surface is observed.

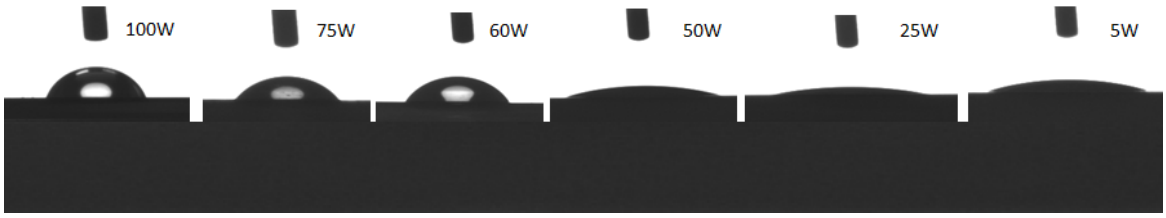

Figure 7.1 OCA_{H2O} measurements performed on PE substrates coated with PPAA films obtained in CW plasma processes

The OCA characterization of PPAA films performed in CW points out the following considerations:

- OCA_{H2O} values decrease as the power decreases itself and generally are lower than the ones calculated on the uncoated substrate showing an hydrophilic behaviour of the surface after PPAA coating deposition
- For $P_{RF} \leq 50$ W, OCA_{H2O} values range from 10° to 20°, so showing a strong hydrophilic behavior of PPAA surface due to the low fragmentation of the acrylic acid monomer during plasma treatment and resulting in low reticulation and high -COOH groups retention. For $Power_{RF} > 50$W, OCA_{H2O} angles are in the range 50°-60

- For $P_{RF} \geq 50$ W, OCA_{H2O} angles are in the range 50°-60°, indicating an hydrophobic behaviour of the materials due to the higher cross-linking degree and so a lower number of –COOH groups exposed at the surface of the PPAA polymers

Increasing the power, the fragmentation of the AA monomer due to plasma discharge increases itself accompanied by a loss of carboxylic functionalities in the final structure as gaseous CO_2 and CO species and with an higher ionic bombardment on the growing plasma-polymer.

The calculation, using the Owens-Wendt-Keable approach, of the surface energy at the interface solid/liquid, divided into its two components, gives information on what type of interactions predominate at the film surface according to carboxylic groups density:

- W_{sl} decreases as the power increases
- W^{d}_{sl} dispersive component (weak forces) is not affected by the power changes
- W^{h}_{sl} polar component (hydrogen bonds) decreases as the power increases

The dispersive interactions at the interface solid/liquid are not depending on the –COOH groups surface density, so the adhesion is only affected from the polar component.

For $P_{RF} \geq 50$ W, adhesion properties remain unchanged, thus suggesting the existence of a certain threshold value for power above which surface properties do not vary anymore. For low power plasma-polymers, the higher density of carboxylic groups at the surface enables the formation of hydrogen-bond interactions with H_2O molecules of the test liquid, thus contributing to the increase of the polar component, W^{h}_{sl}, in the surface energy value $W_{s.}$

W^{h}_{sl} high value suggests another type of interaction at the interface solid/liquid: the formation of intra-molecular H-bonds between the –COOH groups which are close each other in the molecule. Therefore, a thermodynamic equilibrium is established between the intra-molecular H-bonds formed within the carboxylic groups in the PPAA film and the number of inter-molecular H-bonds between –COOH groups exposed at the surface and water molecule of the test liquid phase.

7.1.2. Attenuated Total Reflection-Fourier Transform Infra-Red Spectroscopy (ATR-FTIR) Spectroscopy Results

The qualitative investigation by FTIR-ATR spectroscopy gives information about the chemical composition of the PPAA film and on the type of interaction existing between the chemical groups.

In Continous Wave processes, the chemistry of the polymers performed at high power conditions is different compared to the chemical composition of films obtained at low power input.

For all the PPAA spectra a broad band between 3600-2800 cm^{-1} is present both for high and low power processes.

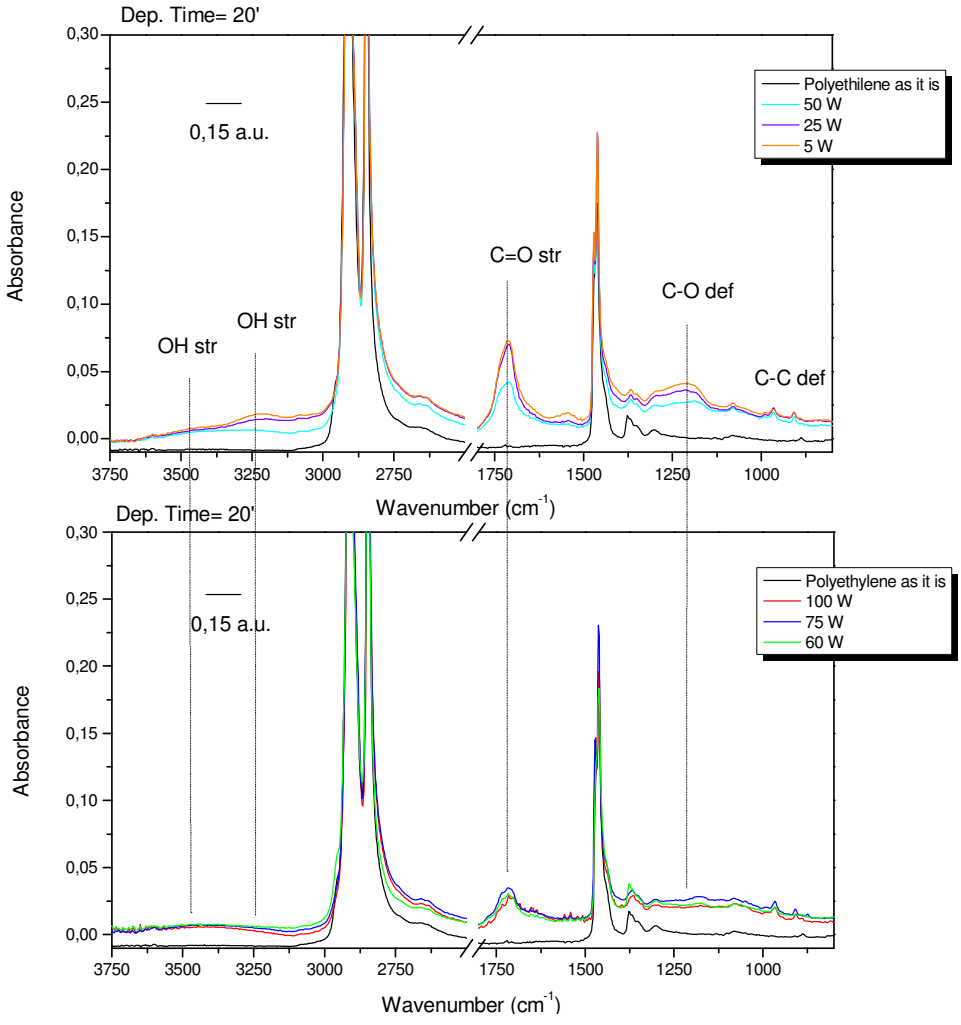

Figure 7.2 FTIR-ATR spectra measured on PE substrates coated with PPAA films obtained in CW plasma processes

In Figure 7.2 and 7.3 the band between 3470 and 3450 cm^{-1} assigned to the absorption of the isolated O-H stretching mode [1] appears more intense (orange line) in CW films obtained at high $Power_{RF}$ regime respect to PPAA obtained at low $Power_{RF}$; on the other hand, the signals related to inter-molecule interacting O-H species centered at 3223 cm^{-1} [1] increases as the power decreases. This feature confirms, in accordance with OCA characterization, that, at high $Power_{RF}$, the molecule fragmentation dominates throughout the process while, for low power processes, due to the higher retention of carboxylic monomer structure, the higher surface density of -OH groups promote the formation of hydrogen bonds.

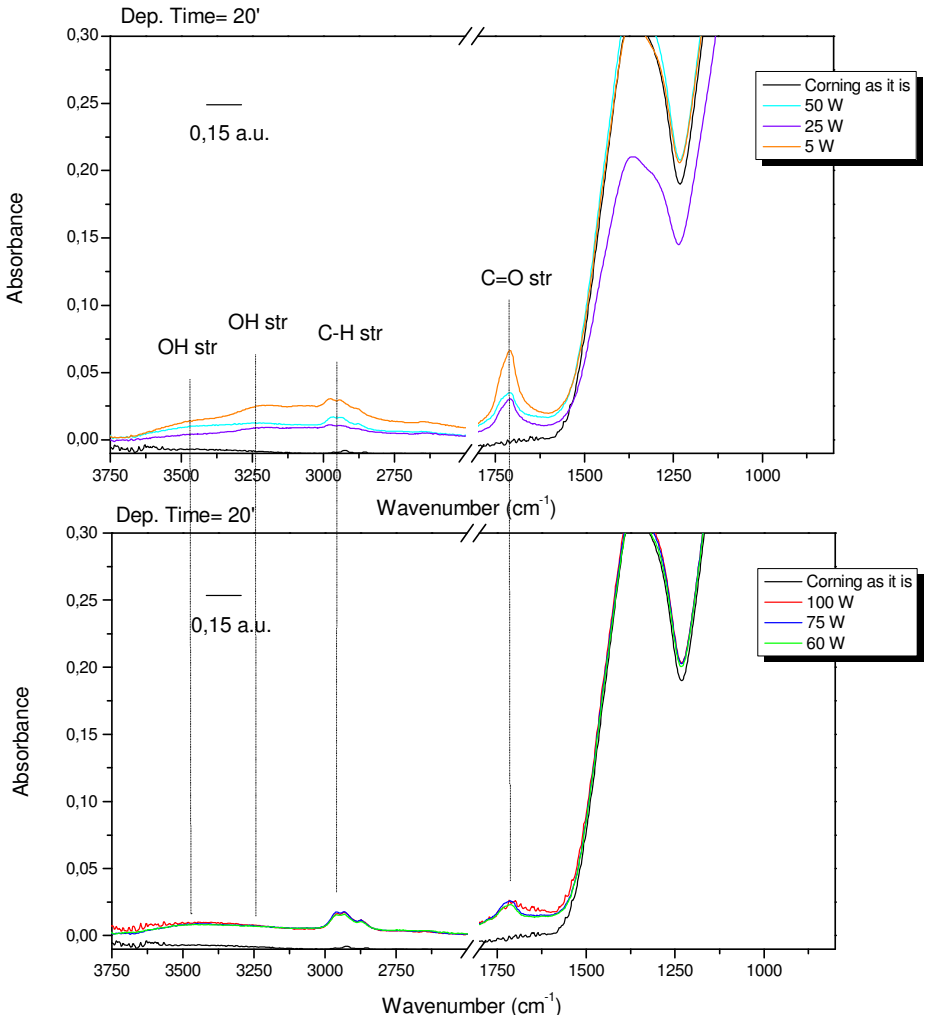

Figure 7.3 FTIR-ATR spectra measured on Corning substrates coated with PPAA films obtained in CW plasma processes

In addition, CW films spectra show, at 2980-2870 cm^{-1} the signals related to aliphatic C-H stretching mode (Fig 7.3) and at 1730-1710 cm^{-1} the absorption related to C=O stretching, corresponding to both carboxylic and carbonylic functionality [1].

The intensity of this absorption is higher for PPAA films obtained in low $Power_{RF}$ regime, as expected from previous results. Finally, the C-H bending mode at 1460 -1370 cm^{-1} and the C-O stretching mode at 1200 cm^{-1} are observable in all spectra of Fig. 7.2.

FTIR-ATR results are in accordance with the previous considerations related to OCA characterization analysis: in low power plasma-processes, molecule fragmentation and ionic bombardment of the growing polymer are reduced, resulting in an higher monomer structure retention and an higher carboxylic groups surface density; on the other hand PPAA films obtained in high power conditions show an opposite behavior with a loss of carboxylic functionalities and more reticulated polymeric structure.

7.2. Modulated Wave (MW) plasma-polymerized acrylic-acid films

Concerning Modulated Wave (MW) plasma-processes, several conditions were tested in order to tune experimental parameters according to the final film properties. Also in this case plasma-polymerized thin films were deposited on Silicon, Corning glass and Polyethylene.

7.2.1. Contact Angle Results

Several process parameters related to MW conditions were tested (Table 6.2) .

Processes Parameters	**Measured Value**
Ar flow	20 sccm
AAc flow	3 sccm
Working Pressure	206-248 mTorr
Deposition Time	5, 10, 20 min
Power (P_{RF})	100W, 200W
Duty Cycle (D.C.%)	5, 10, 20, 50
(T_{on}; T_{off})	(5;95) ms (20;80) ms (10;90) ms (50;50) ms (50;450) ms (20;180) ms

Table 6.2 Process parameters for plasma-polymerization of acrylic acid in Modulated Wave

As for CW processes, the resulting MW plasma-polymerized acrylic-acid (deposited on Si, Corning and PE substrates) were analyzed by contact angle measurements using two different liquids (water, H_2O and diiodomethane, CH_2I_2), in order to investigate not only on hydrophilic/hydrophobic properties of the polymers but also to calculate the surface energy W_{sl} of these films expressed in the two components (see Chapter VI).

P_{RF} Watt	*D.C.* %	t_{on} ms	t_{off} ms	P_{AVE} Watt	Time min	OCA_{H_2O} deg	$OCA_{CH_2I_2}$ deg	W_{sl} mN/m	W^d_{sl} mN/m	W^h_{sl} mN/m
100	5	5	95	5	20	14±1	39±2	70,99	24,99	46
200	5	5	95	10	20	9±1,4	35±5	72,33	26,76	45,57
200	10	10	90	20	20	13,3±0,6	33±2	71,47	27,69	43,78
200	10	50	450	20	20	49±4	32±3	54,8	32,82	21,98
200	10	20	180	20	20	29±2	35±2	65,03	28,06	36,97
200	10	10	90	20	10	25±2	32±2	67,24	29,19	38,05

Table 7.5 OCA measurements performed on PE substrates coated with PPAA films obtained in MW plasma processes

P_{RF} Watt	*D.C.* %	t_{on} ms	t_{off} ms	P_{AVE} Watt	Time min	OCA_{H_2O} deg	$OCA_{CH_2I_2}$ deg	W_{sl} mN/m	W^d_{sl} mN/m	W^h_{sl} mN/m
100	5	5	95	5	20	11±3	30±3	72,24	29,02	43,22
100	50	50	50	50	20	49±3	29±2	53,71	32,84	20,87
200	5	5	95	10	20	9±2	36±4	72,26	26,33	45,93
200	10	10	90	20	20	14±1	34±3	71,37	27,4	43,97
200	10	50	450	20	20	47±3	30±3	53,59	32,54	21,05
200	10	20	180	20	20	26±2	30±3	67,23	29,86	37,37
200	10	10	90	20	10	25±4	33±4	67,2	28,9	38,3

Table 7.6 OCA measurements performed on Corning substrates coated with PPAA films obtained in MW plasma processes

P_{RF} Watt	*D.C.* %	t_{on} ms	t_{off} ms	P_{AVE} Watt	Time min	OCA_{H_2O} deg	$OCA_{CH_2I_2}$ deg	W_{sl} mN/m	W^d_{sl} mN/m	W^h_{sl} mN/m
100	5	5	95	5	20	14±2	40±5	70,94	24,49	46,45
100	20	20	80	20	20	14±1	34±4	71,29	27,23	44,06
100	50	50	50	50	20	55±2	32±4	51,86	33,96	17,9
200	5	5	95	10	20	11±1,5	39±3	71,72	25	46,72
200	10	10	90	20	20	18±3	30±3	70,34	29,39	40,95
200	10	50	450	20	20	55±2	32±2	49,67	32,95	16,72
200	10	20	180	20	20	28±2	34±3	66,07	28,72	37,35
200	10	10	90	20	10	24±2	33±4	67,76	28,34	39,42

Table 7.7 OCA measurements performed on PE substrates coated with PPAA films obtained in MW plasma processes

Also in case of MW PPAA films, OCA angles show very similar values for the three type of substrates, confirming the coating homogeneity.

As for CW processes, also in case of pulsed plasma, the general trend shows an increase in the surface hydrophilicity, after PPAA deposition.

OCA results concerning Modulated Wace processes reveal the following behavior:

- OCA_{H2O} values decrease as the P_{AVE} decreases itself
- low Duty Cycle (*D.C.*) plasma-processes give films similar to the conventional acrylic acid polymers, exposing an high number of -COOH groups and showing high monomer structure retention
- as the T_{on} decreases, OCA_{H2O} angles decrease due to the predominance of radical-monomer reactions taking place during the T_{off} step and so retaining carboxylic groups structure

Concerning processes performed in MW mode, OCA_{H_2O} values (Tables 7.5, 7.6, 7.7) decrease from 50° to 10° as the Average $Power_{RF}$ $\left(P_{AVE} = P_{RF}\ \frac{T_{on}}{T_{on}+T_{off}}\right)$, regardless of P_{RF} starting value, diminishes.

Deposition time (20 min and 10 min) can vary the properties of reconstructed surface: the shorter process seems to produce a slightly less hydrophilic surface, suggesting that the chemistry of the coatings is not homogeneous along the growth profile owing to the coexistence of fragmentation, film deposition and surface ablation weighting each one differently along time process.

Furthermore, for low *D.C.%* values (Processes nr 1 and 4), the surface show higher hydrophilicity, regardless the applied $Power_{RF}$ (100W and 200W, respectively) as the monomer structure is strongly retained owing to the short T_{on} discharge pulse that leads to a very low P_{AVE} and so to an applied low net energy for fragmentation.

The results of OCA measurements suggest that using MW processes is possible to more finely play with process parameters.

7.2.2. Attenuated Total Reflection-Fourier Transform Infra-Red Spectroscopy (ATR-FTIR) Spectroscopy Results

As for Continous Wave FTIR-ATR characterization, also for Modulated Wave plasma processes the spectra of the resulting films reveal the qualitative chemical composition of the PPAA coatings.

Figures 7.4 and 7.5 show FTIR-ATR spectra of PPAA films obtained by pulsed plasma processes.

The same vibrational features observed for low power CW processes are accounted for low $Power_{AVE}$ and low *D.C.%* regime MW PPAA films (Figure 7.4 and 7.5).

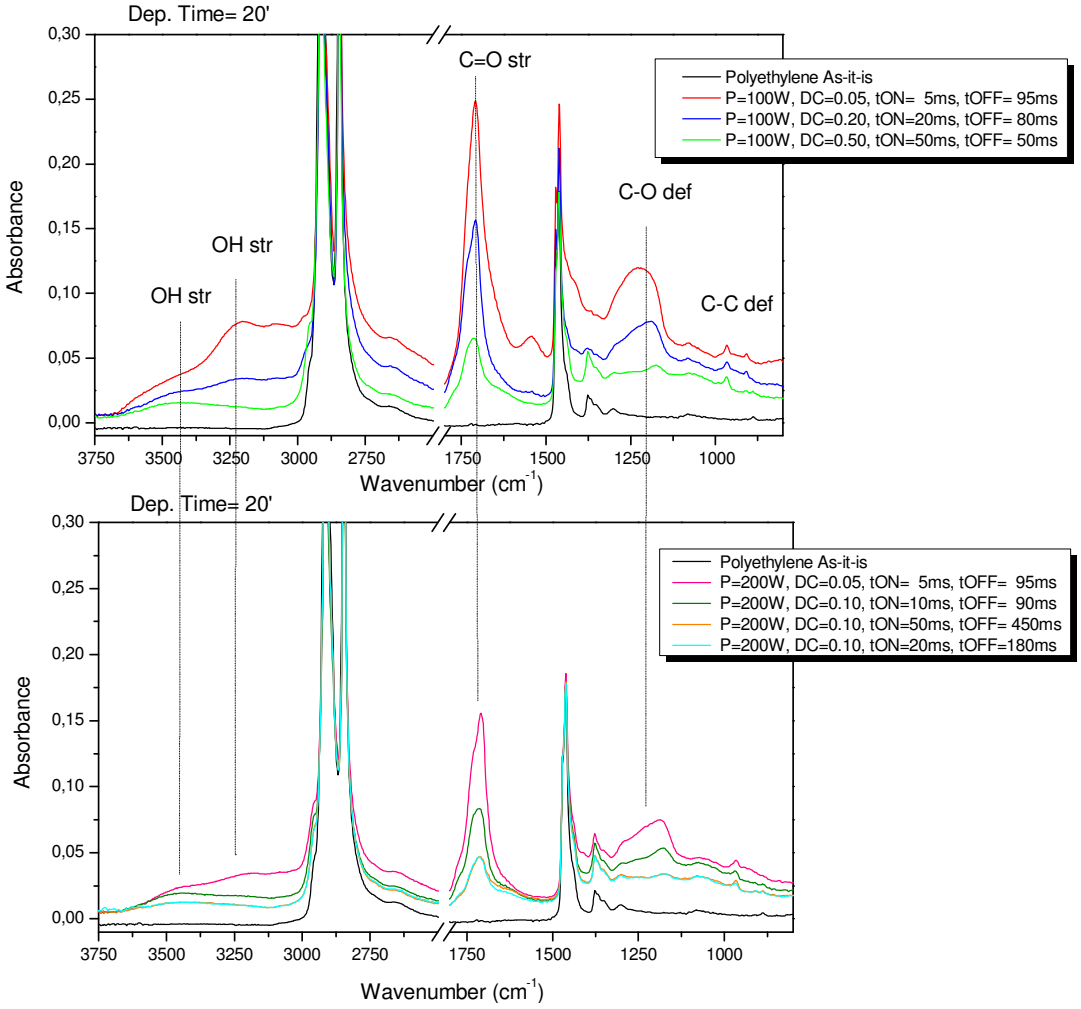

Figure 7.4 FTIR-ATR spectra measured on PE substrates coated with PPAA films obtained in MW plasma processes

The C-O stretching mode at 1200 cm^{-1} and the broad band assigned to interacting –OH groups show significant intensities due to the reduced fragmentation of the –COOH groups and to the reassembly of the growing film during the long T_{off} pause. As already shown by OCA characterization, a high amount of -COOH groups interconnected through aliphatic chains is reliable. If a starting $Power_{RF}$ (200W) is applied, along with the increase of *D.C.%*, intensities of the above cited bands decrease due to the resulting higher networking.

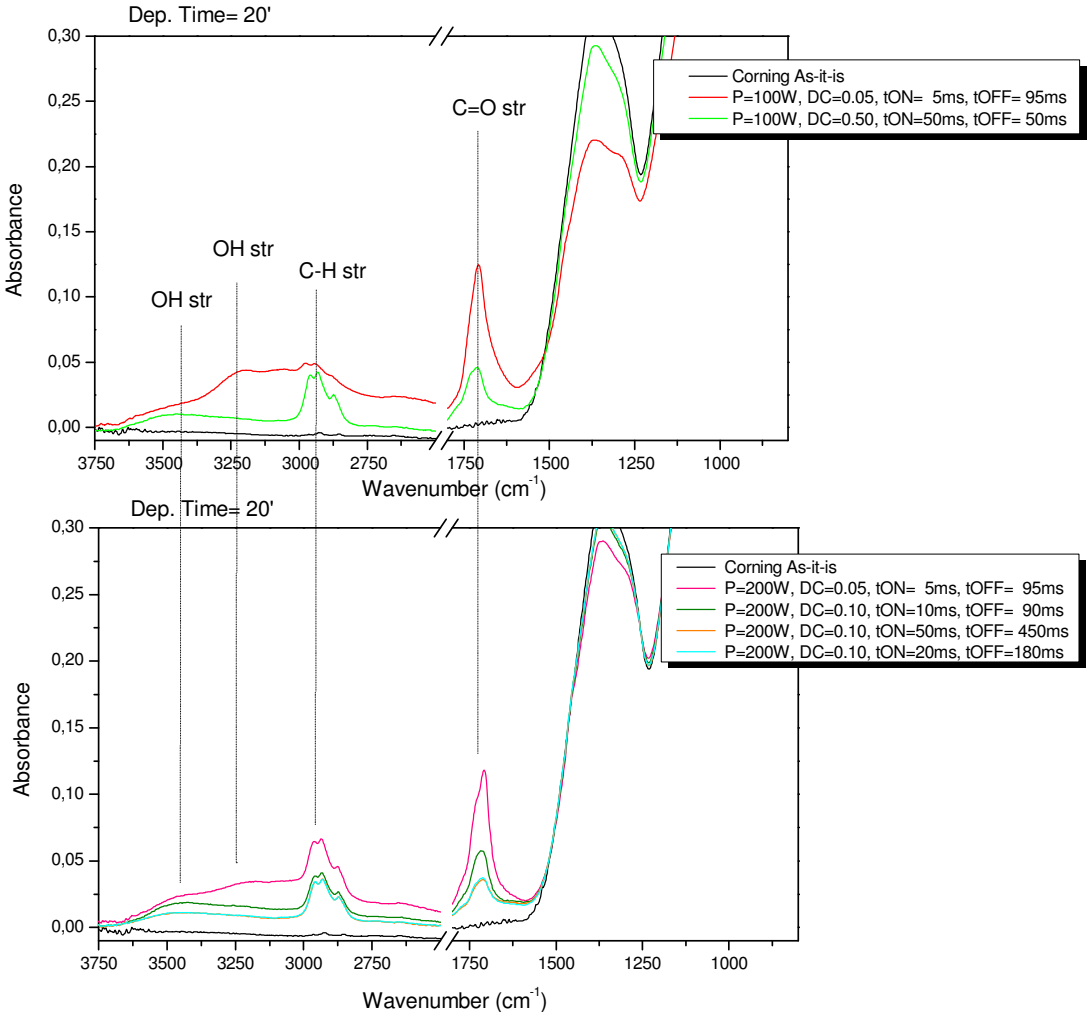

Figure 7.5 FTIR-ATR spectra measured on Corning substrates coated with PPAA films obtained in MW plasma processes

Moreover the great increase in the intensity of the band assigned to the C=O stretching is not followed by a similar behavior of the peaks related to the backbone chain (C-C deformation) absorption modes which are the unique features exclusively assignable to a higher or lower amount of investigated material, thus suggesting that the peaks intensity variation does not depend on the observed differences in films thickness.

This preliminary characterization suggest that MW processes not only allow the activation of simple organic molecules without destroying their chemical functionality but also enable the polymerization reaction in the gas phase according to a mechanisms that closely resemble the traditional radical chain polymerization, though with a low degree of order.

7.3. Study of the PPAA films stability after rinsing in water

The preliminary study carried out on plasma-polymerized acrylic acid films has revealed that tuning plasma parameters the resulting chemical properties can be modified, and mainly by applying "soft" plasma conditions (low power or low $Power_{AVE}$ and low *D.C.%* regime), thin films with an higher retention of carboxylic functionalities suitable for the binding with biomolecules amino groups could be obtained.

Stability after contact with aqueous solutions and/or body fluids of such functional polymers to be applied in biological assays as biomaterials or biocompatible grafting surfaces is a crucial step.

After rinsing, PPAA films are expected to show not only chemical stability but also resistance to delamination or to dissolution in the aqueous mean.

7.3.1. Attenuated Total Reflection-Fourier Transform Infra-Red Spectroscopy (ATR-FTIR) Spectroscopy Results

Some of the more promising PPAA films in terms of surface properties and chemical features (considerable functional groups amount and/or high reticulation) have been rinsed in de-ionized H_2O for 1 h and subsequently characterized by ATR FT-IR spectroscopy.

Figure 7.6 reports the comparison of the spectra collected on 60W and 5W CW films and on films obtained by MW processes with *Duty Cycle* 50% (T_{on}=50 ms) and Duty Cycle 10% (T_{on}=10ms) respectively.

PPAA spectra collected after polymer rinsing in water reveal a loss of carboxylic functionalities at the surface.

Monitoring the behavior of band centered at 1715 cm^{-1}, it is worth of notice that the decrease of intensity due to the H_2O rinsing is evident only for the coating obtained at 5W $Power_{RF}$ in CW mode. For process performed in Modulated Wave *(Duty Cycle*=10%), a negligible decrease of vibrational absorptions is observed.

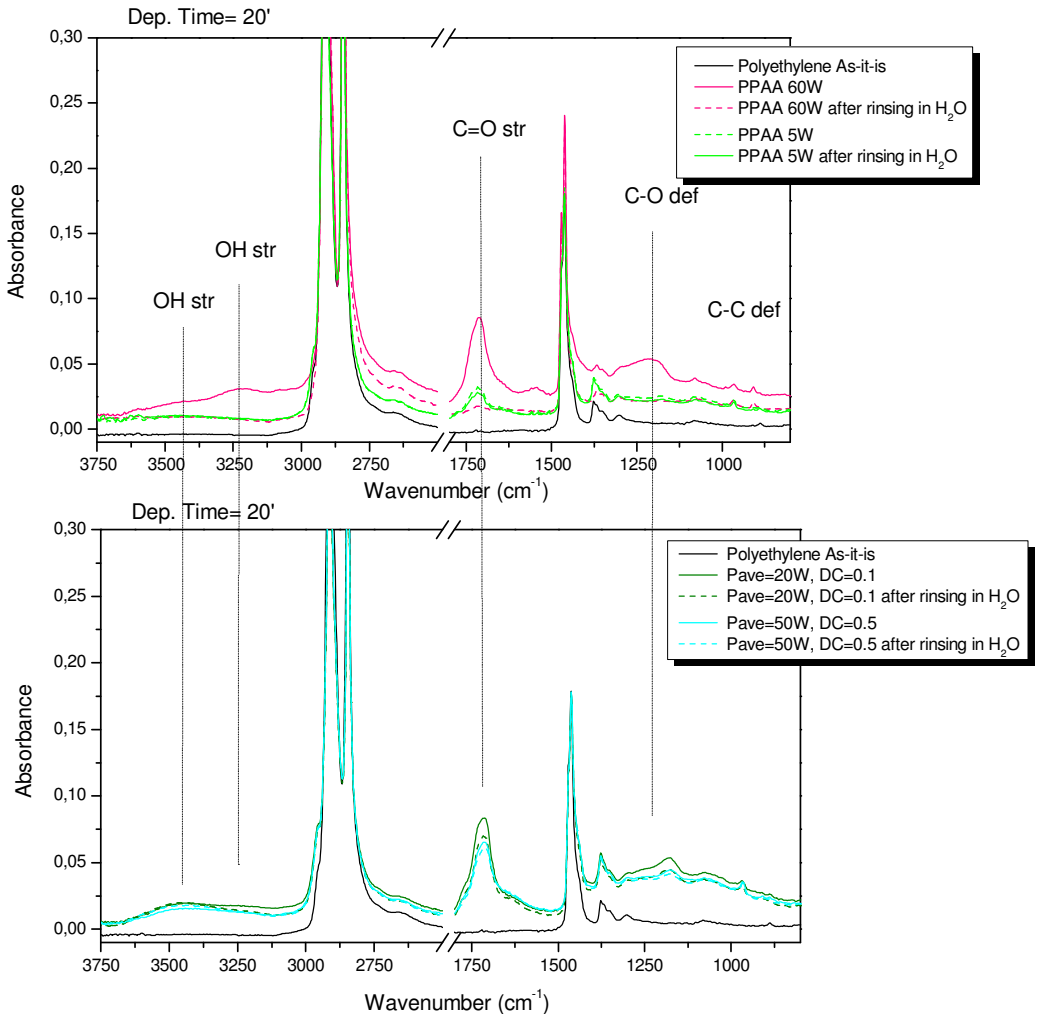

Figure 7.6 FTIR-ATR spectra measured on PE substrates coated with PPAA films obtained in different processes conditions measured before and after rinsing in H_2O

To summarize, for low power CW conditions, PPAA coatings show a higher solubility in aqueous means due to the lower degree of cross-linking, as the molecule fragmentation performed by plasma is reduced, and, for low *Duty Cycle* and high starting $Power_{RF}$ MW processes, this effect is not dominant allowing an acceptable stability and a substantial content of carboxylic groups.

Concerning the PPAA films in figure 7.6, the film showing the best compromise between surface hydrophilicity/hydrophobicity and –COOH groups retention is the one obtained in Modulated Wave at 200W applying a *Duty Cycle* of 10% (T_{on} = 10 ms; T_{off} = 90 ms).

This particular coating was the most suitable for the test with biological species.

The incubation with a fluorescent protein (FITC-Protein A) 0,1 mg/ml solution (10 µl), for 1 h, has shown that, notwithstanding the increment of hydrophobicity, the surface of the last

one is the more efficient, after observation by Fluorescence Microscopy, in the irreversible grafting of tested biomolecules through an amidic bond.

OCA_{H2O} has been successively evaluated on the above selected processes. Except 60W CW coating, the others have shown an amazing increase after water rinsing. OCA_{H2O} related to MW plasma process (*D.C.*=10%), was 71°.

7.3.2. Ellipsometric Results

In order to investigate film optical properties and to determine the thickness and the refractive index of PPAA films before and after rinsing in water, some of the plasma-polymerized films were characterized by ellipsometry.

PPAA films were deposited on Silicon substrates previously oxidized (SiO_2). Deposition time was set to 7,5 minutes in order to obtain a resulting thickness of ~ 50 nm. The thickness of the Si reference was determined by ellipsometry and the refractive index was taken from the literature. These values were used in the model for the measure of plasma-polymers optical properties. First film refractive index was determined by the use of a spectroscopic ellipsometer to obtain more reliable values that have been used in the model for the subsequent thickness measurements performed by the use of single wavelength ellipsometer.

In Table 7.8 average values about thicknesses and relative refractive indexes are reported. Concerning the refractive index, the values are not affected by time of rinsing in de-ionized water: 15 minutes and 48 minutes respectively.

Type of process (Dep Time=7,5')	**Thickness after deposition (nm)**	**Thickness after rinsing in H_2O (15') (nm)**	**Thickness after rinsing in H_2O (48') (nm)**	**Refractive Index**
60 W CW Etch Ar	41,05±0,44	39,45±0,37	38,56±0,34	1,49
100 W DC=0,5 Etch Ar	49,65±0,31	44,73±0,68	43,33±0,50	1,5
200 W DC=0,1 Etch Ar	43,25±0,25	42,65±0,37	41,69±0,49	1,51

Table 7.8 Ellipsometric characterization on PPAA films (Deposition Time =7,5 min): thickness and refractive index values

Thickness values confirm results related to FTIR-ATR characterization. PPAA films show high stability even after test of water rinsing over 72 hours, as film thickness of few nanometers only is observed.

Swelling behavior was also investigated by measuring thickness after putting in contact PPAA films with different pH solutions. Results are reported for PPAAc obtained in CW (60 W) and PPAAc obtained in MW (P=200W, *DC*=10%) respectively (both preceded by Ar etching).

Type of process (Dep Time=7,5')	**Thickness after deposition**	**MilliQ H_2O (pH=6,5)**	**HCl 1 M (pH=2,5)**	**NaOH 1 M (pH=11,5)**
60 W CW Etch Ar	41,05 nm	35,2 nm	36,5 nm	43,3 nm
200 W DC=0,1 Etch Ar	43,25 nm	41,7 nm	42,4 nm	49,3 nm

Table 7. 9 Thickness characterization results on PPAA films (Deposition Time =7,5 min) to measure swelling at different pH solutions

Results show the absence of swelling due to the high cross-linking degree. The type of polymerization mediated by plasma discharge is responsible for the high reticulation degree. The differences related to the particular process conditions resulting in different cross-linking degree of the plasma-polymerized polymers are not revealed by this type of analysis.

7.4. Study of the PPAA films stability (peripheral homogeneity) during deposition

Thickness measurements were repeated in order to study the pripheral homogeneity of the deposition related to the position in the sample holder (distance from the centre of the sample holder).

During plasma polymerization processes Silicon substrates were placed on the sample-holder along its diameter as shown in Figure 7.7 to study the effect on the deposition-rate of the distance from the center position.

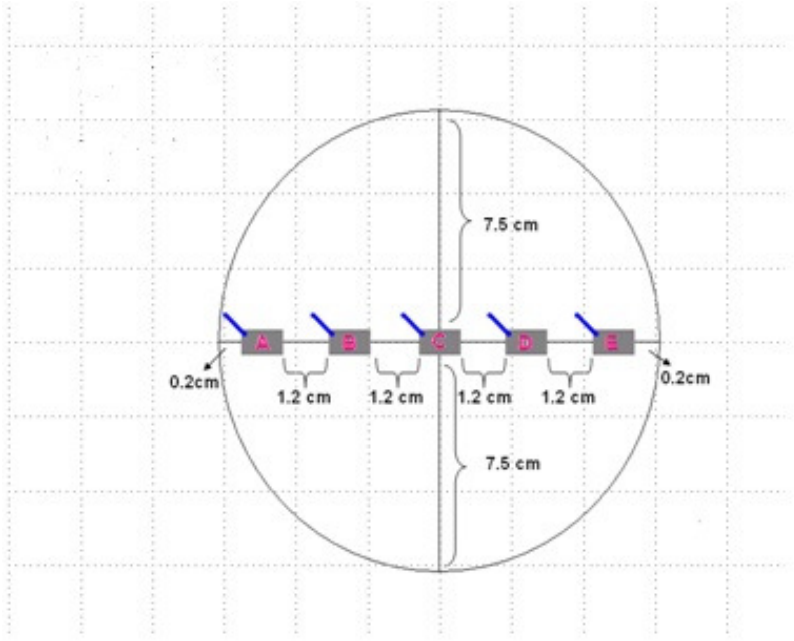

Figure 7.7 Disposition of Silicon substrates (1*2 cm) along the sample-holder diameter (15,2 cm)

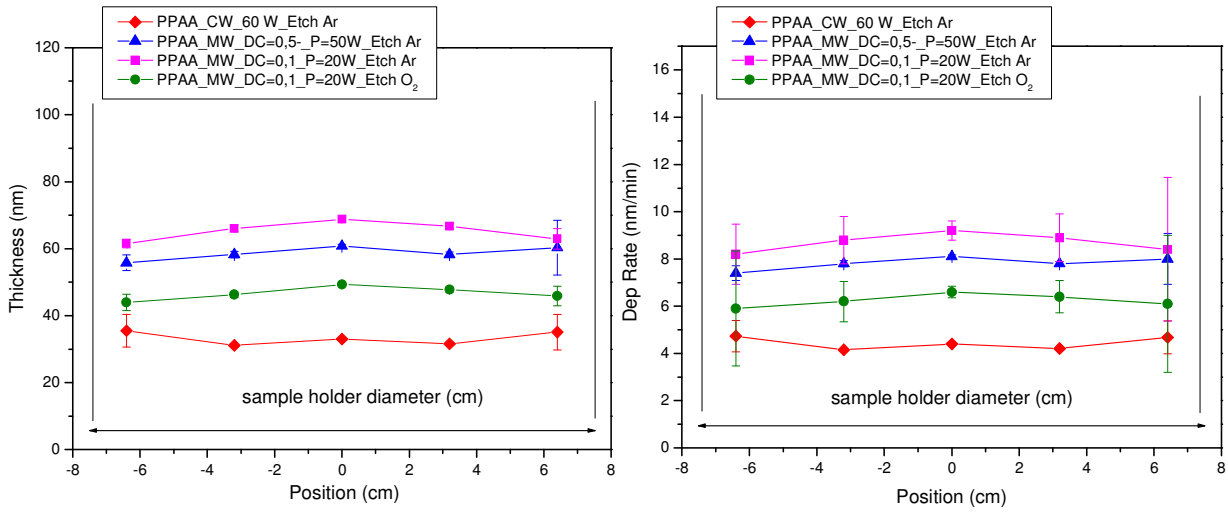

Figure 7.8 Study on the lateral surface homogeneity: the effect of the sample position on the polymer deposition rate

Results related to the thickness and the deposition rate (nm/minutes) show slight decrease of the film thickness from the center position to the edge.

7.5. The effect of pre-deposition plasma etching on coatings final properties

In this study, the effect on the film adhesion of the nature of the gas (Ar and O_2) used for the etching pre-deposition step of the selected substrates (Si, Corning Glass, PE) was also investigated. Ar plasma is known to produce a morphological modification (physical effect due to material ablation) of the surface, more relevant compared to the effect on the surface chemical composition [2], on both inorganic and organic materials. Oxygen etching, due to the O_2 dissociation by plasma discharge in O^* radicalic highly reactive species, mainly affects the surface chemistry of Si and Corning Glass by oxidising and enhancing the oxidised state, respectively, but, in the case of polymers (e.g. PE), in addition to oxidation, is known to impact also on surface morphology. In particular, the chemical oxidation of the surface of substrates enhances surface energy and efficiency of adhesion towards the deposited coating [3]. In general oxygen pre-treatment can introduce several functional groups in the resulting polymer such as -CO-, -C=O, -COOH, -COO, O-COO, with an increase in the surface wettability.

P_{RF} Watt	Pre-etching	D.C. %	T_{on} ms	T_{off} ms	OCA_{H_2O} deg	$OCA_{CH_2I_2}$ deg	W_{sl} mN/m	W^d_{sl} mN/m	W^h_{sl} mN/m
200	**Ar**	10	10	90	27±2	33±2,5	66,18	28,74	37,44
200	**O_2**	10	10	90	16,1±0,3	33±3	70,7	28,07	42,63

Table 7.10 OCA values of plasma polymerization processes (T dep=20 min) performed with Ar and O_2 pre-etching respectively on PE substrate

P_{RF} Watt	Pre-etching	D.C. %	t_{on} ms	t_{off} ms	OCA_{H_2O} deg	$OCA_{CH_2I_2}$ deg	W_{sl} mN/m	W^d_{sl} mN/m	W^h_{sl} mN/m
200	**Ar**	10	10	90	26±2,5	30±2	67,05	30,08	36,97
200	**O_2**	10	10	90	13±2	32±1,4	71,5	28,06	43,44

Table 7.11 OCA values of plasma polymerization processes performed with Ar and O_2 pre-etching respectively on Corning substrate

P_{RF} Watt	Pre-etching	D.C. %	t_{on} ms	t_{off} ms	OCA_{H_2O} deg	$OCA_{CH_2I_2}$ deg	W_{sl} mN/m	W^d_{sl} mN/m	W^h_{sl} mN/m
200	**Ar**	10	10	90	29±2,4	32±3	65,52	29,36	36,16
200	**O_2**	10	10	90	12,3±0,9	33±2	71,72	27,48	44,24

Table 7. 12 OCA values of plasma polymerization processes performed with Ar and O_2 pre-etching respectively on Silicon substrate

Tables 7.10, 7.11 and 7.12 report the OCA values for the plasma process carried out at 200W, with *D.C.*=10% (T_{on}=10 ms and T_{off}=90 ms) preceded by Ar plasma etching and O_2 plasma etching respectively.

The selected process (*D.C.*% = 10; T_{on}= 10 ms; T_{off}= 90 ms; $Power_{RF}$=200W) has been performed both with Ar and O_2 to explore the effect of gas nature (Ar and O_2) used in the pre-deposition etching step on PE, Corning and Silicon substrate (Table 7.6, 7.7 and 7.8).

The OCA_{H2O} angles related to O_2 pre-etching plasma process reveal lower values indicating more hydrophilic behaviour of the these films compared to Ar pre-etching plasma-polymers.

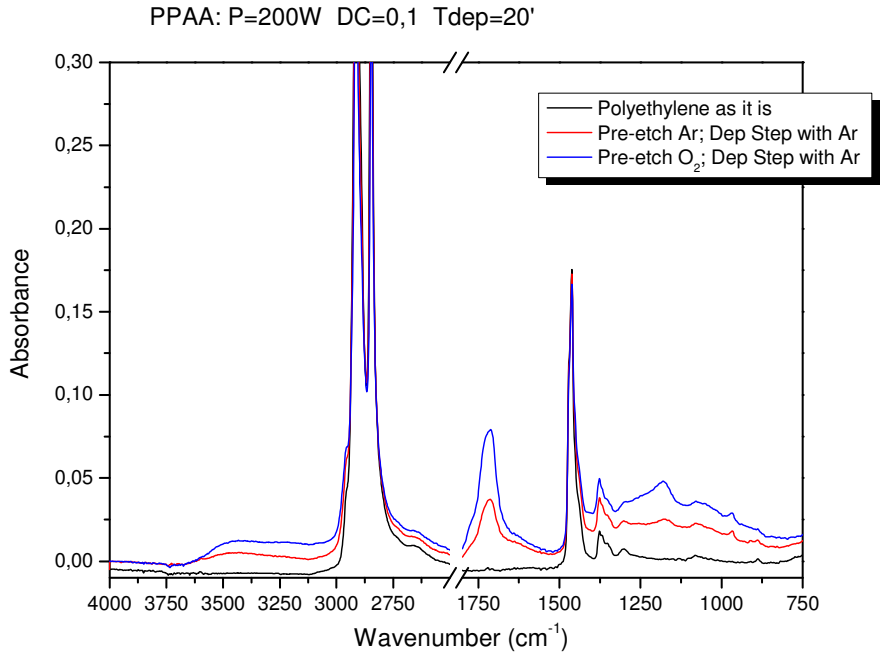

Figure 7.9 FTIR-ATR spectra measured on PE substrates coated with PPAAc films obtained in the same deposition conditions but preceded by two different plasma etching step

The observation (Figure 7.9) of the subsequently deposited films by ATR FT-IR reveals a sensible growth in intensity of vibrational features previously discussed. In particular, signals (at 3223, 1715 and 1200 cm^{-1}) related to oxygen containing species, increase, hence suggesting that the etching gas affects the final chemical properties of the polymeric coatings.

Also in this case, the related peaks intensities are not strictly connected to the measured thickness values (80 nm, for the PPAA obtained by O_2 pre-deposition treatment and 120 nm, for the PPAA obtained by Ar pre-deposition treatment). As a matter of fact, the band assigned to the C=O stretching mode shows a higher intensity for the thinner film, thus confirming the impossibility to observe an effect of such a small variation in film thickness on the spectral features, owing to the prevailing contribution of the chemical composition changes.

This effect was investigated also by means of X-ray Photoelectron Spectroscopy (XPS). This analysis was carried out in order to go into the observed phenomenon thoroughly, for providing a quantitative evaluation of the difference in terms of Oxygen surface amount. A sampling depth of 8.5 nm is reported for plasma deposited Acrylic Acid, by Leber and Ratner [4].

The fitted high resolution (HR) C1s and O1s spectra of the given samples (P_{REF}=200W, *D.C.*=10% preceded by Ar and O_2-etch respectively) are shown in Figure 7.10.

The binding energies assigned to each of these peaks are in accordance with accepted values for these functionalities [5,6]. The peak representative of the carbon (i.e., 285.5 eV) in position to the carboxylic group is assumed to include contributions from C-C, C-O, C=O, O-C=O groups, thus accounting for the somewhat broader peak width assigned for this component [7].

Concerning HR C1s, the difference between the selected samples is related to the C-C bond and to the O-C=O bond: with Ar etching an higher percentage of carbon atoms involved in C-C bond (79.41%) is obtained, whereas this component decreases if O_2 etching (72.72%) is carried out. On the other hand, O_2 etching makes nearly double the weight of O-C=O component, leaving unaffected C-O and C=O ones. This behaviour returns in HR O1s: after O_2 etching the component related to carbonyl of carboxylic group (***O***=C-OH) increases (25.23%) with respect to that related to Ar etching (22.10%) [8].

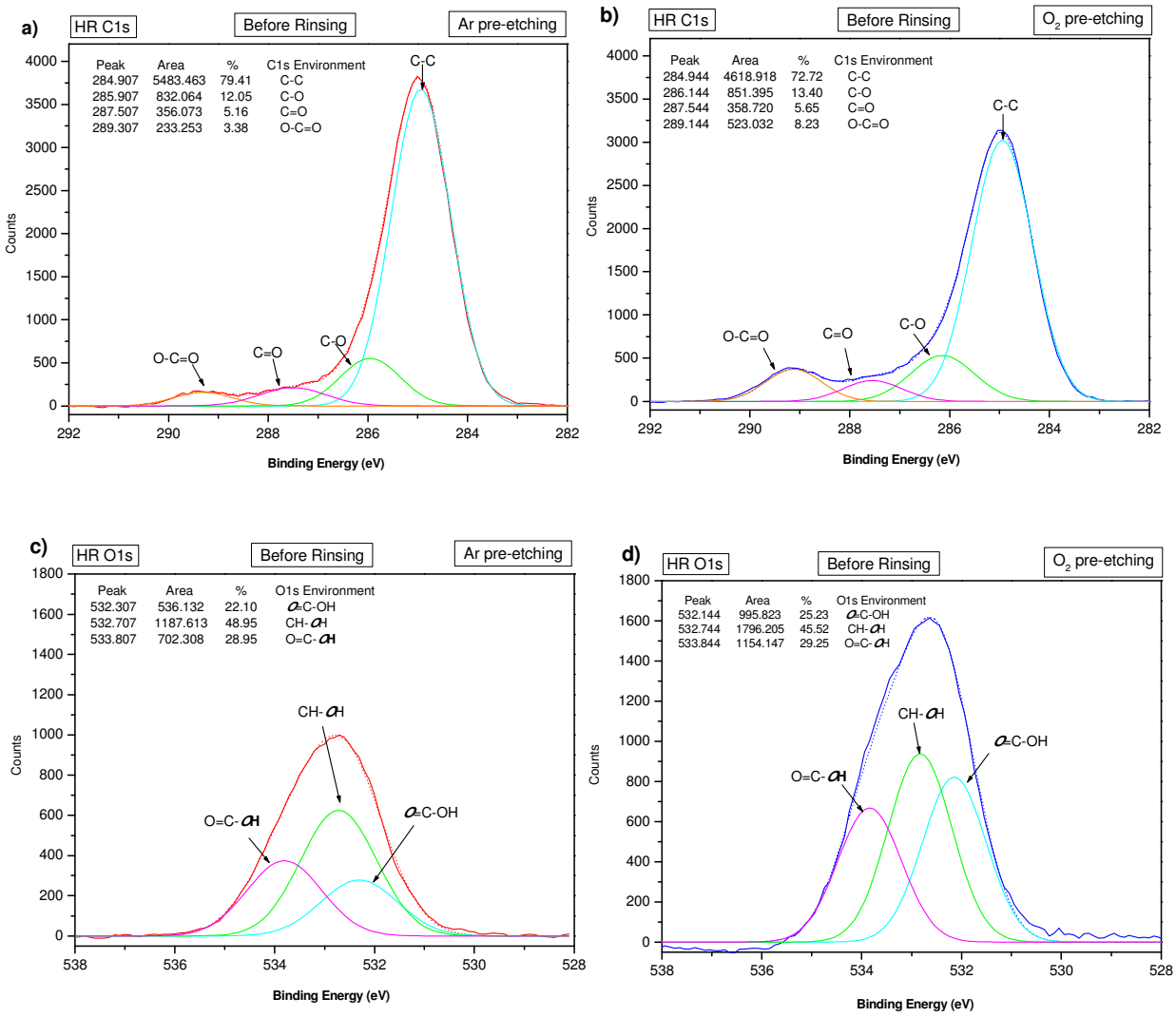

Figure 7.10 XPS spectra of PPAA films deposited after Ar and O_2 etching: a) HR C1s Ar etching; b) HR C1s O_2 etching; c) HR O1s Ar etching; d) HR O1s O_2 etching

Concerning other components, the CH-***O***H shows a higher percentage after Ar etching, while the O=C-***O***H seems unvaried.

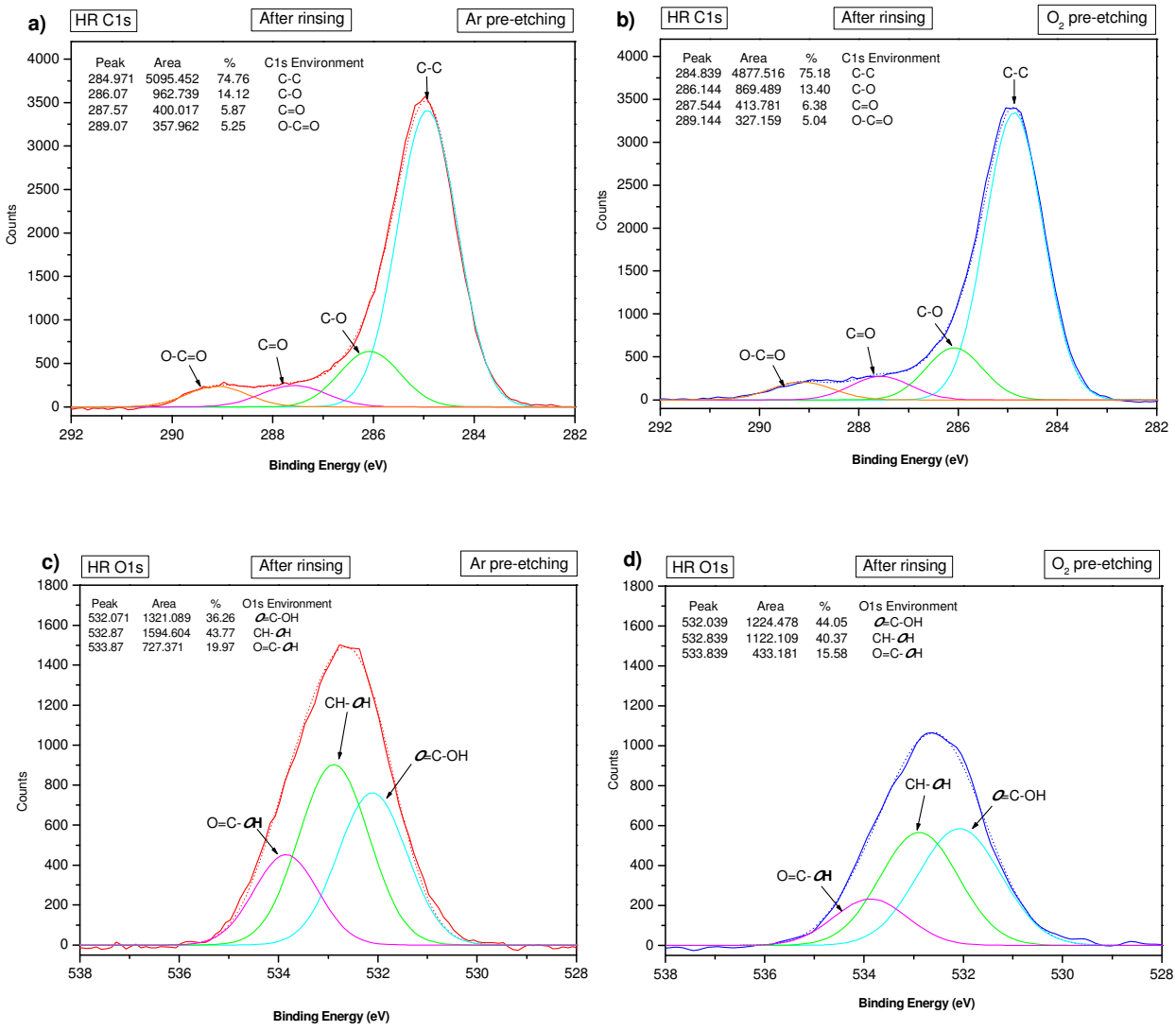

Figure 7.11 XPS spectra collected after rinsing of PPAA films deposited after Ar and O_2 etching: a) HR C1s Ar etching; b) HR C1s O_2 etching; c) HR O1s Ar etching; d) HR O1s O_2 etching

After rinsing in H_2O, HR C1s and O1s spectra, reported in Figure 7.11, evidence the following results: intensity of the C1s peak and areas of the related components seems comparable for both the processes, whereas O1s peak strongly decreases, mainly due to partial depletion of CH-***O***H and O=C-***O***H components.

When O_2 plasma is activate for substrate etching, the reactive species coming from the dissociation of O_2 molecules reside in the process chamber due to the low pumping speed and

so, reacting with the monomer vapors introduced when the deposition process starts, are embedded in the coating under formation.

This mechanism accounts for the resulting high content of oxygen in the film obtained after O_2 etching, as summarized in Table 7.13 where the differences in O/C ratio are reported.

PPAA films	O/C atomic percentage ratio
Ar Etching + PPAAc	0,16
O_2 Etching + PPAAc	0.32
Ar Etching + PPAAc after H_2O rinsing	0,28
O_2 Etching + PPAAc after H_2O rinsing	0,22

Table 7.13 O/C atomic ratio referred to elements percentage obtained from survey spectra of PPAA films obtained after Ar or O_2 plasma etching, before and after H_2O rinsing

The described side effect seems to easily lead to the production of O-rich films where oxygen enhances the formation of a higher number of functional carboxylic groups. But, the subsequent rinsing step demonstrates that these species located at the plasma-polymerized upper layer are highly unstable. As shown by C1s peaks of Figure 7.9 and by O/C ratio (Table 7.13) of rinsed coatings which are quite similar, an effect of "uniformity" of surface is achieved, maybe due to the removal of unstable still reactive water soluble oligomers, known to be formed at plasma polymers surface, at the end of the process.

Therefore, a feasible advantage of O_2 pre-deposition etching for PPAA final chemistry with respect to the employment of it in bio-devices is not obtained.

7.6. Carboxylic groups quantification with Toluidine Blue O (TBO)

In order to quantitatively estimate the concentration of the –COOH groups available at the film surface for biomolecules grafting a colorimetric titration with Toluidine Blue O has been

performed on different PPAA coatings deposited on PE, Si according to different process parameters after H_2O rinsing.

Table 7.14 reports data related to several processes obtained at CW and MW mode on different substrates. Results are in accordance with previous characterizations: as the $Power_{RF}$ or $Power_{ave}$ increases, PPAA films show a lower carboxylic groups surface density.

Processes Parameters	**N°COOH/cm^2**
PE - CW P_{RF}=5W; Ar Etch	4 x 10^{16}
Si – CW P_{RF}=60 W ; Ar Etch	5 x 10^{15}
Si – CW P_{RF}=100 W ; Ar Etch	2 x 10^{15}
PE - MW P_{ave}= 20W; D.C.=10%; T_{on}=10ms, T_{off}=90ms; Ar Etch	(1,15 ±0,35) x 10^{16}
Si - MW P_{ave}= 50W; D.C.=50%; $T_{on=}$50 ms, T_{off}=50ms; Ar Etch	5 x 10^{15}
Si - MW P_{ave}= 20W; D.C.=10%; T_{on}=50 ms, T_{off}=450ms; Ar Etch	1 x 10^{16}
Si - MW P_{ave}= 20W; D.C.=10%; T_{on}=50 ms, T_{off}=450ms; Ar Etch; Rinsed	9 x 10^{15}

Table 7.14 Carboxylic groups density for different types of Plasma Processes

When H_2O rinsing is performed, samples with high -COOH surface density loose half order of magnitude. But only for process performed at 200W in Modulated Wave (*D.C.*=10%, Ton=10 ms, Toff =90 ms) obtained with the Ar pre-deposition etching (Table 7.11), reproducible starting conditions (1.15±0.35 x 10^{16} -COOH/cm^2) and subsequent removal of unstable upper layers occur. Therefore, this is the process showing the best compromise between chemical stability and resulting amount of available and accessible surface groups after rinsing, in the order of 10^{15}/cm^2 confirming results obtained by FTIR-ATR characterizations.

7.7. Study of the acid-base features of polymers: electrokinetic results

After the determination of the number of carboxylic groups exposed at the surface of the plasma-polymerized films an important characterization performed on these coatings was the investigation on the acid-base properties of these functional films (correlated to the presence of a certain number of carboxylic functionalities) performed by the measure of the zeta (ζ) potential.

Electrical surface charge has been found to be relevant for the biocompatibility of polymers applied in medical devices as well as for polymer adhesion in technical systems and numerous other areas.

The apparatus used for the electrokinetic characterization was described in chapter VI (paragraph 6.4.5). Several process conditions were investigated performing different plasma-polymerization processes on specific substrates (Silicon samples constituting the two walls of the channel across which measurements take place as described in paragraph 6.4.5) (Figure 7.13).

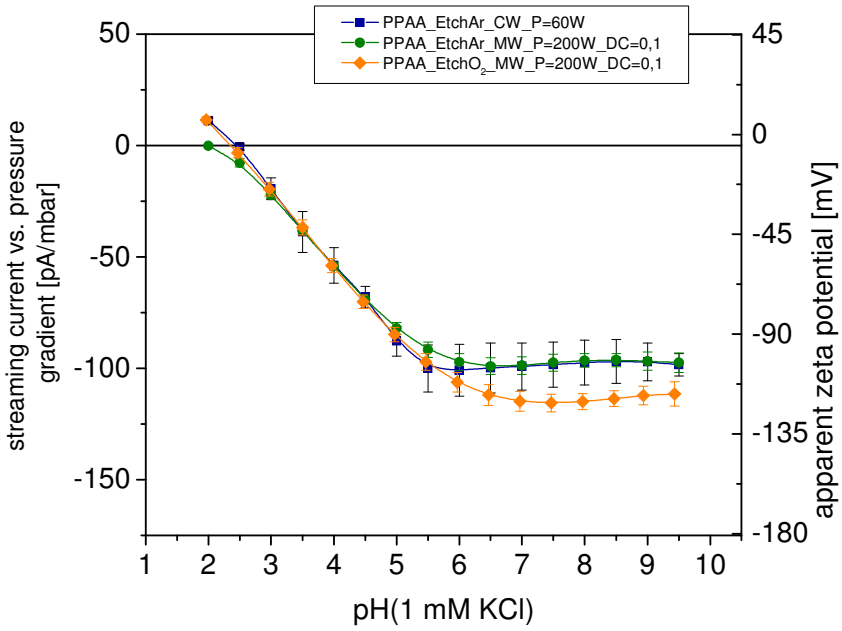

Figure 7.13 Curves related to streaming current measurements in dependence of different pressures across the measuring channel in 10^{-3} M KCl solutions of PPAA films obtained in different process conditions

If a polymer (or a particle) in suspensions has a negative zeta potential when more alkali is added to this suspension, the polymers will tend to acquire a more negative charge. If an acid

moiety is then added to this suspension, a point will be reached where the negative charge is neutralised. Any further addition of acid can cause a build up of positive charge. Therefore a zeta potential versus pH curve will be positive at low pH and lower or negative at high pH.

Concerning PPAA films, the dIS/dp versus pH plot and the position of the isoelectric point at pH=2.1 (Fig. 7.13) indicate that the surface charge originates from the dissociation of the carboxylic acid groups of the PPAA chains. This isoelectric point is typical of acidic behavior, and above the isoelectric point (pH>2.1), the magnitude of the negative streaming current increases with the degree of deprotonation of the carboxylic acid groups at increasing pH values, until a plateau is reached in the basic region corresponding to full dissociation of the carboxylic acid.

7.8. Study of the bio-reactivity towards biomolecules: fluorescence analysis

To investigate on the bio-adhesion properties of plasma-polymerized acrylic acid films and obtain preliminary results on the bio-reactivity of the PPAA coatings toward biomolecules, the functional film of poly-acrylic acid (P=200W, *D.C.*=10%, T_{on}+T_{off}=10+90 ms, Ar pre-etching) was deposited on the surface of a corning-glass substrate.

After PPAA deposition, samples were incubated for 30 minutes with a solution of Protein A (PtA) labelled with a fluorescent marker (Alexa Fluor 546 or FITC). A protein solution of 0,1 mg/ml (volume dispensed=10 μl) was used for the incubation.

Finally, PPAA samples were rinsed in de-ionized water to remove not-specifically adsorbed protein and then dried under N_2 flux and analyzed both by fluorescence microscopy and fluorescence spectroscopy.

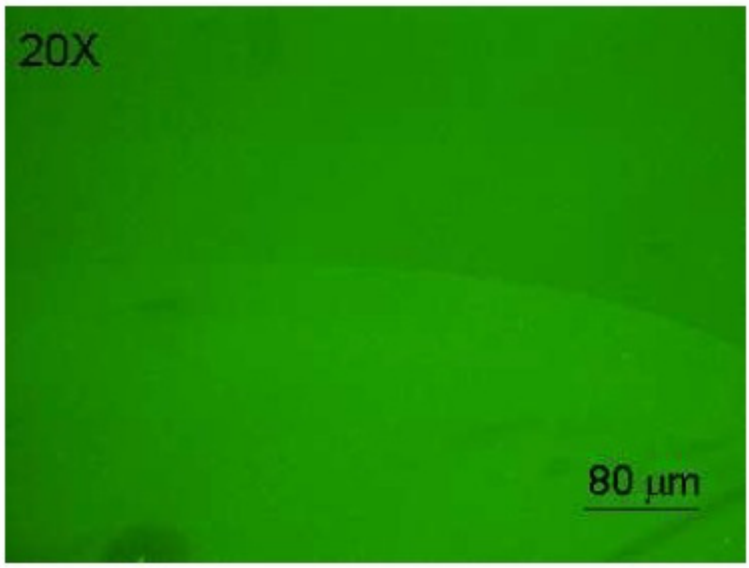

Figure 7.14 Fluorescence Microscopy images: the brighter zone corresponds to the PtA-Alexa Fluor binding to PPAA film, deposited with Ar pre-etching on glass substrate

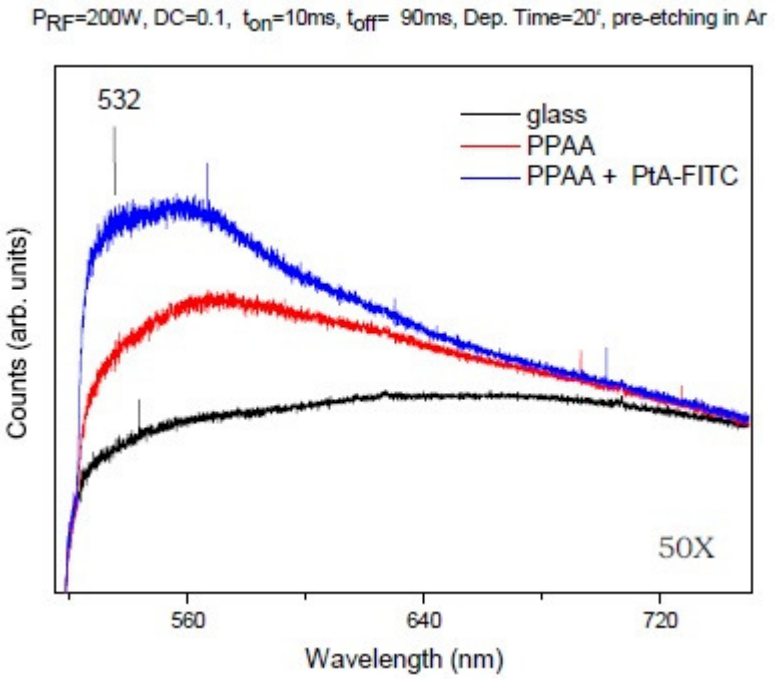

Figure 7.15 Comparison of fluorescence emission spectra of PtA-FITC binded to PPAA coating deposited on glass and to glass substrate as it is

Figure 7.14 show images related to Fluorescence Microscopy analysis: the brighter zone is related to fluorescence emission of PtA-Alexa Fluor binded to PPAA film functional groups

while in Figure 7.15 it is possible to observe how signal intensity related to fluorescence emission of PtA-FITC on PPAA sample is higher compared to the emission related to PtA-FITC on glass substrate uncoated.

Fluorescence characterization results, in the case of both fluorescence microscopy and fluorescence spectroscopy show the efficiency of the acrylic-acid polymer in protein binding due to the successful functionalization mechanism mediated by plasma modification.

7.9. Study of the bio-reactivity towards biomolecules: quartz microbalance analysis

In order to investigate the reactivity of these surfaces, PPAA films deposited on QCM gold substrates have been characterized by QCM-D technique (described in Chapter VI) to study the binding of these films with a BSA (bovine serum albumin) protein solution.

A solution of BSA (0,1 mg/ml) was used to investigate the absorption of the protein on the PPAA films (P=200W, *D.C.*=10%, T_{on}+T_{off}=10+90 ms, Ar pre-etching).

PBS has been used as solvent for the protein solution (pH=5,2) while, for the desorption of the un-specifically binded protein, PBS at 7,6 pH value and Sodium Dodecyl Sulphate (SDS) (10 mg/ml) were tested.

According to Figure 7.16, BSA thickness on PPAA-QCM substrate is higher compared to BSA thickness on.

Since BSA protein dimensions are comparable to the value corresponding to protein thickness on the substrate (~ 4,2 nm), it is possible to affirm that protein immobilization on PPAA film results as monolayer configuration.

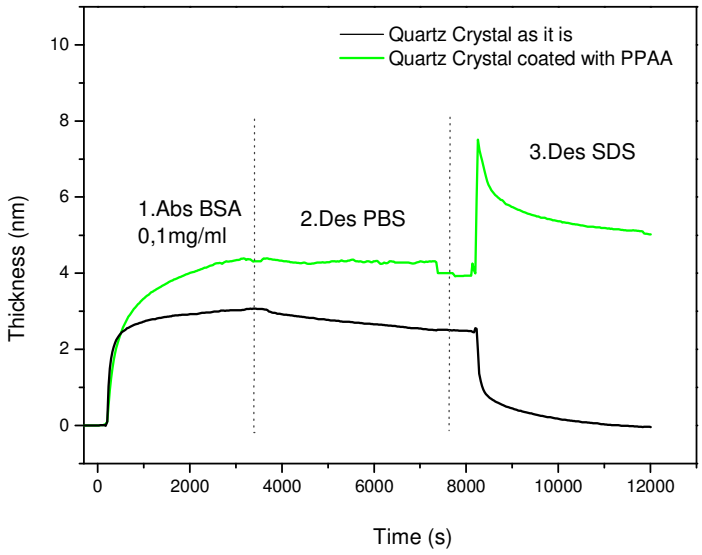

Figure 7.16 Kinetic of BSA adsorption/SDS desorption on PPAA film deposited on QCM substrate

After 1 hour, protein adsorption reaches its plateau so that thickness remains constant as the time increases. Protein desorption was carried out in PBS and in SDS ($CH_3(CH_2)_{11}OSO_3Na$).

SDS is an anionic surfactant used in many cleaning and hygiene products and was used to perform a stronger desorption after PBS desorption. In case of SDS, Figure 7.16 show complete displacement of the protein previously absorbed to the substrate by non-specific binding for uncoated QCM substrate while, for QCM coated with acrylic acid the binding with protein resist not only to PBS desorption but also in case of SDS desorption showing an increase in the thickness compared to PBS desorption, may be due to the interaction of SDS to the protein which still remains anchored to the film by a stable binding.

Figure 7.17 show the same type of interaction but in this case the third step was desorption in PBS at pH 7,6.

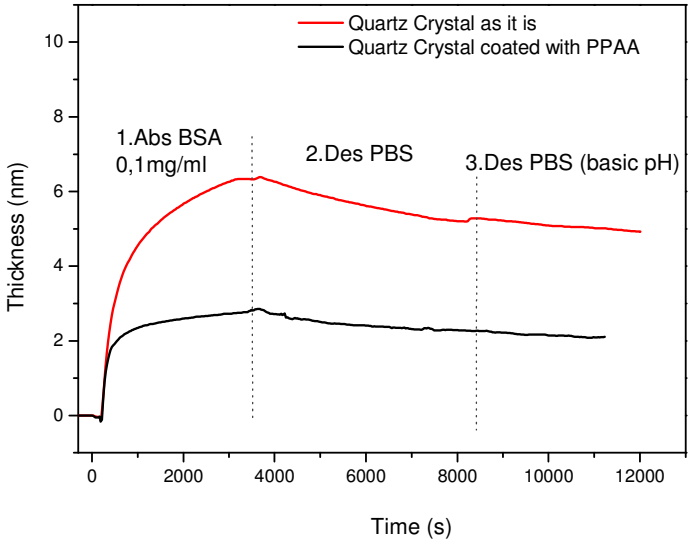

Figure 7.17 Kinetic of BSA adsorption/PBS (pH 7,6) desorption on PPAA film deposited on QCM substrate

Also in this case, protein thickness adsorbed on PPAA-QCM substrate is higher compared to protein thickness on uncoated QCM and after increasing pH of PBS solution from 5,2 to 7,6 to desorb protein non covalently attached to the film it is possible to observe a slight decrease in the thickness of protein linked to PPAA film, thus confirming the stability of the protein on the functional layer of acrylic acid.

Conclusions

In this chapter an accurate study on plasma polymerization processes of acrylic acid was presented. By the optimization of process parameters in a PECVD reactor it was possible to obtain a plasma polymerization process, aimed to yield a –COOH functional polymer, exploitable as active coating in several biomedical applications. Film properties were investigated by different techniques in order to correlate working conditions adopted during plasma process to the final chemical features of the resulting films.

The thin coating obtained in MW mode, at *D.C.%* = 10; t_{on}= 10 ms; t_{off}= 90 ms; $Power_{RF}$=200W, with a Deposition Time of 20', exhibits a considerable surface density of approximately more than 1 x 10^{16} accessible carboxylic groups/cm^2. The content of functional groups is slightly diminished by the contact with aqueous means due to the removal of

unstable oligomers of the film upper layers, without any detrimental effect on the final application. Moreover, no evident advantages have been observed on chemical stability and group surface density of the resulting PPAA by enriching with oxygen species the reactive atmosphere during the plasma process.

Due to these reasons the "selected" coating was deposited on specific substrates in order to stably functionalize the surface and obtain a biosensor device suitable for several biomedical applications.

References

[1] Lin-Vien D., Colthup N. B., Fately W. G., Grasselli J. G., *The Handbook of Infrared and Raman Characteristic Frequencies of Organic Molecules*, Academic Press, New York, **1991.**

[2] Shi L.-S., Wang L.Y.,. Wang Y.-N, "The investigation of argon plasma surface modification to polyethylene: Quantitative ATR-FTIR spectroscopic analysis", *Eur. Polym. J*., **2006**, 42, p. 1625-1633.

[3] Ataeefard M., Moradian S., Mirabedini M., Ebrahim M., Asiaban S.," Surface Properties of Low Density Polyethylene upon Low-Temperature Plasma Treatment with Various Gases, *Plasma Chem. Plasma P*rocess, **2008**, 28, p. 377-390.

[4] Leber R.E., Ratner B.D., "Introduction of Carboxyl Functional Groups onto Platinum by RF Plasma Deposition", *Plasma Process. Polym.,* **2009***,* 4, *p.* 219-227.

[5] Beamson G., Briggs D., *High Resolution XPS of Organic Polymers, The Scienta ESCA300 Database,* Wiley, Chichester, UK, **1992.**

[6] Briggs D., Seah M.P., *Practical Surface Analysis - Auger and X-ray Photoelectron Spectroscopy, second ed.*, J. Wiley and Sons, Chichester , **1990.**

[7] Alexander M. R., Duc T. M, "The chemistry of deposits formed from acrylic acid plasmas", *J. Mater. Chem.* , **1998,** 8, p. 937-943.

[8] De Giglio E., Cometa S., Cioffi N., Torsi L., Sabbatini L., "Analytical investigations of poly(acrylic acid) coatings electrodeposited on titanium-based implants: a versatile approach to biocompatibility enhancement", *Anal. Bioanal. Chem*., **2007**, 389, p. 2055-2063.

Chapter VIII

Plasma polymerization from styrene vapours: thin film deposition of styrene-polymers and styrene-co-polymers with acrylic acid

As described in the previous chapters, the control of the deposition parameters in plasma-polymerization processes, allows the fabrication of films that feature a high degree of retention of the chemical functionality of the monomer precursor. For example, in this work, it was demonstrated (by OCA and FTIR-ATR characterizations, carboxylic groups colorimetric titration, etc.) how low plasma power or in general "soft plasma conditions" cause high levels of retention.

Retention of monomer functionality offers the exciting possibility of exercising a very high degree of control over processes that depend on surface chemistry. Further significant benefits would accrue if an exact control over the concentration of a specific surface functionality could be achieved.

Concerning plasma parameters, plasma power, plays an important role particularly in relation to physical properties which can vary from low molecular weight oil to highly cross-linked powder. Therefore, plasma power is not an ideal variable for achieving the purpose of controlling functional groups concentration. Another variable that affects the level of functional group retention is the monomer flow rate. However, this variable can also produce considerable changes in the deposit's physical properties. The choice of the monomer offers some control, but only a limited range of monomers are available for polymerization, in particular those that have a significant vapour pressure at 10^{-2} mbar [1].

A possible approach to the problem of controlling polymer functionalities is the plasma copolymerization: the vapours of a monomer containing chemical active functionalities (acrylic acid) are mixed, in the reaction chamber, with the vapours of a chemically inert aliphatic chain monomer, such as styrene, to achieve a sort of "dilution" of the first in the

second. Styrene is an aromatic molecule (C_6H_6-CH=CH_4) which, by decomposing, allows to introduce aliphatic fragments among carboxylic groups arising from acrylic acid monomer.

8.1. Plasma-polymerization of styrene: optimization of process parameters

Plasma polymerization of styrene was carried out using the same PECVD reactor described in 6.2 for the acrylic acid.

Liquid styrene was stored into a different reservoir but the working conditions applied during deposition were the same described for acrylic acid. Ar was the carrier gas used at 20 sccm and made bubbled in the styrene reservoir to have the gas/vapour mixture passage throughout the specific line related to styrene monomer.

Styrene vapour pressure is 5 Torr at 20°C but monomer flow, measured when the manual valve intercepting the reservoir is open, is not easily controllable and it is highly sensitive to external temperature variations. This creates problems for the reproducibility of the processes and does not allow the measure of the vapour flow of styrene as in the case of acrylic acid (paragraph 6.2.1). Anyway, several process conditions were tested in order to optimize experimental conditions and obtain the desired properties in the resulting films. In particular process parameters related to acrylic acid plasma processes showing the best results were repeated for styrene depositions.

Processes Parameters	**Measured Value**
Ar flow	20 sccm
ST partial pressure	5 mTorr; 10 mTorr
Working Pressure	206-248 mTorr
Deposition Time	5 min
Power (P_{RF})	60 W (Continous Wave) 200W, 250W (Modulated Wave)
Duty Cycle (D.C.%)	10, 50
(T_{on}; T_{off})	(20;80) ms (50;50) ms

Table 8.1 Process parameters for plasma-polymerization of styrene in continous and modulated wave conditions

8.1.1. Contact Angle Results

For sake of simplicity only OCA results concerning plasma-polymerized styrene (PPST) polymers deposited on Polyethylene substrates are reported in Table 8.2

As expected, an hydrophobic behavior is shown by PE substrates after PPST deposition due to the chemical composition of the resulting polymers.

During plasma processes a crucial step was the stabilization of Styrene partial pressure during the deposition step. Increasing styrene vapor pressure, plasma power was not enough intense to break chemical bonds in the monomer molecule thus causing the formation of solid particles during deposition.

Moreover when plasma power is not sufficient to activate the polymerization mechanism, cross-linking between the growing coating and the substrate surface is not completely achieved, so the water delamination occurs during water rinsing.

P_{RF} Watt	D.C. %	t_{on} ms	t_{off} ms	P_{AVE} Watt	$Press_{Sty}$ mTorr	OCA_{H_2O} deg	$OCA_{CH_2I_2}$ deg	W_{sl} mN/m	W^d_{sl} mN/m	W^h_{sl} mN/m
60	/	/	/	/	8-10	84,1	22,3±0,9	47,15	45,70	1,45
250	50	50	50	5	8-10	68,4±2,7	3,4±1,2	51,88	45,26	6,61
200	10	20	180	20	10	90,4	16,4±0,7	49,86	49,65	0,21
200	10	20	180	20	5	68,4±1,4	21,7	47,25	41,55	5,71

Table 8 2 OCA measurements performed on PE substrates coated with PPST films obtained in different process conditions (T dep= 5 min)

The best compromise between an hydrophobic coating and an high reticulated film showing stability after rinsing in de-ionized water (OCA results not shown) was achieved by modulating plasma discharge (P_{REF}=200W, *D.C.*=10%, T_{on}=20 ms; T_{off}=180 ms; P_{ST}=5 mTorr). OCA_{H2O} and OCA_{CH2I2} images are represented in Figure 8.1.

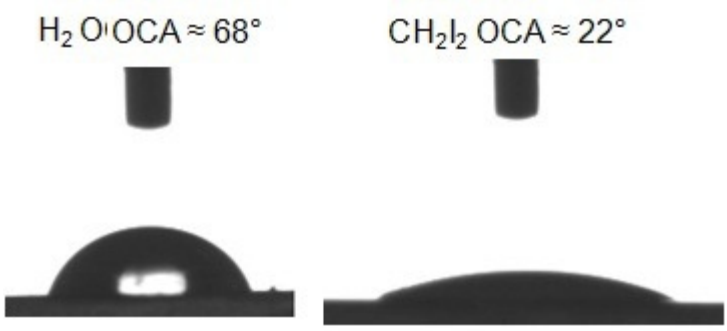

Figure 8.1 OCA results for PPST performed on PE substrate in Modulated Wave (P_{REF}=200W, DC=10%, Ton=10 ms; Toff=90 ms; PST=5 mTorr)

8.1.2. ATR-FTIR Results

The Infra-Red Spectroscopy analysis (ATR-FTIR characterization) is shown in Figure 8.2. PPST plasma-polymers deposited on PE were compared to the atactic polystyrene taken from the polymer IR database.

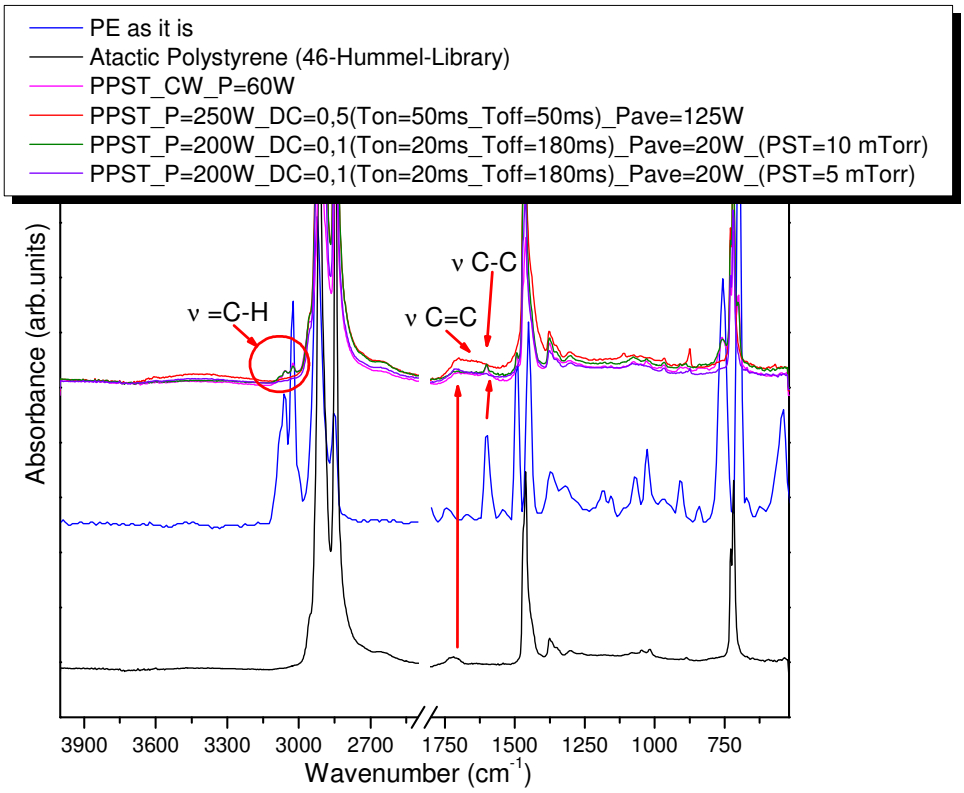

Figure 8.2 ATR-FT-IR spectra measured on PE substrates coated with PPST films obtained in different process conditions

Spectra of Figure 8.2 show two bands related to C=C and C-C stretching vibrations associated to the backbone chain absorption modes. In the case of MW plasma at 200W (DC = 10% and PPST pressure =5mTorr) spectrum show at 2980-2870 cm^{-1} the signals related to aliphatic C-H stretching mode.

8.2. Plasma-copolymerization of acrylic acid and styrene: optimization of process parameters

Plasma co-polymerization from vaporized acrylic acid monomer, carrying the functional group and vaporized styrene monomer, conferring an higher reticulation degree, was performed in the PECVD reactor in order to exercise a further control on the number of carboxylic functionalities exposed at the film surface.

P_{fwd} (W)	*DC*	t_{on} (ms)	t_{off} (ms)	*Time (min)*	P_{AA} (mTorr)	P_{STY} (mTorr)	P_{pro} *(mTorr)*	Ar_{AA} *(sccm)*	Ar_{STY} *(sccm)*
200	0,1	10	90	5	5	10	240-258	10	10
200	0,1	10	90	10	5	10	241-264	10	10
200	0,1	50	450	5	5	12	242-266	10	10
200	0,1	20	180	5	5	10	240-266	10	10
200	0,1	10	90	5	7	11	240-263	15	5
200	0,1	10	90	5	8	8	241-266	18	2
200	0,1	10	90	5	7	10	237-263	19	1
100	0,1	10	90	5	6	9	236-259	15	5
200	0,1	10	90	5	7	8	237-256	5	15
200	0,1	10	90	5	7	9	240-255	1	19

Table 8.3 Process parameters for plasma-copolymerization of acrylic acid and styrene

Acrylic acid and styrene were stored in two different *reservoirs* and made to flow throughout two different lines; for this reason the vapor mixture was formed directly into the vacuum chamber where copolymerization takes place. Different conditions were tested in

order to optimize monomer vapor flows and establish a good equilibrium between the two flows during co-polymerization obtaining the desired final film properties.

8.2.1. Contact Angle Results

In table 8.2 OCA results of PPAA-PPST films deposited on Polyethylene substrates are reported.

P_{fwd} (W)	T_{on}+T_{off} (ms)	Ar_{AA} (sccm)	Ar_{STY} (sccm)	OCA_{H_2O} deg	$OCA_{CH_2I_2}$ deg	W_{sl} mN/m	W^d_{sl} mN/m	W^h_{sl} mN/m
200	10+90	10	10	200	0,1	10	90	5
200	10+90	10	10	200	0,1	10	90	10
200	50+450	10	10	200	0,1	50	450	5
200	20+180	10	10	200	0,1	20	180	5
200	10+90	15	5	200	0,1	10	90	5
200	10+90	18	2	200	0,1	10	90	5
200	10+90	19	1	200	0,1	10	90	5
100	10+90	15	5	100	0,1	10	90	5
200	10+90	5	15	200	0,1	10	90	5
200	10+90	1	19	200	0,1	10	90	5

Table 8.4 OCA measurements performed on PE substrates coated with PPAA-PPST films obtained by plasma-copolymerization processes

OCA values show an hydrophobic behaviour: comparing the results of table 8.2 with results of Table.7.7 related to only acrylic acid plasma polymers, for the same process conditions plasma copolymers of acrylic acid and styrene show higher OCA_{H2O} values due to the presence of the styrene.

8.2.2. Attenuated Total Reflection-Fourier Transform Infra-Red Spectroscopy (ATR-FTIR) measurements

In graph 8.2 some FTIR-ATR spectra related to films obtained by plasma copolymerization processes are reported.

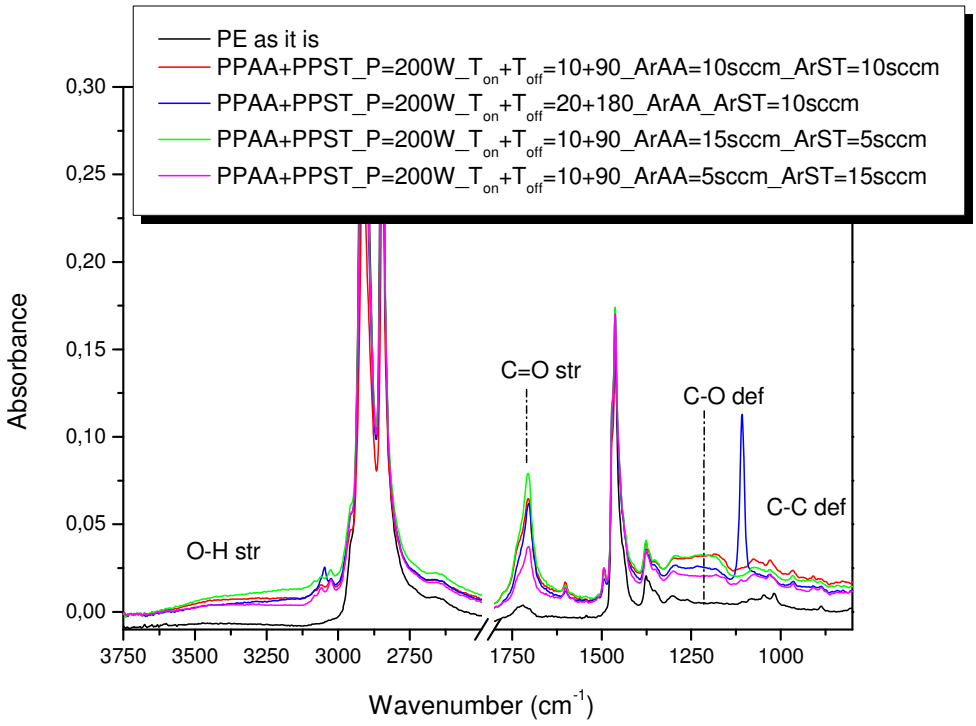

Figure 8.3 ATR FT -IR spectra measured on PE substrates coated with PPAA-PPST copolymerized films obtained in MW plasma processes

Plasma copolymers, derived from deposition of acrylic acid and styrene mixture, reveal the same chemical composition compared to plasma polymers obtained by acrylic acid vapor only; the difference is concerning the lower intensity of the signals related to the O-H and C=O stretching vibrations, confirming a lower number of carboxylic functionalities exposed at the surface of the copolymers due to the presence of the styrene component.

8.2.3. Ellipsometric Results

In order to estimate film thickness of plasma copolymerized films and compare film optical properties of PPAA-PPST with PPAA films, coatings obtained by plasma co-polymerization carried out in modulated wave (P=200W, *D.C.*=10%, T_{on}+T_{off}=10ms+90ms, Ar_{AA}=10sccm, Ar_{ST}=10sccm) were characterized by ellipsometry.

Plasma polymerized and copolymerized coatings were deposited on Silicon substrates as described in paragraph 7.4. Plasma depositions were carried out for 7,5 minutes for all the functional films.

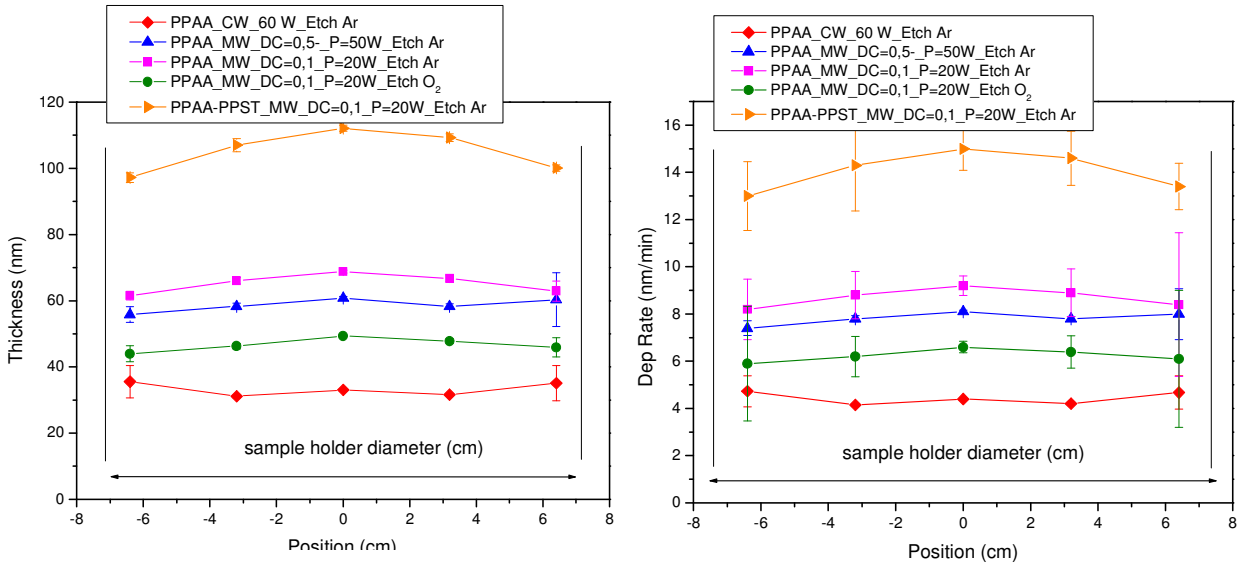

Figure 8.4 Study on the lateral surface homogeneity: the effect of the sample position on the co/polymer deposition rate

Figure 8.4 shows that in case of PPAA-PPST copolymers the deposition rate reached during polymerization is higher compared to PPAA films, in fact the thickness reached during plasma copolymerization for the deposition time (7,5 minutes) is nearly twice as the thickness of PPAA films, demonstrating that the reaction mechanisms and so the deposition rate are different. With respect to all PPAA films, peripheral homogeneity during deposition is achieved; the position of the sample along the diameter of the sample-holder does not affect thickness constant distribution except in case of PPAA-PPST copolymers where moving from the center to edges the homogeneity in the thickness slightly decreases.

8.2.4. Electrokinetic Results

The same plasma copolymerization process (MW, P=200W, *D.C.*=10%, T_{on}+T_{off}=10ms+90ms, Ar_{AA}=10sccm, Ar_{ST}=10sccm) was performed on silicon substrates used for the zeta potential characterization as described in paragraph 7.7. The introduction of styrene in the vapor mixture result in thin functional films with a lower number of carboxylic groups exposed at the surface as described in the previous paragraphs thus affecting the acid-base properties expressed by the plasma copolymers.

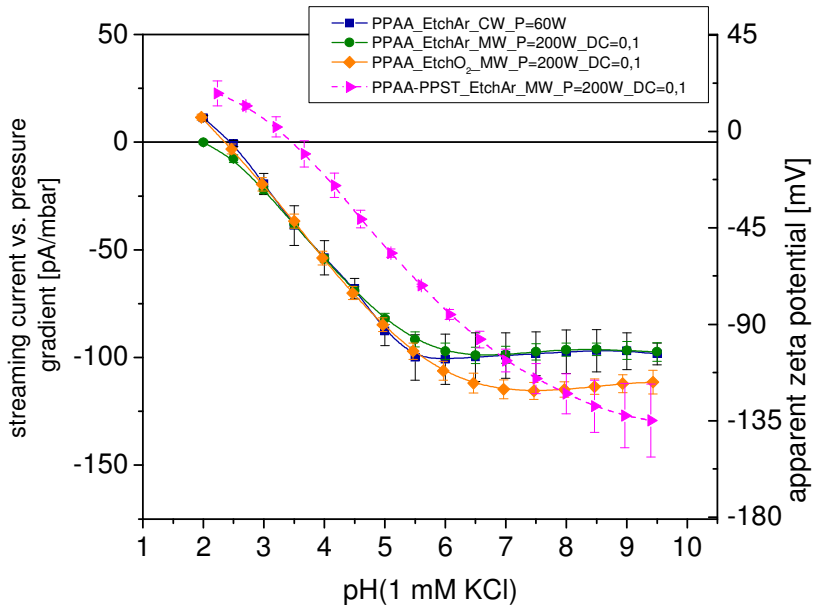

Figure 8.5 Curves related to streaming current measurements in dependence of different pressures across the measuring channel in 10^{-3} M KCl solutions of PPAA/PPAA-PPST films obtained in different process conditions

Comparing PPAA-PPST films with PPAA films shown in figure 7.13, it is really evident the different trend in the behaviour of the two processes.

The introduction of styrene in the vapour mixture and the subsequent lower number of the carboxylic groups (-COOH) resulting in the final films, reduces the ionizable surface.

In fact, results show a different isoelectric points (IEP): PPAA is characterized by an IEP close to pH 2 (typical of acidic behaviour) while PPAA-PPST show an IEP close to pH 4 typical of inert surfaces.

The two curves related to these two different films are also characterized by a different shape.

For PPAA polymers, increasing the ionic strength, the curve reaches the plateau due to the fact that, at a certain value of pH, an equilibrium in the exchange between OH^- ions from the solution and H^+ ions from the polymers is reached; this behaviour is different in the case of styrene copolymers where the plateau of the is reached at higher pH values due to the presence of a less ionizable surface.

Conclusions

The optimization of the plasma parameters carried out for the deposition of acrylic acid thin films has led to the study and to the optimization of the process conditions for the plasma polymerization processes of styrene vapours. A hydrophobic, stable coating was realized starting from styrene (P_{REF}=200W, *D.C.*=10%, T_{on}=20 ms; T_{off}=180 ms; P_{ST}=5 mTorr), showing a potential behavior as anti-fouling film to prevent biomolecules adsorption in biosensing applications.

Starting from styrene vapours it was possible to perform a plasma copolymerization process with acrylic acid monomer in order to improve film stability as a control on carboxylic surface density was achieved by styrene introduction in the vapor mixture.

References

[1] Beck A.J., Jones F.R , Short R.D, "Plasma copolymerization as a route to the fabrication of new surfaces with controlled amounts of specific chemical functionality", *Polymer*, **1996**, 37, p. 5537-5539.

Chapter IX

Application of a functional thin film of plasma-polymerized acrylic acid

Plasma-Polymerized Acrylic Acid thin functional films (PPAA) exposing at the surface carboxylic groups (-COOH) able to react with the amino groups (-NH_2) of 5'end amino-modified single-strand DNA probes was exploited for the surface functionalization of a Microarray DNA biochips for the detection of *Listeria monocytogenes,* a bacterium responsible of enteritis. The detection method selected for this purpose is relevant to get a low cost disposable diagnostic tool, usable for Point-Of -Care (POC) analyses.

These functional groups will be readily accessible without any adding step of activation such as the use of N-hydroxysuccinimide (NHS) and 1-ethyl-3-(3-dimethyl aminopropyl) carbodiimide (EDC), as reaction catalyst, reported by Jafari et al. [1].

For the Microarray diagnostic Assay, PPAA films were deposited on a Polyvinylchloride-Unplasticised (UPVC) substrates (thickness 0.5 mm) purchased by Goodfellow, after cutting in 75 mm x 2.5 mm, i.e. compatible with slide shape used for both manual and automatic microarray DNA probes spotting facilities.

For comparison with commercial microarray diagnostics supports, 3-wells Dr. Chip (LifeLineLab – LLL) biochips were purchased.

9.1. Experimental: the functionalization procedure

Plasma Process

The UPVC substrate, after rinsing in ethanol and drying with N_2 flux for cleaning, was introduced in the PECVD reactor for plasma deposition. The process used for the functionalization procedure was carried out at 200W (DC=10%, Ton+Toff=10+90 ms) with Ar pre-etching for 20 minutes as deposition time. After the process, the PPAA-UPVC samples were rinsed in de-ionized water in order to stabilize the functional layer (by removal of unstable oligomers at the surface) and optimize the subsequent binding to the probes.

Grafting of the Amino-modified biotinylated ss-DNA probes

The DNA probes were spotted according to the designed array by CRIBI (Padova, IT), with the layout described in **Figure 8-II**. The biotinylated probes were used as a reference control for the colorimetric detection. The DNA probe sequences CGC TTT CAG GTT TAA CTA GTC TAC AGC A were specifically designed for the hybridization of *L. monocytogenes*, while CTA CCG CTT CAG GCA AGT TAG ACC ACA G DNA probe was used as a negative control. Moreover, a biotinylated probe with arbitrary sequence was used as positive control. The DNA probes were spotted on UPVC slides pre-functionalized with a PPAAc film and on commercial slides (DR. Chip Biotech Inc.) to compare the results.

PCR reaction and hybridization with targets

The *L. monocytogenes* Polymerase Chain Reaction (PCR) product were obtained with a PCR mix composed of 5 µL of Master Mix 10X (BioAtlas), 2 µL of 10 µM forward primer (5'-ACT ATC TAG TAA CAC GAT TAG TGA-3') and 2 µL of reverse 5' biotinylated primer (5'-CAA ATT TGT TAA AAT CCC AAG TGG-3'). After that, 2 µL of plasmid DNA template (ng/µL) was added and finally H_2O to obtain a final volume of 25 µL. The thermal cycles for amplification were set as follows: 15 min for pre-denaturing at 95°C, 20 s for denaturing at 95°C, 30 s for annealing and extension at 63°C, and finally 5 min at 72°C for the post-extension. PCR products were loaded on an 3% agarose (Sigma Aldrich) gel stained with Gel Red (Biotium), using a 100 bp DNA ladder (Fermentas, Gene Ruler) for the evaluation of amplicons size and the semi-quantitave analysis (GelAnalyzer, http://www.gelanalyzer.com/).

The PCR products were mixed with the Hybridization buffer, following the recipes and the procedures described elsewhere [2].

Colorimetric Detection

The colorimetric detection was based on the use of Silver Quant® Kit (Eppendorf) and is depicted in Figure 9.1

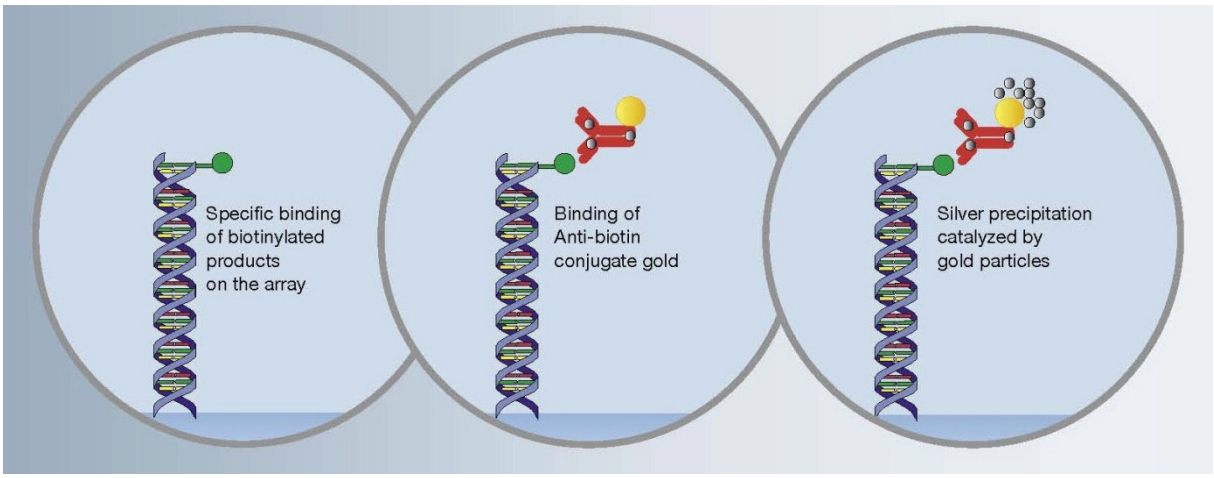

Figure 9.1 Colorimetric detection of amino-biotinylated probes by colorimetric detection based on Silver Quant® Kit (Eppendorf)

After hybridization of the biotinylated probes with specific oligonucleotide targets, anti-biotin molecules conjugated with gold particles were dispensed on the microarray chip for the binding with the biotinylated products on the array.

The subsequent dispensing of silver salts causes the precipitation of silver, reduced to the metallic form, in the solution and so the formation on the array of colored spots corresponding to the positions where DNA probes were immobilized.

9.2. Results of the Microarray functionalization procedure

The PPAA film (P=200W, DC=10%, Ton+Toff=10+90 ms, Ar pre-etching, Tdep=20 min) deposited on UPVC substrate was characterized by OCA_{H2O} measurements.

The OCA_{H2O} mean value on the sample soon after deposition is 10°, after H_2O rinsing is 57° (UPVC as it is OCA_{H2O} mean value is 86°, OCA_{CH2I2} mean value is 31°). The same measurement on Dr. Chip surface is 60°. In microarray diagnostics, an high contact angle of nanolitric drops (low spreading) is preferred in order to avoid the dilution with respect to contacted surface area of DNA probes to be grafted on the functional film and to promote an efficient intensity of the colorimetric signal to be detected after the hybridization assay.

The –COOH surface density of PPAc deposited on UPVC is comparable with value related to the same process performed on PE (Table 7.13).

9.2.1. DNA Microarray Experiment: proof of concept

The so prepared PPAA-UPVC slides were used to test the successful probes binding to the surface thanks to the formation of a covalent bond between the –COOH groups exposed at the surface of the PPAA coating deposited on the substrate and the $–NH_2$ groups of the oligonucleotide probes.

The first experiment was carried out by a manual 32 pin micro-arrayer (Microarray Printer XMM

47.832, Xenopore, Hawthorne, NJ). The droplet dimension is 300 micron in diameter.

The UPVC-PPAA slides, after probes deposition were incubated over night in a humid chamber at 37° C (humidity = 80%) then rinsed with a blocking solution (100 mm ethanolamine, 0.2 M Tris, pH 9,0).

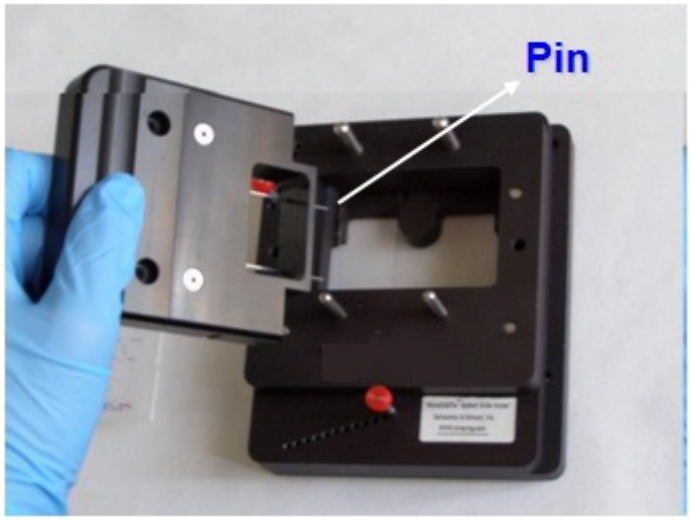

Figure 9.2 Manual-arrayer (32 pins) for spots deposition

This experiment was performed to verify the efficiency in the functionalization mechanism when modified probes were spotted on the PPAA-UPVC substrate and to test the activity of the probes after their binding when the complementary target hybridizes on the microarray.

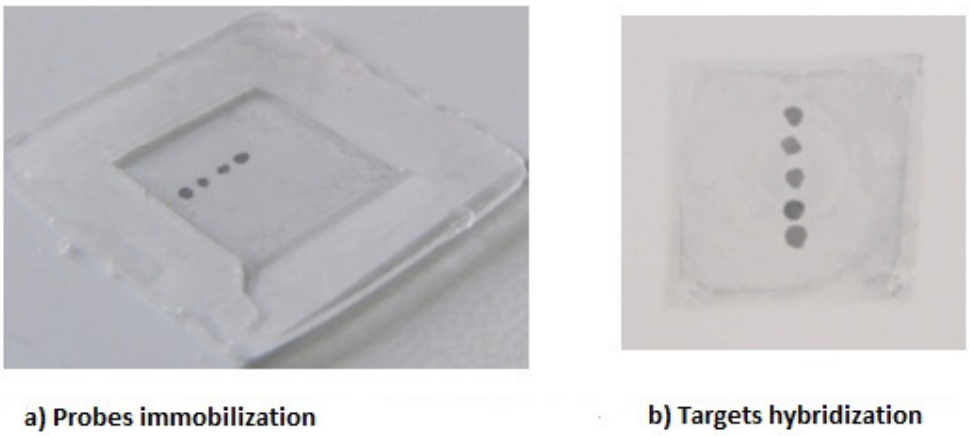

Figure 9.3 a) Successful probes immobilization on the UPVC-PPAAc surface and b) subsequent successful targets hybridization

Figure 9.3 shows the successful probes immobilization on PPAA functionalized microarray surface and the subsequent successful targets hybridization of DNA oligonucleotides.

At this point it was possible to test the UPVC-PPAAc slides for a real protocol of detection for biodiagnostic applications

9.2.2. DNA Microarray Experiment: real strategy

The so prepared PPAA-UPVC slides were finally used to obtain a DNA MicroArray able to detect the presence of *L. monocytogenes* through a DNA hybridization experiment.

Enteritis is usually caused by eating or drinking substances that are contaminated with bacteria or viruses. The germs settle in the small intestine and cause inflammation and swelling, which may lead to abdominal pain, cramping, diarrhea, fever, and dehydration. Enteric infections are second only to respiratory tract infections as common medical problems, thus it is crucial to develop robust and inexpensive biological tools to determine the causes of these pathologies, which, nowadays, are still carried out by in-solution classical assays.

I

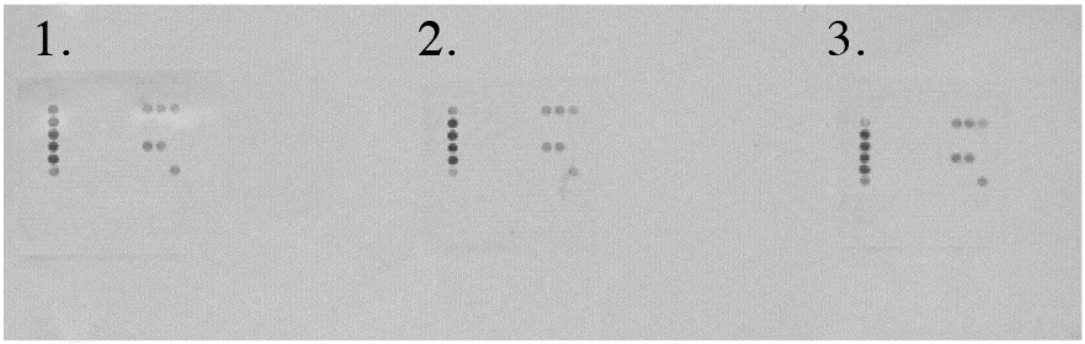

II

C1	2	2	2	N	N	2	C1	C1	C1
1	2	2	2	N	N	2	2	2	2
1	2	2	2	N	N	2	2	2	2
1	2	2	2	N	N	2	C1	C1	2
1	2	2	2	N	N	2	2	2	2
C1	2	2	2	N	N	2	2	2	C1

III

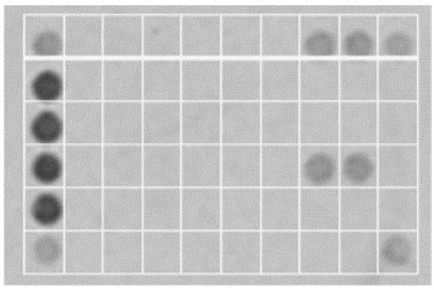

Figure 9.4 Photograph of PPAAc- UPVC slide after colorimetric detection of Listeria *monocytogenes* hybridization (1. 300 ng; 2. 600 ng; 3. 6 µg) II – grid corresponding to position of spotted solutions: C1: biotinylated control probes, 1: Listeria *monocytogenes*, 2: aspecific probes, N: hybridization buffer; III – enlargement of region 1. of image I.

The hybridization tests (Figure 9.3) were performed on PPAA-UPVC slides and replicated on commercial slides (Dr. Chip – LifeLineLab), in order to compare the performances of the substrates According to the grid in Figure 9.3-II, C1 corresponds to the position in which control biotinylated probes have been spotted, 1 position hosts the *L. monocytogenes* probes, 2 position is related to aspecific probes (*Escherichia*, *Salmonella*, etc.); on N zone hybridization Buffer, used as a control for spotting contamination has been spotted. Figure 9.3-I reports the image of the PPAA– UPVC slide on which, after DNA probe positioning, the hybridization of the PCR products containing the complementary *L. monocytogenes* DNA s-strands and the colorimetric detection by SilverQuant® have been carried out. Arrayed dark spots with intensity comparable with the control biotinylated probes have been yielded only in correspondence of positions 1. Regions 1. 2. 3. of Figure 9.3-I concerns the different content of *Listeri*a target in used solutions: 1. → 300ng; 2. → 600ng; 3. → 6µg. It is worth of notice that region 1. (enlarged in III) shows spots intensity comparable with the other region where a higher *Listeria* content solution has been put in contact and with the biotinylated probes spots. The comparison of the results obtained through the PPAA-PVC slide hybridization with respect to the commercial ones, revealed no signal differences. This gave evidence of the robustness and efficiency of the PPAA films to induce the correct biological response upon

immersion into a physiological medium, so opening the possibility of its usage for the development of DNA Microarray able to perform a whole hybridization experiment.

Conclusions

The plasma-polymerized acrylic acid thin film was successfully applied to a DNA Microarray biochip for biosensing applications. The functional layer deposited on the substrate shows reactivity towards biomolecules, exposing carboxylic groups readily accessible without any adding step of activation such as the use of N-hydroxysuccinimide (NHS) and 1-ethyl-3-(3-dimethyl aminopropyl) carbodiimide (EDC), as reaction catalyst.

DNA Microarray experiment described in this study shows a successful and innovative detection test of hybridization of *L. monocytogenes* suggesting that an efficient and unique combination of surface properties has been achieved in this PPAA polymer so that it can be generally proposed for functionalization of the surface of biosensing devices.

References

[1] Jafari R., Arefi-Khonsari F., Tatoulian M., Le Clerre D., Talini L., Richard F.," Development of oligonucleotide microarray involving plasma polymerized acrylic acid", *Thin Solid Films* **2009**, 517, p. 5763-5768.

[2] Marasso S. L., Giuri E., Canavese G., Castagna R., Quaglio M., Ferrante I., Perrone D., Cocuzza M.,"A multilevel Lab on chip platform for DNA analysis", *Biomed. Microdevices,* **2011**, 13, p. 19-27.

Chapter X

Application of a functional patterned plasma-polymerized layer of acrylic acid and styrene to a photonic crystal for optical biosensing

Molecular medicine represents a new frontier for the public health.

New approaches for biological target therapies, and new tools for the early diagnosis of chronic diseases including cancer are being developed.

Recent improvements in molecular medicine together with the advances of micro and nanotechnologies are opening very interesting perspectives in the interdisciplinary field of therapy and diagnostics in cancer research. A main challenge for nanotechnology is the need f integrated devices performing thousands of complex biochemical analysis with high sensitivity and short execution time. The actual limits of nowadays technologies (high costs, difficult automation, low sensitivity, accuracy and precision for quantitative methods) are hampering the development of future applications, especially in the sensing domain. As a consequence, a clear strategic road-map in the development of innovative bio-oriented devices having high-tech content must first converge on medical and diagnostic applications of outstanding importance.

Concerning these fields of applications, a relevant and largely unsolved issue is the lack of methods increasing the sensitivity and reliability of biological measurement including proteins and nucleic acid sequences [1]. Actually the measurement of very low amount of specific biomarkers is required for both early diagnoses and to follow the outcome of therapies to control a specific biological process.

10.1. Photonic Biosensors

In the last years, a large interest has been addressed to optical biosensing based on **Surface Plasmon Polaritons** (**SPP**). These optical surface waves are interesting because of the strong electromagnetic field enhancement, the spatial confinement at interfaces and thus an high sensitivity upon perturbations. **SEW**s, similar to SPP, can be obtained on dielectric photonic

structures such as planar multilayers (one dimensional photonic crystal 1DPC) [2,3]. Although the idea of using SEWs for sensing purposes is not completely new, very few works have been published on this subject, as compared to the huge literature on SPPs. Specific biomarkers selectivity is provided by chemical functionalization of the sensor active area. Surface functionalization of the last structure layer is performed by vapour self-assembled monolayers of amminosilane. Organosilane self-assembled monolayers (SAM) have been widely used to tailor the surface of glass, quartz, oxidized Si wafers and silica particles [4]. Specific antibodies (Abs) immobilized on the 1DPC free surface will induce a change in the refractive index at the interface, thus changing the coupling conditions of SEWs upon binding of the cognate biomolecules. The accurate monitoring of such changes will allow an high precision and sensibility in the measurement [5].

10.2. Surface Plasmon Resonance

Surface plasmon resonance spectroscopy (SPR) has emerged, over the last two decades, as a powerful surface analytical technique for the study of biomolecular and biomolecule-surface interactions. It was probably the demonstration of its sensitivity for protein adsorption studies, the facile construction of SPR instruments, and the introduction of commercial SPR equipment that spurred such interest in this technique over a broad range of disciplines and research groups around the world. One of the earliest reports on the SPR phenomenon dates back to the beginnings of the 20th century when dark and light bands were observed in the background when a continuous source irradiated a metal grating with light polarized in the plane of incidence. This was subsequently explained as the excitation of surface electromagnetic waves at the metal-air interface. Years later, the concept of volume plasmons in metals was introduced. These volume plasmons were described as longitudinal fluctuations of volume electron density. The concept of fluctuating electron density allowed the description of volume plasmons in a theoretical format. In 1959, an experimental confirmation of Ritchie's theory was reported. Ritchie's theory also described `lowered' plasmon modes at metallic foils boundaries. These `lowered' plasmon modes were later described as surface plasmons. It was not until the early 1980s that the first demonstrations on the use of SPR for biosensing applications were first reported and it took almost another decade for the advent of commercial SPR instruments (BIAcore, IASYS, IBIS, SPREETA, Bio Tul, GWC Instruments, and others).

Today, research laboratories around the world routinely use SPR to study adsorption, biospecific molecular recognition, self-assembly, and other phenomena occurring at the surface of metallic thin films.

The SPR phenomenon is also responsible for the unique optical properties of colloidal metals such as gold. It was Michael Faraday who first proposed, through a series of qualitative experimental observations, that the bright red color of ruby glass and his colloidal gold preparations was due to finely divided gold particles. The optical properties of colloidal gold (and other metals) have only recently begun to be exploited for colorimetric detection assays and the analysis of biospecific interactions. It is likely that novel applications of metallic nanoparticles exploiting the SPR phenomenon will emerge in the near future. Thus, offering complementary advantages to planar substrates and/or an entirely new set of nanomaterials with unique optical properties.

Surface plasmon resonance finds widespread uses in biochemistry, biomaterials and surface science. However, a detailed understanding of this technique requires knowledge of optics, solid-state physics, and surface chemistry. Often, the user has only a superficial understanding of these fields [6].

10.3. Bloch Surface Waves (BSWs) propagation

In alternative to SPPs, electromagnetic modes propagating at the interface between a homogeneous medium and a truncated periodic structure [7], such as a one-dimensional photonic crystal (1DPC) have been recently proposed [8]. This kind of surface modes, also referred to as Bloch Surface Waves (BSW), share some common characteristics with SPPs. In analogy to dielectric loaded waveguides for surface plasmon polaritons (SPP) on smooth metallic films [9], BSWs can be confined to some extent on ultra-thin relieves having a micrometer-sized lateral dimension [10,11]. Their dispersion is located within forbidden bands of the 1DPC, beyond the light line of the homogenous medium. This results in an exponential decay of the field envelope inside the periodic structure and an exponential decay of the field in the homogeneous medium because of total internal reflection. Moreover, BSWs offer several possible advantages as compared to SPPs. In fact, the BSW dispersion is not limited by the properties of a particular material and can be designed at almost any wavelength by properly choosing the refractive index and thickness of the layers constituting

the 1DPC. Since dielectrics for energy lower than the optical gap, are characterized by much lower extinction coefficients than metals, BSW resonances appear much narrower than those observed for SPP [12], with an expected increase of sensor performances. The possibility to excite simultaneously several different surface modes in the same 1DPC allows for self referencing sensing [13]. Such BSW waveguides are furthermore wavelength scalable and fully compatible with the fabrication technologies for integrated photonic and plasmonic structures. Moreover, the use of dielectric materials offers a wide variety of biochemistry routes for surface functionalization not limited to the thiol-based chemistry, such as carboxylic or amino-terminated organo-silanes [14]. Such features make dielectrics, and biosensors based on dielectric 1DPC, even more attractive.

10.3.1. Functionalization of the 1DPC photonic device

The photonic crystal object of this study is a multilayer (**1DPC**) based on hydrogenated amorphous silicon nitride (a-Si1-xNx:H) grown by Plasma Enhanced Chemical Vapor Deposition (PECVD) on Corning glass substrates. Depending on the nitrogen content, a-Si1-x Nx:H can have tunable refractive. Moreover, such a deposition technique allows a nanometric control of the growth process. This basic structure is constituted by stacks of high and low refractive index layers with properly designed thicknesses. Here, we consider a 1DPC made of a high index material H (silicon nitride, n_H=1.99 at λ=532.0 nm) and low index material L (silicon dioxide, nL=1.48 at λ=532.0 nm) grown by plasma enhanced chemical vapour deposition (Oxford Plasmalab 80þ PECVD) and arranged in 15 layers as follows: glass/$(HL)^7$L1/air. Each layer in the periodic stack has a respective thickness t_H=79 nm, t_L=134 nm, while the last tailoring layer at the air side has a thickness t_{L1}=28 nm.

Thanks to a set of computational tools developed in our research group, a rigorous simulation of the interaction of light with 1DPC can be performed. Based on calculations, a customized design of photonic structures can be obtained, depending on practical parameters such as the spectral range of operation and illumination angles. Moreover, the structure can be tailored by adding specific additional layers (silicon oxide) where chemical functionalization will be performed.

The experimental setup for BSWs propagation is depicted in Figure 10.1

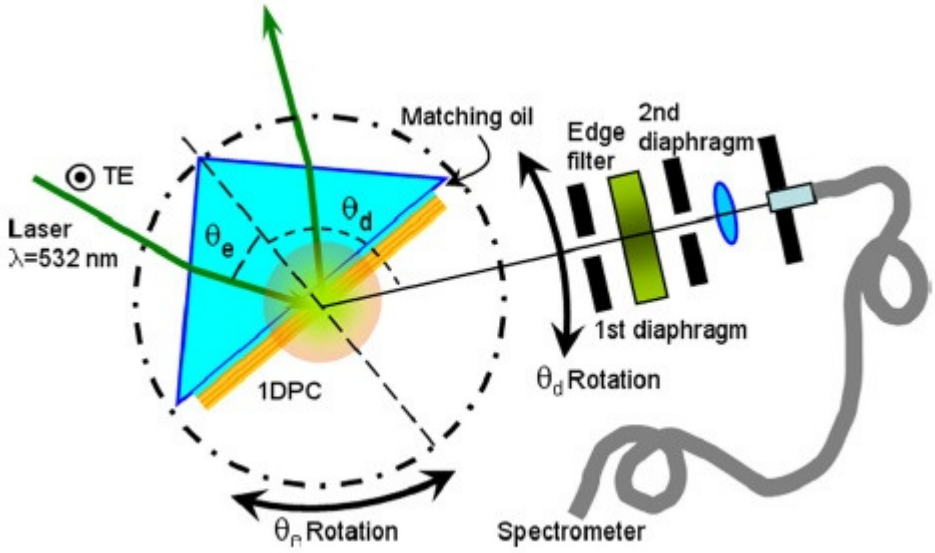

Figure 10. 1 Sketch of the experimental setup of the photonic crystal

A TE-polarized collimated CW Nd:YAG laser beam (λ=532.0 nm) illuminates the 1DPC oil-contacted to a glass prism according to the Kretschmann-Raether configuration. The prism is held on a motorized rotational stage allowing to accurately adjust the angle of incidence θ_e. The detection arm is mounted on an independent homocentric rotational stage, in such a way that the radiation leaving the sample with an angle θd, with respect to the normal to the sample, can be detected on either the prism or the air side of the 1DPC. Light is angularly filtered by two diaphragms (resulting in an angular acceptance of about 0.2°), spectrally filtered with an edge filter (RazorEdge from Semrock) for 532.0 nm radiation, and eventually focused into a fibered dispersive spectrometer (Ocean Optics USB2000þ).

The aim of surface functionalization of the photonic crystal is to render the surface of 1DPC device homogenously active for biosensing through a multi-step controlled and reproducible functionalization method.

Imparting a chemical specificity to the surface through the formation of covalent bonds, at every step of functionalization, it will be possible to ensure the invariability of the zero detection conditions before the target molecule are immobilised by the probes grafted at the surface. Due to the bonds stability, the detachment of molecules from the receptor layer or the aspecific adhesion of impurities is strongly limited.

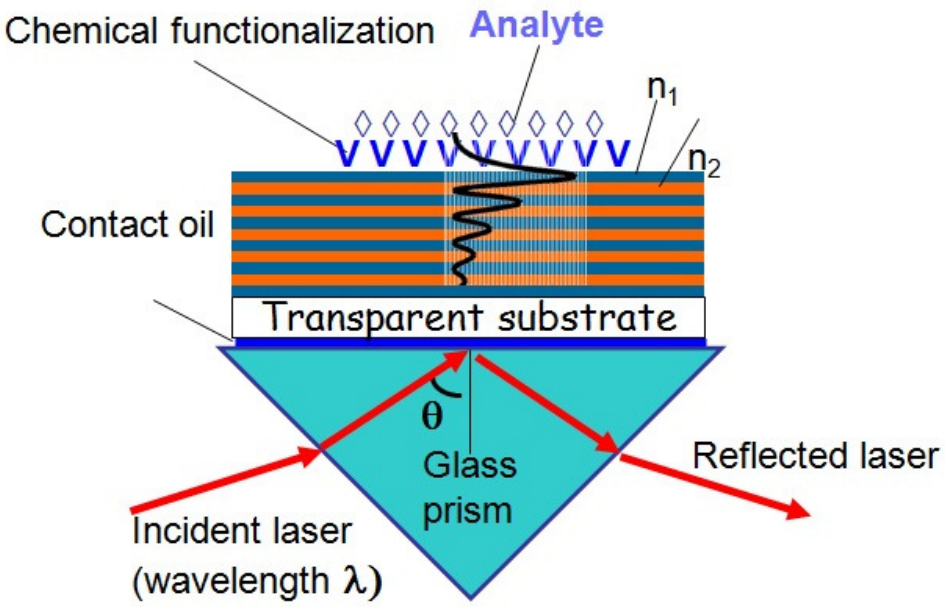

Figure 10.2 The multilayer photonic device functionalized for analyte detection mediated by Bloch Surface Waves (BSWs) propagation on the top layer after opportune light eccitation

The chemical selectivity for probes biomolecules avoids, during target molecules detection, unspecific interaction of targets with the surface. These unwanted phenomena would both heavily affect the sensibility of quantitative measurements of very low moieties of biomolecules, that is the core of the device, and render vane the efficiency of biological models achievable at the surface.

The process will be optimized regarding the activity, selectivity and homogeneity properties of the functionalized surfaces in order to be compatible with integration of the multilayer structure in the apparatus based on surface electromagnetic waves (SEWs) detection. The most difficult task will be the choice of minimal moieties of reactants to be anchored at surface, but however efficient for grafting, in order to minimize the decrease of the potential high sensibility of the as-it-is photonic structure.

A functionalizing method based on plasma-polymerized thin functional layers was applied with good results on 1DPC [15]: in this paper an alternative method for the detection of the enhanced fluorescence based on Bloch surface waves (BSWs) propagating at the truncation surface of the one dimensional photonic crystal (1DPC) is proposed.

The use of surface plasmon polaritons (SPPs) for the modification of the emission properties of a fluorophore in close proximity of a metal surface has been well documented [16]. In particular mainly two SPP-based techniques have emerged for controlling the enhancement, polarization, and direction of the emitted fluorescence, namely, the surface

plasmon field-enhanced fluorescence (SPFS) and the surface plasmon-coupled fluorescence (SPCE) [17,18]. In the SPFS, one benefits from the enhanced excitation of the emitters upon a resonant coupling of the illuminating (laser) radiation to the SPP sustained by the metallic film, leading to an overall measured enhanced fluorescence. Conversely, SPCE is based on the coupling of fluorescence into the SP mode of the metal film, which is re-irradiated only at angles that satisfy the SPR dispersion relation. In particular, this latter method has been proposed as a tool to significantly improve the detection performances. SPCE is most useful for the strong directionality of fluorescence emission, which results in a higher signal-to-noise ratio, and for applications where multiplexing is desired.

Compared to the mentioned techniques, the benefits of using BSW is twofold. Firstly, BSW-based detection does not suffer from signal losses, being the enhancing medium made of dielectrics. Secondly, the distance between the emitters and the 1DPC surface is less critical due to the absence of quenching and strong absorption effects played by metals.

To realize this purpose, the 1DPC device, able to sustain BSW, realized with the parameters described before, was functionalized by plasma polymerization of acrylic acid, with the deposition on the top of a 30 nm thin polymeric PPAA layer (n=1.53).

PPAA can expose up to 10^{16} -COOH functional groups/cm^2 suitable for protein binding.

Subsequently, a solution containing protein A labeled with Alexa Fluor 546 was incubated at concentration 0,1 mg/ml for 30 min on the polymeric layer. After washing, a 1DPC with a homogeneously fluorescent polymeric cap is obtained.

The advantage derived from this type of functionalization is evident when the 1DPC is aimed at specific sensing application; in this case it is possible to explicitly take into account and thus compensate the presence of a functionalization/tailoring layer (such as a 30 nm thick PPAA layer, as used herein). In such a way, the emitters can always be located at a suitable distance to the structure in order to optimize the radiated power after coupling to the BSW modes. If a functional/ tailoring layer is surface patterned, complex emitting structures for guiding BSW can be obtained (Figure 10.3)

To obtain a patterned surface composed of strips guides on the 1DPC structure a combination of lithographic techniques and plasma polymerization processes was used.

Acrylic-acid plasma polymer was deposited on the substrate as thin guides, for this reason strips deposition was achieved on the 1DPC surface by lithography. The scheme of the functionalization procedure is represented in Figure 10.3.

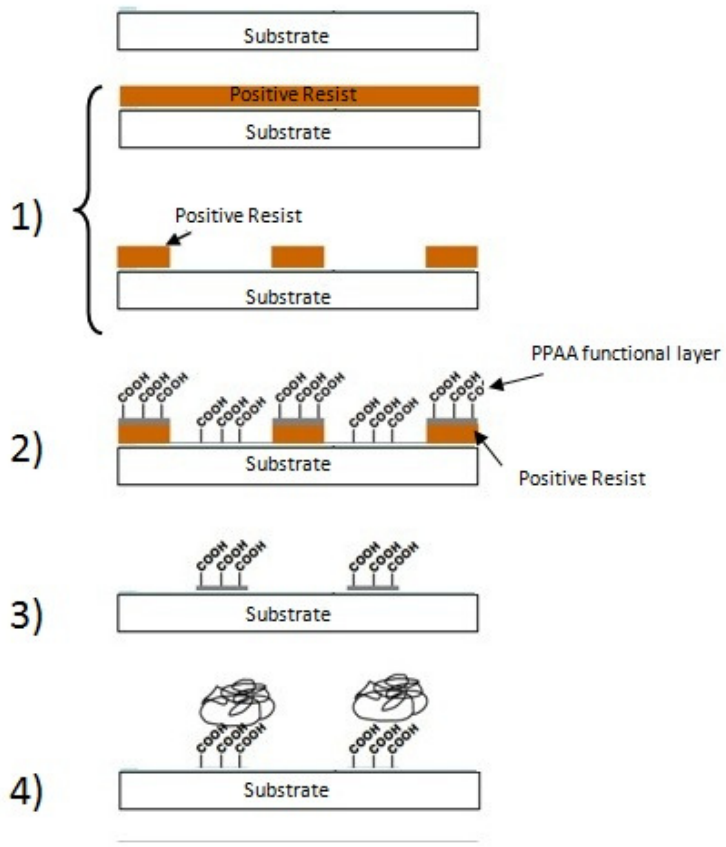

Figure 10. 3 Scheme of the functionalization procedure realized by combination of plasma-polymerization and lithography techniques to obtain acrylic-acid functional guides

After rinsing in ethanol and baking the sample to remove solvent residuals, spin coating for resist (AZ5214E image reversal) deposition was performed by lithography technique (step 1 Figure 10.3). The procedure used was the following:

- spinning of the resist on the multilayer (3500 rpm for 30 seconds)
- UV exposure (with an appropriate mask) for 65 seconds
- hard bake (110°C for 3 minutes)
- developing with AZ Developer and Water (1:1)

This procedure is showed in Figure 10.4 and it results in strips characterized by 1µm as thickness.

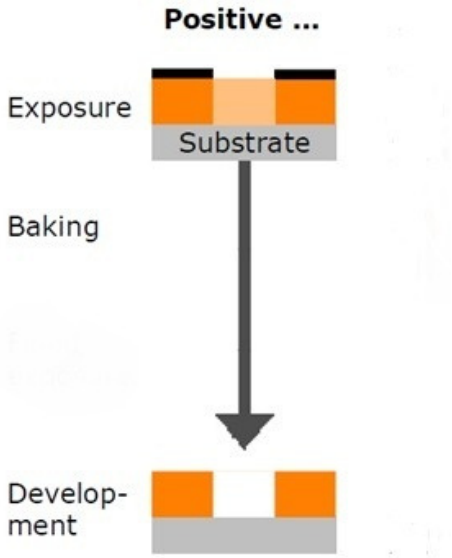

Figure 10.4 Different steps in strips deposition by resist AZ5214E image reversal used as positive resist

The following step (step 2 Figure 10.3) was the deposition by plasma polymerization of the acrylic-acid thin functional film with the optimized working parameters as described in Chapter 7 (P= 200W, DC=10%, T_{on}+T_{off}=10+90 ms, Ar pre-etching) using a deposition time of 4,5 minutes in order to have a final thickness of ~ 30 nm. After PPAA deposition the lift-off procedure for strips removal was performed by sonicating the sample in acetone for 60sec and drying it with N_2 flux (step 3 Figure 10.3).

At each step of the procedure the substrate was investigated by AFM.

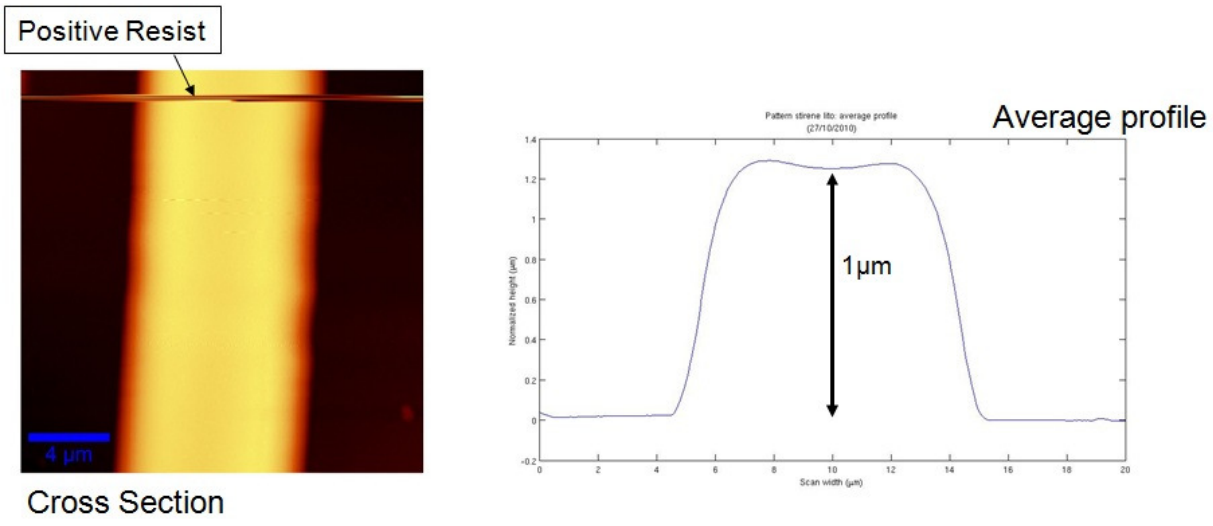

Figure 10.5 Resist strips deposited on the 1DPC surface: cross section and profile investigation by AFM

The 1DPC photonic crystal after the deposition of plasma-polymerized acrylic acid thin film (4,5 minutes as deposition time), before the lift-off step, was investigated by AFM to verify the presence of the resist strips (Figure 10.5). After strip removal by lift-off in acetone, acrylic acid functional guides remain deposited on the surface of the multilayer (Figure 10.6).

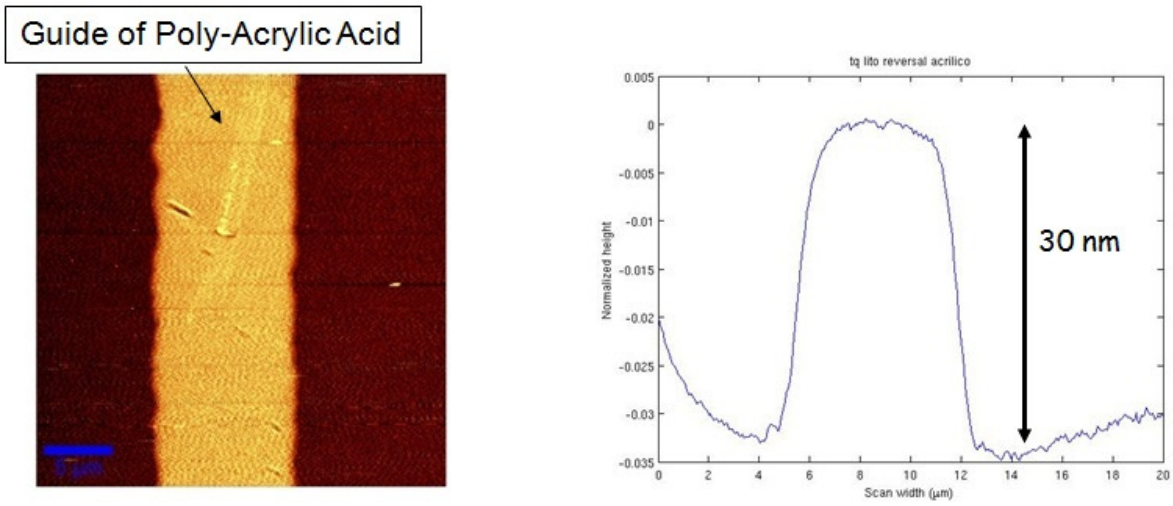

Figure 10.6 PPAA strips deposited on the 1DPC surface after lift-off procedure: cross section and profile investigation by AFM

After strip removal a well-definite guide characterized of a thickness of 30 nm and a micrometric width is obtained on the surface.

The last step was the test of the protein binding on acrylic acid guides (step 4 Figure 10.3) to verify their reactivity towards biomolecules after the functionalization procedure. Figure 10.5 show the detection of Protein A (PtA) labeled with a fluorescent marker (Alexa-Fluor) on the PPAA-1DPC substrate by Fluorescence Microscopy analysis.

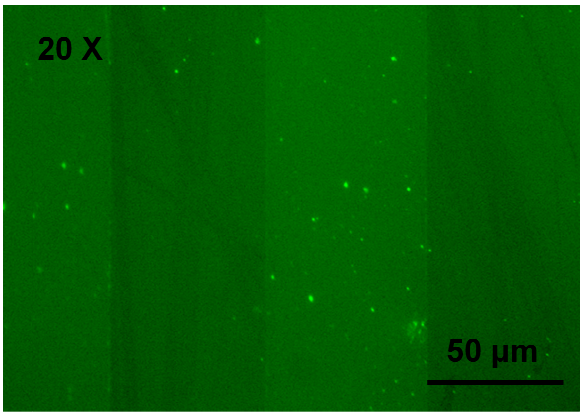

Figure 10.7 PtA-Alexa Fluorescence Emission on 1DPC coated by plasma-polymerized acrycic-acid guides

As it is observable from Figure Protein A is able to bind specifically to PPAA guides (brighter zone corresponds to protein fluorescence emission), as fluorescence emission is higher in correspondence to these strips. Good previous results were obtained with PPAA strips functionalization, anyway Figure 10. show a slight fouling effect due to unspecific protein A binding to uncoated substrate.

10.4. A patterned polymer-based surface functionalization of the photonic device

In order to optimize the sensitivity towards biomolecules and avoid unspecific adsorption especially in case of trace elements detection an interesting alternative to the deposition of a unique functional layer on the top of the photonic device is the functionalization of the surface of the crystal with a functional pattern based on the alternation of two different layers: a functional one, represented by the plasma-polymerized acrylic acid film and an anti-fouling coating represented by the styrene polymer deposited by plasma polymerization. To realize this functional pattern strips deposition by lithography techniques coupled with plasma polymerization processes were used.

As described before, on smooth metallic films, BSWs can be spatially confined on ultra-thin relieves similarly to dielectric-loaded waveguides for surface plasmon polaritons (SPP). This effect is due to a combined role of the remarkably narrow energy/momentum BSW resonance and the redshift experienced by the BSW resonance upon slight surface perturbations, such as the deposition of a small amount of patterned organic add-layers. As described in the previous paragraph, recent works have demonstrated that such a lateral confinement of BSW-coupled fluorescence can be pushed down to approximately 500 nm in

a suitable photonic structure consisting of AlexaFluor 546-labeled polymeric ridges 30nm thick patterned on a silicon nitride/silicon dioxide 1DPC [18].

In the case of a functional pattern, the spatially-selective BSW coupling conditions on a similar patterned 1DPC are exploited in order to perform an angular/spectral multiplexing of BSW-coupled fluorescence.

In order to localize protein binding only to specific zones and to avoid unspecific adsorption to the surface of SiNx multilayer constituting the photonic device a scheme of functionalization was realized to obtain a functional patterned polymer on the top of the 1DPC.

The first step was the deposition of an anti-fouling layer represented by the plasma-polymerized styrene (Figure 10.4). Applying working conditions described in chapter 8 (P=250 W, *DC*=10%, T_{on}+T_{off}=20+180 ms, Partial $Press_{ST}$= 5 mTorr, T dep= 5 min, Ar pre-etching) an hydrophobic-non bio-adhesive coating, stable after rinsing in water, was deposited on the surface of the multilayer. Due to the chemical composition (C6H5CH=CH2) styrene plasma polymer avoid protein adsorption to the photonic crystal surface.

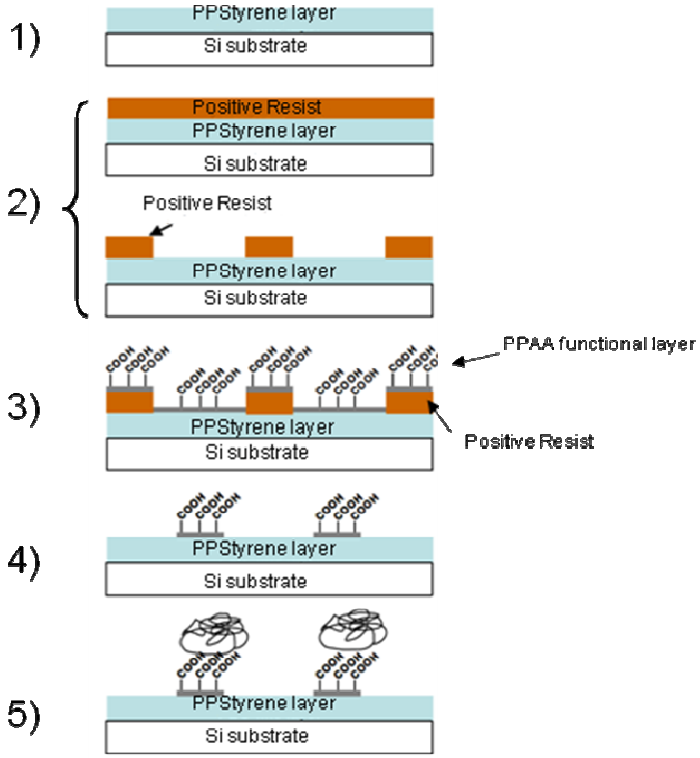

Figure 10.8 Scheme of the functionalization procedure realized by a patterned functional polymer deposition

For the other steps it was followed the same procedure of functionalization described in paragraph 10.3.1 for acrylic-acid guides.

The patterned functionalized surface of the 1DPC multilayer was incubated with protein A solution. The scheme of the procedure is represented in Figure

10.4.1. Pattern of functionalization: fluorescence emission mediated by Bloch Surface Waves

The functionalization procedure carried out at the surface of the 1DPC device for specific BSWs coupling to Fluorescence emission, resulted in the deposition of the micrometric ridges (width 50 μm, height 30 nm, length 1 cm) on 1DPC surface by means of photo-lithography, followed by a Plasma-Polymerized Acrylic Acid (PPAA) deposition (20 nm thickness) and a liftoff procedure in acetone. Before performing the photo-litographic and the lift-off process, a 5 nm thick Plasma-Polymerized Styrene film (PPST) is deposited on the silicon oxide surface of the 1DPC (paragraph 10.4) is represented in Figure 10.9 (a).

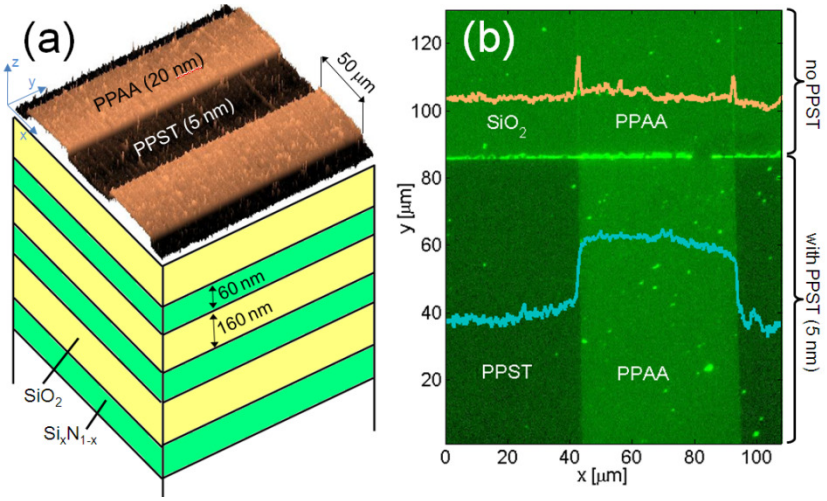

Figure 10.9 (a) Combined view of a sketch of the 1DPC deposited on glass and an AFM topography of the polymeric pattern on top (vertical dimension not to scale); (b) fluorescence micrograph of a AF546-labelled 1DPC structured with PPAA stripes on regions with and without the underlying 5 nm thick PPST layer. The fluorescence contrast in the two regions is illustratively depicted by means of the cross-sectional curves displayed

The success full protein binding only to acrylic acid strips is observable in Figure 10.8. The presence of a non-bioadhesive layer represented by the plasma-polymerized styrene coating combined with PPAAc allows to enhance the selective binding of labeled PtA only on PPAA functional strips by exploiting the different chemical properties of the two polymers (hydrophobic PPST "trenches" and –COOH-rich PPAA "ridges"). In Fig.10.9 (b) a fluorescence micrograph of the sample surface is presented, in which it is possible to clearly see the gain in fluorescence contrast (in/out ridge) due to the presence of the underlying 5 nm thick PPST layer. Without the PPST film, the fluorescent PtA is non-specifically adsorbed over the whole surface. The proposed combination of hydrophobic/functional materials such as PPST/PPAA for fabricating ultra-thin photonic structures can be fruitfully exploited in biosensing applications.

Fluorescence coupled to the two BSWs is presented in Fig.10.10. Measurements are performed collecting the fluoresence at several detection angles θ_d, provided a direct, normal illumination of the patterned 1DPC surface from the air side (θ_e=180 deg). With this kind of illumination, no resonance effects are expected to occur and both regions of the sample (with and without the PPST layer) are illuminated with the same intensity. Moreover, since the presence of the underlying PPST layer makes the relative amount of fluorescent PtA different from trenches to ridges, fluorescence intensities associated to the two BSWs are different (Fig.10.10 (a)). This observation confirms the fact that the two BSW modes are associated to separate spatial regions. When a PPST-free region is illuminated, the two BSW-coupled fluorescent curves show almost equal fluorescence intensity levels (Fig.10.10 (b)). The comparison among dispersion curves within a single fluorescence map is made easier by the insets, where a plot showing the normalized angle-resolved integrated-fluorescence intensity in a spectral region 10 nm wide (as indicated in the figure) is reported. It can be clearly seen that the contrast between the normalized fluorescence intensities is larger in the case the PPST layer is present.

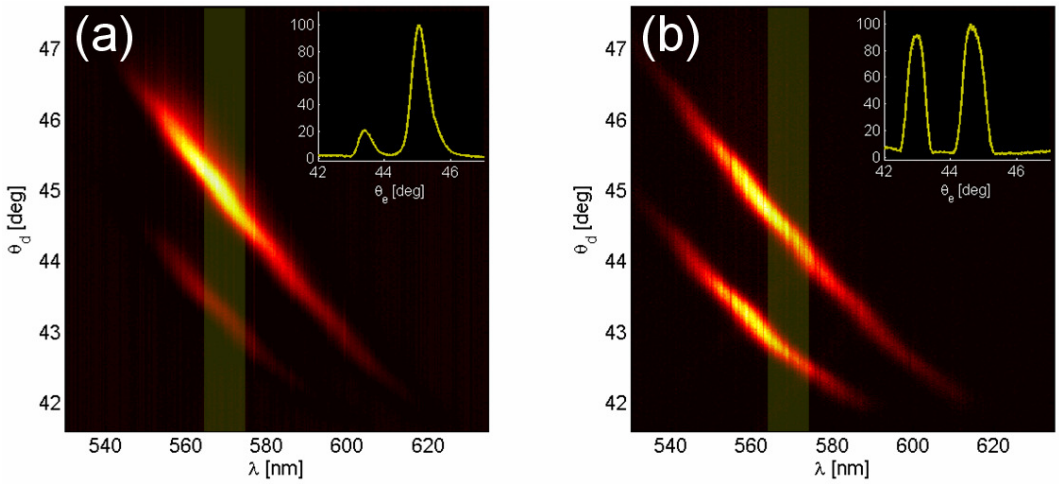

Figure 10. 10 Fluorescence maps collected upon illumination from the air side, normally to the patterned 1DPC surface. (a) Sample with 5-nm thick PPST layer; (b) sample with no PPST layer. The vertical band indicates the spectral interval used for calculating the integrated fluorescence as a function of the detection angle as shown in the inset

Figure 10.10 shows the angle-resolved fluorescence maps obtained by prism-illuminating the sample at the angle of coupling of the high-momentum BSW for the two cases in which the PPST layer is present (Fig.10.10 (a)) or not present (Fig.10.10 (b)). It can be seen that when the PPST layer is used, the fluorescence coming from the non-specific binding of the PtA is strongly suppressed (on/off resonant illumination [19]). The benefits of a scheme using both the selective binding of a fluorescent dye through a PPST layer and the selective BSW-coupled illumination can be summarized by comparing Fig.10.10 (b) with Fig.10.11 (a). In the former case, there is no chemical selectivity within the different areas of the sample. The fluorescent ptA is grafted homogeneously all over the surface and no resonant illumination occurs. Under these conditions, the collected fluorescence from the inside and the outside of ridges is comparable. In the latter case, the binding of PtA is strongly conditioned by the role played by the PPST layer, and mostly occurs on the top of the ridges. In addition, the resonant excitation is such that only the fluorescence from the ridges experiences an intensity enhancement. The combination of these two effects results in a drastic suppression of the detected fluorescence from non-specific sites.

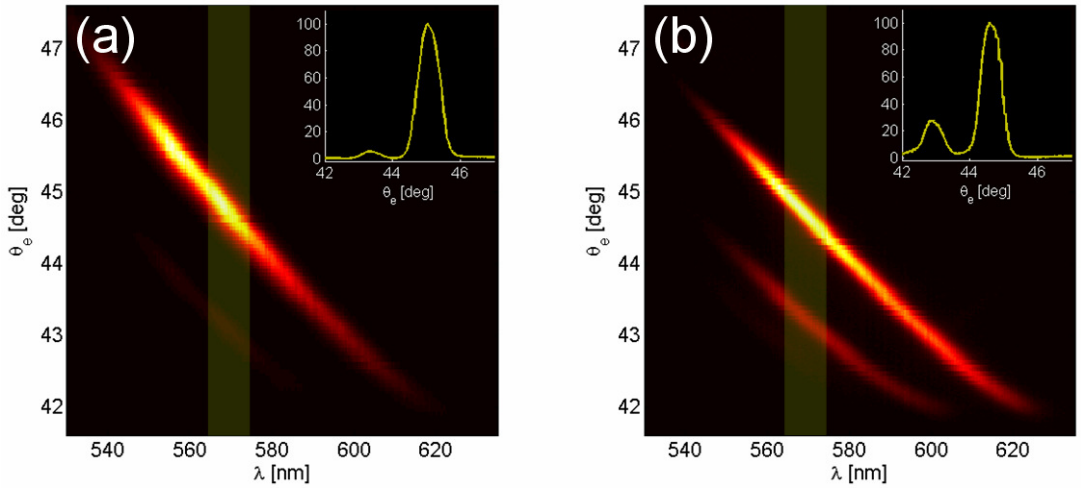

Figure 10. 10 Fluorescence maps as measured by a resonant prism-illumination of the high-momentum BSW (localized on ridges). (a) Sample with 5-nm thick PPST layer; (b) sample with no PPST layer. The vertical band indicates the area used for calculating the integrated fluorescence as a function of the detection angle as shown in the inset

Conclusions

In this study it was presented a particular type of functionalization procedure based on a polymer functional pattern, composed of functional guides (PPAAc) alternated to anti-fouling guides (PPSTc), realized on the surface of a photonic crystal able to sustain Bloch Surface Waves.

Since different regions of the patterned 1DPC can sustain BSWs belonging to different and well separated dispersion curves, distributed emitters will provide a fluorescence emission coupled to different BSW dispersion curves, depending on the location where they are grafted on. BSW-coupled fluorescence could be finally detected under different leakage angles out of the prism. In such a way it is possible to angularly and spectrally differentiate fluorescence emitted from different regions of the structure, without the use of any imaging technique. In the present case, a proof of principle of such an effect is presented on a micrometer-sized stripes, but an extension to higher-density patterns is expected to work as well.

The feasibility of laterally-confined BSW-controlled fluorescence on tiny guiding structures with nanometer-sized polymeric relieves implementing photonic and chemical functionalities at the same time. This finding may be mostly useful for sensing applications but it could be applied also to other domains such as gain-assisted surface waves on doped structured media.

References

[1] Woodcock J.,"Molecular Medicine: How, what, and when", *Clin. Pharmacol. Ther*., **2007,** 82, p. 376.

[2] Yeh P., Yariv A., "Optical surface waves in periodic layered media", *Appl. Phys. Lett*., **1978,** 32, p. 104-107.

[3] Robertson W. M., May S., "Surface electromagnetic wave excitation on one-dimensional photonic band-gap arrays", *Appl. Phys. Lett*., **1999**, 74, p. 1800-1810.

[4] Plueddemann E. P., *Silane coupling agents*, 2nd ed.; Plenum Press: New York, **1991.**

[5] Guillermain E., Lysenko V., Orobtchouk R., Benyattou T.,. Roux S, Pillonnet A., Perriat P., "Bragg surface wave device based on porous silicon and its application for sensing ", *Appl. Phys. Lett*., **2007,** 90, p. 241116 – 241119.

[6] Surfaces and Interfaces

[7] Yeh P., Yariv A., Hong C.-S., "Electromagnetic propagation in periodic stratified media. I. General theory", *J. Opt. Soc. Am*., **1977**, 67, p. 423–438

[8] Shinn M., Robertson W.M., "Surface plasmon-like sensor based on surface electromagnetic waves in a photonic band-gap material", *Sens. Actuators B*, **2005**, 105 (8), p. 360–364.

[9] Goto T., Katagiri Y., Fukuda H., Shinojima H., Nakano Y., Kobayashi I., Mitsuoka Y., "Propagation loss measurement for surface plasmon-polariton modes at metal waveguides on semiconductor substrates", *Appl. Phys. Lett.,* **2004**, 84, p.852-855.

[10] Descrovi E., Sfez T., Quaglio M., Brunazzo D., Dominici L., Michelotti F., Herzig H.P., Martin O.J.F., Giorgis F.," Guided Bloch Surface Waves on ultra-thin polymeric ridges", *Nano Lett.*, **2010**, 10, p.2087- 2091.

[11] Sfez T., Descrovi E., Yu L., Quaglio M., Dominici L., Nakagawa W., Michelotti F., Giorgis F., Herzig H. P., "Two-dimensional optics on silicon nitride multilayer: Refraction of Bloch surface waves ", *Appl. Phys. Lett*., **2010**, 96, p.151101-151104..

[12] Barnes W.L., "Surface plasmon-polariton length scales: a route to sub-wavelength optics*", J. Opt. A: Pure Appl. Opt.*, **2006**, 8, p. 87–93.

[13] Konopsky V.N., Alieva E.V., "A biosensor based on photonic crystal surface waves with an independent registration of the liquid refractive index", *Biosens. Bio-electron*., **2010**, 25, p.1212–1216.

[14] Fiorilli S., Rivolo P., Descrovi E., Ricciardi C., Pasquardini L., Lunelli L., Vanzetti L., Pederzolli C., Onida B., Garrone E., "Vapor-phase self-assembled monolayers of aminosilane on plasma-activated silicon substrates", *J. Colloid Interface Sci.*, **2008,** 321, p. 235–241

[15] Ballarini M., Frascella F., Michelotti F., Digregorio G., Rivolo P., Paeder V., Musi V., Giorgis F., Descrovi E., "Bloch surface waves-controlled emission of organic dyes grafted on a one-dimensional photonic crystal", *Appl. Phys. Lett*., **2011**, 99, p.043302.

[16] Lakowicz J. R., *Principles of Fluorescence Spectroscopy,* 3rd ed., Springer: New York, **2006**.

[17] Liebermann T. , Knoll W.," Surface-plasmon field-enhanced fluorescence spectroscopy", *Colloids Surf. A,* **2000,** 171, p.115-130.

[18]. Lakowicz J. R, Ray K., Chowdhury M., Szmacinski H., Fu Y., Zhang J., Nowaczyk K., "Plasmon-controlled fluorescence: a new paradigm in fluorescence spectroscopy", *Analyst*, **2008,** 133, p. 1308-1346.

[18] Ballarini M., Frascella F., Enrico E., Mandracci P., De Leo N., F. Michelotti F., Giorgis F., Descrovi E., "Bloch Surface Waves-controlled fluorescence emission: coupling into nanometer-sized polymeric waveguides," *Appl. Phys. Lett.* (accepted)

[19] Chaudhery V., Huang C.-S., Pokhriyal A., Polans J.,. Cunningham B.T., "Spatially selective photonic crystal enhanced fluorescence and application to background reduction for biomolecule detection assays," *Opt. Express* , **2011**, 19, p. 23327-23340.

Chapter XI

Surface modification of cell culture carriers: Routes to anhydride functionalization of polystyrene

Functional surface modifications of polymers for biomedical applications are of wide interest [1-3]. This applies in particular to cell culture carriers. Several works [4] document how surfaces functionalized with anhydride moieties provide a versatile platform for defined coupling of cell stimulating biomolecules. Anhydride moieties can react directly (i.e. without activating agents like EDC/NHS) with primary amines or hydroxyl groups from proteins. Furthermore, the ability to covalently bind biomolecules can be reversibly deactivated by simple means. After hydrolysis these surfaces possess only physisorptive properties for non-covalent coupling while an elevated temperature leads to recyclization and restores the anhydride ring (annealing). Using this technique the biological response of a cell culture can be controlled in a well-defined way [5, 6]. Combining this method of protein immobilization with lateral microstructuring allows to create patterns of cell adhesive and non-adhesive sites [7] which is a key to guided cell growth or to carry out single cell studies.

Towards this goal the study aims to provide a toolbox mainly for Research&Development purposes. A variety of approaches for anhydride functionalization of polystyrene is presented. Mostly, well-defined model surfaces are used to demonstrate the functionalization procedure. However, also the problem of 3D well plates with its geometrical restrictions is addressed. All surfaces can be sterilized without elevated temperatures (e.g. by gamma sterilization).

Since the examples were taken from different studies, a different range of materials and analytical techniques was applied in some cases. However, the results allow to compare the approaches with respect to the efficiency of anhydride functionalization. Also other peculiarities of the techniques, e.g. providing anhydride moieties either on a soft or on a rigid surface, are considered.

Plasma polymerization of functional thin films [8] is a well-known approach to surface engineering of polymers. For coatings containing anhydride moieties, maleic anhydride (MA) can be used as a precursor [9]. This was demonstrated by different research groups [10–13]. However, operating a low pressure plasma setup with gaseous MA usually requires an elevated temperature of the system. This includes the MA supply to obtain an appropriate vapor pressure and to establish a defined gas flow but also other parts of the apparatus like the vacuum chamber, the substrate holder, etc. to prevent condensation. A simplified approach working at room temperature was introduced by Gaboury and Urban [14,15]. Here, the solid MA precursor is placed in a vacuum chamber next to the polymer surface to be functionalized while a short microwave exposure is used to ignite a plasma. Based on this concept (referred to as maleic anhydride plasma reaction) an improved process was developed for the present study (Fig. 11.1a): solid MA and the polymer surface to be functionalized were placed next to each other in a remote argon discharge. The low pressure plasma simultaneously activates released MA molecules in the gas phase as well as the exposed polymer surface which leads to an efficient and durable anhydride functionalization.

Contrary to the plasma based MA surface functionalization from the gas phase, anhydride moieties can be introduced by the immobilization of MA copolymers [16] using different mechanisms. The first process of this type that is discussed here is plasma immobilization (Fig. 11.1 b) [17]. A low pressure argon plasma is used for covalent fixation of a thin polymer film on a polymeric substrate. Cross-linking and immobilization is achieved while functional groups are preserved. The technique works for a variety of materials [18,19] and is applied here to a MA copolymer system.

Replacing the plasma treatment by energetic electron irradiation leads to the approach of electron beam immobilization (Fig. 11.1 c) [20]. Once again the process is demonstrated for a MA copolymer system.

Furthermore, UV light can be applied to immobilize functional polymers on a polymeric surface. In this case a photoinitiator is required since the photon energy is lower compared to the energy of the active species in plasma or electron beam based processes. UV immobilization (Fig. 11.1 d) is demonstrated for a benzophenon functionalized MA copolymer. Instead of simultaneous cross-linking and immobilization by means of energetic irradiation, MA copolymers can be immobilized on a polymeric surface by a grafting to process. Functional groups that allow for covalent grafting can be provided by a low pressure

plasma treatment. Here, the grafting of functional polymers to plasma activated surfaces (Fig. 11.1 e) is shown for a MA copolymer and an ammonia plasma pretreatment.

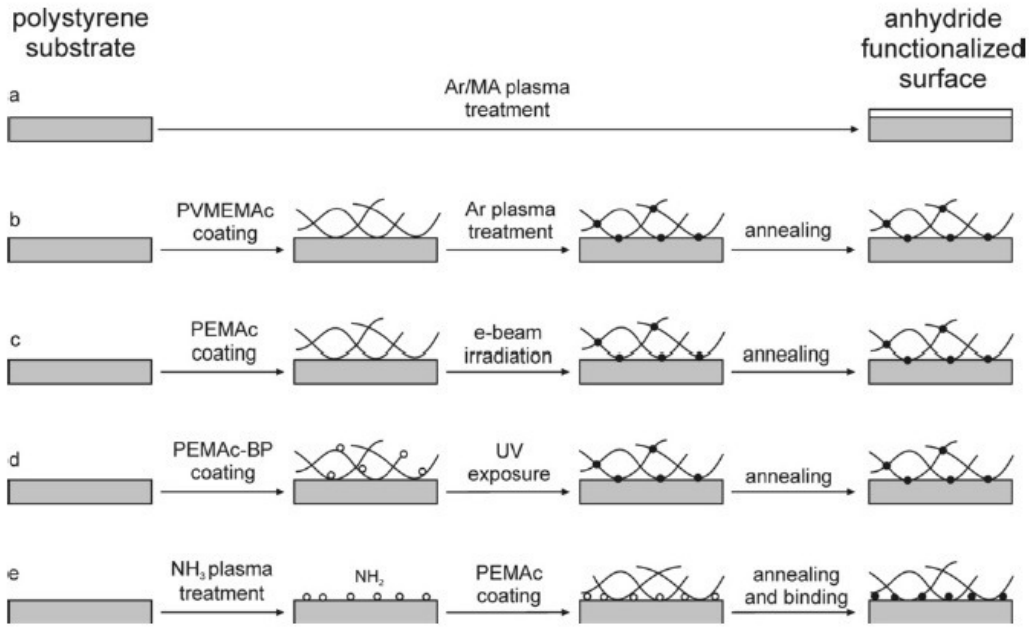

Figure 11.1 Approaches to anhydride functionalization of polystyrene surfaces

11.1. Materials used for surface modification

Surface functionalization experiments of this study were carried out on polystyrene (PS). To provide well-defined model surfaces, thin polystyrene films (PS type 148H, BASF) were prepared by spin coating (PS 1% (wt/wt) in toluene, 3000 rpm, 3000 rpm/s, 30 s) on various substrates: silicon wafers with 30 nm oxide thickness 15 mm*20 mm for ellipsometry, 7 mm*7 mm for XPS and attenuated total reflection (ATR) elements for infrared spectroscopy as described below. Furthermore, polystyrene well plates for cell culture (Greiner Bio-One, Frickenhausen, Germany) were used as samples.

For the plasma reactions maleic anhydride (MA) (99%, Aldrich) was used as received. For immobilization and grafting to experiments poly(vinyl methyl ether-alt-maleic acid) (PVMEMA) (MW 216.000 g mol^{-1}, Aldrich), and poly(ethylene-alt-maleic acid) (PEMA) were used.

PEMA was obtained by hydrolysis of poly(ethylene-alt-maleic anhydride) (PEMA) (MW 125.000 g mol−1, Aldrich). For that purpose 10 g of PEMA were immersed in 90 g de-ionized water and strirred for 5 days at room temperature. Subsequently the solution was dried and the conversion was verified by infrared spectroscopy.

11.2. Maleic Anhydride surface functionalization: working conditions

11.2.1. Maleic Anhydride plasma reaction

PS surfaces were reacted with MA in a low pressure argon plasma using the apparatus depicted in Figure 11.2 (P1).

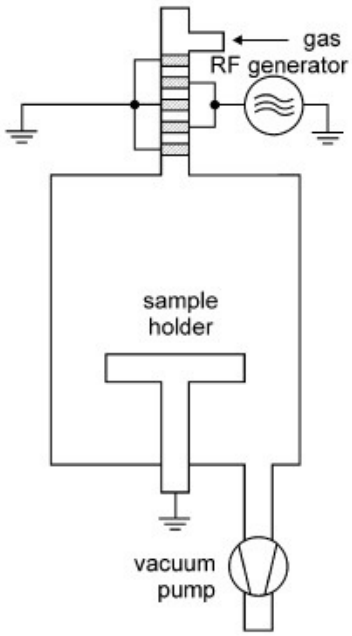

Figure 11.2 Schematic representation of the plasma device P1

The vacuum system of this setup consists of a quartz tube with a inner diameter of 20 mm and a length of 300 mm on top of a cylindrical part with an inner diameter of 200 mm and a length of 800 mm connected to a rotary vane pump (base pressure 1×10^{-3} mbar). The process gas is introduced into the chamber by a gas flow control system. A butterfly valve between the pump and the chamber allows to set a particular pressure for a given gas flow. For plasma

generation electrodes are attached to the outer surface of the quartz tube. The electrodes are connected to a 13.56 MHz radio frequency (RF) generator PFG300RF (Hüttinger, Freiburg, Germany) via an automatic matching network. This leads to an argon discharge in the small diameter tube. The bottom part of the chamber houses a grounded sample holder. The distance between the discharge region and the sample holder is set to 60 cm, i.e., the sample holder is placed in the afterglow region of the plasma. The gas flow, the pressure, the RF power and the duty cycle can be tuned to optimize the process.

Using this system plasma treatments were carried out placing PS model surfaces and a small amount of the solid precursor MA (0.15 g or 0.45 g) on the sample holder within a distance of 5 cm. The chamber was evacuated to the base pressure for 10 min. The argon flow was introduced into the chamber. After stabilizing the process pressure, plasma treatments were carried out using the following parameters: power 200W, pulse frequency 1000Hz, Duty cycle (*D.C.*)10–50%, Ar gas flow of 5–20 sccm, pressure $6*10^{-2}$ mbar, treatment time 300 s. Subsequently the gas flow was stopped and the system was evacuated for another 10 min.

11.2.2. Plasma immobilization of functional polymer thin films

PVMEMA was immobilized on PS using low pressure argon plasma in the apparatus represented in Figure 11.3 (P2).

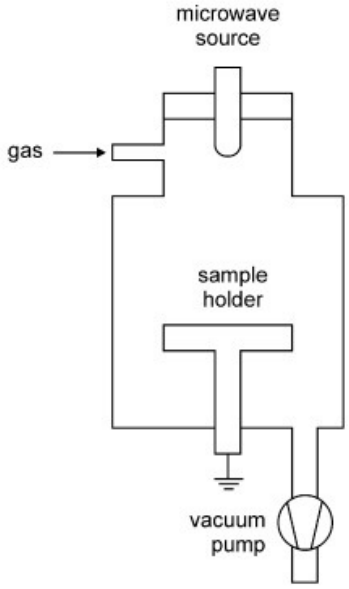

Figure 11. 3 Schematic representation of the plasma device P2

This set-up is a computer controlled MicroSys apparatus (Roth&Rau, Wüstenbrand, Germany). The cylindrical vacuum chamber, made of stainless steel, has a diameter of 350

mm and a height of 350 mm. The base pressure obtained with a turbomolecular pump is <10−7 mbar. On the top of the chamber a 2.46 GHz electron cyclotron resonance (ECR) plasma source RR160 by Roth&Rau with a diameter of 160 mm and a maximum power of 800 W is mounted. The process gas is introduced into the active volume of the plasma source via a gas flow control system. When the plasma source is on, the pressure is measured by a capacitive vacuum gauge.

Thin PVMEMA films were prepared by spin coating (1% (wt/wt) PVMEMA in methanol, 3000 rpm, 3000 rpm/s, 30 s) on top of PS model surfaces. The samples were introduced by a load-lock-system and placed on a grounded holder near the center of the chamber.

The distance between the sample and the excitation volume of the plasma source is about 200 mm. For the subsequent Ar plasma treatment the following parameters were used: effective power 120 W, argon gas flow 38 sccm, pressure 8×10^{-3} mbar, treatment time 7 s, 10 s and 15 s. To remove unbound material, the samples were rinsed in methanol at room temperature and dried under vacuum. Anhydride formation was achieved by annealing the samples up to 64 h at 90 ◦C (Figure 11.5).

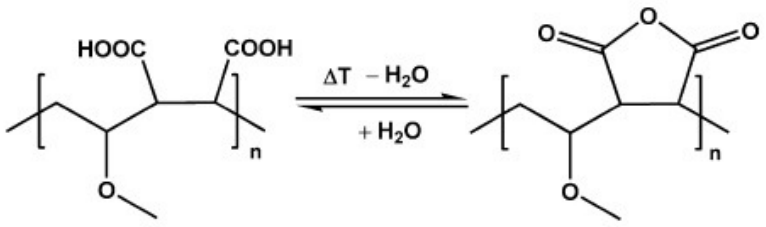

Figure 11.4 Conversion of the copolymers PVMEMA to the respective anhydride form

11.2.3. Electron Beam immobilization of functional polymer thin films

PEMA was immobilized on PS by electron beam cross-linking. For that purpose thin films of PEMA were prepared by spin coating (1% (wt/wt) and 2% (wt/wt) PEMA in methanol, 3000 rpm, 3000 rpm/s, 30 s) on top of PS model surfaces. Two different absorbed doses of 257 kGy and 770 kGy were applied. To remove unbound material, the samples were rinsed in methanol at room temperature and dried under vacuum. Anhydride formation was achieved by annealing the samples up to 64 h at 90 ◦C (Figure 11.5).

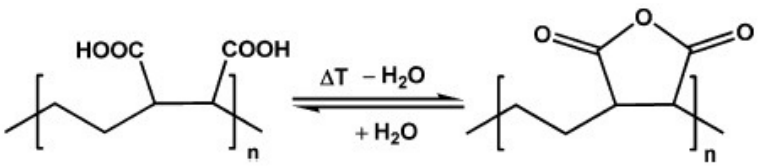

Figure 11. 5 Conversion of the copolymers PVMEMA to the respective anhydride form

11.2.4. UV immobilization of functional polymer thin films

For UV immobilization experiments the photoinitiator 4-amino benzophenone (BP) (98%, Merck) was covalently coupled to PEMA (PEMA-BP). This prevents the release of toxic low molecular weight residuals into the cell culture medium after cross-linking and immobilization. Three different modifications of PEMA-BP have been synthesized with a functionalization density of 5 mol% (PEMA-BP5), 10 mol% (PEMA-BP10) and 20 mol% (PEMA-BP20).

For that purpose 5 mmol of PEMA were dissolved in 15 ml acetone. 0.25 mmol, 0.50 mmol or 1.00 mmol BP were dissolved in 2 ml acetone respectively. The solution of BP was added stepwise at room temperature to the PEMA solution under stirring and left for 24 h. The polymer was precipitated in 40 °C warm n-hexane and washed three times with warm n-hexane before drying in vacuum at 60 °C. For hydrolysis, the dried polymer was stirred in de-ionized water for 48 h at room temperature. The water soluble product was freeze dried and analyzed by ^{1}H NMR.

Thin films of PEMA-BP were prepared by spin coating (1% (wt/wt) and 2% (wt/wt) PEMA-BP in methanol, 3000 rpm, 3000 rpm/s, 30 s) on top of PS model surfaces. After 10 min of UV irradiation, the samples were rinsed in methanol at room temperature and dried under vacuum. Anhydride formation was achieved by annealing the samples for 48 h at 90◦C.

11.2.5. Grafting of functional polymers to plasma activated surfaces

To provide free amino groups for the grafting procedure, PS well plates were treated with low pressure ammonia plasma in apparatus described in paragraph 11.2.2 (P2) using the following parameters: effective power 600 W, ammonia gas flow 15 sccm, pressure 7×10−3 mbar, treatment time 10 s. After that wells were filled with 150 µl cm−2 PEMA 0.2% (wt/wt)

in ethanol. The solution was allowed to dry up. Recyclization of maleic acid to maleic anhydride and covalent binding of anhydride to the amino functionalized PS surface was achieved by keeping the well plates for 24 h at 90 ◦C under vacuum. A subsequent rinsing for 24 h in de-ionized water was applied to hydrolyze and remove unbound copolymer. Finally, anhydride formation of the covalently bound PEMA was achieved by another annealing step for 24 h at 90 ◦C under vacuum.

11.3. Maleic Anhydride surface functionalization: characterization techniques

PS functionalized samples were characterized by XPS, Ellipsometry and FTIR-ATR for all the different approaches.

Ellipsometric measurements of thin polymer films on reflecting surfaces were performed using a SE400adv ellipsometer (Sentech Instruments, Berlin, Germany). Δ and Ψ values for four angles of incidence, 50°, 60°, 65° and 75°, were acquired for a wavelength of 633 nm. To calculate the thickness and the optical properties of the polymer films under investigation, fit procedures based on optical multi-layer models were applied to the ellipsometric data.

Values for the refractive indices were taken from the literature. Nine measurements from different spots across each sample were averaged.

XPS was carried out using an Amicus spectrometer (Kratos Analytical, Manchester, UK) equipped with a non-monochromatic Mg K_α X-ray source operated at 240 W and 8 kV. The kinetic energy of the photoelectrons was determined using an analyzer with a pass energy of 75 eV. The take-off angle between the sample surface normal and the electron optical axis of the spectrometer was 0◦. In this case, the information depth is about 8 nm. Spectra were

referenced to the 1s peak of aliphatic carbon at 285 eV. A satellite subtraction procedure was applied. Quantitative elemental compositions were calculated from peak areas using experimentally determined sensitivity factors and the spectrometer transmission function. High-resolution C1s spectra were deconvoluted by means of CasaXPS (Casa Software Ltd., UK) assuming the same full width at half maximum for all components.

FTIR-ATR spectra were obtained with a Vector 22 FTIR spectrometer (Bruker, Ettlingen, Germany) using trapezoidal shaped ATR elements made of chalcogenide glass IRG100 [21] with 45◦ incident angle and 17 reflections (9 effective reflections on the coated side). Sample spectrum and background spectrum were acquired with the coated ATR element and the clean ATR element respectively.

For the film thickness used in this work, the thin-film case of ATR spectroscopy applies [22]. In this case the film thickness limits the sampling depth, i.e., there is no variation of the sampling depth with wavelength. Consequently, absorbance units are given instead of ATR units.

11.4. Maleic Anhydride surface functionalization: results

11.4.1. Maleic Anhydride plasma reaction

Fig. 11.6 shows the XPS C1s spectrum for polystyrene functionalized by maleic anhydride plasma reaction. The spectrum can be deconvoluted into three clearly separated components at 285.0 eV (A) 286.8 eV (B) and 289.2 eV (C). While peak C is a first hint to anhydride surface functionalization, peak B suggests the simultaneous formation of other structures as a result of the plasma process.

The ratio A:B:C = 60:20:20 remains the same upon rinsing in organic solvents indicating a stable surface modification (results not shown).

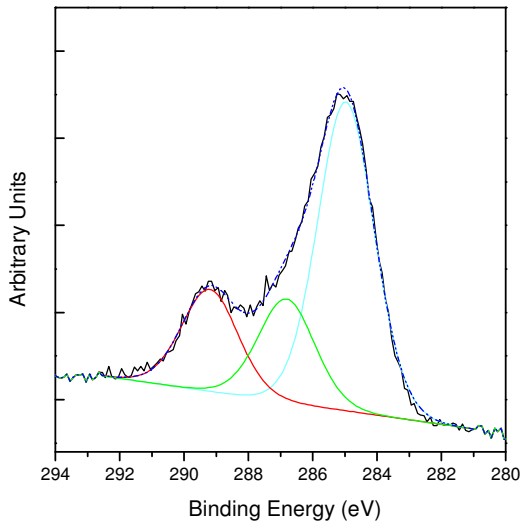

Figure 11.6 XPS C1s spectrum of PS functionalized by maleic anhydride plasma reaction (power 200 W, duty cycle 10%, Ar flow 20 sccm, pressure 6*10^{-2} mbar, MA 0.45 g, treatment time 5 min)

Infrared spectroscopy was used to prove the formation of anhydride structures. The two bands appearing at 1775 cm^{-1} and 1860 cm^{-1} (Fig. 11.7) correspond to the C-O stretching

vibration of cyclic anhydrides while the signal at lower wavenumbers arises from other carbonyl structures [23]. Both facts corroborate the XPS results mentioned above. Several attempts were made to enhance the fraction of the 1775 cm^{-1}/1860 cm^{-1} bands with respect to the total C O stretching signal. While the variation of the Duty Cycle or the carrier gas flow did not improve the efficiency of the process at all (data not shown), the gas composition was found to be an effective parameter. A higher amount of anhydride in the argon plasma (by providing a higher amount of solid precursor) led to a more distinct anhydride signal in the spectrum. Upon hydrolysis of the functionalized surface the two anhydride bands at 1775 cm^{-1} and 1860 cm^{-1} disappear and are replaced by a band at 1725 cm^{-1} (C-O stretching in COOH).

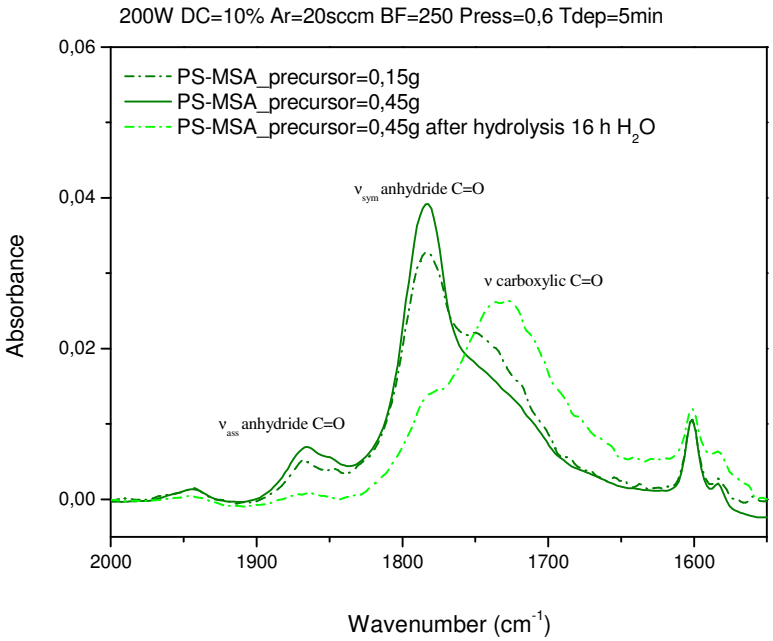

Figure 11.7 FTIR-ATR spectra of PS functionalized by maleic anhydride plasma reaction (power 200 W, duty cycle 10%, Ar flow 20 sccm, pressure 6*10^{-2} mbar, treatment time 5 min) related to different working conditions

11.4.2. Plasma immobilization of functional polymer thin films

Low pressure plasma immobilization of PVMEMA was investigated. The initial film thickness obtained by spin coating was 14 nm.

This is less than the interaction depth of the microwave argon plasma [17] and allows the grafting process at the PS-PVMEMA interface (otherwise no immobilization occurs). To optimize the efficiency of the process, the experiment was carried out with different treatment times. The amount of immobilized PVMEMA after plasma treatment and rinsing was

evaluated by ellipsometry. While no effect was observed for a plasma exposure of 7 s or less, treatment times of 10 s and 15 s led to an immobilized layer of 2 nm and 5 nm respectively.

Type of plasma treatment	PVME-MA (7 s plasma) rinsed	PVME-MA (10 s plasma) rinsed	PVME-MA (15 s plasma) rinsed
thickness (nm)	Ø nm	2 nm	5 nm

Table 11. Thickness values measured by ellipsometry on PVMEMA plasma immobilized on PS after different plasma treatment times (power 120 W, argon gas flow 38 sccm, pressure 8×10^{-3} mbar)

Structure retention was investigated by XPS. The C1s spectrum of immobilized PVMEMA on polystyrene after 15 s of plasma treatment and subsequent rinsing (Fig. 11.4) can be deconvoluted into three components at 285.0 eV (A), 286.8 eV (B) and 289.2 eV (C).

The chemical shifts of the components correspond to the values expected for the spectrum of pure PVMEMA while the relative intensities are different. The ratio of A:B:C = 63:24:13 (instead of 3:2:2 for pure PVMEMA) indicates a certain degradation of the original polymer structure upon argon plasma exposure (B and C should contribute equally).

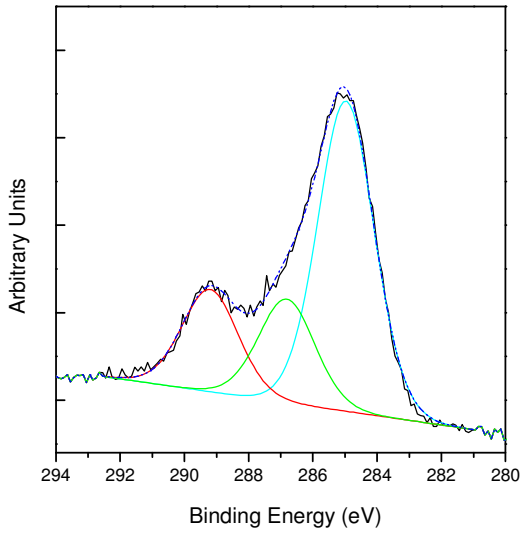

Figure 11. 8 XPS C1s spectrum of PS functionalized by PVMEMAc plasma immobilization (power 120 W, argon gas flow 38 sccm, pressure 8×10^{-3} mbar, treatment time 15s)

The excess in component A can be attributed to the fact, that the thickness of the immobilized material is less than the XPS sampling depth and, consequently, the PS substrate contributes to the spectrum.

Also in this case, a slight variation in the XPS spectrum is registered after rinsing (results not shown).

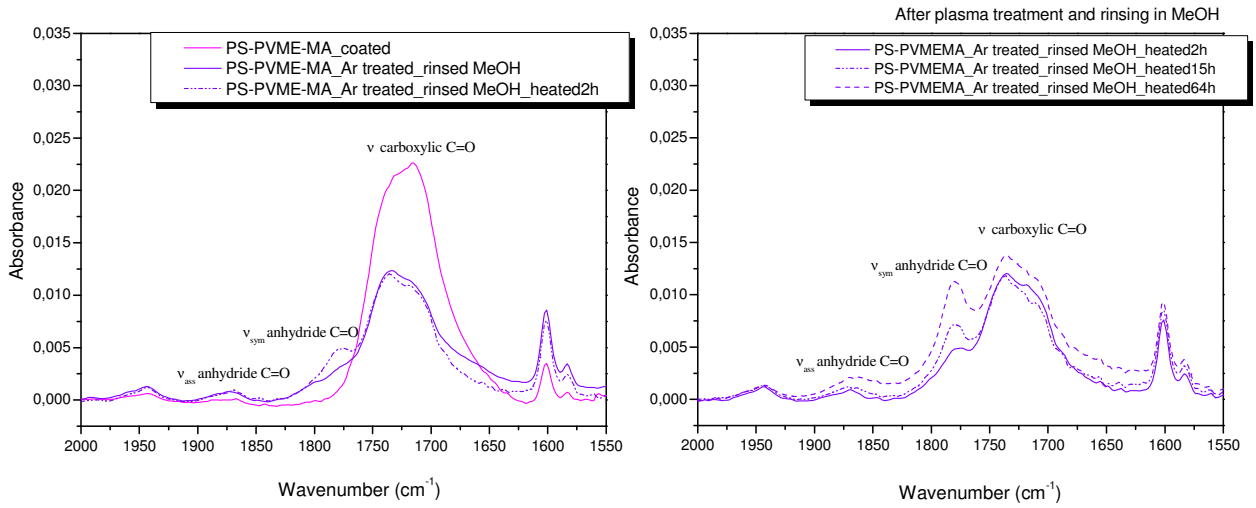

Figure 11. 5 FTIR-ATR spectra of PS functionalized by PVMEMA plasma immobilization (power 120 W, argon gas flow 38 sccm, pressure 8×10^{-3} mbar, treatment time 15s) before and after heating (left) and after different heating treatment times (right)

Differently from MA plasma reaction treatment, the formation of anhydride moieties for PVMEMAc plasma immobilization in the plasma immobilized layer is evident in FTIR-ATR results after annealing at 90 ◦C by the appearance of the 1775 cm^{-1}/1860 cm^{-1} bands in the corresponding infrared spectra (Fig. 11.5).

FTIR-ATR PVMEMA spectra in Figure 11.5 (left) show how the duration of the heating treatment can affect the final chemical properties: increasing the time, the resulting maleic anhydride fraction increases itself how it is observable form the graph, as consequence of a higher conversion from the carboxylic form to the anhydride one. The same effect could be achieved by increasing the temperature of the heating treatment (from 90°C to 120°C) but such higher temperature are not compatible with the thermal stability of polystyrene substrate thus allowing as maximum a temperature of 90°C for the heating treatment (results not shown).

11.4.3. Electron beam immobilization of functional polymer thin films

Electron beam immobilization of PEMA on PS was investigated as a function of the initial PEMAc film thickness and the absorbed irradiation dose. PEMA films of different thickness were prepared on PS model surfaces by different spin coating parameters. Before and after irradiating and rinsing, the amount of PEMA was determined by ellipsometry. For an absorbed dose of 257 kGy 2 nm or less were found independent of the initial film thickness. Increasing the absorbed dose to 770 kGy improved the efficiency of the process.

For an initial film thickness of 16 nm and 45 nm (before rinsing) an immobilized film thickness of 5 nm and 18 nm was obtained respectively (Table 11.2).

Type of plasma treatment	**PE-MA 1% EB 257 kGy rinsed**	**PE-MA 2% EB 257 kGy rinsed**	**PE-MA 1% EB 770 kGy rinsed**	**PE-MA 2% EB 770 kGy rinsed**
thickness (nm)	~ 1,5 nm	2 nm	5 nm	17,8 nm

Table 11.2 Thickness values measured by ellipsometry on PEMA (1% and 2%) electron beam immobilized on PS with different adsorbed doses (257 and 770 kGY)

Fig. 11.6 shows the results for the most favorable case with an initial PEMA film thickness of ~18 nm and an absorbed dose of 770 kGy. The peak deconvolution of the XPS C1s spectrum results in three components at 285.0 eV (A), 286.8 eV (B) and 289.0 eV (C) with A:B:C = 66:8:26. Comparing this to the expected values for pure PEMA (only component A and C with A:C = 2:1) the appearance of component B can be attributed to the material degradation upon electron beam exposure (as for previous treatments). However, the structure retention of the immobilized molecule seems to be better than in the case discussed above for plasma immobilization.

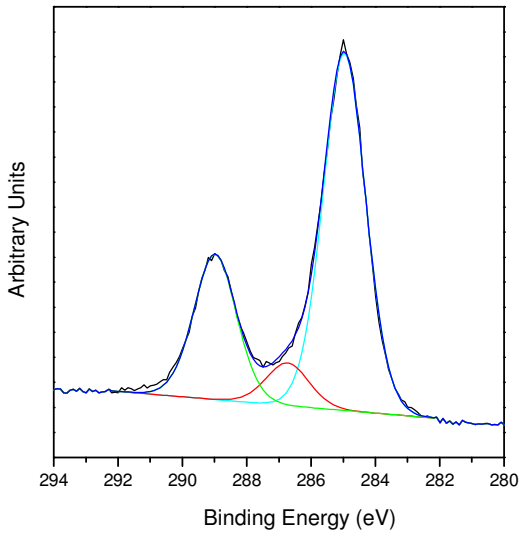

Figure 11.6 XPS C1s spectrum of PS functionalized by PEMA (2%) electron beam immobilization (770 kGy)

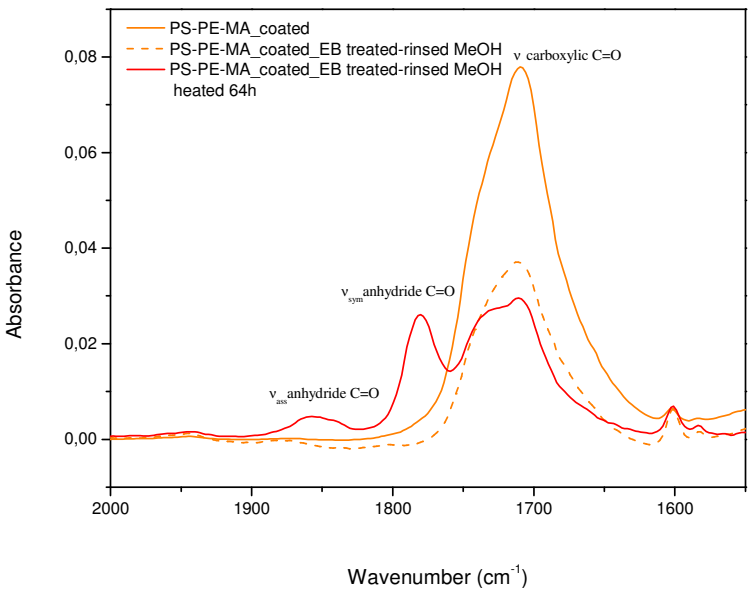

Figure 11.7 FTIR-ATR spectra of PS functionalized by PEMA (2%) electron beam immobilized (770 kGy) before (orange solid line) and after rinsing (orange dash line) and after heating treatment for 64 h at 90°C (red solid line)

The formation of anhydride moieties upon annealing at 90°C was proven by the appearance of the 1775 cm^{-1}/1860 cm^{-1} bands in the infrared spectrum (Fig. 11.7), similarly to other FTIR-ATR results.

11.4.4. UV immobilization of functional polymer thin films

UV immobilization of PEMA-BP on PS was investigated as a function of the initial PEMA-BP film thickness and the BP functionalization density. PEMA-BP films of different thickness were prepared on PS model surfaces by variation of spin coating parameters. Only 2% was used as concentration for the polymer preparation since it resulted the more efficient from electron beam characterization in the final polymer immobilization.

Before and after UV irradiation and rinsing, the amount of PEMA-BP was determined by ellipsometry. Results are reported in Table 11.2.

Type of plasma treatment	**PE-MA 2% PBZ 5% UV 10 min rinsed**	**PE-MA 2% PBZ 10% UV 10 min rinsed**	**PE-MA 2% PBZ 20% UV 10 min rinsed**
thickness (nm)	34,5 nm	35 nm	36 nm

Table 11.2 Thickness values measured by ellipsometry on PEMA (2%)-PBZ (5,10,20%) UV immobilized on PS after 10 minutes of irradiation

Corresponding experiments for PEMA-BP5 and PEMAc-BP20 showed very similar results. Independent of the functionalization density, simultaneous UV cross-linking and grafting allows to immobilize the major part of the pre-deposited polymer film (XPS results not shown).

Again, the formation of anhydride moieties upon annealing at 90°C was proven by the appearance of the 1775 cm^{-1}/1860 cm^{-1} bands in the infrared spectrum (Fig. 11.8) as for previous FTIR-ATR results.

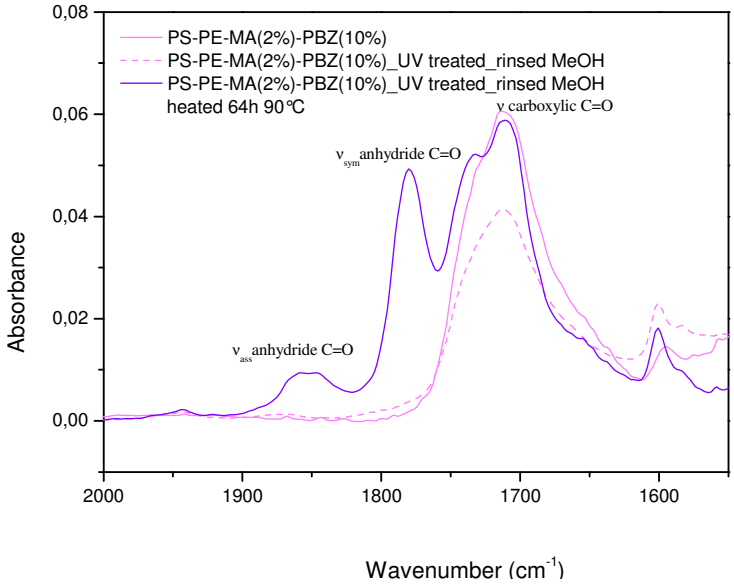

Figure 11. 8 FTIR-ATR spectra of PS functionalized by PEMAc (2%) UV immobilized (770 kGy) before (pink solid line) and after rinsing (pink dash line) and after heating treatment for 64 h at 90°C (violet solid line)

11.4.5. Grafting of functional polymers to plasma activated surfaces

The last approach based on plasma ammonia activation and subsequent polymer grafting was characterized only by XPS measurements.

Fig. 11.8 shows the XPS C1s spectrum of the PS surface after grafting PEMA and removing unbound material. A peak deconvolution similar to the cases discussed above results in a ratio A:B:C = 73:8:19. This indicates a thickness of the grafted PEMA layer (only component A and C with A:C = 2:1) less than the XPS sampling depth of about 8 nm. Since there is no reason for radiation-induced degradation of the immobilized copolymer in this procedure, the appearance of component B can be attributed only to the modified PS surface underneath the grafted PEMA layer. NH_3 plasma treatments typically lead to the formation of primary amine groups but also to other structures with similar C1s binding energies of the adjacent carbon atom [24].

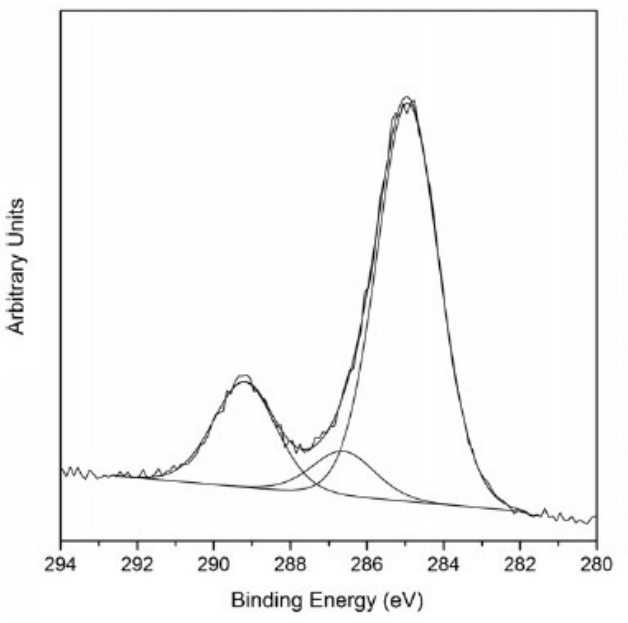

Figure 11 9 XPS C1s spectrum PEMA grafted to ammonia plasma activated

Anhydride formation was proven by fluorescence labeling (Fig. 11.10). To prove the formation of anhydride groups and to check the lateral homogeneity of the functionalization, the reaction of 5-aminofluorescein with the surface anhydride was used. For that purpose samples were incubated over night with a 5 mM solution of 5-aminofluorescein in DMSO and subsequently rinsed with borate buffer (pH 10) to remove any unbound label molecules. The fluorescence of the samples was quantified with a fluorescence imaging system FLA 5100 (Fuji Photo Film Europe, Düsseldorf, Germany).

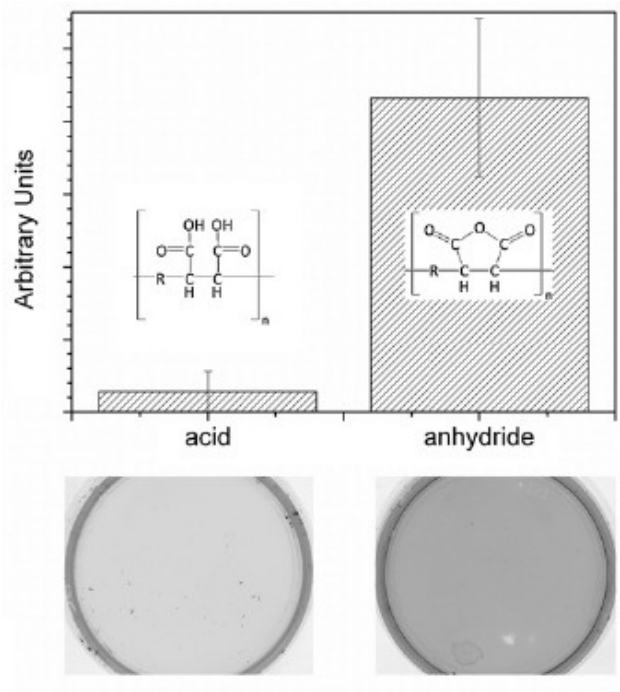

Figure 11.10 Proof of anhydride formation for PEMA grafted to ammonia plasma activated PS multiwell plates. Fluorescence intensities (top) and fluorescence images (bottom) of the unreactive surface (acid form of the maleic anhydride copolymer, left) and the reactive anhydride surface (right) after labeling with 5-aminofluorescein.

A covalent coupling of 5-aminofluorescein on the surface anhydride by reaction with amino groups gives rise to a high fluorescence intensity on this surfaces. In contrast, no covalent binding with the fluorescent reagent is expected for the acid form of the copolymer. Consequently, only a slight fluorescence appears after rinsing with borate buffer.

Conclusions

Various routes to anhydride surface functionalization of polymeric materials, in particular polystyrene, were introduced including (a) maleic anhydride plasma reaction, (b) low pressure plasma immobilization, (c) electron beam immobilization and (d) UV immobilization of functional polymer thin films as well as (e) grafting of functional polymers to plasma activated surfaces. In every case a stable surface functionalization with a sufficient anhydride density for subsequent protein binding was achieved. Considering the advantages of each technique for a particular application, concerning the simplicity of the procedure process maleic anhydride plasma reaction from solid precursor (a) is the most favorable one. Anhydride moieties are formed straightforward in a single step. No thin film preparation from polymer solution is required. Regarding the complexity of the set-up (i.e. the cost of the

apparatus) the UV technique (d) outperforms any high vacuum (a, b, e) and electron beam based approach (c).

In any case this type of functionalization based on maleic anhydride reactive groups gives the advantage to change the functionality from the carboxylic form to the anhydride one by simply annealing the sample and to reversibly re-obtain the carboxylic functionality by immersing in water the sample so performing a high hydrolysis reaction. The advantage is the possibility to have on the same surface two different type of functionalities according to environmental conditions. Moreover, the anhydride functionality can act as protective group for the carboxylic one, known to be less stable during surface aging and reactive with contaminants.

References

[1] Dubiel E.A, Martin Y., Vermette P., "Bridging the Gap Between Physicochemistry and Interpretation Prevalent in Cell−Surface Interactions", *Chemical Reviews,* **2011,** 111, p. 2900-2936.

[2] Mrksich M., "What can surface chemistry do for cell biology? ", *Current Opinion in Chemical Biology*", **2002**, 6, p. 794-797.

[3] Morent R., De Geyter N., Desmet T., Dubruel P., Leys C., "*Plasma Processes and Polymers,* "Plasma Surface Modification of Biodegradable Polymers: A Review"**, 2011**, 8, p.171-190.

[4] Pompe T., Zschoche S., Herold N., Salchert K., Gouzy M.F., Sperling C., Werner C., *Biomacromolecules,* "Maleic Anhydride Copolymers: a Versatile Platform for Molecular Biosurface Engineering", **2003,** 4, p.1072-1079.

[5] Alberti K., Davey R.E., Onishi K., George S., Salchert K., Seib F.P., Bornhäuser M., Pompe T., Nagy A.*,* " Functional immobilization of signaling proteins enables control of stem cell fate", *Nature Methods*, **2008,** 5, p. 645-650.

[6] Pompe T., Salchert K., Alberti K., Zandstra P., Werner C., "Immobilization of growth factors on solid supports for the modulation of stem cell fate", *Nature Protocols*, **2010,** 5, p. 1042-1050.

[7] Lehmann K., Herklotz M., Espig M., Paumer T., Nitschke M., Werner C., Pompe T., "A new approach to biofunctionalisation and micropatterning of multi-well plates", *Biomaterials*, **2010,** 31, p. 8802-8809.

[8] Biedermann H., Osada Y., *Plasma Polymerization Processes*, Elsevier: Amsterdam, **1992**.

[9] Mishra G., McArthur S.L., "Plasma Polymerization of Maleic Anhydride: Just What Are the Right Deposition Conditions? ", *Langmuir,* **2010,** 26, p. 9645-9658.

[10] Drews J., Goutianos S., Kingshott P., Hvilsted S., Rozlosnik N., Almdal K., Sorensen B.F., "Plasma Polymerised Thin Films of Maleic Anhydride and 1,2-Methylenedioxybenzene for Improving Adhesion to Carbon Surfaces", *Journal of Vacuum Science and Technology A*, **2007,** 25, p. 1108-1117.

[11] Ryan M.E., Hynes A.M.,. Badyal J.P.S, "Pulsed Plasma Polymerization of Maleic Anhydride", *Chemistry of Materials*, **1996,** 8, p. 37-42.

[12] Schiller S., Hu J., Jenkins A.T.A.,. Timmons R.B, Sanchez-Estrada F.S., Knoll W., Forch R., "Chemical Structure and Properties of Plasma-Polymerized Maleic Anhydride Film, *Chemistry of Materials,* **2002**,14, p. 235-242.

[13] Siffer F., Ponche A., Fioux P., Schultz J., Roucoules V., "A chemometric investigation of the effect of the process parameters during maleic anhydride pulsed plasma polymerization", *Analytica Chimica Acta*, **2005**, 539, p. 289-299.

[14] Gaboury S.R., Urban M.W., "Microwave plasma reactions of solid monomers with silicone elastomer surfaces: a spectroscopic study", *Langmuir,* 9, **1993,** p. 3225-3233.

[15] Gaboury S.R., Urban M.W., *Langmuir,* 10, **1994,** p. 2289.

[16] Rzayev Z.M.O., "Graft Copolymers of Maleic Anhydride and Its Isostructural Analogues: High Performance Engineering Materials", *International Review of Chemical Engineering*, **2011**, 3, p.153-215.

[17] Nitschke M., Zschoche S., Baier A., Simon F., Werner C., "Low pressure plasma immobilization of thin hydrogel films on polymer surfaces", *Surface and Coatings Technology*, **2004**, 185, p.120-125

[18] Cordeiro A.L., Zimmermann R., Gramm S., Nitschke M., Janke A., Schäfer N., Grundke K., Werner C., "Temperature dependent physicochemical properties of poly(N-isopropylacrylamide-co-N-(1-phenylethyl) acrylamide) thin films", *Soft Matter,* **2009**, 5, p.1367-1377.

[19] Nitschke M., Gramm S., Götze T., Valtink M., Drichel J., Voit B., Engelmann K., Werner C., "Thermo-responsive poly(NiPAAm-*co*-DEGMA) substrates for gentle harvest of human corneal endothelial cell sheets", *Journal of Biomedical Materials Research A*, **2007**, 80, p. 1003-1010.

[20] Gramm S., Teichmann J., Nitschke M., Gohs U., Eichhorn K.-J., Werner C., "Electron beam immobilization of functionalized poly(vinyl methyl ether) thin films on polymer

surfaces – Towards stimuli responsive coatings for biomedical purposes", *Express Polymer Letters,* **2011,** 5, p. 970-976.

[21] Kloceck P., *Handbook of Infrared Optical Materials*, Marcel Dekker: New York, **1991**.

[22] Harrick N.J., *Internal Reflection Spectroscopy*, Interscience: New York, **1975**.

[23] Lin-Vien D., Colthub N.B., Fately W.G., Grasseli J.G., *The Handbook of Infrared and Raman Characteristic Frequencies of Organic Molecules*, Academic Press: London, **1991**.

[24] Meyer-Plath A.A., Schröder K., Finke B., Ohl A., "Current trends in biomaterial surface functionalization-nitrogen containing plasma assisted processes with enhanced selectivity", *Vacuum*, **2003**, 71, p. 391-406.

Conclusion

a. The study and the optimization of a **plasma-polymerized acrylic acid** and a **plasma-polymerized styrene** thin film presented in this thesis, has led to the following important results:

1. By selecting specific working conditions (Power, *Duty Cycle.*, Time of Deposition), a pulsed-plasma polymerization process performed by Acrylic Acid vapours on a RF - PECVD system has been optimized to obtain a **hydrophilic**, **water resistant** thin functional film exposing **carboxylic groups** (-COOH) at the surface
2. The optimized parameters (pulsed plasma, applied Power, carrier gas flow) were tested for plasma-polymerization of Styrene: by tuning the experimental conditions, a **stable hydrophobic** thin film was deposited by a plasma process.
3. The stability towards water soaking and rinsing in solutions at different pH, investigated by ellipsometry, XPS and FTIR-ATR spectroscopy, was successfully verified showing a slight decrease in the film thickness and a **high-reticulated structure** derived from the plasma process.
4. The high number of carboxylic functionalities was qualitatively characterized by XPS technique and quantitatively investigated by colorimetric titration and electrokinetic characterization. The possibility to tune functional groups density exposed at the film surface has been studied by exploring the effect of nature of gas (**Ar** and $\mathbf{O_2}$) used in the pre-deposition etching step of the substrate. It was demonstrated (by FTRIR-ATR and XPS Spectroscopy) that Ar pre-etching allows a lower number of carboxylic groups exposed at the film surface and this can be exploited in specific biosensing applications.
5. The availability and the **bioreactivity** of carboxylic (-COOH) groups towards biomolecules amino ($-NH_2$) groups has been studied and successfully validated by Fluorescence Microscopy for the detection of Protein A conjugated to a fluorescent marker and by Quartz Microbalance technique for the study of kinetic of the binding of BSA protein to PPAA films.
6. In order to optimize the –COOH groups retention for the subsequent biological applications, a **plasma copolymerization process** performed starting from a vapour mixture of Acrylic Acid and Styrene was performed with successful results.

7. From **styrene** vapours, a **hydrophobic film** showing antifouling properties was successfully deposited by a pulsed plasma-polymerization process and exploited for biosensor applications.

b. On the basis of these outcomes, in particular, two successful applications have been explored:

1. A **Microarray biochip** platform constituted of a polymeric substrate (UPVC) has been functionalized by **plasma-polymerized acrylic acid film**. The efficiency in Microarray applications was tested by a hybridization protocol for the detection of *Listeria monocytogenes* oligonucleotides. This work has given rise to a patent registration Nr TO2011A000559.

2. A **polymer-based functional pattern** composed of **PPAA** guides (binding a labeled protein) and **PPST** guides (preventing the non-specific protein binding) has been developed and successfully implemented to an **optical biosensor** device able to couple Block Surface Waves to Fluorescence Emission specifically localized to PPAA guides.

c. A new procedure for **maleic anhydride surface functionalization** has been applied with success to standard polystyrene substrates by different approaches (plasma reaction, electron beam and UV immobilization), to get functional films exposing anhydride groups at the surface for protein binding in cell cultures assays.

Appendix

Surface Characterization Techniques

A biomaterial surface presents different levels of crystallinity, roughness and chemical groups towards the biological environment into which it is introduced. Immediately after implantation, the adsorption of a variety of biological molecules such as proteins and lipids further change the surface (Fig. A.1). In order to be able to construct the ideal biomaterial, the surface has to be characterized and this is achieved by a variety of techniques.

In order to determine the composition and structure of a biomaterial surface, different methods which provide several levels of information are commonly used. ATR-IR (Attenuated Total Reflectance Infra-Red) or ATR-FTIR (Attenuated Total Reflectance Fourier Transform Infra-Red) spectroscopy supplies the characteristic absorption bands of functional groups with an informational depth of 0.1-10 μm. The achieved informational depths are usually larger than the thickness of the modified section of the substrate so that the collected spectra obtained could include absorption peaks due to the bulk.

X-ray photoelectron spectroscopy (XPS) (or ESCA, electron spectroscopy for chemical analysis) is a more surface-sensitive analytical method which supplies information not only about the type and amount of present elements but also about their oxidation state and chemical surroundings. Depths of approximately 10 nm can be achieved with this method (about 50 atomic layers).

For the morphological surface characterization microscopic techniques are exploited. The application of atomic force microscopy (AFM) in comparison to scanning electron microscopy (SEM) delivers information about surface properties as far as molecular dimensions. Another advantage of AFM compared with SEM is that the sample is investigated in the original state (no sputtering).

The understanding of the structural and morphological chemical composition of the functional coatings obtained by plasma-polymerization at the surface and interface level is

fundamental to tune and to optimize plasma process parameters in order to obtain the desired properties in the resulting thin films.

For this reason an exhaustive chemical and morphological study on the surface characteristics of the plasma-polymers has been carried out using different surface analytical techniques

A very large number of bioanalytical methods deal with monitoring interactions occurring at surfaces or at least uses surface bound ligands or receptors to monitor changes in analyte concentration even within a homogeneous phase. For all these detection methods there is a need for very special and smart surface properties.

Selectivity, sensitivity, stability, and reversibility are examples of such requirements for these sensor systems which must be provided in part by the surface properties. In the case of biosensors, the user expects a rather high signal-.to-noise ratio, short response times, low limits of detection, high sensitivity, and the possibility to use sensors also in real samples, not just in lab applications.

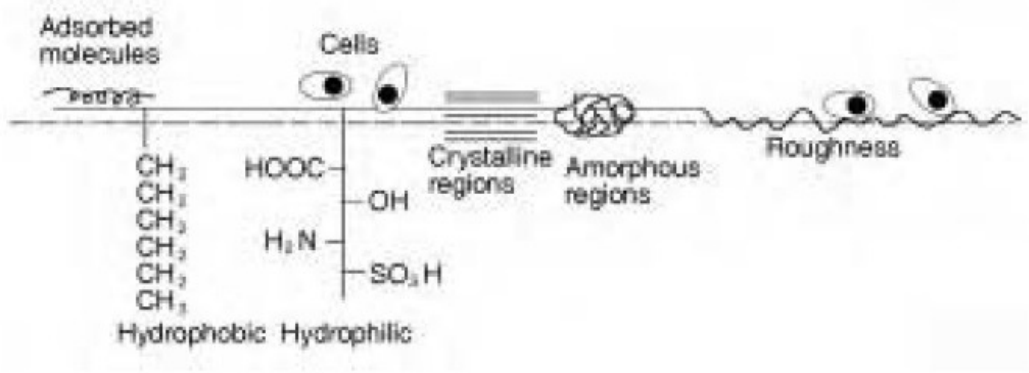

Figure A.1 A typical biomaterial surface in the *in-vivo* environment

Microscopic Techniques

To investigate about the structural and morphological properties of the functionalized surfaces three microscopic techniques have been extensively used throughout this study:

a) Contact Angle

The investigation of surface wettability by means of contact angle determination is of special interest in the characterization of solid surfaces. Wetting involves the interaction of a liquid with a solid, including the formation of a contact angle at the solid/liquid/fluid interface, the spreading of a liquid over a surface (displacing the fluid initially in contact with that surface), or the penetration of a liquid into a porous solid medium. Wetting and non-wetting phenomena are ubiquitous in the natural and technological worlds. The flow of oil and water through the porous rock of an oil reservoir and the rise of nutrient-bearing fluids in the stem of a plant are examples of cases strongly influenced by capillary forces. Such forces are, at least in part, determined by the wetting of a solid surface by the two involved fluid phases. Wetting phenomena are also of considerable technical interest.

The importance of wettability in adhesion is also well-known: the quality of adhesive bondings and coatings depends strongly on the spreading of these materials on the adherent or solid substrate. The reason is that for good adhesion to take place, the adhesive and the adherent must come into intimate contact.

Contact angles are often used simply as empirical parameters to quantify the wettability in technical solid–liquid systems. However, it is of great fundamental, but also practical interest, to know *how the contact angle depends on the chemical composition of both the solid and the liquid* [1].

Contact angle measurements are believed to be the simplest methods in the estimation of solid surface tension. The determination of solid-vapor (γ_{sv}) and solid-liquid ($\gamma_{s\ell}$) interfacial tensions. Contact angle measurement is easily performed by establishing the tangent (angle) of a liquid drop with a solid surface at the base. It can be defined as the angle between the tangent to the liquid–fluid interface and the tangent to the solid interface at the contact line between the three phases. The contact angle is usually measured on the liquid side. The attractiveness of using contact angles θ to estimate the solid-vapor and solid-liquid interfacial tensions is due to the relative ease with which contact angles can be measured on suitably prepared solid surfaces.

The possibility of estimating solid surface tensions from contact angles relies on a relation which has been recognized by Young [2] in 1805. The contact angle of a liquid drop on a solid surface is defined by the mechanical equilibrium of the drop under the action of three interfacial tensions (Figure A.2): solid-vapor, γ_{sv}, solid-liquid, $\gamma_{s\ell}$, and liquid-vapor, $\gamma_{\ell v}$.

This equilibrium relation is known as Young's equation:

$$\gamma_{\ell v} \cos \theta Y = \gamma_{sv} - \gamma_{s\ell} \quad \text{(Eq. 1)}$$

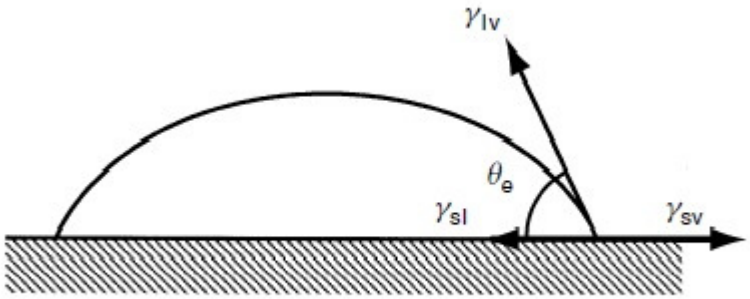

Figure A.2 Young's force balance giving the equilibrium contact angle

where θY is the Young contact angle, i.e. a contact angle which can be inserted into Young's equation. It will become apparent later that the experimentally accessible contact angles may or may not be equal to θY. Young's Eq.6.1 contains only two measurable quantities, the contact angle θ and the liquid-vapor surface tension, $\gamma_{\ell v}$. In order to determine and $\gamma_{s\ell}$, an additional relation relating these quantities must be sought. Nevertheless, Eq. 1 suggests that the observation of the equilibrium contact angles of liquids on solids may be a starting point for investigating the solid surface tensions, γ_{sv} and $\gamma_{s\ell}$. This has inspired many studies which attempt to develop methodologies for determining solid surface tensions.

From the point of view of thermodynamic equilibrium, complete and partial wetting are two distinct equilibrium regimes. Complete wetting means that the contact angle between a liquid and a flat solid surface is zero (θe = 0, see Fig. 7). In this case, the liquid forms a very thin film on the solid surface and the long-range character of the molecular interactions must be taken into account [3,4].

Partial wetting occurs if the contact angle is finite (θe > 0, see Figures 7(a) and 7(b)). The liquid does not spread down to a mesoscopic or a microscopic thickness. Thus, it can be described in terms of macroscopic quantities, as will be discussed in this section.

Partial wetting, with contact angles greater than 90° (Figure A.3) are often called "non-wetting" situations when the liquid tends to "ball-up" and run off the surface easily. In the case of partial wetting, the liquid drop deposited on a solid surface will form an equilibrium shape.

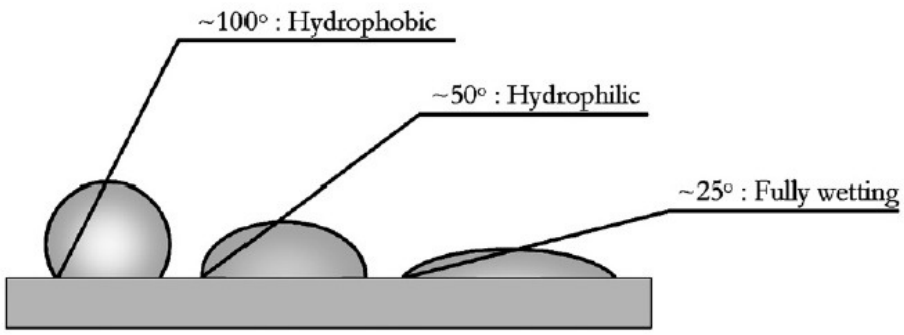

Figure A.3 Different wettability situations

Classical capillarity predicts this equilibrium shape, which obeys the Laplace law, as follows

$$\Delta P = \gamma \left(\frac{1}{R_1} + \frac{1}{R_2}\right) \quad \text{(Eq. 2)}$$

According to this well-known equation, the pressure difference P across a liquid–fluid interface is related to its interfacial tension γ and curvature, where $R1$ and $R2$ are the principal radii of curvature.

The equilibrium in the boundary region between two bulk phases can be treated mathematically, by using either the concept of "surface tension" or the (mathematically) equivalent concept of "surface free energy". Because of this mathematical equivalence, both terms can generally be used interchangeably. Frequently, the terms "surface tension" or "surface free energy" are used if one of the phases is a gas or a vapour.

The term "interfacial tension" is often used to describe the tension between two immiscible liquids, i.e., water and oil. The terms "interfacial tension" or "interfacial free energy" are also used in a more general sense to describe the free energy of solid–liquid, solid–vapour, liquid–vapour and liquid–liquid interfaces.

The surface tension can be defined as a force per unit length [5]. If the value of this force per unit length is denoted by γ, then the work done in extending a movable side by a distance dx is given by the following

$$work = \gamma\, l\, dx \quad (\text{Eq. } 3)$$

Since l dx = dA, this gives the change in area and Eq.6.3 can be equally written as follows

$$work = \gamma\, dx \quad (\text{Eq. } 4)$$

Now, γ represents the work required by any reversible process to form a unit area of new surface. This parameter is generally reported in dyn/cm or mN·m, but also in erg/cm^2 or mJ/m2, which have the same numerical values. In the case of normal pure liquids, only plastic deformation is possible and the total work in deforming the surface is just γ . In the case of solids, both plastic and elastic deformations are possible.

Surface tension component: Fowkes approach

The approach of surface tension components was pioneered by Fowkes [6]. He postulated that the total surface tension can be expressed as a sum of different surface tension components, each of which arises due to a specific type of intermolecular forces:

$$\gamma = \gamma^d + \gamma^h + \gamma^{di} \ldots \quad (\text{Eq. } 5)$$

where γ, γ^d, γ^h are, respectively, the total surface tension, dispersive surface tension component, and surface tension components due to hydrogen and dipole-dipole bonding. Eq. 5 is often rearranged into

$$\gamma = \gamma^d + \gamma^n \quad (\text{Eq. } 6)$$

i.e. the total surface tension g is a sum of only the dispersive γ^d and non-dispersive γ^n surface tension components. The former is claimed to result from molecular interaction due to London forces, the latter from all other interactions due to non-London forces. A geometric mean relationship was postulated both of the solid-liquid and liquid-liquid interfacial tensions

$$\gamma_{12} = \gamma_1 + \gamma_2 - 2(\gamma_1^d + \gamma_2^d)^{1/2} \quad (\text{Eq. } 7)$$

For solid-liquid systems, combining Eq.7 with Young's equation yields

$$\gamma_l \, cos\Theta_Y \; = \; -\gamma_l + 2(\gamma_s^d + \gamma_l^d)^{1/2} \quad (\text{Eq. } 8)$$

Typically, experimental contact angles of different liquids with known γ_l^d on a dispersive solid surface $\gamma_s = \gamma_s^d$ are employed to determine the surface tension of a solid.

The Fowkes approach, can be easily tested with dispersive non-dispersive liquid pairs. Results will simply illustrate the fact that the perceived 'surface tension components' in Fowkes' sense do not reflect physical reality. In principle, this is obvious from the experimental results that $\gamma_{lv} \, cos\Theta$ changes smoothly with γ_{lv}, independent of intermolecular forces and liquid structures.

Thus, the basic postulate of the Fowkes approach is false and any generalization of this approach must suffer from the same deficiency.

Surface tension component: Owens-Wendt-Kaelble approach

Owens and Wendt [7] extended Fowkes' concept to cases where both dispersion and hydrogen bonding forces may operate. They regarded the surface tension as being composed of two components such that

$$\gamma = \; \gamma^d + \gamma^h \quad (\text{Eq. } 9)$$

where $\boldsymbol{\gamma^h}$ denotes the component of surface tension due to both hydrogen bonding and dipole-dipole interactions. They postulated

$$\gamma_{sl} = \gamma_s + \gamma_l - 2\sqrt{\gamma_s^d \gamma_l^d} - 2\sqrt{\gamma_s^h \gamma_l^h} \quad (\text{Eq. } 10)$$

Combining this equation (called Owens-Wendt-Kaelble equation) with Young's equation yields

$$\gamma_l\,(1 + cos\Theta_Y) = 2\sqrt{\gamma_s^d \gamma_l^d} + 2\sqrt{\gamma_s^h \gamma_l^h} \quad (\text{Eq. } 11)$$

Nearly at the same time, Kaelble [8] also published a very similar equation in terms of dispersion and polar forces.

Clearly, for the applicability of Young's equation in this equation containing two unknowns (γ_s^d and γ_s^h) of the solid, it is suggested to use contact angle measurements of at least two different liquids on one and the same solid surface, by solving two simultaneous equations. Such procedures also imply constancy of the solid surface tension from liquid to liquid; if

the operative solid surface tension is not constant from one liquid to the next, simultaneous solution of different equations (from contact angles of different liquids) would be meaningless.

b) Atomic Force Microscopy (AFM)

Atomic force microscopy (AFM) is a method increasingly being used to study and quantify surface properties of materials in their untreated, natural form.

It can produce three-dimensional images of solid surfaces at very high resolution, and unlike scanning tunneling microscopy (STM), it can also image non-conducting samples such as polymers and ceramics.

It is essentially a scanner that creates topographical maps of surfaces. A very sharp tip, located at the free end of a cantilever follows the contours of the surface as it is moved over it.

When the force microscope is operated in 'contact mode', the sample surface is scanned by a sharp tip, which is mounted on a soft spring, also referred to as 'cantilever'. The sample is positioned on a piezoelectric tube ortripod, which controls the scanning motion. Features on the sample surface cause a deflection of the cantilever. This deflection is most commonly measured by an optical beam technique: laser light is focused onto the end of the cantilever, and reflected onto a split photodiode. The feedback signal from the photodiode is used to control the height of the piezoelectric crystal as the sample is scanned. The corresponding height adjustment signal is directly related to the topography of the surface. Interaction

between the sample surface and the AFM tip is determined by the interaction between the molecules or atoms on the surface of the sample and the tip.

Interaction between the sample surface and the AFM tip is determined by the interaction between the molecules or atoms on the surface of the sample and the tip. The relevant forces in force microscopy (e.g. electrostatic forces, dipolar actions, van der Waals forces, H-bonding) have been summarized e.g. by Schönherr.

When AFM is used to obtain topographic information on soft samples such as adsorbed biolayers, the lateral force exerted by the tip can lead to image artefacts due to disrupture of the surface.

This problem has been solved recently by the development of a new AFM technique, known as tapping mode AFM (TM-AFM). This tapping mode employs a cantilever oscillating with a high amplitude. The vibration is set such that the tip contacts the sample surface once in every vibration period. Since the tip only intermittently 'taps' the surface, the tip-sample interactions (especially shear forces) are greatly reduced, which ensures minimal disturbance of the adsorbed molecules [9].

The use of this technique has enabled researchers to image the molecular packing and aggregation of proteins on surfaces such as silicon, [10] methylated silicon, [11] self-assembled monolayers, [12] spin-cast polymer films, and on mica.

An advantage of AFM is with polymers that can be highly hydrated in vivo, and thus treatments for visualization as in SEM (high vacuum, conductive coats, etc.) would not maintain their actual surface topography. With AFM, however, it was possible to examine very fragile hydrogel materials like soft contact lenses in their swollen form and measure their surface roughness. It is also possible to monitor real-time events like hydrolytic degradation.

c) Fluorescence Microscopy

There is a huge variety of optical microscopies and spectroscopies which are all mainly used to study biological molecules, but not so often biomaterials.

Fluorescence microscopy is one of the most widely used techniques in biology. Biological molecules are labelled with a fluorescent marker (or label), i.e., are chemically modified, if they do not contain fluorescing entities like tryptophan themselves. A fluorescence

microscope is a classical optical microscope in which different wavelengths can be detected visually, usually by selecting a wavelength by putting a filter between sample and detector. One advantage of fluorescence microscopy is the fact that some dyes quench the fluorescence of another dye by the so-called Förster energy transfer. If two parts of a large biomolecule or two different molecules are labelled with these two dyes, one can study the distance dependence of the interaction. Another advantage is that the fluorescence wavelength is influenced by the environment; this can also be used to get more insight in the structural properties of a biomolecule. This method is, therefore, mainly used for studies on molecules attached to a biomaterial surface but not to study the biomaterials themselves.

The resolution is limited to that of an optical microscope, i.e., to some hundred nanometers.

Scanning nearfield optical microscopy (**SNOM**) is an optical microscope which is not operated in the far field as classical microscopies, but in the near field. Because the resolution limitations result from the diffraction of light in the far field, they are not valid in the near field. In the near field, the short-range interactions of an evanescent light field with a sample

surface are detected. There are several practical solutions to near field microscopy. The first and most commonly used method uses a glass fiber (often metal coated) which is sharpened at its end so that light from a laser source at the other end of the fiber cannot propagate through the small exit hole and an evanescent field evolves. If this fiber is at a short distance from the sample surface, the evanescent near field interacts with the surface. The reflected or transmitted light is then collected in the far field. The resolution limit is given only by the geometrical parameter of the fiber opening.

Resolutions at around 100 nm are commonly reached. The approach to the wobbling amplitude by a sensor such as a tuning fork. The amplitude is decreased when the fiber comes close to the surface [13].

Spectroscopic Techniques

The surface chemistry of a polymer intended for biomedical applications can be investigated by a number of several spectroscopic approaches:

a) X-ray photoelectron spectroscopy (XPS)

XPS (X-ray Photoelectron Spectroscopy) or ESCA (Electron Spectroscopy for Chemical Analysis) is a method for studying the energy distribution of electrons ejected from a material that has been irradiated with a source of ionizing radiation such as X-rays.

XPS is probably the most frequently applied analytical method in surface sciences. Its application is established in all fields of materials sciences (e.g. metals, ceramics, polymers and their composites), life sciences, electronic and several other industries [14].

This powerful tool is an extremely surface sensitive method able to identify and quantify the chemical elements in the surface region of a solid and to provide quantitative information about basic properties such as binding energy, charge, and valence state, examining the atom as a part of its chemical environment. The impact of ESCA in polymeric characterization has been twofold: it can analyze relatively intractable materials without the need for special sample preparation and it is a surface sensitive method. In principle, when any material is bombarded by photons with energy greater than the binding energy of an electron in a given atomic shell or sub-shell, there is a finite probability that the incident photon will be absorbed by the atom and an electron is either prompted to move to an unoccupied level or ejected as a photoelectron. This depends on the energy of the incident photon and the atomic number of the target element. The kinetic energy of the photoelectron is:

$$KE = h\nu - BE \quad \text{(Eq. 11)}$$

where KE and BE are the kinetic energy and the binding energy of the photo-electron, and $h\nu$ is the energy of the incident photon.

Concerning the instrumentation, photoelectron spectrometer must be consisted of few basic units (Fig A.4): First, a X-Ray source is required to emit a white spectrum (Bremsstrahlung spectrum) which additionally contains intensive peaks of well defined energies (characteristic X-Ray radiations). Usually, for XPS the $K\alpha_{1,2}$ radiation of magnesium ($h \cdot \nu = 1253.6 \pm 0.35$ eV) or aluminium ($h \cdot \nu = 1253.6 \pm 0.45$ eV) is used [15].

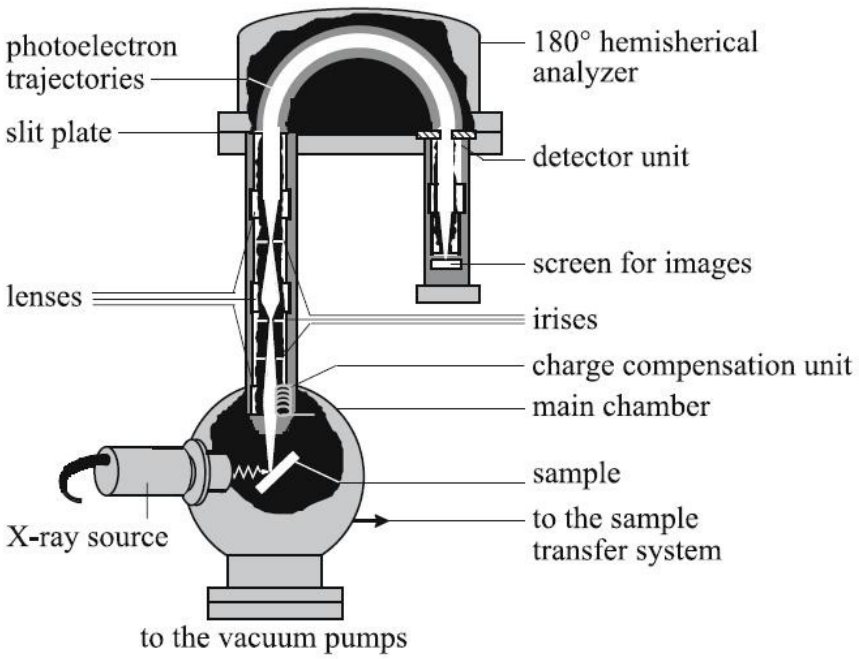

Figure A 4 Typical build-up of a simple photoelectron spectrometer

In order to enhance the energetic resolution of the spectrometer a crystal monochromator can be employed to cut a small line of the $K\alpha_1$ transition out. The X-Rays pass the sample and there is a certain probability that photons release electrons which are now denoted photoelectrons. The actual aim of the spectrometer is to determine the kinetic energies of the photoelectrons escaping the sample surface. Usually in XPS a hemispherical analyser is used for this purpose.

The photoelectrons which have passed the electron-optics of the spectrometer introduce a slit between two hemispheres. There an electric field is applied and forces the linearly moving photoelectrons on a circular path. The radius of this circular path depends on the applied field strength as well as the kinetic energy of the photoelectrons. At a given field strength only photoelectron with a definite kinetic energy can arrive the count unit (e.g. set of channeltrons) at the end of the hemispherical analyser. Hence, the variation of the field strength allows us to separate the photoelectrons concerning their different kinetic energies. In praxis, the field strength is mostly constant. A slit plate with an adjustable electric potential slows the photoelectrons with higher kinetic energies down to pass the hemispherical analyser and arrive at the count unit. In this case the voltage applied to the slit plate is a measure for the kinetic energy of the photoelectrons.

As mentioned above, the photoelectrons which have passed the hemispherical analyser are counted over a defined time interval. Hence the *y*-axis in the XPS spectra is indicated *count rate* and its unit is *cps* (counts per second). Today, mostly a series of channeltrons is used to count the photoelectrons.

The forth essential and fundamental module of all XPS spectrometers is the vacuum system requiring also a suitable sample transfer and handle system. To prevent interactions between photoelectrons and gas molecules which would result in a partial lost of the photoelectron's kinetic energy the base pressure in the analysis chamber must be better than 10–8 mbar. To produce and preserve the ultra-high vacuum different pumps have to work permanently.

Although the X-ray may penetrate deeply into the sample to produce photoelectrons, most of these electrons lose energy in numerous inelastic collisions; only those atoms residing in the top few mono-layers give rise to undistorted photoelectron spectra. The typical analysis depth in ESCA and in Auger electron spectroscopy (AES) is about 3±50 Å, and they are truly surface analysis methods.

In AES, an incident primary electron creates an excited ion near the surface which decays by the emission of a secondary Auger electron, whose kinetic energy is measured. As in XPS, the escaping Auger electron's kinetic energy limits the depth from which it can emerge, giving AES its high surface sensitivity and nanometer sampling depth. Auger images or maps can also be generated for specific elements with approximately 200 nm resolution. Auger finds its greatest strength in the analysis of inorganic materials not susceptible to electron-beam damage.

b) Fourier Transform InfraRed spectroscopy in Attenuated Total Reflectance (ATR)

The name means below red, from the Latin infra = "below" and red that is the color of the longest wavelengths of visible light, in other words it has a longer wavelength than that of red light. A longer wavelength means it has a lower frequency than red, hence below. Infrared radiation is an electromagnetic radiation that encompasses all the wavelengths between the visible and the microwave regions of the electromagnetic spectrum. The infrared region can also be subdivided into three smaller categories known as near-IR, mid-IR and far-IR, the ranges of which are neatly summed up in Table A.1.

Region	Wavenumber range	Vibrational information
near IR	14000 – 4000	Changes in vibrational and rotational levels
mid IR	4000 – 400	Changes in fundamental vibrational levels of most molecules
far IR	400 – 20	Rotational energy level changes

Table A. 1 The three different regions in which infra-red is divided

FTIR (Fourier Transform Infrared) Spectroscopy is an analytical technique, that provides information about the chemical bonding or molecular structure of materials, whether organic or inorganic. The technique works on the fact that bonds vibrate at characteristic frequencies. A molecule that is exposed to infrared rays absorbs infrared energy at frequencies, which are characteristic to that molecule. An absorption spectrum reveals the chemical species present and shifts in frequencies from those expected from the `free' molecules in solution indicate interactions with the surface or other surface species.

During FTIR analysis, a spot on the sample is subjected to a modulated IR beam. Material's transmittance and reflectance of the infrared rays at different frequencies is translated into an IR absorption plot consisting of reverse peaks. The resulting FTIR spectral pattern is then analyzed and matched with known signatures of identified materials in the FTIR library.

Traditional (dispersive) infrared techniques experience difficulties due to the 'one wavenumber at a time' nature of data acquisition. This leads to either a poor signal to noise ratio in a spectrum or a very long time needed to obtain a high quality spectrum.

These problems can be overcome using Fourier transform infrared spectroscopy (FTIR), which is based on the interferometer originally designed by Michelson and a mathematical procedure developed by Fourier that converts response from the time to the frequency domain. In the *Michelson interferometer* a parallel, polychromatic beam of radiation from a source (A) is directed to a beam splitter (B), made from an infrared transparent material, such as KBr. The beam splitter reflects approximately half of the light to a mirror, known as the fixed mirror (C), which in turn reflects the light back to the beam splitter. The rest of the light passes through to a mirror, called moving mirror (D), moving continuously, at a known velocity, back and forth along the direction of the incoming light. Upon reflection from the moving mirror, radiation is then directed back to the beam splitter. At the beam splitter some of the light that has been reflected from the fixed mirror combines with light reflected from the moving mirror and is directed towards the sample. After passing through the sample (E) the radiation is focused onto the detector (F). Detectors are sufficiently fast to work on time domain signal changes from the modulation in the interferometer. As the distance of the moving mirror from the beam splitter changes, different wavelengths of radiation are in-phase and out-of-phase at a frequency, that is dependent both upon the rate at which the mirror moves and the frequency of radiation. The complex pattern of overlaid sinusoidal waves of light (in the time domain) is known as an interferogram. The interferogram can be converted back to the original frequency distribution (spectrum) by means of a Fourier transform, which can be done very rapidly on a computer.

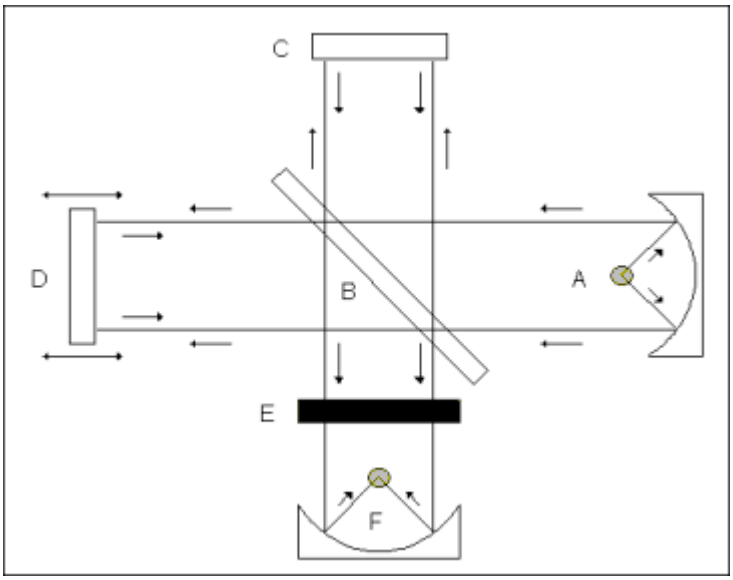

Figure A.5 The schematic of the Michelson interferometer, which forms the basis of most FTIR instruments

Before the advent of ESCA the only reliable method for polymer surface studies was infra-red spectroscopy (either attenuated total reflectance (ATR) or multiple internal reflectance (MIR) spectroscopy). This method require es fairly large samples with flat or easily deformable surfaces and typically gives information pertaining to surfaces and gives information penetrating to 1 μm into the material.

In **attenuated total reflectance** (**ATR**) FTIR, the incident IR beam first passes through a ZnSe, Ge, or diamond crystal, improving the surface sensitivity of the technique. The resulting plot is of absorbance (or transmittance) versus wave-number. Sampling depth is dependent on the infrared transmitting crystal used to internally reflect the incident IR beam as well as the refractive index of the sample, and is on the order of microns [16]. Although ATR-FTIR has a relatively deep sampling depth, it does not require ultra high vacuum conditions, as do XPS and ToF-SIMS, and an analysis can therefore be conducted in less than ten minutes.

In recent years, Fourier transform infra-red (FTIR) has allowed analysis sensitivity to be improved, but even then FTIR can neither match the sensitivity of ESCA nor can it be as focused on the surface. In systems with variable composition within the range 0±1 μm, the two methods could be applied to complement each other effectively.

c) UV-vis Spectroscopy

Molecules containing π-electrons or non-bonding electrons (n-electrons) can absorb the energy in the form of ultraviolet or visible light to excite these electrons to higher anti-bonding molecular orbitals. The more easily excited the electrons (i.e. lower energy gap between the HOMO and the LUMO) the higher the wavelength of light it can absorb. Spectrophotometry investigates the absorption of the different substances between the wavelength limits 190 nm and 780 nm (visible spectroscopy is restricted to the wavelength range of electromagnetic radiation detectable by the human eye, that is above ~360 nm; ultraviolet spectroscopy is used for shorter wavelengths).

Spectrophotometry is used for both qualitative and quantitative investigations of samples. The wavelength at the maximum of the absorption band will give information about the structure of the molecule or ion and the extent of the absorption is proportional with the amount of the species absorbing the light. Quantitative measurements are based on Beer's

Law (also known as “Lambert Beer Law” or even “Bouguer-Lambert-Beer Law”) which is described as follows:

$$A_\lambda = \varepsilon_\lambda \, b \, C$$

where

- A is the absorbance and is calculated by the following equation

$$A = \log_{10} I_0/I$$

where I_0 is the incident light’s intensity and I is the light intensity after it passes through the sample.

- e = molar absorbance or absorption coefficient (in L mol^{-1} cm^{-1} units)
- c = concentration (molarity) of the compound in the solution (in mol L^{-1} units)
- b = path length of light in the sample (in cm units)

The Beer-Lambert law states that the absorbance of a solution is directly proportional to the concentration of the absorbing species in the solution and the path length. Thus, for a fixed path length, UV/Vis spectroscopy can be used to determine the concentration of the absorber in a solution. It is necessary to know how quickly the absorbance changes with concentration. This can be taken from references (tables of molar extinction coefficients), or more accurately, determined from a calibration curve.

UV/Vis spectroscopy is routinely used in analytical chemistry for the quantitative determination of different analytes (colorimetric titration), such as transition metal-ions, highly conjugated organic compounds, and biological macromolecules. Determination is usually carried out in solutions.

Energetics

Surface energetics is very important in defining the biocompatibility of a polymer because this determines the type of molecules that do and do not adsorb on the surface. Tissue in growth, blood coagulation, cell damage to blood elements and immune signalling are all influenced by the energetics of the surface.

a) Zeta potential (ζ potential)

A charged molecule in motion produces an electric field. The zeta potential is the electric potential of a charged particle at the plane of shear. The shear plane, or the plane of slip, is the distance from the surface to the distance in solution where the solvent molecules are not bound to the surface and are not moving as a unit with the particle. At this boundary, zeta potential can be determined. The surface potential is a very difficult parameter to characterize and it is far easier to determine zeta potential. It is measured at a shear plane near the particle surface and is therefore proportional to surface potential. It is affected by ionic strength; at high ionic strength, potential decreases much more sharply over the distance from the surface to the shear plane. This means a smaller zeta potential. It is therefore important to maintain a relatively constant ionic strength while characterizing the zeta potential of a dispersion as a function of pH.

Zeta potential and the Electrical double layer

The development of a net charge at the particle surface affects the distribution of ions in the surrounding interfacial region, resulting in an increased concentration of counter ions (ions of opposite charge to that of the particle) close to the surface. Thus an electrical double layer exists around each particle. The liquid layer surrounding the particle exists as two parts; an inner region, called the Stern layer, where the ions are strongly bound and an outer, diffuse, region where they are less firmly attached. Within the diffuse layer there is a notional boundary inside which the ions and particles form a stable entity. When a particle moves (e.g. due to gravity), ions within the boundary move with it, but any ions beyond the boundary do not travel with the particle. This boundary is called the surface of hydrodynamic shear or slipping plane. The potential that exists at this boundary is known as the Zeta potential.

If all the particles in suspension have a large negative or positive zeta potential then they will tend to repel each other and there is no tendency to flocculate. However, if the particles have low zeta potential values then there is no force to prevent the particles coming together and flocculating. The general dividing line between stable and unstable suspensions is generally taken at either +30mV or -30mV. Particles with zeta potentials more positive than +30mV or more negative than -30mV are normally considered stable.

The most important factor that affects zeta potential is pH. A zeta potential value on its own without a quoted pH is a virtually meaningless number. Imagine a particle in suspension with a negative zeta potential. If more alkali is added to this suspension then the particles will

tend to acquire a more negative charge. If acid is then added to this suspension a point will be reached where the negative charge is neutralised. Any further addition of acid can cause a build up of positive charge. Therefore a zeta potential versus pH curve will be positive at low pH and lower or negative at high pH.

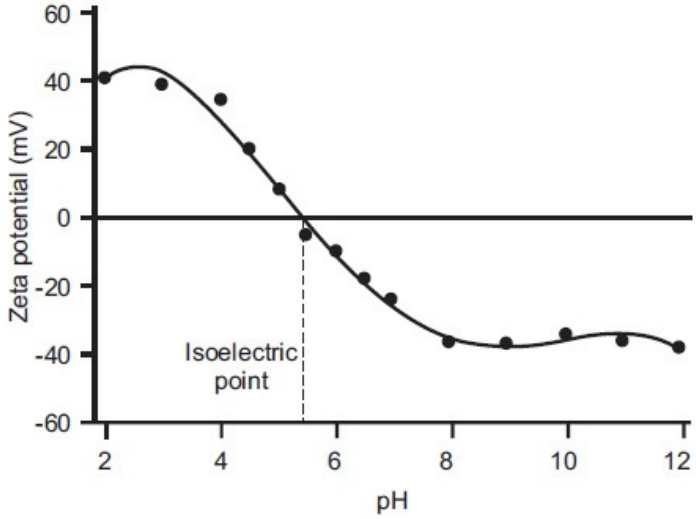

Figure A.6 A typical plot of zeta potential versus pH showing the position of the isoelectric point and the pH values where the dispersion would be expected to be stable

The point where the plot passes through zero zeta potential is called the Isoelectric point and is very important from a practical consideration. It is normally the point where the colloidal system is least stable (Figure A.6).

An important consequence of the existence of electrical charges on the surface of particles is that they will exhibit certain effects under the influence of an applied electric field. These effects are collectively defined as electrokinetic effects.

Another aspect influencing the zeta potential is the conductivity. The thickness of the double layer (κ-1) depends upon the concentration of ions in solution and can be calculated from the ionic strength of the medium. The higher the ionic strength, the more compressed the double layer becomes. The valency of the ions will also influence double layer thickness. A trivalent ion such as Al^{3+} will compress the double layer to a greater extent in comparison with a monovalent ion such as Na^{+}. Inorganic ions can interact with charged surfaces in one of two distinct ways (i) non-specific ion adsorption where they have no effect on the isoelectric point. (ii) specific ion adsorption, which will lead to a change in the value of the isoelectric point. The specific adsorption of ions onto a particle surface, even at low

concentrations, can have a dramatic effect on the zeta potential of the particle dispersion. In some cases, specific ion adsorption can lead to charge reversal of the surface.

Also the concentration of a formulation component can give information to assist in formulating a product to give maximum stability thus affecting zeta potential. The influence of known contaminants on the zeta potential of a sample can be a powerful tool in formulating the product to resist flocculation for example [17].

Electrokinetic Effects

An important consequence of the existence of electrical charges on the surface of particles is that they interact with an applied electric field. These effects are collectively defined as electrokinetic effects. There are four distinct effects depending on the way in which the motion is induced.

These are:

- Electrophoresis: the movement of a charged particle relative to the liquid it is suspended in under the influence of an applied electric field.
- Electroosmosis: the movement of a liquid relative to a stationary charged surface under the influence of an electric field.
- Streaming potential: the electric field generated when a liquid is forced to flow past a stationary charged surface (the one exploited for the characterization presented in this thesis).
- Sedimentation potential: the electric field generated when charged particles move relative to a stationary liquid.

b) Ellipsometry

When linearly polarised light, of a known orientation, is reflected at an oblique incidence from a surface, then the reflected light is elliptically polarised. The shape and orientation of the ellipse and thus the result of the interaction of the light beam with the surface depends on the angle of incidence, the direction of the polarisation of the incident light, and the reflective properties of the surface. Ellipsometric measurement is a non-invasive and sensitive technique

for determining the optical properties of surfaces and thin films by measuring the changes in the polarisation state of light when it is reflected from or transmitted through a sample. If the sample undergoes a change, as for example occurs when a thin film on a surface changes its thickness, then its reflection properties will also change. The ability to monitor these changes by measuring the state of the polarisation of the light, before and after the interaction with the substrate, permits an investigation of the processes occurring at the substrate or a characterising of the optical properties of the sample, illustrated schematically in Figure A.7.

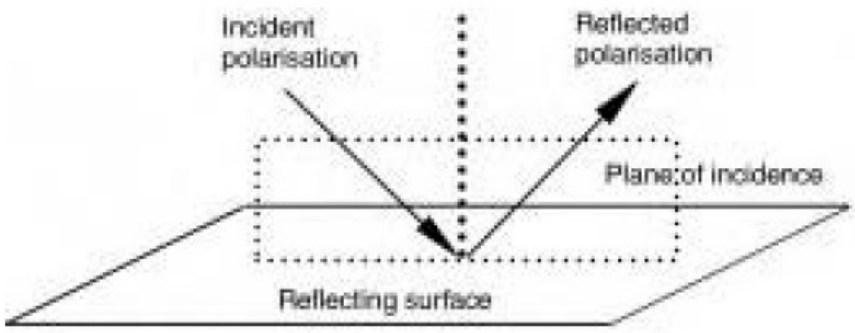

Figure A.7 The geometry of reflection ellipsometry. The change in polarization upon reflection carries informations about the characteristics of the sample

The most important application of ellipsometry in physical measurements is to study thin films and surfaces, and as a result this provides a means to study (and design) devices which contain them. In the context of ellipsometry, a thin film is one that ranges from essentially zero to several hundred nanometers in thickness. The sensitivity of an ellipsometer is such that a change of film thickness of a few tenths of a nanometer is usually relatively easy to detect by optical means.

The process of ellipsometry requires a measurement of the change of the state of polarisation of light. This change involves the amplitude ratio, Ψ of the two orthogonal polarisation components and/or a change in their relative phase difference, Δ. These parameters, which are fundamental to the ellipsometric measurement cannot, however, be measured instantaneously. Such an averaged measurement representation of polarised, partially polarised or unpolarised

The measured response depends on optical properties and thickness of individual materials. Thus, ellipsometry is primarily used to determine film thickness and optical constants. However, it is also applied to characterize composition, crystallinity, roughness, doping concentration, and other material properties associated with a change in optical response.

Since the 1960s, as ellipsometry developed to provide the sensitivity necessary to measure nanometer-scale layers used in microelectronics, interest in ellipsometry has grown steadily. Today, the range of its applications has spread to the basic research in physical sciences, semiconductor and data storage solutions, flat panel display, communication, biosensor, and optical coating industries. This widespread use is explained by increased dependence on thin films in many areas and the flexibility of ellipsometry to measure most material types: dielectrics, semiconductors, metals, superconductors, organics, biological coatings, and composites of materials [13].

References

[1] Grundke K., *Wetting, Spreading and Penetration* from *Handbook of Applied Surface and Colloid Chemistry* edited by Krister Holmberg, John Wiley & Sons, Ltd, **2001**

[2] Young T., "An Essay on the Cohesion of Fluids", *Philos. Trans. R. Soc. London*, **1805,** 95, p. 65-87

[3] De Gennes P.G., "Wetting: statics and dynamics", *Rev. Mod. Phys*., **1985,** 57, p. 827-863

[4**]** Leger L., Joanny J.-F, "Liquid spreading", *Rep. Prog. Phys*., **1992,** 55, p. 431-486

[5**]** Adamson A. W., *Physical Chemistry of Surfaces*, 5th Edn,Wiley, New York, **1990**

[6**]** Fowkes F.M., "Attractive Forces at Interfaces", *Ind. Eng. Chem*., **1964,** 12, p. 40-52

[7] Owens D. K., Wendt R.C., "Estimation of the surface free energy of polymers", *J. Appl. Polym. Sci.*, **1969,** 13, p. 1741-1747

[8**]** Kaelble D.H., Adhesion J., "Dispersion-polar surface tension properties of organic solids" **1970,** 2, p.66-81

[9] Baty A.M., Leavitt P.K., Siedlecki C.A., Tyler B.J., Suci P. A.; Marchant R. E.; Geesey G. G., "Adsorption of adhesive proteins from the marine mussel, mytilus edulis, on polymer films in the hydrated state using angle dependent X-ray photoelectron spectroscopy and atomic force microscopy" *Langmuir* **1997,** 13, p. 5702-5710

[10] Ortega-Vinuesa J. L., Tengvall P.; Lundström I., "Molecular packing of HSA, IgG, and fibrinogen adsorbed on silicon by AFM imaging", *Thin Solid Films* **1998,** 324,p. 257-273

[11] Ortega-Vinuesa, J. L.; Tengvall, P.; Lundström, I., "Aggregation of HSA, IgG, and fibrinogen on methylated silicon surfaces", *J. Coll. Interface Sci.* **1998,** 207, p. 228-239

[12] Lin J. N., Drake B., Lea A. S., Hansma P. K., "Direct observation of immunoglobulin adsorption dynamics using the atomic force microscope", *Langmuir* **1990,** 6, p. 509-511

[13] Vadgama P., *Surfaces and Interfaces for Biomaterials*, Woodhead Publishing Ltd, **2005**.

[14] Seah M.P., "The quantitative analysis of surfaces by XPS", *Surf. Interface Anal.*, **1980**, 2, p. 222-239

[15] Pleul D., Simon F., "X-ray Photoelectron Spectroscopy" from M. Stamm editor. Polymer Surfaces and Interfaces. Berlin: Springer, p. 71-85, **2008**

[16] Desai S., Singh R.P., "Surface modification of polyethylene" from Albertsson AC, editor. Long-term properties of polyolefins. New York: Springer, p. 231, **2004**

[17] Zetasizer Nano series, *Zeta Potential Theory*, Chapter 16